STUDY OF SHALLOW WATER INTERACTION BETWEEN SHIPS

by

Pål Wold

This thesis is submitted for the degree of Master of Science

Department of Naval Architecture and Ocean Engineering University of Glasgow

November 1998

ProQuest LLC.
789 East Eisenhower Parkway
P.O. Box 1346
Ann Arbor, MI 48106 – 1346

DECLARATION

Except where reference is made to the work of others, this thesis is believed to be original.

TABLE OF CONTENT

NOMENCLATURE

$_{ij}A_{mn}^{(k)}$: normal velocity evaluated at the m^{th} control point of the i^{th} body due to the vortex at the n^{th} vortex point of the j^{th} body, for the k^{th} time-step

$_{ij}B_{mn}^{(k)}$: normal velocity evaluated at the m^{th} control point of the i^{th} body due to the vortex at the n^{th} vortex point of the wake of the j^{th} body for the k^{th} time-step

Bs_i : underwater hull-surface of the i^{th} ship

C : submerged surface of the fixed object

CF_i : lateral force coefficient acting on the i^{th} ship

$C_i(x_i)$: blockage coefficient of the i^{th} ship

CM_i : yaw moment coefficient acting on the i^{th} ship

D_i : draught of the i^{th} ship

$G^{(\gamma)}$: distribution of sources along the body axis

$G^{(\sigma)}$: distribution of vortices along the body axis

H : water depth

$H^{(\gamma)}$: harmonic function

$H^{(\sigma)}$: harmonic function

M_i : number of elements the i^{th} body is divided into

N : number of ships

L_i : length of the i^{th} ship

N_i : two-dimensional unit vector sectional area of the i^{th} ship

$S'_i(x_i)$: total flux from the body of the i^{th} ship

$S_i(x_i)$: sectional area of the body sectional area from the i^{th} ship

Sp_{ij} : separation distance between the i^{th} and the j^{th} ship

U_i : the forward speed of the i^{th} ship

V_i^* : actual cross flow velocity at the section $\Sigma_i(x_i)$ of the i^{th} ship

ST_{ij} : longitudinal distance, or stagger, between the i^{th} and j^{th} ship

ds_j : element on the x_j axis

g : acceleration of gravity

$g_{im}^{(k)}$: total normal velocity evaluated at the m^{th} control point of the i^{th} body for the k^{th} time-step

k	:	time-steps
m	:	1,2...M
t	:	time in general
w	:	channel width
w_j	:	the wake of the j^{th} ship
θ_i	:	angular displacement of the i^{th} ship
ε	:	slenderness parameter
$\vec{n}$	:	unit normal vector
ϕ	:	velocity potential
$\vec{V}$	:	velocity vector of the fluid motion
Δp	:	linearized pressure jump across the x-axis
Δt	:	size of the time-step
Δx_i	:	element length of the i^{th} ship
$\Delta\phi$	:	difference in potential across the x_i-axis
Φ_i	:	velocity potential in the inner region of the i^{th} ship
$\Phi_i^{(1)}$	:	velocity potential due to the longitudinal motion at unit speed of the i^{th} ship
$\Phi_i^{(2)}$	:	velocity potential related to a cross-flow of unit magnitude of the i^{th} ship
Γ_i	:	circulation of the i^{th} ship
$\Sigma_i(x_i)$	:	section contour of the i^{th} ship
γ_j	:	vortex distribution strengths of the j^{th} ship
η	:	vortex point
ρ	:	fluid density
σ_j	:	source distribution strengths of the j^{th} ship
ξ	:	source point

LIST OF FIGURES

CHAPTER 2

CHAPTER 3

CHAPTER 4

CHAPTER 5

CHAPTER 6

LIST OF TABLES

CHAPTER 3

CHAPTER 4

CHAPTER 5

CHAPTER 6

ACKNOWLEDGEMENTS

I would like to thank my supervisors; Dr. K.S. Varyani and Dr. R.C. McGregor for giving me support and constructive advice throughout the research.

The author would like to extend his gratitude to Professor N. Barltrop for his assistance and help.

The author would like to express his gratitude to Mr. D. Brown for the private discussions, which have been helpful for the research.

Thanks must also be given to my good friends Mr. T. Tveitnes, Mr. A. Mærli and Mr. R. Olsen for valuable support and encouragement.

Finally, I would like to express my gratitude to my very special friend Miss J. Juvik, for encouraging me to finish this thesis.

SUMMARY

When a ship operates in a harbour, in a channel or in confined waters, it usually does so close to other ships or some fixed structures. This is unavoidable because of the inherently restricted nature of these waters. The proximity of these other objects is potentially hazardous and it is important that the ship operator is able to maintain full control of the ship during operations in these waters. For this to be possible, the hydrodynamic interaction forces and moments, which are amplified in close encounters in restricted waters, should be properly understood.

This thesis presents an investigation into the lateral forces and yaw moments experienced by a ship in transit near other ships. In the theoretical development, up to three ships are involved in the manoeuvre. For the conditions where two ships are interacting, new empirical formulae are derived for calculating the maximum lateral force and yaw moment coefficients.

The first chapter presents an introduction and history of the ship-ship interaction problem, which has been investigated by other researchers.

The second chapter is concerned with the problem formulation that the present method is based on. The interaction forces and moments acting on several ships are calculated using a numerical scheme based on the discrete vortex distribution method.

In the third and fourth chapter, the lateral force and yaw moment coefficients are examined for the two ships interaction problem. The effect of varying several parameters (such as water depth, separation distance, ship size and ship speed) is analysed. Based on the parametric study, new empirical formulae are derived for calculating the maximum lateral force and yaw moment coefficients, both for the two ships meeting and two ships passing manoeuvre.

Chapter 5 and 6 presents an investigation into the situations where three ships interacting. Again, effect of the water depth, separation distance, ship size and ship speed on the hydrodynamic forces and moments is examined, both for three ships meeting and three ships passing manoeuvre.

In the last chapter the major findings and conclusions from the research are drawn. Recommendations for future work are made.

CHAPTER 1

INTRODUCTION

1.1 GENERAL

In restricted waters such as harbours, estuaries, channels or fairways, a ship is commonly in the close proximity of other vessels or fixed structures. This is unavoidable because of the inherent nature of ship operations in such waterways. These operations are potentially hazardous and it is important to be able to predict and control the course of each ship in these waters. It is therefore necessary, from viewpoint of navigation, to know the precise manoeuvring characteristics of ships, including the effects of water depth, proximity of channel bank and the other ships. In narrow waterways especially, the effects of the channel geometry and hydrodynamic interactions between ships are strongly inter-related and particularly significant.

1.2 REVIEW OF LITERATURE

E.O. Tuck (1966) made a systematic investigation of the problem of shallow water flow past a fixed slender obstacle in a stream. This problem had a particular bearing on, and was suggested by, the behaviour of ships moving in still water of restriction only in depth, but had also application to a variety of problems involving shallow water, such as river flows past obstacles. However Tuck referred to the slender obstacle as a ship, and its surface as the hull. Adopting the assumptions of linearized shallow water theory, this problem was entirely congruent to the steady aerodynamics of a thin wing. The analysis assumed the ship to be slender in the sense that it is longer than it is broad or deep, and used the technique of matched asymptotic expansions (or 'inner' and 'outer' expansions) to construct an approximate solution. This technique has been used to solve a number of difficult singular perturbation problems. Tuck obtained expressions for the vertical force and moment at both sub- and supercritical speeds. The latter are used to give the sinkage and trim displacements of a ship

E.O. Tuck (1967) also presented a theory for ship dynamics in shallow water of restricted width. This was a straightforward extension of the earlier method. Beck, Newman, and Tuck (1975) further extended the analysis to include the case of a ship operating in a dredged channel surrounded on both sides by shallow water. E.O. Tuck and J. Newman (1974) also investigated the hydrodynamic interaction between ships.

The method of matched asymptotic expansions was also used by J.N. Newman (1969) to determine the lateral flow of an ideal fluid past a slender body. The flow was constrained

by a pair of closely spaced walls parallel to the long axis of the body. The walls introduced an effective blockage in the cross flow plane, which caused the flow field to become three-dimensional. Approximate solutions were derived to determine the added mass and moment of inertia for accelerated body motions and the lift force and moment acting on a wing of low aspect ratio. Newman used a simplified formula (which Taylor (1973) investigated more thoroughly) for the blockage effect. Each cross section of a ship has a blockage coefficient, which is uniquely dependent on its shape, and Newman derived a general numerical procedure for finding this coefficient when the cross section takes an arbitrary shape.

R.F. Beck (1977) applied the matched asymptotic expansions to the problem of a ship moving with constant velocity in a channel of rectangular cross section. Beck examined the case of a ship travelling parallel to, but displaced from, the centre line of a shallow channel, and calculated the lateral forces and yaw moments acting on the ship. Because of the asymmetry of this configuration, there were not only a sinkage force and trimming moment but also a side force and yaw moment.

R.W. Yeung (1978) examined the unsteady hydrodynamic interaction of two bodies moving in a shallow fluid by applying slender body theory. The bodies were assumed to be in each other's far field and the free surface was assumed to be rigid. By matched asymptotic, the inner and outer problems are formulated and a pair of coupled integral-differential equations for determining the unknown cross flows were derived. The degree of coupling was shown to be related to a bottom clearance parameter. Expressions are given for the unsteady sinkage force, trimming moment, sway force, and yaw moment. Numerical calculations for two weakly coupled cases were presented. One corresponds to the interaction of a stationary body with a passing one, and the other to the interaction of two bodies moving in a steady configuration. Theoretical results were compared with existing experimental data.

W. Tan (1979), and R. Yeung and W. Tan (1980) considered interaction of a single ship with a circular island, a finite breakwater, and an elliptical island. It was found that a ship has a dangerous tendency to veer towards the fixed object during the approach if the object has a sharp tip. Results for the interaction of two ships in a channel were also presented.

K. Kijima and H. Yasukawa (1984) investigated the hydrodynamic behaviour of ships during meeting and passing in narrow water channel using slender body theory. Furthermore, ship motions with rudder control during passing in channel by using these hydrodynamic forces were discussed. Kijima and Furukawa (1994) obtained the ship motion for a single ship in the vicinity of a pier.

I.W. Dand (1976a), (1976b), and (1981a,b,c) has produced a large database of experimental data regarding interaction forces and moments between two ships in a channel. Both two ships meeting and passing manoeuvres were investigated for different water depths and separation distances.

K.S. Varyani et al (1997) and (1998) examined the interaction forces and moments acting on several ships, using a numerical scheme based on the discrete vortex distribution method. The effect of water depth was studied and it was found that as the water gets shallower, the lateral forces and yaw moments become larger.

1.3 OBJECTIVES OF STUDY

As explained earlier, in narrow waterways, the hydrodynamic interactions between ships are strongly inter-related and particularly significant from the viewpoint of safety of navigation.

The aim of this research is to calculate interaction forces and moments on two and three ships in meeting and passing conditions using a computer program based on discrete vortex distribution method. A number of parameters (such as water depth, separation distance between ships, ship size and ship speed) are investigated to obtain a large database of the hydrodynamic forces and moments, and new empirical formulae are derived to calculate the maximum lateral force and moment coefficients. This can be used by simulation program developers to inform the vessel operators of hazards of variation of certain parameters while navigating in crowded waterways.

The theoretical approach of previous research in this subject area has been broadly similar for all studies. The present work continues this accord that this is the best way forward and the analysis is developed along these lines. Emphasis is placed on the application for which the analysis can be used. In particular it is the notation and method of Kijima and Yasukawa (1985), which is most closely adhered to.

CHAPTER 2

PROBLEM FORMULATION

2.1 GENERAL FORMULATION

Let Oxyz be a coordinate system fixed in space and $O_ix_iy_iz_i$ a coordinate system fixed on the midship of the i^{th} ship with the $O_iy_iz_i$ – plane located at the midship and the $O_ix_iy_i$ – plane coinciding with the undisturbed free surface. Positive x_i corresponds to a position forward of the midship. Each ship is assumed to move in a straight line in the water channel. The ships are assumed to be moving in calm water of uniform depth H and in water channel with vertical-sided walls. The speed of each ship can be a function of time and is denoted by $U_i(t)$.

To describe the fluid motion, a time-dependent velocity potential, ϕ (x,y,z;t), is introduced where[1]:

$$\vec{V}(x,y,z;t) = \nabla\phi(x,y,z;t) \tag{2.1}$$

$\vec{V}$ is the velocity vector of the fluid motion which is assumed to be irrotational. If the fluid is further assumed to be incompressible, the continuity equation is reduced to $\nabla\cdot\vec{V} = 0$. Thus, ϕ satisfies the Laplace equation:

$$\nabla^2\phi = 0 \tag{2.2}$$

At the rigid fluid boundaries, the velocity potential has to satisfy the condition that the fluid velocity normal to the surface is equal to the normal velocity of the surface. If there are N ships, this results in the following boundary conditions:

$$\left[\frac{\partial\phi}{\partial n_i}\right]_{Bs_i} = U_i(t)(n_x)_i \qquad i = 1, 2,\ldots,N \tag{2.3}$$

$$\left[\frac{\partial\phi}{\partial n}\right]_C = 0 \tag{2.4}$$

$$\left[\frac{\partial\phi}{\partial z}\right]_{z=-H} = 0 \tag{2.5}$$

$$\left[\frac{\partial\phi}{\partial z}\right]_{z=0} = 0 \tag{2.6}$$

[1] For a fuller explanation of the theoretical development see Kijima and Yasukawa (1985)

where Bs_i represents the underwater hull-surface of the i^{th} ship and C the submerged surface bounding the floor. $\partial/\partial n_i$ and $\partial/\partial n$ are the derivatives in the direction normal to Bs_i and C respectively with the unit normal vectors, $\vec{n}_i$ and $\vec{n}$, directed outwards from the fluid domain. $(\vec{n}_x)_i$ is the component of the unit normal vector $\vec{n}_i$ in the x_i-direction.

Equation (2.6) expresses the assumption that the free-surface is rigid. This assumption allows one to treat the problem as a "double-body" problem. In this case, Bs_i and C denote not only the submerged portion of the hull surface and the fixed object, but also their images reflected about the free surface. Equation (2.5) and (2.6) can now be combined into a single equation:

$$\left[\frac{\partial \phi}{\partial z}\right]_{z=\pm H} = 0 \tag{2.7}$$

To complete the general formulation of the problem, the following condition at infinity is imposed:

$$\phi \to 0 \quad \text{as} \quad \sqrt{x_i^{\,2} + y_i^{\,2} + z_i^{\,2}} \to \infty \tag{2.8}$$

2.2 SIMPLIFYING ASSUMPTIONS

It is a difficult task to solve the full three-dimensional problem as formulated above directly. In order to make it more tractable, some assumptions are made which will permit its decomposition into two sub-problems, the so-called "inner problem" and "outer problem".

Let ε be the slenderness parameter ($\varepsilon << 1$), then the slenderness assumption restricts beam and draught of the ships to be small as compared to their lenghts, i.e:

$$L_i = O(1), \qquad B_i = O(\varepsilon), \qquad D_i = O(\varepsilon) \qquad i = 1, 2, \ldots, N \tag{2.9}$$

where L_i, B_i and D_i denote length, breadth and draught of the i^{th} ship respectively.

An assumption that the water is shallow is made, i.e. H = O(ε). A seemingly more restrictive assumption is described by Tan (1979) where the minimum ship-ship separation distances are comparable to the lengths of the ships. This assumption ensures that the inner problem for each ship is uncoupled. However, it does not necessary entail that the theoretical method developed will yield erroneous results for small separation distances and existing experimental and theoretical data appears to justify the use of the theory also for small separation distances.

2.3 METHOD OF SOLUTION

This section describes the method for obtaining the solution to the problem formulated in section 2.1. Briefly, the representations of the inner and outer solutions are first obtained. The outer limit of the inner solution ($y_i >> \varepsilon$) and the inner limit of the outer solution ($y_i << 1$) are then derived. Using these limits, the two solutions are matched in the intermediate region defined by $\varepsilon << y_i << 1$. This ensures the compatibility of the inner and outer solutions. The matching results in an integral equation, which can be solved numerically. The information obtained from solving the integral equation is sufficient for determining the lateral force and moment.

2.3.1 Inner problem

The inner region for the i^{th} ship is defined as the region where the coordinates have the following orders of magnitude:

$$x_i = O(1), \qquad y_i, z_i = O(\varepsilon) \qquad i = 1, 2, \ldots, N \tag{2.10}$$

Since the minimum ship-ship and ship-wall separation distance are comparable to the length of the ships, neither the fixed object nor the other ship will appear in the inner problem of the i^{th} ship. However, since the water depth is assumed to be O(ε) the water bottom will be a part of the inner problem.

Using Φ_i to denote the velocity potential in the inner region of the i^{th} ship, eqns (2.2), (2.3) and (2.7) can be replaced by the following:

$$\frac{\partial^2 \Phi_i}{\partial y_i^{\,2}} + \frac{\partial^2 \Phi_i}{\partial z_i^{\,2}} = 0 \tag{2.11}$$

$$\left[\frac{\partial \Phi_i}{\partial N_i}\right]_{\sum_i(x_i)} = U_i(n_x)_i \tag{2.12}$$

$$\left[\frac{\partial \Phi_i}{\partial z_i}\right]_{z=\pm H} = 0 \tag{2.13}$$

where N_i is the two-dimensional unit vector normal to the section contour $\Sigma_i(x_i)$ of the i^{th} ship.

The inner potential, Φ_i, can be decomposed into two components -- one associated with the longitudinal motion and the other with the lateral flow -- and it is expressed as follows:

$$\Phi_i(y_i, z_i; x_i, t) = U_i(t)\Phi_i^{(1)}(y_i, z_i) + V_i^*(x_i, t)\Phi_i^{(2)}(y_i, z_i) + f_i(x_i, t) \tag{2.14}$$

$\Phi_i^{(1)}$ is the velocity potential due to the longitudinal motion at unit speed and $\Phi_i^{(2)}$ is related to a cross-flow of unit magnitude. V_i^* is the actual cross flow velocity at the section $\Sigma_i(x_i)$ of the i^{th} ship. This cross-flow is a consequence of the presence of the fixed structure and the other ships. $f(x_i,t)$ is an unknown function independent of y_i and z_i coordinates.

$\Phi_i^{(1)}$ corresponds to the problem of a two-dimensional dilating body confined between two parallel walls. $\Phi_i^{(2)}$ corresponds to the lateral-flow problem of a rigid two-dimensional body in an uniform stream of unit strength (Fig 2.1a).

The outer limits of these potentials are defined by Newman (1969) and Yeung (1978) and take the following forms:

$$\lim \Phi_i^{(1)} = \frac{-S_i'(x_i)}{4H}|y_i| \qquad \text{as } |y_i| >> \varepsilon \qquad (2.15)$$

$$\lim \Phi_i^{(2)} = y_i \pm C_i(x_i) \qquad \text{as } |y_i| >> \varepsilon \qquad (2.16)$$

The total flux from the body can be shown to be $S'_i(x_i)$ where $S_i(x_i)$ is the sectional area of the body. The blockage coefficient $C_i(x_i)$ is a hydrodynamic coefficient associated with the virtual-mass characteristics of the section in cascade flow (Sedov 1965), and are estimated by using the approximate formulas given by Taylor (1973). Finally, the outer limit of the inner solution is obtained (as $|y_i| >> \varepsilon$):

$$\lim \Phi_i(y_i, z_i; x_i, t) = \frac{-U_i(t)S_i'(x_i)}{4H}|y_i| + V_i^*(x_i, t)[y_i \pm C_i(x_i)] + f_i(x_i, t) \qquad (2.17)$$

2.3.2 Outer problem

The region, which is far away from any of the ships, is called the outer region of the problem. In terms of orders of magnitude of the coordinates, this region is defined as follows:

$$x_i, y_i = O(1) \qquad z_i = O(\varepsilon) \qquad i = 1, 2, \ldots, N \qquad (2.18)$$

In this region, it is possible to express the velocity potential, ϕ, as a Taylor expansion:

$$\phi_i(x_i, y_i, z; t) = \phi_i(x_i, y_i, 0; t) + \phi_{iz}(x_i, y_i, 0; t)z + \frac{1}{2}\phi_{izz}(x_i, y_i, 0; t)z^2 + \ldots$$

$$= \phi_{0i}(x_i, y_i; t) + \phi_{1i}(x_i, y_i; t)z + \frac{1}{2}\phi_{2i}(x_i, y_i; t)z^2 + \ldots \qquad (2.19)$$

where eqn (2.1) has been used to arrive at the second quality, and ϕ_0 and ϕ_1 are potentials independent of z.

By using eqn (2.7) :

$$\frac{\partial^2 \phi_{0i}}{\partial x_i^{\,2}} + \frac{\partial^2 \phi_{0i}}{\partial y_i^{\,2}} = 0 \qquad (2.20)$$

Hence, the leading-order outer potential ϕ_{0i} (x,y,t) satisfies Laplace equation in x-y plane. This problem is the same as the two-dimensional flow around ships in a water channel. With the understanding that only the leading-order potential ϕ_{0i} is being considered the subscript 0 will henceforth be omitted. The outer solution can be represented by a distribution of sources $G_i^{(\gamma)}(x,y;\xi,\eta)$ and vortices $G_i^{(\sigma)}(x,y;\xi,\eta)$ along the body axis.

$G_i^{(\gamma)}$ and $G_i^{(\sigma)}$ are defined as follows:

$$G_i^{(\sigma)}(x,y;\xi,\eta) = \ell n\sqrt{(x-\xi)^2+(y-\eta)^2} + H_i^{(\sigma)}(x,y;\xi,\eta) \qquad (2.21)$$

$$G_i^{(\gamma)}(x,y;\xi,\eta) = \tan^{-1}\left(\frac{y-\eta}{x-\xi}\right) + H_i^{(\gamma)}(x,y;\xi,\eta) \qquad (2.22)$$

where $H_i^{(\sigma)}$ and $H_i^{(\gamma)}$ are functions harmonic in the physical domain and so constructed that the no-flux condition on C is satisfied, namely:

$$\left[\frac{\partial G_i^{(\sigma,\gamma)}}{\partial n}\right]_C = 0 \qquad (2.23)$$

In the preceding, (ξ,η) is the source or vortex point, and (x,y) is a field point. The outer velocity potential is then written as:

$$\phi_i(x,y;t) = \sum_{j=1}^{N} \frac{1}{2\pi}\left[\int_{L_j} \sigma_j(s_j,t) G_j^{(\sigma)}(x,y;\xi,\eta)\,ds_j + \int_{L_j w_j} \gamma_j(s_j,t) G_j^{(\gamma)}(x,y;\xi,\eta)\,ds_j\right] \qquad (2.24)$$

where σ_j and γ_j are distribution source and vortex strengths of the j^{th} ship, respectively, ds_j denotes the element on the x_j axis, while L_j is the ship axis and w_j is the wake. ξ and η are parametric functions of s_j (Fig 2.1b).

The inner limit ($y_i \rightarrow 0$) of the outer solution as expressed by eqn (2.24) are obtained by means of making a Taylor expansion of ϕ for small values of y_i.

The limit of $\phi_i(x,y;t)$ as $|y_i| << 1$ is given by:

$$\lim \phi_i(x,y;t) = \sum_{\substack{j=1 \\ j\neq i}}^{N} \frac{1}{2\pi} \Bigg[\int_{L_j} \sigma_j(s_j,t) G_j^{(\sigma)}(x_0,y_0;\xi,\eta)\,ds_j + \int_{L_j w_j} \gamma_j(s_j,t) G_j^{(\gamma)}(x_0,y_0;\xi,\eta)\,ds_j$$

$$+ \left\{ \int_{L_j} \sigma_j(s_j,t) \frac{\partial G_j^{(\sigma)}}{\partial y_i}(x_0,y_0;\xi,\eta)\,ds_j + \int_{L_j w_j} \gamma_j(s_j,t) \frac{\partial G_j^{(\gamma)}}{\partial y_i}(x_0,y_0;\xi,\eta)\,ds_j \right\} y_i \Bigg]$$

$$+ \frac{1}{2\pi} \int_{L_i} \sigma_i(s_i,t) \left[\ell n |x_i - \xi_i| + H_i^{(\sigma)}(x_0,y_0;\xi,\eta) \right] ds_i$$

$$+ \frac{1}{2\pi} \int_{L_i w_i} \gamma_i(s_i,t) \left[\theta_i + H_i^{(\gamma)}(x_0,y_0;\xi,\eta) \right] ds_i$$

$$\pm \frac{1}{2} \int_{x_i}^{\frac{L_i}{2}} \gamma_i(\xi_i,t)\,d\xi_i$$

$$+ \Bigg[\frac{1}{2\pi} \int_{L_i} \sigma_i(s_i,t) \frac{\partial H_i^{(\sigma)}}{\partial y_i}(x_0,y_0;\xi,\eta)\,ds_i$$

$$+ \frac{1}{2\pi} \int_{L_i w_i} \gamma_i(s_i,t) \left\{ \frac{1}{x_i - \xi_i} + \frac{\partial H_i^{(\gamma)}}{\partial y_i}(x_0,y_0;\xi,\eta) \right\} ds_i \Bigg] y_i$$

$$+ \frac{\sigma_i(x_i)}{2} |y_i| \qquad (2.25)$$

The point denoted by (x_o, y_o) in the space-fixed Oxy coordinate system corresponds to the point (x_i, $y_i = 0^{\pm}$) in the moving $O_i x_i y_i$ coordinate system.

2.3.3 Equation of interactive forces and moments

Compatibility of the inner and outer solutions is required so that they match in the intermediate region $\varepsilon << y_i << 1$, i.e. they must satisfy the following condition:

$$\lim \Phi_i \quad \text{as} \quad |y_i| >> \varepsilon \equiv \lim \phi_i \quad \text{as} \quad |y_i| << 1 \qquad i = 1,2,\ldots,N \tag{2.26}$$

Figure 2.1c shows the matching in the intermediate region where the interaction effect is included in the effect of the cross flow (V^*). Using the expression obtained for the outer limit of the inner solution, eqn (2.17), and for the inner limit of the outer solution, eqn (2.25), the matching condition is shown by the following equations obtained by the term of similar nature:

$$\sigma_i(x_i,t) = -\frac{U_i(t)S_i'(x_i)}{2H} \tag{2.27}$$

$$V_i^*(x_i,t)C_i(x_i) = \frac{1}{2}\int_{x_i}^{\frac{L_i}{2}} \gamma_i(\xi_i,t)d\xi_i \tag{2.28}$$

$$\begin{aligned} V_i^*(x_i,t) = \sum_{\substack{j=1 \\ j\neq i}}^{N} \frac{1}{2\pi}\Bigg[& \int_{L_j} \sigma_j(s_j,t)\frac{\partial G_j^{(\sigma)}}{\partial y_i}(x_0,y_0;\xi,\eta)ds_j + \int_{L_j w_j} \gamma_j(s_j,t)\frac{\partial G_j^{(\gamma)}}{\partial y_i}(x_0,y_0;\xi,\eta)ds_j \Bigg] \\ & + \frac{1}{2\pi}\int_{L_i} \sigma_i(s_i,t)\frac{\partial H_i^{(\sigma)}}{\partial y_i}(x_0,y_0;\xi,\eta)ds_i \\ & + \frac{1}{2\pi}\int_{L_i w_i} \gamma_i(s_i,t)\left[\frac{1}{x_i-\xi_i} + \frac{\partial H_i^{(\gamma)}}{\partial y_i}(x_0,y_0;\xi,\eta)\right]ds_i \end{aligned} \tag{2.29}$$

The integral equation for γ_i can be obtained using eqn (2.28) and (2.29) as:

$$\frac{1}{2C_i(x_i)}\int_{x_i}^{\frac{L_i}{2}}\gamma_i(\xi_i,t)d\xi_i-\frac{1}{2\pi}\int_{L_iw_i}\gamma_i(s_i,t)\left[\frac{1}{x_i-\xi_i}+\frac{\partial H_i^{(\gamma)}}{\partial y_i}(x_0,y_0;\xi,\eta)\right]ds_i$$

$$-\sum_{\substack{j=1\\ j\neq i}}^{N}\frac{1}{2\pi}\int_{L_jw_j}\gamma_j(s_j,t)\frac{\partial G_j^{(\gamma)}}{\partial y_i}(x_0,y_0;\xi,\eta)ds_j$$

$$=\frac{1}{2\pi}\int_{L_i}\sigma_i(s_i,t)\frac{\partial H_i^{(\sigma)}}{\partial y_i}(x_0,y_0;\xi,\eta)ds_i+\sum_{\substack{j=1\\ j\neq i}}^{N}\frac{1}{2\pi}\int_{L_j}\sigma_j(s_j,t)\frac{\partial G_j^{(\sigma)}}{\partial y_i}(x_0,y_0;\xi,\eta)ds_j$$

for i = 1, 2,...,N (2.30)

The additional conditions imposed on γ_i are the wake conditions, Kelvin's theorem and Kutta condition, i.e.:

$$\gamma_i(x_i,t)=\gamma_i(x_i) \qquad \text{for } x_i < -L_i/2 \tag{2.31}$$

$$\int_{-\infty}^{\frac{L_i}{2}}\gamma_i(\xi_i,t)d\xi_i=0 \tag{2.32}$$

$$\gamma_i\left(x_i=-\frac{L_i}{2},t\right)=-\frac{1}{U_i}\frac{d\Gamma_i}{dt} \tag{2.33}$$

where Γ_i is the circulation of the i^{th} ship. Using Bernoulli's theorem for unsteady flow, the following expression for the linearized pressure jump across the x_i-axis is obtained.

$$\Delta p(x_i,t)=-\rho\left(\frac{\partial}{\partial t}-U_i\frac{\partial}{\partial x_i}\right)\Delta\phi(x_i,t) \tag{2.34}$$

The difference in potential across the x_i-axis, $\Delta\phi$ can be obtained from eqn (2.25),

$$\Delta\phi(x_i,t)=\int_{x_i}^{\frac{L_i}{2}}\gamma_i(\xi_i,t)d\xi_i \tag{2.35}$$

The lateral force and moment acting on the i^{th} ship is then obtained by integrating the pressure difference over the length of the ship as follows,

$$F_i(t) = -\int_{-\frac{L_i}{2}}^{\frac{L_i}{2}} \Delta p(x_i,t)dx_i \tag{2.36}$$

$$M_i(t) = -\int_{-\frac{L_i}{2}}^{\frac{L_i}{2}} x_i \Delta p(x_i,t)dx_i \tag{2.37}$$

The above expression for the lateral force and moment corresponds to the "equivalent" two-dimensional bodies which means they are the values per unit depth. In order to get the total lateral force and yaw moment acting on the ships, simply multiply eqns (2.36) and (2.37) by the water depth H.

Furthermore, the lateral forces and yaw moments are presented in a non-dimensionalized form and are as follows for the i^{th} ship:

$$CF_i = \frac{F_i}{\frac{1}{2}\rho U_1 U_2 B_i D_i} \tag{2.38}$$

$$CM_i = \frac{M_i}{\frac{1}{2}\rho U_1 U_2 B_i D_i L_i} \tag{2.39}$$

2.4 METHOD OF NUMERICAL SOLUTION

The objective of the numerical procedure to be developed here is to solve the integral eqn (2.30). Once the distribution of vorticity $\gamma_i(x_i,t)$ is known, the unsteady hydrodynamic sway force and yaw moment can be obtained using eqns (2.36) and (2.37).

Each body is first divided into M_i elements of equal length, Δx_i. Within each of these segments the distribution of the vortex strength is assumed to take a certain form. The simplest is the discrete vortex representation where all the vorticity within the element is assumed to be concentrated at one point, the vortex point. This distribution permits the direct use of the Green function of any object once it is known. Other forms of

vortex-strength distribution like the step-wise and the linear, require a further step of integrating the Green function over the element which can be very difficult for complex configurations. Moreover, this representation has been found to be reliable for solving aerodynamic problems and techniques, which have been used, are adapted from that field.

Using the discrete-distribution assumption, the integral equation (2.30), can be immediately transformed into a system of linear simultaneous equations. Some notations are now introduced to facilitate the expression of these and other equations. Let the total vorticity within the n^{th} element of the i^{th} body at time t_k be denoted by $\gamma_{in}^{(k)}$, n = 1,2...M_i. Let $\tilde{\gamma}_{in}$, n=1,2...k be the vorticity in the wake element of the i^{th} body where n=k corresponds to the wake element nearest the trailing edge of the body. The system of simultaneous equation derived from eqn (2.30) can now be written in a concise form. For the i^{th} body, we can have:

$$\sum_{j=1}^{N}\left[\sum_{n=1}^{M_j} {}_{ij}A_{mn}^{(k)}\gamma_{in}^{(k)} + \sum_{n=1}^{k} {}_{ij}B_{mn}^{(k)}\tilde{\gamma}_{in}^{(k)}\right] = g_{im}^{(k)}, \qquad \begin{matrix} m = 1,2...M_i \\ i = 1,2...N \end{matrix} \qquad (2.40)$$

where

$${}_{ij}A_{mn}^{(k)} = \begin{cases} \dfrac{1}{2\pi}\left[\dfrac{1}{x_{im}-\xi_{jn}} + \dfrac{\partial H^{(\gamma)}}{\partial y_i}\right] & \text{for } j = i,\ \xi_{jn} < x_{im} \\ -\dfrac{1}{2\pi}\left[\dfrac{1}{x_{im}-\xi_{jn}} + \dfrac{\partial H^{(\gamma)}}{\partial y_i}\right] + \dfrac{1}{2C_i(x_i)} & \text{for } j = i,\ \xi_{jn} > x_{im} \\ -\dfrac{1}{2\pi}\dfrac{\partial G^{(\gamma)}}{\partial y_i} & \text{for } j \neq i \end{cases} \qquad (2.41)$$

$${}_{ij}B_{mn}^{(k)} = \begin{cases} -\dfrac{1}{2\pi}\left[\dfrac{1}{x_{im}-\tilde{\xi}_{jn}} + \dfrac{\partial H^{(\gamma)}}{\partial y_i}\right] & \text{for } j = i \end{cases}$$

$$-\frac{1}{2\pi}\frac{\partial G^{(\gamma)}}{\partial y_i} \qquad \text{for } j \neq i$$

(2.42)

$$g_{im}^{(k)} = \frac{1}{2\pi}\sum_{n=1}^{M_i} -\frac{U_i S_i'(\hat{\xi}_{in})}{2H}\frac{\partial H^{(\sigma)}}{\partial y_i} + \frac{1}{2\pi}\sum_{\substack{j=1 \\ j\neq i}}^{N}\sum_{n=1}^{M_j} -\frac{U_j S_j'(\hat{\xi}_{jn})}{2H}\frac{\partial G^{(\sigma)}}{\partial y_i} \tag{2.43}$$

Here, x_{im} is the control points located at the m^{th} segment of the i^{th} body while ξ_{jn} and $\tilde{\xi}_{jn}$ are the vortex points on the n^{th} segment of the j^{th} body and on the n^{th} segment of its wake respectively. The source points – the location of the discrete sources – are denoted by $\hat{\xi}_{jn}$. The normal velocities $\frac{\partial G^{(\gamma,\sigma)}}{\partial y_i}$ and $\frac{\partial H^{(\gamma,\sigma)}}{\partial y_i}$ are evaluated at the body axes, $y_i = 0^{\pm}$. However, the Green functions are usually expressed in the fixed Oxy coordinate system. Thus, even though it is convenient to use the moving $O_i x_i y_i$ coordinate system to indicate the location of the vortex, source and control points relative to the bodies, the coordinates of these points have to be transformed to the Oxy system before the Green functions can be used. Since this coordinate transformation is time-dependent, the Green functions are thus time-dependent also.

The term ${}_{ij}A_{mn}^{(k)}$ can be interpreted as the normal velocity evaluated at the m^{th} control point of the i^{th} body due to the vortex at the n^{th} vortex point of the j^{th} body, for the k^{th} time-step. A similar interpretation can be given for ${}_{ij}B_{mn}^{(k)}$ except that the vortex point is now located in the wake of the j^{th} body. $g_{im}^{(k)}$ is the total normal velocity evaluated at the m^{th} control point of the i^{th} body, due to the presence of all the sources in the field. The source strength, in eqn (2.43) has been substituted by eqn (2.27). Once the body speeds, $U_i(t)$, and the sectional area distributions, $S_i(x_i)$, are prescribed, $g_{im}^{(k)}$ becomes a known quantity for every time-step. The unknowns at each time-step are the body vorticities, $\gamma_{in}^{(k)}$ for $n = 1,2\ldots M_i$ and $i = 1,2\ldots N$. The other unknowns are the vorticities of the wake elements shed at the k^{th} time-step i.e. $\tilde{\gamma}_{ik}^{(k)}$. The vorticities of the other wake elements are known because they have been evaluated at the previous time-steps and are independent of time:

$$\tilde{\gamma}_{in}^{(k)} = \tilde{\gamma}_{in}^{(k-1)} \qquad \text{for } n = 1,2\ldots k\text{-}1$$

$$k = 2,3\ldots \qquad (2.44)$$

Therefore, the total number of unknown variables at each time-step is $\sum_{i=1}^{N}(M_i+1)$

According to eqn (2.40), satisfaction of the "boundary condition" on each body gives a set of M_i equations. For N bodies, eqn (2.40) gives a system of $\sum_{i=1}^{N} M_i$ equations. The additional equations can be obtained from Kelvin's theorem, eqn (2.32), which discretized form is as follows:

$$\sum_{n=1}^{M_i} \gamma_{in}^{(k)} + \sum_{n=1}^{k} \tilde{\gamma}_{in}^{(k)} = 0 \qquad i = 1,2\ldots N \qquad (2.45)$$

Thus, there is a system of $(N+M_1+M_2\ldots M_N)$ simultaneous equations which can be solved for the $(N+M_1+M_2\ldots M_N)$ unknowns. By transposing the terms which do not involve the unknown variables to the right-hand side of eqns (2.40) and (2.45) the following equivalent set of equations can be obtained:

$$\sum_{j=1}^{N}\left[\sum_{n=1}^{M_j} {}_{ij}A_{mn}^{(k)}\gamma_{in}^{(k)} + {}_{ij}B_{mk}^{(k)}\tilde{\gamma}_{ik}^{(k)}\right] = g_{im}^{(k)} - \sum_{j=1}^{N}\sum_{n=1}^{k-1} {}_{ij}B_{mn}^{(k)}\tilde{\gamma}_{in}^{(k-1)} \qquad m=1,2\ldots M_i \qquad (2.46)$$

$$\sum_{n=1}^{M_i} \gamma_{in}^{(k)} + \tilde{\gamma}_{in}^{(k)} = -\sum_{n=1}^{k-1} \tilde{\gamma}_{in}^{(k-1)} \qquad i=1,2\ldots N \qquad (2.47)$$

Since ${}_{ij}A_{mn}^{(k)}$, ${}_{ij}B_{mn}^{(k)}$ and $g_{im}^{(k)}$ are coefficients which are dependent on time, they have to be evaluated at each time-step. As k increases not only do all the coefficients have to be computed k times, but the number of the first two coefficients increases. This is due to the lengthening of the wake and the corresponding increase in the number of wake vortices present in the field. In order to avoid excessive computational time, the time-step is chosen such that the distance travelled by each body is equal to its element length:

$$U_i \Delta t = \Delta x_i \qquad i = 1,2\ldots N \qquad (2.48)$$

where Δt is the size of the time-step.
In terms of the number of elements[1)] of each body, M_i, and its body length, L_i, this condition can be rewritten as follows:

[1)] Convergence trials indicated that 40 elements ensured accurate results.

In terms of the number of elements of each body, M_i, and its body length, L_i, this condition can be rewritten as follows:

$$\Delta t = \frac{\Delta x_i}{U_i} = \frac{L_i / M_i}{U_i} = \text{constant} \qquad i = 1,2\ldots N \qquad (2.49)$$

The consequence of this choice is that the above coefficients at each instance is related to that of the previous time-step. These relations are of the following form:

$$_{ij}A_{mn}^{(k)} = {}_{ij}A_{m+1,n+1}^{(k-1)} \qquad m = 1,2\ldots M_i - 1, \quad n = 1,2\ldots M_j\text{-}1$$

$$_{ij}B_{mn}^{(k)} = {}_{ij}B_{m+1,n}^{(k-1)} \qquad m = 1,2\ldots M_i - 1, \quad n = 1,2\ldots k\text{-}1$$

$$_{ij}B_{mk}^{(k)} = {}_{ij}A_{m+1,1}^{(k-1)} \qquad m = 1,2\ldots M_i - 1 \qquad (2.50)$$

The term $g^{(k)}_{im}$ is related to its previous value accordingly. In other words, the coefficients that have to be evaluated at each time-step are only those related to the leading-edge element, i.e. $_{ij}A_{M_i,n}^{(k)}$ for $n = 1,2\ldots M_j$. $_{ij}A_{m,M_j}^{(k)}$ for $m = 1,2\ldots M_i$ and $_{ij}B_{M_i,n}^{(k)}$ for $n = 1,2\ldots k$.

The Kutta condition is not explicity imposed. However, if the location of the control points and vortex points are appropriately chosen, this condition is automatically satisfied. This choise is guided by two-dimensional airfoil theory where it was found that the correct choice for steady flow around a flat plate is "quarter chord" for the vortex point and "three-quarter chord" for the control point (James, 1972). Although this is an unsteady problem, which also includes bottom clearance effects, reliable results are obtained using this scheme.

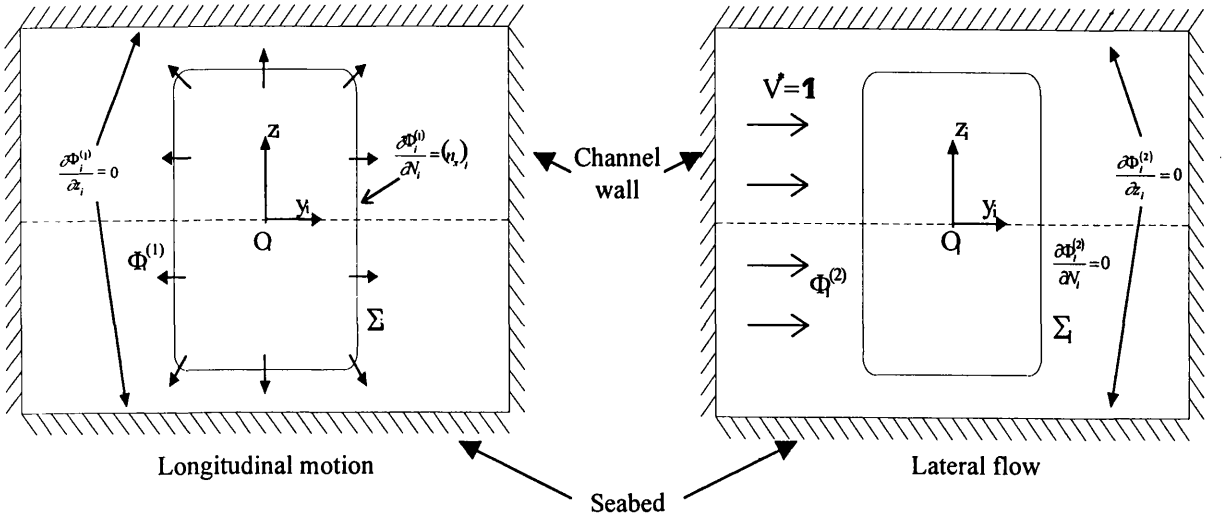

Fig a The inner problem (2D solution for ship and channel wall and its reflection about the water-surface in the transverse plane).

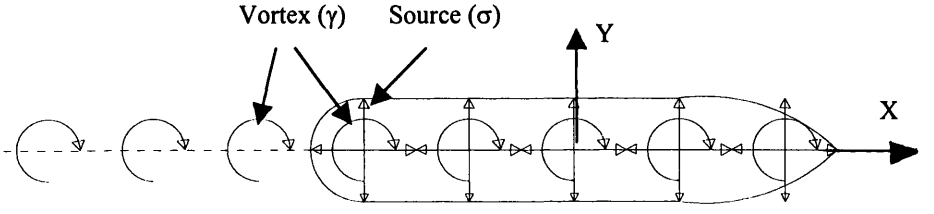

Fig b The outer problem (2D solution involving the source and vortex strengths in the horizontal plane).

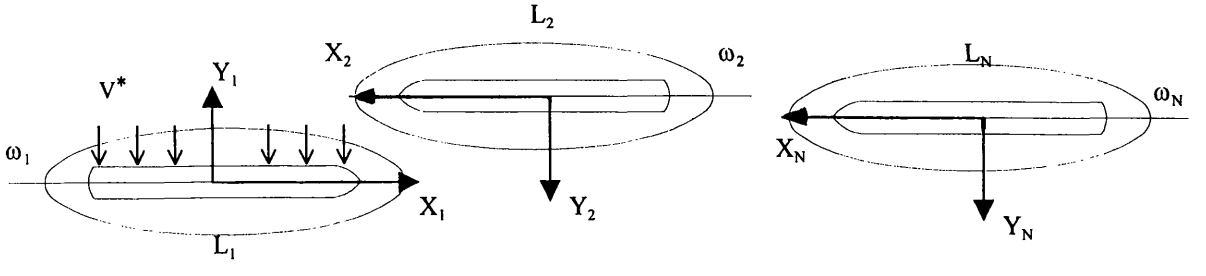

Fig c Matching the inner solution (in term of V^*) with outer solution (in term of σ and γ) at some distance from the hull.

Figs 2.1a,b,c Decomposition of the inner and outer problem.

CHAPTER 3

INTERACTION BETWEEN TWO SHIPS IN MEETING MANOEUVRE.

3.1 INTRODUCTION

This chapter describes an investigation into the hydrodynamic interaction between two ships meeting in a channel. Fig 3.1 gives the plan view of an encounter situation, and the sign convention for the force and moment are indicated in the figure. The stagger, ST_{12}, is defined as follows:

$$ST_{12} = (U_1 + U_2) \times t \qquad U_1, U_2 > 0$$

where the time scale is defined such that t = 0 corresponds to the midship-midship situation. The stagger, ST`{ $= 2.0 \times ST_{12}/(L_1 + L_2)$ }, is non-dimensionalized, such that the values –1, 0, and +1 correspond to the bow-bow, midship-midship, and stern-stern situations respectively, and it is used as the abscissa for the plots.

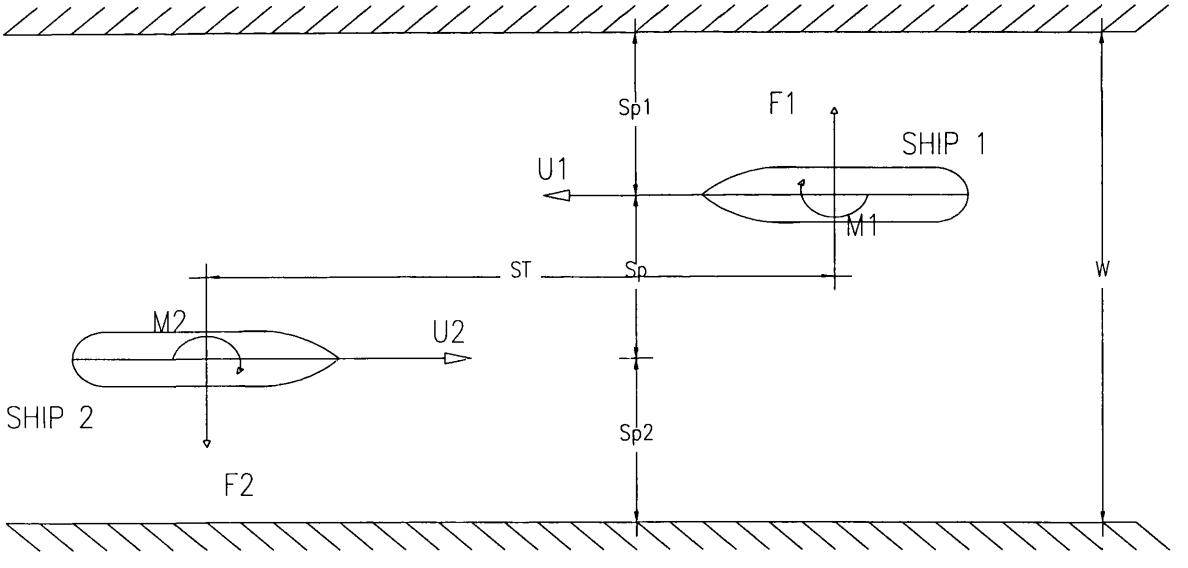

Fig 3.1 Co-ordinate system for two ships meeting.

The effect of several parameters (such as water depth, H, separation distance, Sp, ship speed, U and ship size, L) on the lateral forces and yaw moments has been investigated. From this database new empirical formulae have been derived for the maximum non-dimensional lateral forces and yaw moments that a ship experiences during an encounter situation.

In an encounter manoeuvre both ships experience equal but opposite lateral force and yaw moment during transit. Consequently, only the numerical results from Ship 1 (for characteristics see Table 3.1) are presented. The separation distances and water depths are non-dimensionalized by the length and draught respectively of Ship 1. However, when Ship 1 and Ship 2 are identical, the subscripts are omitted from these non-dimensionals.

Length (m)	155.0
Breadth (m)	26.0
Draught (m)	8.7
C_B	0.7

Table 3.1 Principal particulars for Ship 1.

3.2 VERIFICATION OF NUMERICAL METHOD

The usefulness of any theory depends to a large extent on agreement of its predictions with empirical data. This presentation of a theoretical method for solving unsteady ship interaction problems is not complete unless there are some comparisons between theoretical predictions and experimental results. Comparisons with both experimental and theoretical data from Yasukawa (1983) have been presented, and comparisons with various experimental results from Dand (1981b) have also been made.

3.2.1 Comparisons with Yasukawa's experimental results

Yasukawa (1983) presented experimental results for hydrodynamic interactions for two identical ships meeting in shallow water. The model tests were carried out on a 2.5m model (see Table 3.2). This model is a 1:62 model of Ship 1, which was used in the calculations using the present method. The various lateral forces and yaw moments during the transit were recorded for a set of separation distances. The speed of the ships was the same and the water depth-draught ratio was 1.3.

Length (m)	2.5
Breadth (m)	0.419
Draught (m)	0.140
C_B	0.7

Table 3.2 Principal particulars for Yasukawa's model[1)].

Figures. 3.2a,b show the non-dimensional lateral force and yaw moment obtained by the present method compared with experimental results. The magnitudes agree well, but a phase lag of the peak values for the lateral force and yaw moment coefficients can be seen. Dand (1981b) described problems involving a systematic feature of phase lag in his experimental results, but managed to solve this problem. This may explain why Yasukawa's experimental data have the same force and moment transit for the encountering manoeuvre as the present method but with a constant phase shift of the peak values. Besides, Yasukawa have not a phase lag in his computed data.

The ships initially experience a repulsive force and a bow-out moment, which reaches a maximum as the bows pass each other. The combined effect of this would cause the ships to veer away from each other (if the ships were allowed to do so). The repulsive force then decreases and becomes negligible at around the point where the bow of one is aligned with the midship of the other. The moment, however, changes rapidly from maximum bow-out to maximum bow-in during this part of the encounter. This would result in the bows turning back towards each other. As the midships becomes aligned, the lateral force reaches maximum attraction while the turning moment becomes negligible. The consequence would be a parallel attraction of the ships when they are in the midship-midship position. As they move out of this position, the attractive force decreases while the moment increases in the bow-out direction. At the stern-midship position, the lateral force becomes negligible while the bow-out moment reaches maximum. This third-quarter of the transit is the most dangerous since the combined attractive force and bow-out moment may cause the stern of one to hit the midship of the other. The last part of the transit is relatively safe, since the force increases in the

[1)] Dand does not provide full details of his ship geometry. Consequently the geometry used, while having the same principal design parameters, will be slightly different at section area from the model used in the experiments.

repulsive direction and the moment changes from maximum bow-out to maximum bow-in, i.e. the sterns turn away from each other.

3.2.2 Comparisons with Yasukawa's theoretical results

Yasukawa (1983) derived theoretical results for two ships in a meeting configuration with variations of the following parameters: separation distance, water depth, ship size and speed. These numerical calculations are compared to those obtained using the present method.

Variation of separation distance

Figures. 3.3a,b show the non-dimensional unsteady lateral forces and yaw moments obtained using the present method, and by using Yasukawa for a set of different separation distances. The depth-draught ratio was chosen to be 1.3, the two identical ships meet in a 2L wide channel at the same speed.

Figure 3.3a shows good agreement between the result produced using the present method and Yasukawa, and the calculated lateral force coefficients decrease as Sp/L increases for both theories. The maximum repulsion forces appear at approximately the bow-bow and stern-stern situation, while the ships have maximum attraction force when they are midship-midship. The differences in peak values for the lateral force coefficients are approximately 10% for various separation distances, whereas the present method is more conservative in all cases.

Figure 3.3b shows the variation of the yaw moment coefficients for different separation distances. A similar tendency was revealed by the results from both Yasukawa and the present method; the peak values decrease as the separation distances increase. These peak reductions can best be seen for the maximum bow-in and bow-out moment coefficients, immediately before and after the midship-midship situation respectively, where the peaks tend to flatten out as Sp/L increases. Both the present method and Yasukawa have this feature.

Variation of water depth

The preceding analysis shows that an increase in bottom clearance results in smaller hydrodynamic forces and moments, as can be seen in Figs 3.4a,b for Sp/L = 0.5. Yasukawa is found to have a similar tendency, but there are some differences in maximum values both for the lateral force and yaw moment coefficients.

The present method, when compared to Yasukawa, tends to give more conservative peak values for the maximum repulsion-attraction-repulsion force coefficients for different depth-draught ratios (Fig 3.4a). The amount by which these peak values decrease for increasing bottom clearance is similar to that in Yasukawa's results. The present method produces approximately 10% to15% larger maximum repulsion and attraction force coefficients than Yasukawa's computations.

Figure 3.4b shows a similar decreasing tendency for the yaw moment coefficients as H/D increases. The difference between the present method and Yasukawa for the maximum bow-out and bow-in moment coefficients at the bow-bow and stern-stern situations respectively, is 10% to 15%, the present method being larger. However, the yaw moment coefficients near the midship-midship situation have a different tendency as H/D varies. The present method produces constant maximum bow-in and bow-out moment coefficients, appearing immediately before and after the midship-midship situation respectively, for decreasing H/D. Yasukawa's results, on the other hand, show a small variation in these yaw moment coefficients.

Variation of ship size and ship speed

Comparisons have also been made for the ship size and speeds and they show good agreement with Yasukawa's results, both for the lateral force and yaw moment coefficients, which can be seen in the Appendix 3.

3.2.3 Comparisons with Dand's experimental results

Dand (1981b) presented some measurements of interaction induced by one ship model encountering another. Variations of interaction forces and moments with separation distances and depth-draught ratios were given. Two different ship models were used and their principal characteristics can be seen in Table 3.3 and 3.4. Model 1 was fully instrumented recording lateral forces and yaw moments, while Model 2 was allowed to move independently of the carriage and carrie no recording instrumentation; it simply provided the appropriate pressure system with which to induce interaction forces and moments on Model 1. The experiments were carried out in the enlarged shallow section of the NMI number 2 tank. The shallow section is 90m in length and 6.1m wide, or 1.54 times the length of Model 1.

Length (m)	3.962
Breadth (m)	0.506
Draught (m)	0.213
C_B	0.7

Table 3.3 Principal particulars for Dand's Model 1.

Length (m)	3.323
Breadth (m)	0.473
Draught (m)	0.167
C_B	0.76

Table 3.4 Principal particulars for Dand's Model 2[1)].

Dand's experimental results using Model 1 are compared with calculations carried out on Ship 1 using the present method (Table 3.1). The ratio of the length of Model 1 to the length of Model 2 is 1.19. Ship 2 is geometrically scaled based on this ratio, i.e. $L_1/L_2 = 1.19$. However, the models are not geometrically identical, so the breadth and draught ratios are not the same for the results obtained by experiment and by the

[1)] The details of the geometry were provided in confidence and cannot be disclosed.

present method. The separation distances and water depths are non-dimensionalized by the respective length and draught of Ship 1.

The speed ratio for the model tests is 0.59 where Model 1 is the slower ship. Consequently, the speed ratio for the present method is taken to be equal, i.e. $U_1/U_2 = 0.59$. Numerical calculations for the present method are carried out on Ship 1 in a $1.54L_1$ wide channel for the following situations:

- $Sp/L_1 = 0.2$ & $H/D_1 = 1.2$
- $Sp/L_1 = 0.467$ & $H/D_1 = 1.2$
- $Sp/L_1 = 0.2$ & $H/D_1 = 1.49$

Qualitatively, the calculation results obtained by the present method agree well with Dand's experimental results (Fig 3.5a,b to 3.7a,b). When travelling in the opposite direction, Ship 1 initially experiences a repulsive force and a bow-out moment. These reach maximum as the bows pass each other. The repulsive force then decreases to zero as the bow of Ship1 becomes aligned with the midship of Ship 2 while the moment changes from maximum bow-out to maximum bow-in. As the midships become aligned, the lateral force reaches maximum attraction while the yaw moment becomes zero. Furthermore, at the stern-midship position the attractive force is negligible while the moment turns to maximum bow-out. In the last part of the transit, the force increases in the repulsive direction and the moment shifts gradually from bow-out to maximum bow-in.

There is, however, not such a good agreement of the peak values for the lateral force and yaw moment coefficients between Dand's and the author's results. For $Sp/L_1 = 0.2$ & $H/D_1 = 1.2$, Fig 3.5a, show larger peak values for the repulsion-attraction-repulsion force coefficients obtained from Dand's model tests, and the difference is as large as 56% for the maximum attraction force coefficient. Similar larger peak values from the measurements can be seen in Fig 3.5b for the maximum bow-in and bow-out moment coefficients, where the disagreement can be as much as 88%.

For $Sp/L_1 = 0.467$ & $H/D_1 = 1.2$, the experimental data shows even larger peak values for the lateral force and yaw moment coefficients compared to those of the present method (Figs 3.6a,b).

However, better agreement is obtained for $Sp/L_1 = 0.2$ & $H/D_1 = 1.49$ (Figs 3.7a,b). The maximum lateral force coefficients have very similar values to those of the experimental results. The largest disagreement is only 12% in peak value, Dand's experimental results being more conservative. For the maximum yaw moment coefficients the differences are less also, having a difference at most 30%, the present method being less conservative.

The large disagreements for the $H/D_1 = 1.2$ cases may be explained by the squat effect. A vessel moving through shallow water experiences a hydrodynamic effect that increases the draught, and is influenced by the channel width and proximity of seabed. This effect is known as 'squat' (Wold (1997)). The models in Dand's experiments may have been influenced by this effect, causing them to run with smaller depth-draught ratios than measured when the models were stationary. In the parameter study in chapter 3.4.1, it is shown that the hydrodynamic forces and moments increase as the bottom clearance decreases. Since the present method does not take the squat effect into account, the change in draught when travelling in shallow water may be one explanation for the difference in maximum lateral force and yaw moment coefficients between the experimental results and those of the present method.

A more obvious source of error is that the models used in the experiments do not have the same geometrical shape as the ships used by the author.

3.3 PRESSURE AND VORTICITY DISTRIBUTION

Pressure and vorticity distribution acting on Ship 1 (Figs 3.8a,b) is derived for five different "time steps", encountering an identical ship with the same speed. The depth-draught ratio is chosen as 1.3 and the separation distance 0.5L.

It is can be seen from the graphs that, as the bows meet (position 1), Ship 1 experiences higher pressures around the forward part of the hull facing Ship 2. This results in a repulsive force and a bow-out moment. Then, at position 2, the pressure is distributed nearly evenly around the hull, resulting in zero lateral force on the ship. However, there is a small amount of reduced pressure at the aft sections, causing a small peak value for the yaw moment in the bow-in direction. When the midships become aligned (position 3), the pressure is reduced around the hull-side facing Ship 2, generating a large attractive lateral force. The yaw moment at this situation is insignificant. Furthermore, at position 4, the pressure distribution once more becomes evenly distributed, and consequently the lateral force is zero. The yaw moment is also negligible. As Ship 1 moves out of this position and the sterns becomes aligned (position 5), the stern part of the hull facing Ship 2 experiences an increase in pressure, and hence a repulsive force. This force causes a bow-in turning moment.

3.4 PARAMETRIC STUDY

In this section a parametric study into the interaction forces and moments acting on two ships undertaking encounter manoeuvers in a canal is conducted. The first three sets of results show the effects of separation distance, water depth and ship size on hydrodynamics during an encounter between two ships travelling at the same speed. The ship principal particulars can be seen in Table 3.1. The encounter by two ships of different speeds is then examined. The numerical calculations are carried out on Ship 1. The conditions are given in tables.

The general trend of the force and moment variation is the same for the different encounter configurations considered here. The ships experience a repulsion-attraction-

repulsion transient during the encounter, with the first repulsive peak occurring immediately after the bows pass each other. The attractive maximum occurs when the midships are aligned with each other. In the last part of the transient the ship experiences another repulsion that reaches its maximum immediately before the stern-stern situation.

In the initial stage of the meeting situation, the ships experience a bow-out turning moment, which reaches a maximum at the bow-bow situation. The moment then changes direction and a bow-in peak value appears when the bow of one is aligned with the midship of the other. Furthermore, the moment changes direction towards a bow-out maximum immediately after the midships have been side by side. These two latter peaks flatten out when the lateral separation distance between the ships is large. Finally, the ships experience a maximum bow-in moment immediately before the stern-stern situation.

Plots are made for the maximum lateral force and yaw moment coefficients to describe the behaviour of these peak values. 'Bow-Bow', 'Midship-Midship' and 'Stern-Stern' legend respectively in the graphs, denotes the maximum repulsion-attraction-repulsion peaks. Similar 'Bow-Bow' and 'Stern-Stern' legend signifies the maximum bow-out and bow-in moment coefficients occurring at the beginning and end of the encountering manoeuvre. The peaks appearing immediately before and after the midship-midship situation are represented by 'Fore-Fore' and 'Aft-Aft' respectively.

3.4.1 The effect of water depth

Figures 3.9a,b show how variation of the bottom clearance influences the lateral force and yaw moment coefficients for the following condition:

W	H/D	Sp/L	L_1/L_2	U_2/U_1
2L	Varying	0.5	1.0	1.0

Table 3.5 Condition for the effect of water depth, (two ships meeting).

It is apparent that as the depth-draught ratio decreases, the hydrodynamic forces and moments increase, as anticipated.

The maximum repulsion-attraction-repulsion force coefficients for different water depths can be seen in Fig 3.10a. The curves highlight the fact that the force coefficients tend to increase more rapidly as the depth-draft ratio becomes smaller. This tendency is similar for other separation distances. The maximum repulsion force coefficients at the bow-bow situation are approximately 55% smaller in magnitude compared to the maximum attraction force coefficients. However, the maximum repulsion force coefficients at the end of the transit are around 70% smaller in magnitude than the maximum attraction force coefficients.

The maximum yaw moment coefficients are shown in Fig 3.10b. Similar rapid increases in peak values as the water depth decreases can be seen for the maximum bow-out moment at the bow-bow situation and for the maximum bow-in moment at the stern-stern situation, where the latter's peak magnitudes are between 25% to 35% smaller than the bow-out maximums. However, there are no significant peak values just prior to and after the midship-midship situation for different depth-draft ratios. For smaller separation distances, however, this is not the case, and for Sp/L = 0.2 these peak values are quite notable. This is discussed further in chapter 3.4.2.

3.4.2 The effect of separation distance

Figures 3.11a,b show the effect of lateral separation distance on the lateral force and yaw moment coefficients acting on Ship 1 for the following condition:

W	H/D	Sp/L	L_1/L_2	U_2/U_1
2L	1.3	Varying	1.0	1.0

Table 3.6 Condition for the effect of separation distance, (two ships meeting).

From the figures it is clearly noticeable that as the Sp/L increases, the hydrodynamic forces and moments decrease.

The curves for the maximum repulsion and attraction forces are shown in Fig 3.12a. The peak values increase more rapidly as Sp/L reduces, a trend shared by the water depth variation. The maximum repulsion force coefficients at the bow-bow situation are found to have approximately 50% to 55% less peak magnitude than the maximum attraction force coefficients. Furthermore, the repulsive peaks at the stern-stern situation are around 60% to 70% smaller than the attractive peaks.

Figure 3.12b shows the peak values for the yaw moment coefficients. Similar to the peak value variation for decreasing bottom clearance, here too the maximum bow-out and bow-in moments at the beginning and end of the transit respectively increase rapidly as Sp/L decreases. The maximum bow-in moment coefficients are approximately 25% smaller than the maximum bow-out coefficients. However, contrary to the water depth variation, the ships experience a significant bow-in and bow-out moment immediately before and after the ships are side by side for small separation distances. These peak values also increase sharply as Sp/L decreases.

3D plots are made to illustrate the way in which the maximum repulsion-attraction-repulsion force coefficients tend to increase as H/D and Sp/L decrease (Figs 3.13a,b).

3.4.3 The effect of ship size

So far we have only considered encounters between identical ships. Figs 3.14a,b show the size effect on the interaction force and moment coefficients. The calculations are carried out on Ship 1 and its size is kept constant. Ship 2, on the other hand, is scaled accordingly, maintaining its geometrical shape.

W	H/D_1	Sp/L_1	L_1/L_2	U_2/U_1
$2L_1$	1.5	0.5	Varying	1.0

Table 3.7 Condition for the effect of ship size, (two ships meeting).

It is apparent from Figs 3.14a,b that when Ship 1 is smaller than Ship 2, its lateral forces and yaw moments are larger and, accordingly, when Ship 1 is larger, its hydrodynamic forces and moments are smaller.

Ship 1 experiences the same repulsion-attraction-repulsion trend for the forces as described earlier, and the maximum peak values can be seen in Fig 3.15a for various L_1/L_2 ratios. The graphs show that the lateral force coefficients increase more sharply as the L_1/L_2 ratio decreases. When Ship 1 is 20 % smaller than Ship 2, it experiences 70% larger lateral force peaks than in the case of two identical ships meeting. On the other hand, if Ship 1 is 1.2 times larger than Ship 2, the result is 37% smaller lateral force peaks for Ship 1, as compared to the L_1/L_2=1.0 case.

Figure 3.15b illustrates the behavior of the peak values for the interaction moments as the L_1/L_2 ratio varies. Since the separation distance is chosen as $0.5L_1$, the bow-in and bow-out moments around the midship-midship situation are not significant. However, the bow-out and bow-in moments experienced by Ship 1 at the beginning and end of the transit respectively are not negligible, and increase as the size of Ship 2 increases. The tendencies for the peak values are the same as for the lateral force coefficients; Ship 1, when 20% smaller than Ship 2, experiences 70% larger yaw moment peaks, compared to the case of two identical ships meeting. Ship 1 also has a 37% reduction

in hydrodynamic moment peaks when encountering a ship 1.2 times its size, compared to the $L_1/L_2 = 1.0$ case.

Figures 3.16a,b illustrate the difference in the interaction force and moment between Ship 1 and 2 when Ship 2 is half the size of Ship 1. The depth-draught ratio is 1.3 for Ship 1 and 2.6 for Ship 2. It can be seen from the graphs that the lateral force and yaw moment coefficients are larger for the smaller Ship 2. At certain instances, the force coefficient peaks can be 170% larger and the moment coefficient peaks can be 300% larger. However, it should be noted that due to the non-dimensionalization this does not mean that the actual force and moment magnitude is larger for the smaller ship. It can only be taken to mean that the smaller ship is affected by the interaction to a larger extent in the sense that it experiences a greater sway and yaw acceleration.

3.4.4 The effect of ship speed

In the previous calculations, the two ships in meeting conditions have been travelling at the same speed. Figures 3.17a,b show the effect of a change in relative speed on the hydrodynamic forces and moments acting on Ship 1 for the following situation:

W	H/D	Sp/L	L_1/L_2	U_2/U_1
$2L_1$	1.3	0.5	1.0	Varying

Table 3.8 Condition for the effect of ship size, (two ships meeting).

When $U_2/U_1 < 1.0$, Ship 1 is travelling faster than the ship it encounters and when $U_2/U_1 > 1.0$ it is the slower ship. It is apparent from Figs 3.17a,b that the slower of the two ships in the encounter manoeuver experiences a greater lateral force and yaw moment during the transit.

The peak values for the repulsion-attraction-repulsion lateral force coefficients are shown in Fig 3.18a. When the speed of Ship 2 is gradually increased as compared to the speed of Ship 1, it is evident from the graphs that the lateral force coefficients

acting on Ship 1 increase linearly. When Ship 1 travels at half the speed of Ship 2, the lateral force peaks on Ship 1 are between 40% to 60% higher than when the speeds of the ships are equal. However, if the velocity of Ship 1 is twice that of Ship 2, it has only a 20% to30% reduction of peak values, compared to when $U_2/U_1 = 1.0$.

The peak value variations for the yaw moment coefficients have a tendency different to that described above, as seen in Fig 3.18b. The maximum bow-out moments near the bow-bow instance and the maximum bow-in moment at the end of the transit do not change significantly as the relative speed varies. The extensive differences are in the maximum bow-in moments immediately before the midships are aligned, and the maximum bow-out moments immediately after the midship-midship situation. These peak values again increase linearly but more steeply than the peak values for the lateral force coefficients, as the speed ratio increases above $U_2/U_1 = 1.0$. At the point at which both ships are travelling at the same speed, there is a discontinuity in the curve, and the reduction in maximum bow-in and bow-out moment coefficients, as Ship 1 is the faster ship, becomes less steep, i.e. for $U_2/U_1 < 1.0$.

When Ship 1 has half the speed of Ship 2, there is a 158% increase in maximum bow-in value on Ship 1, as compared to when $U_2/U_1 = 1.0$. However, the reduction of the same maximum bow-in moment coefficient when Ship 1 has twice the velocity of Ship 2 is 42%.

A similar tendency can be seen for the peak values immediately after the midship-midship situation for increasing U_2/U_1. However, it should be noted that for approximately $U_2/U_1 < 0.75$, Ship 1 does not experience a change from bow-in to bow-out turning moment. Instead, it experiences a bow-in moment from just before the ships are side by side and trough-out the transit. Also, here there are large differences in peak values. Ship 1 has a 700% larger maximum bow-out moment coefficient when $U_2/U_1 = 2.0$ compared to when $U_2/U_1 = 1.0$. However, when Ship 1 has twice the speed of Ship 2, it experiences a bow-in moment rather than a maximum bow-out moment, as compared to the case in which the ships have the same velocity. The magnitude of this bow-in moment is comparable to the maximum bow-out moment for $U_2/U_1 = 1.0$.

3.5 NEW EMPIRICAL FORMULAE FOR MAXIMUM CF & CM

In section 3.4, the effect of water depth, separation distance, ship size and ship speed on the hydrodynamic forces and moments are investigated. Here, a set of new empirical formulae is derived for the maximum lateral force and yaw moment coefficients. In order to achieve this, a more thorough examination of the different parameters has been carried out. Firstly, empirical formulae are obtained for a variance in water depth and separation distances for two identical ships meeting at the same speed in a 2L wide channel. Then, the effect of ship size and speed is taken into account. The empirical formulae are based on the calculations carried out on Ship 1, and should only be used within the ranges of data covered by the investigation[1)].

3.5.1 Separation distance and water depth variation

The effect of the water depth on the lateral force and yaw moment in chapter 3.4.1 is only described for one particular separation distance (Sp/L = 0.5). Since more numerical results are needed to derive more accurate empirical formulae for the maximum lateral force and yaw moment coefficients, calculations are carried out for Sp/L = 0.2, 0.25, 0.3, 0.4, 0.5 and 0.7, all for H/D = 1.2, 1.3, 1.5, 1.8 and 2.0.

Maximum lateral force coefficients.

The maximum forces at the bow-bow, midship-midship and stern-stern situation, for a given Sp/L, are found not to increase at the same rate for decreasing H/D. As a result, the new empirical formulae are based on the variations of each of the maximum repulsion-attraction-repulsion force coefficients separately.

The maximum repulsion force coefficients at the bow-bow situation indicate that as the bottom clearance decreases, the peak values increase in the following manner for a given Sp/L:

$$CF_{Bow-Bow} = A\left[1 - 0.85\left(D/H\right)\right]^{-0.9}\left(H/D\right)^{-0.9} \qquad (3.1)$$

[1)] In order to fit the peaks of the distribution, the empirical formulae were found by systematically adjustment of coefficient and power.

where A is a coefficient, and is different for various Sp/L. Investigation into this constant shows that it can be expressed empirically, based on the non-dimensionalized separation distance between the ships, as follows:

$$A = 1.2\left(1 + {}^{Sp}/_{L}\right)^{-5.5} \tag{3.2}$$

The maximum repulsion force coefficient at the bow-bow-situation can now be expressed for different separation distances and water depths by the following empirical formulae:

$$CF_{Bow-Bow} = 1.2\left(1 + {}^{Sp}/_{L}\right)^{-5.5}\left[1 - 0.85\left({}^{D}/_{H}\right)\right]^{-0.9}\left({}^{H}/_{D}\right)^{-0.9} \tag{3.3}$$

Similar empirical formulae are derived for the maximum attraction force coefficient at the midship-midship situation, and the maximum repulsion force coefficient at the stern-stern situation. They have the following form:

$$CF_{Midship-Midship} = -2.0\left(1 + {}^{Sp}/_{L}\right)^{-4.8}\left[1 - 0.85\left({}^{D}/_{H}\right)\right]^{-0.96}\left({}^{H}/_{D}\right)^{-0.96} \tag{3.4}$$

$$CF_{Stern-Stern} = 1.01\left(1 + {}^{Sp}/_{L}\right)^{-6.0}\left[1 - 0.85\left({}^{D}/_{H}\right)\right]^{-0.94}\left({}^{H}/_{D}\right)^{-0.94} \tag{3.5}$$

Maximum yaw moment coefficients

Empirical formulae have also been derived for the maximum yaw moment coefficients for a variety of water depth and separation distances. During the bow-bow condition, Ship 1 experiences a peak value for the moment in the bow-out direction. As the separation distance and the bottom clearance reduce, these peak values increase in a way similar to the maximum lateral force coefficients. The empirical formulae for maximum bow-out coefficients can then be expressed as follows:

$$CM_{Bow-Bow} = A\left[1 - 0.85\left({}^{D}/_{H}\right)\right]^{-0.75}\left({}^{H}/_{D}\right)^{-0.75} \tag{3.6}$$

where A is a coefficient, and is different for various separation distances. This constant is also dependent on Sp/L, in the following manner:

$$A = 0.305\left(1 + {}^{Sp}/_{L}\right)^{-5.0} \tag{3.7}$$

The empirical formulae for the maximum bow-out moment coefficient at the bow-bow-situation can now be expressed for different separation distances and water depths as follows:

$$CM_{Bow-Bow} = 0.305\left(1 + {}^{Sp}/_{L}\right)^{-5.0}\left[1 - 0.85\left({}^{D}/_{H}\right)\right]^{-0.75}\left({}^{H}/_{D}\right)^{-0.75} \tag{3.8}$$

The behavior of the yaw moments around the midship-midship situation is somewhat different. As described in section 3.4.2, concerning the separation distance effect, the yaw moments for large separation distances are insignificant in this part of the transit. However, when the ships pass each other closely, these bow-in and bow-out moments can not be ignored, and the investigation of the water depth effect in chapter 3.4.1 shows that these peak values do not change at the same rate as the first bow-out moment coefficients.

The empirical formula for the maximum bow-in moment coefficients, just before the midships are aligned, is as follows:

$$CM_{Fore-Fore} = -0.81\left(1 + {}^{Sp}/_{L}\right)^{-8.0}\left({}^{H}/_{D}\right)^{-1.0} \tag{3.9}$$

Similarly, the maximum bow-out moment coefficient, immediately after the midship-midship situation, can be obtained by using the following empirical formulae:

$$CM_{Aft-Aft} = 0.95\left(1 + {}^{Sp}/_{L}\right)^{-10.0}\left({}^{H}/_{D}\right)^{-1.2} \tag{3.10}$$

At the end of the encounter, the ships experience a maximum bow-out moment at the stern-stern situation. These peak values for Ship 1 vary in a similar way for different

separation distances and water depths, as the maximum bow-out moment coefficients at the bow-bow situation. Based on this, the following empirical formula is obtained:

$$CM_{Stern-Stern} = -0.21\left(1+{}^{Sp}/_{L}\right)^{-5.0}\left[1-0.85\left({}^{D}/_{H}\right)\right]^{-0.9}\left({}^{H}/_{D}\right)^{-0.9} \quad (3.11)$$

3.5.2 Ship size variation

So far, the new empirical formulae have not taken the variation of ship size into account. As described in section 3.4.3, the smaller ship in the encounter experiences larger lateral forces and yaw moments. In order to incorporate this size effect into the new empirical formulae for the maximum lateral force and yaw moment coefficients, the various L_1/L_2 ratios are investigated for a wider range of water depths and separation distances. Numerical calculations are carried out on Ship 1, whose size is kept constant, while Ship 2 is scaled geometrically. The various L_1/L_2 cases are investigated for different separation distances and water depths that are non-dimensionalized by the length and draught respectively of Ship 1.

Maximum lateral force coefficients

It is evident from the results that the maximum lateral force coefficients for different L_1/L_2 cases show the same increasing trend for decreasing Sp/L_1 when $H/D_1 = 2.0$. This is also true for both $H/D_1 = 1.5$ and $H/D_1 = 1.3$ (See Appendix 3). The water depth in the two latter depth-draught ratios limits the possible size of Ship 2, i.e. range of L_1/L_2 ratios. It became clear that by adding a multiplication factor to the existing empirical formulae for the maximum lateral force coefficients, the different L_1/L_2 cases can be expressed by the $L_1/L_2 = 1.0$ case. This multiplication factor has the following form:

$$\left({}^{L_1}/_{L_2}\right)^{-2.19} \quad (3.12)$$

and is the same for all the maximum repulsion-attraction-repulsion force coefficients.

Maximum yaw moment coefficients

The maximum bow-out moment coefficients at the bow-bow situation have exactly the same tendency as described for the maximum force coefficients. Consequently, these peak values can be obtained by employing the same multiplication factor as described in eqn 3.12 for various L_1/L_2. This is also true for the maximum bow-in moment coefficients at the stern-stern situation.

However, the tendency of the maximum bow-in and bow-out moments immediately before and after the midship-midship situation is somewhat different. Here, there is no clear trend for the yaw moment coefficients when L_1/L_2 decreases. The L_1/L_2 = ratio of 1.0 gives larger peak values than other L_1/L_2 ratios when varying Sp/L (See the Appendix 3). However, the discrepancies are small and, as a result, using the new empirical formulae without correction for the ship size effect gives more conservative yaw moment coefficients.

3.5.3 Ship speed variation

This section examines how the relative speed between the ships is incorporated into the empirical formulae. Calculations are carried out for Ship 1 meeting Ship 2 at a lateral distance of 0.5L. The depth-draught ratio is chosen as 1.3, and L_1/L_2 = 1.0. This present method assumes that the maximum lateral force and yaw moment coefficients for U_2/U_1 variations are not affected by the separation distance, water depth and ship size. As in section 3.4.4, Ship 1 is the faster ship when $U_2/U_1 < 1.0$ and the slower ship when $U_2/U_1 > 1.0$.

Maximum lateral force coefficients

It is apparent from the previous analysis that the slower ship experiences larger lateral forces, and that the peak values increase linearly as the U_2/U_1 ratio increases. This trend is similar both for the maximum repulsion forces and the maximum attraction force. However, Ship 1 does not experience the same amount of increasing tendency for the different peak values. Based on the empirical formulae for the maximum

repulsion force coefficients when $U_2/U_1 = 1.0$, the ship speed effect can be expressed as a multiplication factor with the following linear formulae at the bow-bow situation:

$$M.CF_{Bow-Bow} = 1 + 0.434\left(\Delta U / U_1\right) \tag{3.13}$$

where $\Delta U = U_2 - U_1$

Similarly, the ship speed effect can be expressed in terms of a multiplication factor to the maximum attraction force coefficients at the midship-midship situation as follows:

$$M.CF_{Midship-Midship} = 1 + 0.492\left(\Delta U / U_1\right) \tag{3.14}$$

and finally for the stern-stern situation, the maximum repulsion force coefficients include the following addition to the $U_2/U_1 = 1.0$ case.

$$M.CF_{Stern-Stern} = 1 + 0.626\left(\Delta U / U_1\right) \tag{3.15}$$

Maximum yaw moment coefficients

For the maximum bow-in and bow-out moment coefficients, the tendency is slightly different for increasing U_2/U_1 ratios. The peak values are found not to change significantly for the maximum bow-out and bow-in moment coefficients, at the bow-bow and stern-stern situation respectively. As a result, there is no addition to the empirical formulae for the $U_2/U_1 = 1.0$ case for these maximum yaw moment coefficients.

In contrast, the maximum bow-in and bow-out moment coefficients immediately before and after the midship-midship situation do vary significantly. Since there is a discontinuity in the curve at $U_2/U_1 = 1.0$ for these conditions, there is a difference between the situations where Ship 1 is the faster and where it is the slower ship.

The additional multiplication factor to the $U_2/U_1 = 1.0$ case for maximum bow-in coefficients becomes, then, as follows:

$$M.CM_{Fore-Fore} = 1 + 1.585\left(\Delta U / U_1\right) \quad \text{when } U_2/U_1 > 1.0 \quad (3.16)$$

$$M.CM_{Fore-Fore} = 1 + 0.839\left(\Delta U / U_1\right) \quad \text{when } U_2/U_1 < 1.0 \quad (3.17)$$

Similarly, the maximum bow-out moment coefficients can be expressed empirically by adding the following factor:

$$M.CM_{Aft-Aft} = 1 + 7.059\left(\Delta U / U_1\right) \quad \text{when } U_2/U_1 > 1.0 \quad (3.18)$$

$$M.CM_{Aft-Aft} = 1 + 3.926\left(\Delta U / U_1\right) \quad \text{when } U_2/U_1 < 1.0 \quad (3.19)$$

3.5.4 Overall new empirical formulae

The empirical formulae for the different peaks can now be gathered into an overall new empirical formula for the maximum lateral force coefficient and overall new empirical formulae for the maximum yaw moment coefficient. The new formulae take into account the effect of separation distance, water depth, ship size and speed, and are as follows:

$$CF_i = Y_i^{ms}\left(1 + Sp/L_1\right)^{\alpha_i}\left[1 + Y_i^{md}\left(D_1/H\right)\right]^{\beta_i}\left(H/D_1\right)^{\beta_i}\left(L_1/L_2\right)^{\delta}\left[1 + Y_i^{mu}\left(\Delta U/U_1\right)\right] \qquad i = 1,2,3$$

where m denotes the meeting manoeuvre and
- i = 1 denotes the bow-bow situation
- i = 2 denotes the midship-midship situation
- i = 3 denotes the stern-stern situation

and $\Delta U = U_2 - U_1$

The different constants for maximum lateral force coefficients can be seen in the Table 3.9 below:

	Bow-Bow	Midship-Midship	Stern-Stern
Y^{ms}	1.20	-2.00	1.01
Y^{md}	-0.85	-0.85	-0.85
Y^{mu}	0.434	0.492	0.626
α	-5.50	-4.80	-6.00
β	-0.90	-0.96	-0.94
δ	-2.19	-2.19	-2.19

Table 3.9 Coefficients for the maximum lateral force coefficients acting on Ship 1, (two ships meeting).

For the maximum yaw moment coefficients the following new empirical formulae is derived:

$$CM_i = N_i^{ms}\left(1+{Sp}/{L_1}\right)^{\varepsilon_i}\left[1+N_i^{md}\left({D_1}/{H}\right)\right]^{\varphi_i}\left({H}/{D_1}\right)^{\varphi_i}\left({L_1}/{L_2}\right)^{\delta}\left[1+N_i^{mu}\left({\Delta U}/{U_1}\right)\right] \qquad i = 1,2,3,4$$

where m denotes the meeting situation and

i = 1 denotes the bow-bow situation
i = 2 denotes the immediately before midship-midship situation (Fore-Fore)
i = 3 denotes the immediately after midship-midship situation (Aft-Aft)
i = 4 denotes the stern-stern situation

and $\Delta U = U_2 - U_1$

Similarly, the constant for the maximum yaw moment coefficients are given in Table 3.10 below:

	Bow-Bow	Fore-Fore	Aft-Aft	Stern-Stern
N^{ms}	0.305	-0.81	0.95	-0.21
N^{md}	-0.85	0	0	-0.85
$(U_2/U_1>1.0)$ N^{mu}	0	1.585	7.059	0
$(U_2/U_1<1.0)$ N^{mu}	0	0.839	3.926	0
ε	-5.00	-8.00	-10.00	-5.00
φ	-0.75	-1.00	-1.20	-0.90
δ	-2.19	-2.19	-2.19	-2.19

Table 3.10 Coefficients for the maximum yaw moment coefficients acting on Ship 1, (two ships meeting).

3.6 PRACTICAL APPLICATION

When encountering a ship in a shallow channel, it is important for the master of the ship to know the potential hazards involving the interaction forces and moments. To identify in which conditions the rudder can not produce adequate moments to oppose the hydrodynamic yaw moments is especially important. A set of graphs is made based on the new empirical formulae to identify the regions where safe operations are satisfied.

Firstly, an estimation of the rudder area on Ship 1 is carried out. Usually, the area of the rudder is determined as an arbitrary proportion of the area given by multiplying the length of the ship (L) by the design draught (D), the proportion varying with the character, and to some extent with size of the ship. For merchant ships, the area of the rudder is usually about two percent of the product L times D (William H. Hunley 1969). Furthermore, this estimation of the rudder area is checked against a recently built ship with similar features as Ship 1 (The Motor Ship 1998), where the rudder area is found to be two percent of the product L times D.

Secondly, Clark's formula, based on the rudder area, is used for calculating the maximum yaw moment a rudder can produce (Appendix 2). It can now be identified in which conditions the rudder can withstand the hydrodynamic moments occurring in a meeting manoeuvre, and hence find the regions where safe operations occur.

Figures 3.19a,b,c,d identify which regions are below the point of rudder adequacy. If Ship 1 is encountering a ship in conditions below the curves, the rudder moment is lower than the maximum interaction moment. In most cases the maximum yaw moments occur in the bow-bow situation but shift to the aft-aft situation for small Sp/L and large U_2/U_1. As expected, the minimum separation distance for safe operations gets larger for various water depths as the size and speed of Ship 1 becomes smaller compared to those of Ship 2. However, since the separation distances are non-dimensionalized by the length of Ship 1, the condition where there are zero distance between the ship-sides are illustrated by the dotted line in the figures with the legend "Zero distance". Linear interpolation between the curves can be used

to find the minimum separation distances, which satisfies safe operations for different speed ratios than those in the figures.

It should be noted that even if Ship 1 is travelling in conditions, which are below the point of rudder adequacy, a collision does not necessarily take place. It only means that the rudder moment is smaller than the interaction moments and it becomes very difficult for Ship 1 to maintain a straight line of travel. An encounter manoeuvre where the ships are allowed to change paths has to be simulated to determine if a collision will take place. Such simulation is a natural extension to the work presented here but beyond the objectives in this thesis.

3.7 CONCLUDING REMARKS

- The comparison with experimental data shows good qualitatively agreement, but quantitatively the result are not so good. However there are many uncertainties such as the width of test tank, ship speed etc.

- The comparisons with Yasukawa (1983) theoretical predictions of the lateral force and yaw moment coefficients, shows good tendency and value agreement. Similar good agreement in tendency is found with Dand's (1981b) experimental data too. Again the peak values for the lateral force and yaw moment coefficients do not give such good similarity.

- The parametric study shows an increase in the interactive forces and moments as the separation distance and water depth decrease. It is also evident that a slower and smaller ship experiences larger lateral forces and yaw moments.

- New empirical formulae are derived based on the peak values from the non-dimensionalized force and moment curves, that describes the variation in forces and moments acting on Ship 1 during transit.

- Graphs are made which identifies the regions where safe and unsafe operations occur based on the maximum yaw moment formulae.

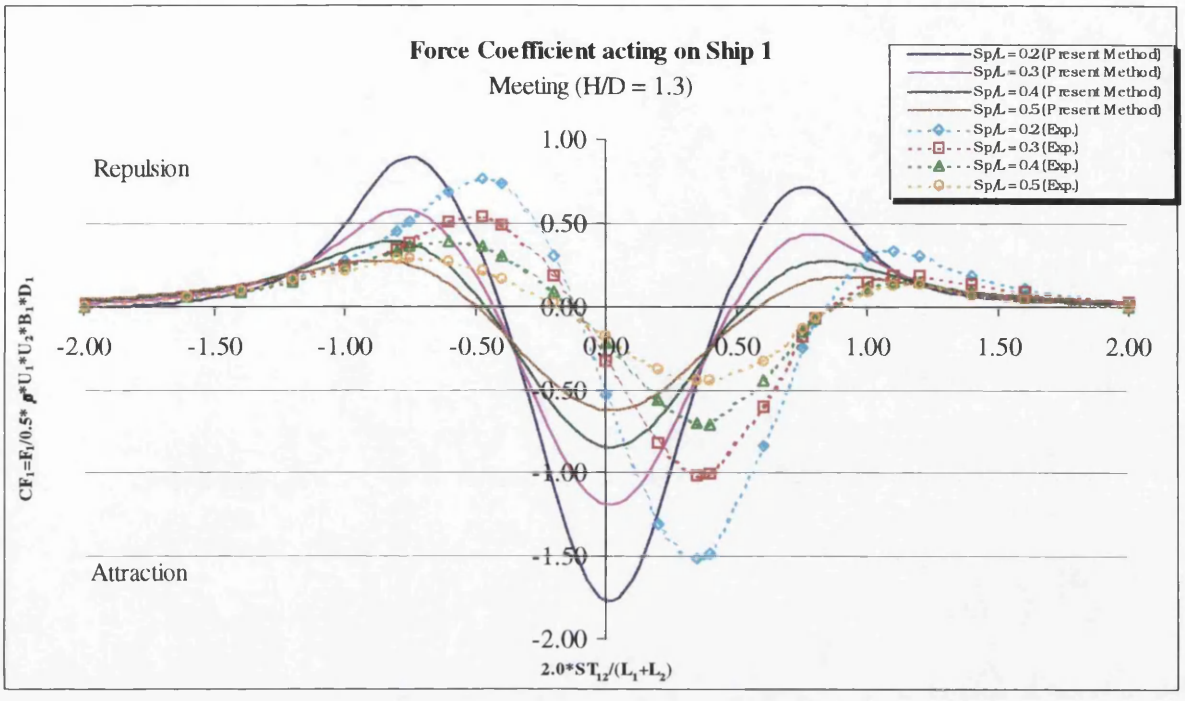

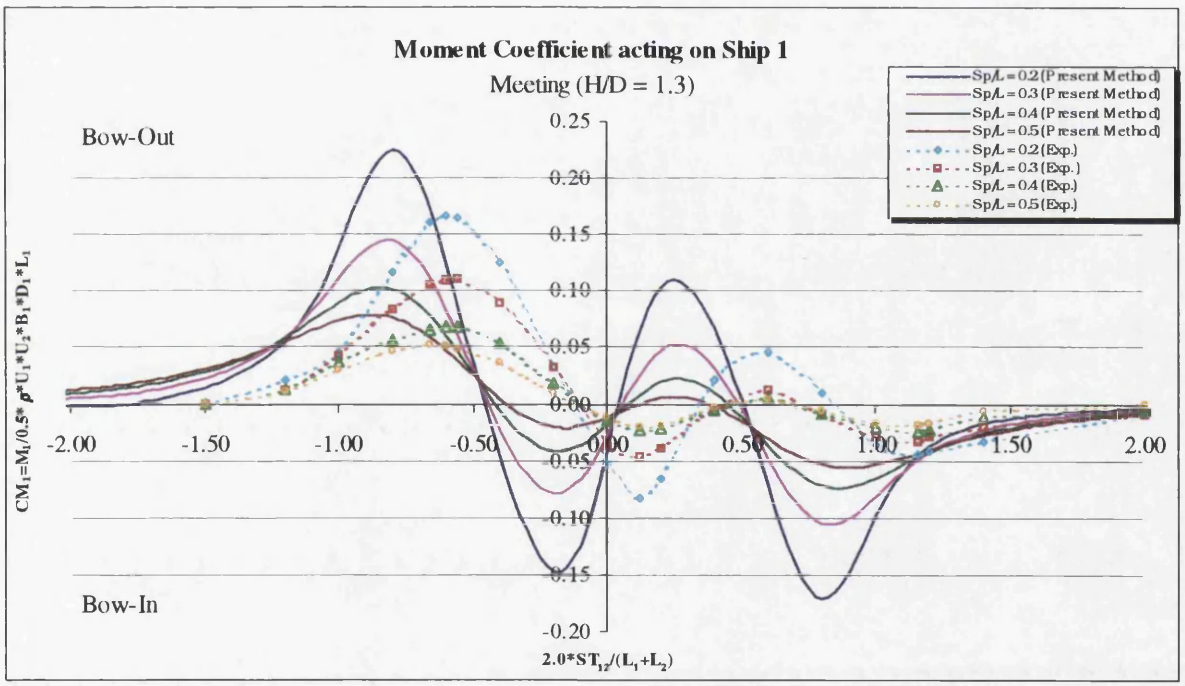

Figs 3.2a,b Comparison of the lateral force and yaw moment coefficients with Yasukawa's experimental data for various separation distances, (two ships meeting)

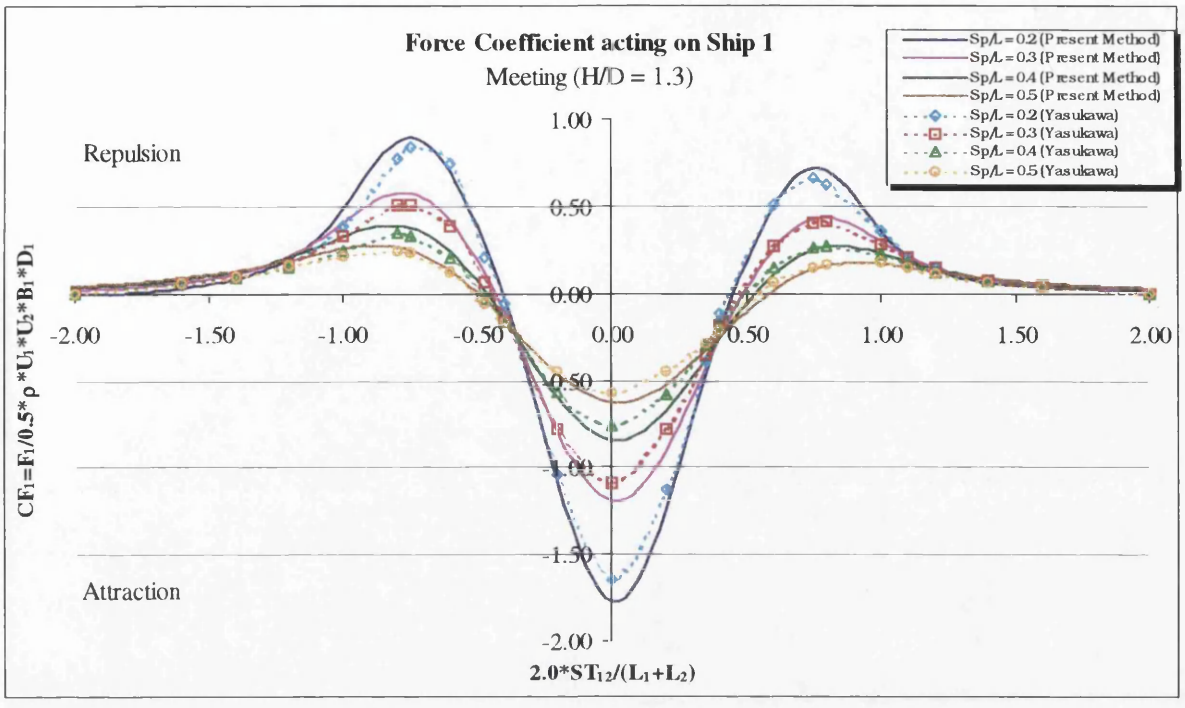

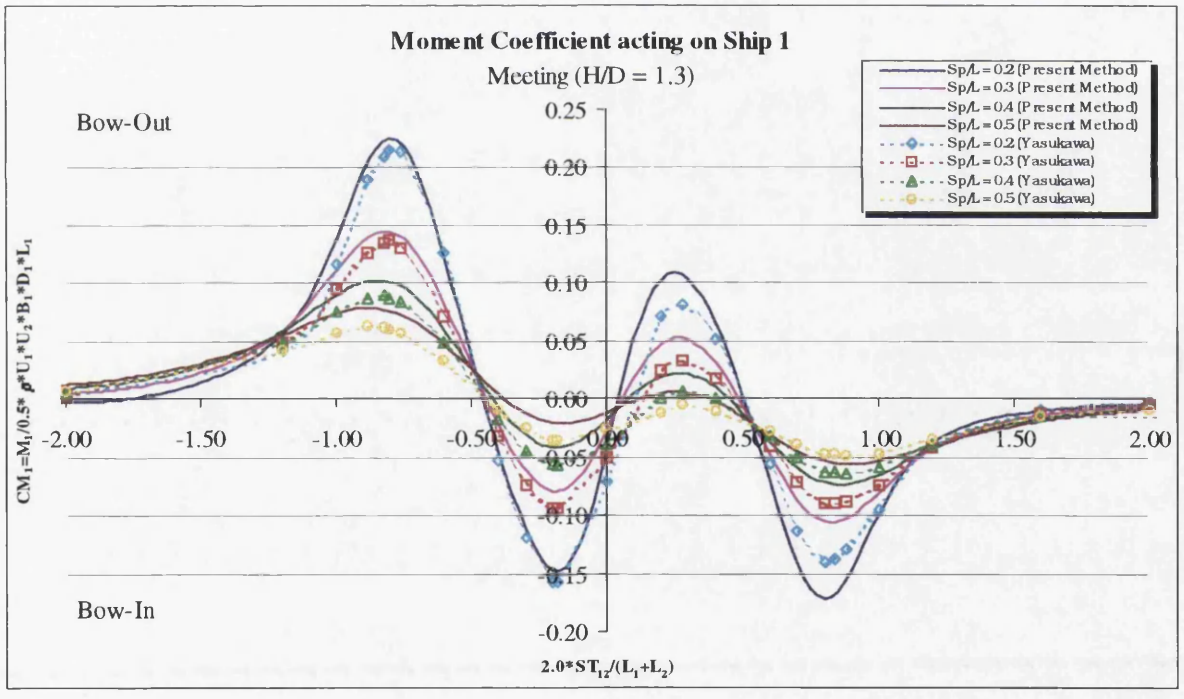

Figs 3.3a,b Comparison of the lateral force and yaw moment coefficients with Yasukawa's theoretical data for various separation distances, (two ships meeting)

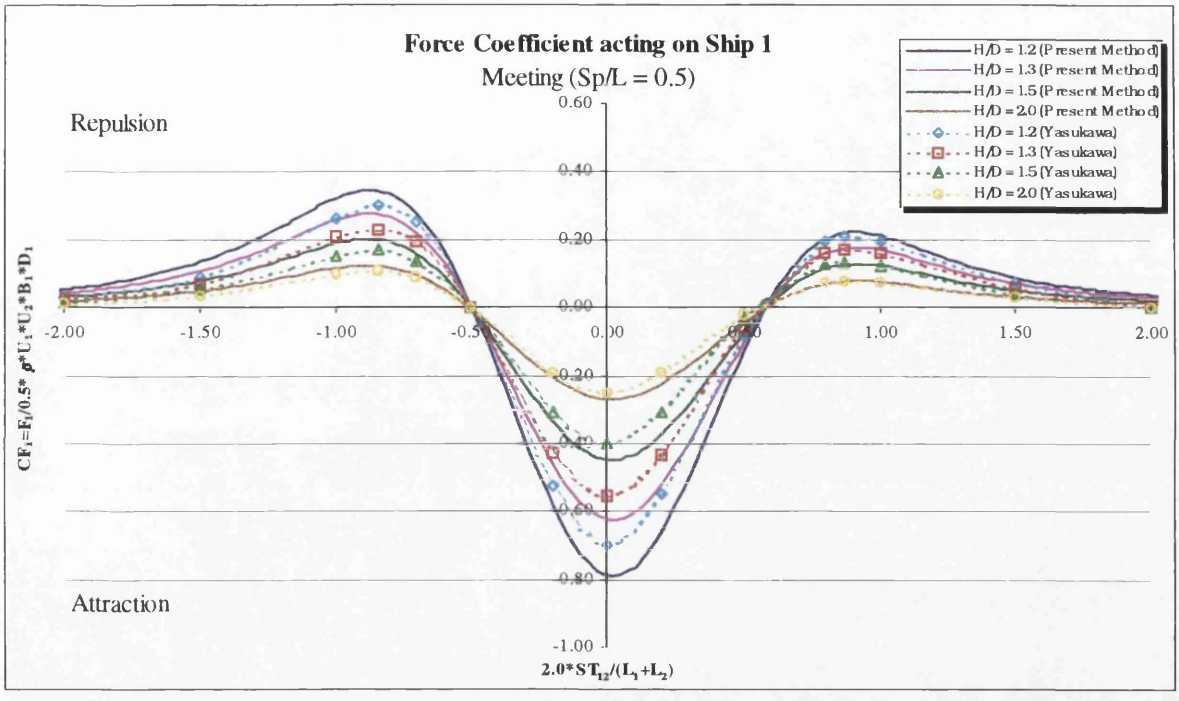

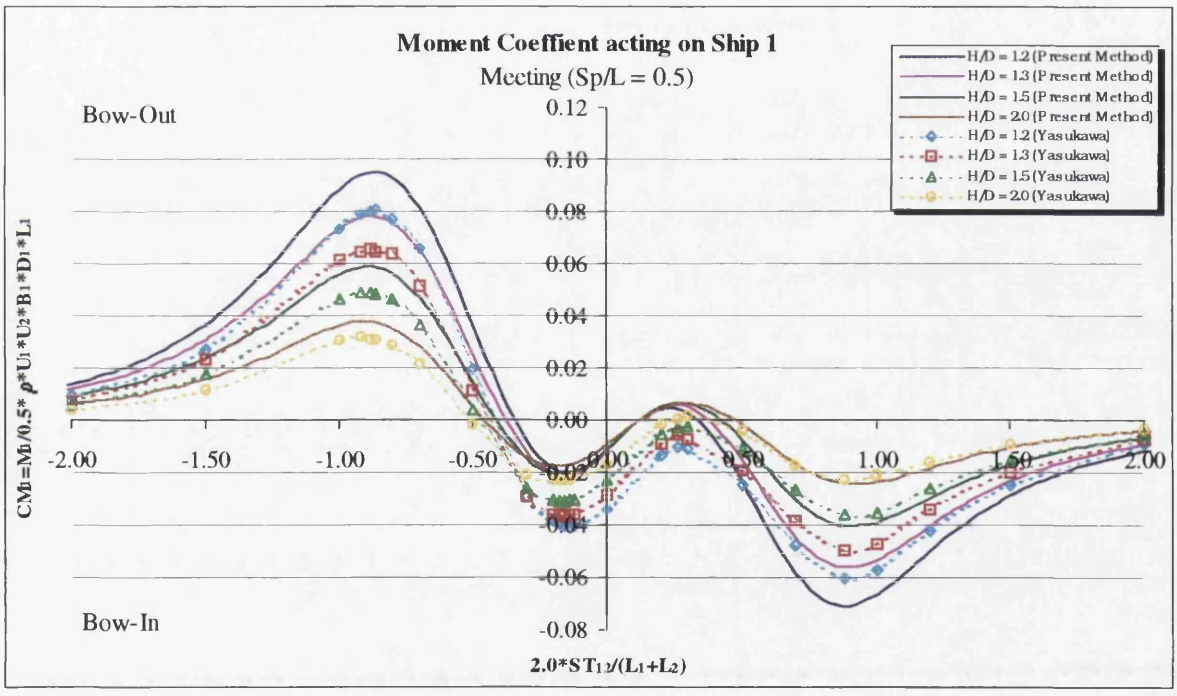

Figs 3.4a,b Comparison of the lateral force and yaw moment coefficients with Yasukawa's theoretical data for various water depths, (two ships meeting)

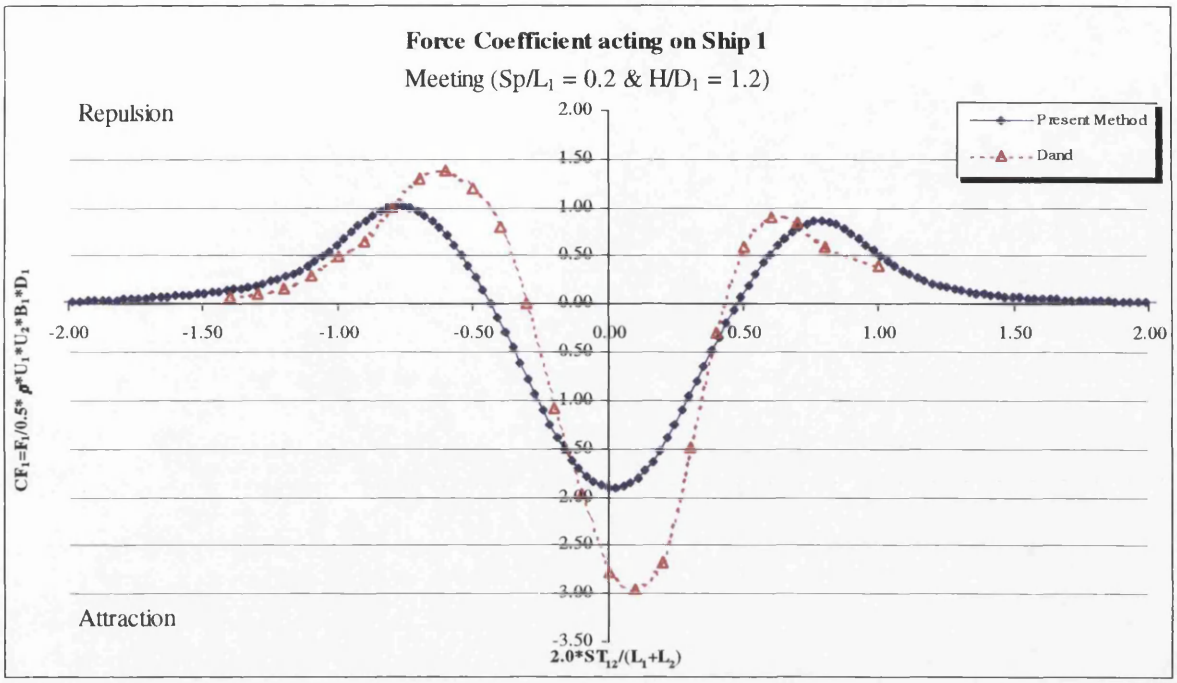

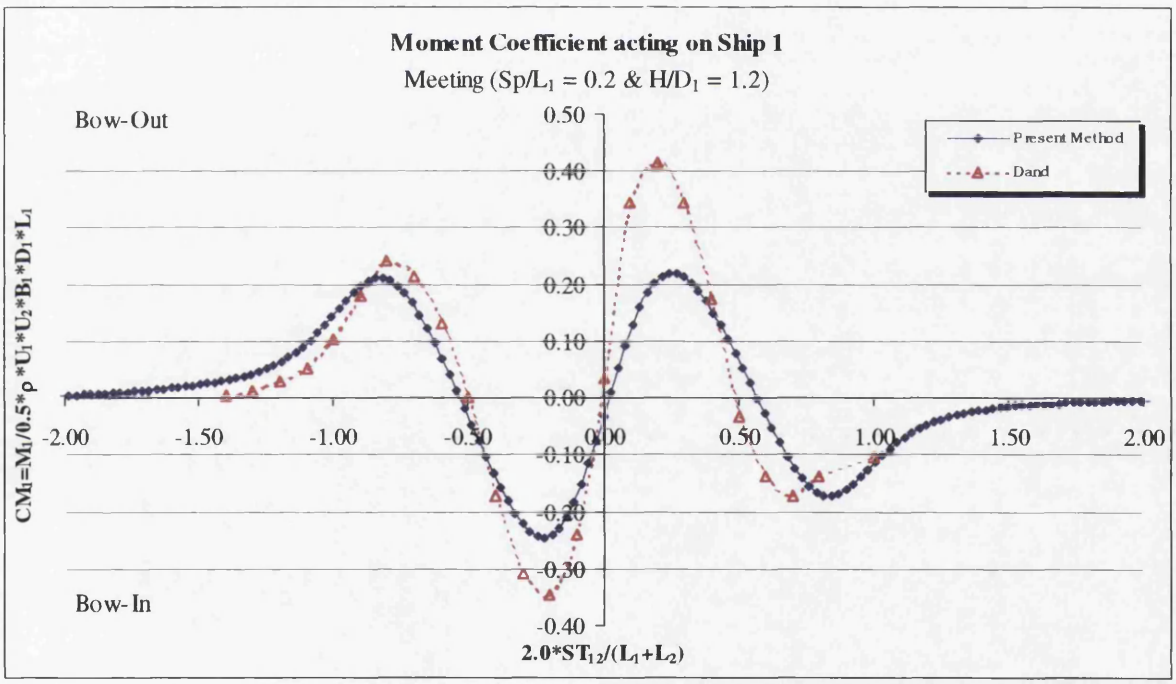

Figs 3.5a,b Comparison of the lateral force and yaw moment coefficients with Dand's experimental data. ($Sp/L_1 = 0.2$ and $H/D_1 = 1.2$, two ships meeting)

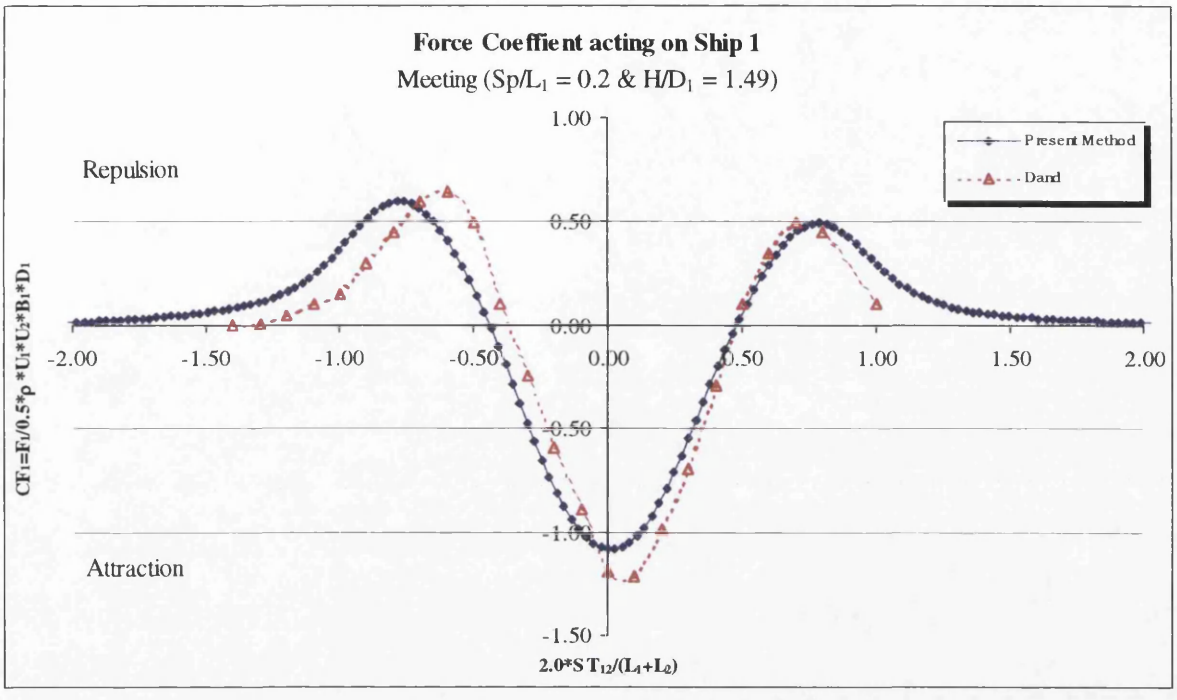

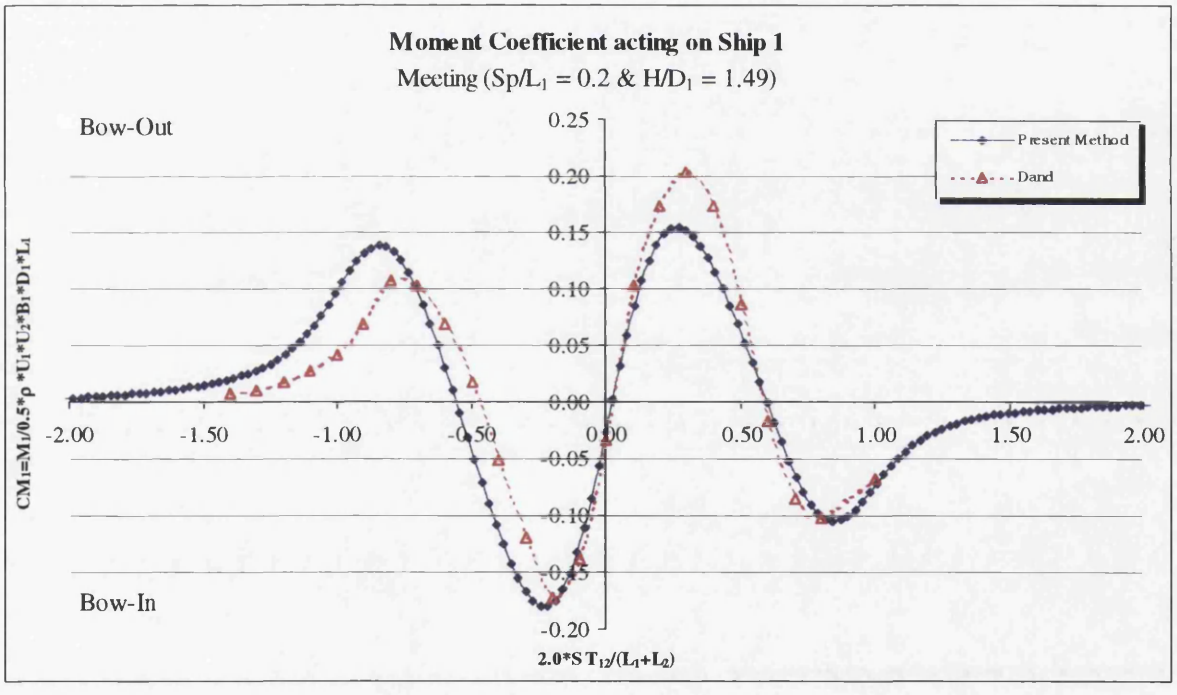

Figs 3.6a,b Comparison of the lateral force and yaw moment coefficients with Dand's experimental data. ($Sp/L_1 = 0.2$ and $H/D_1 = 1.49$, two ships meeting)

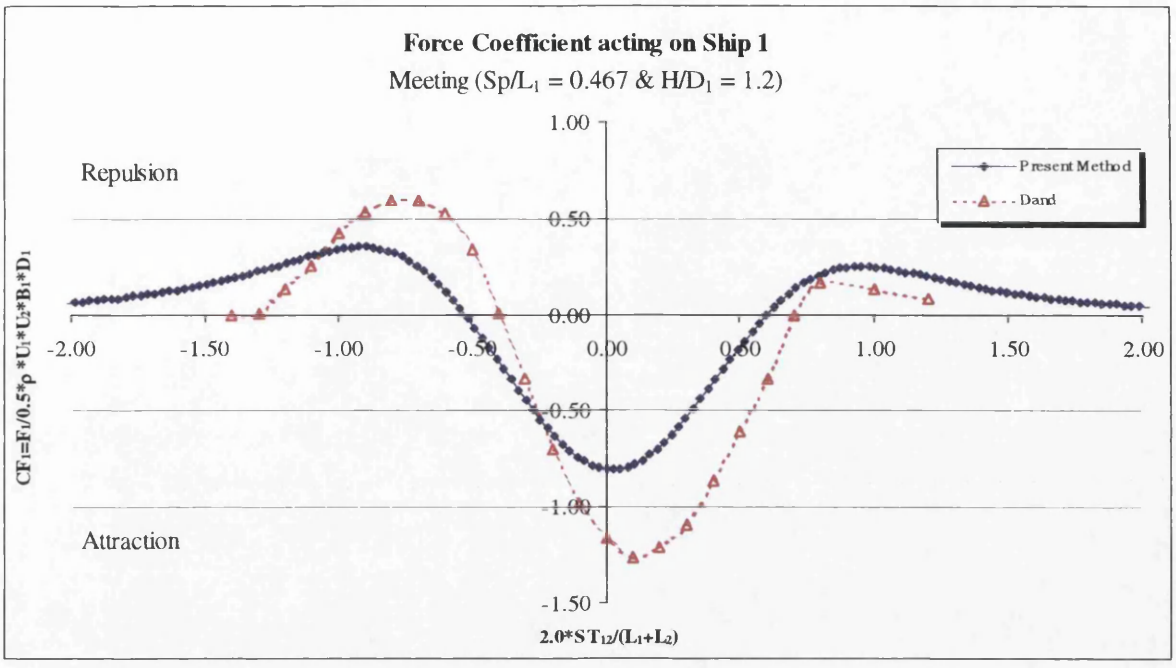

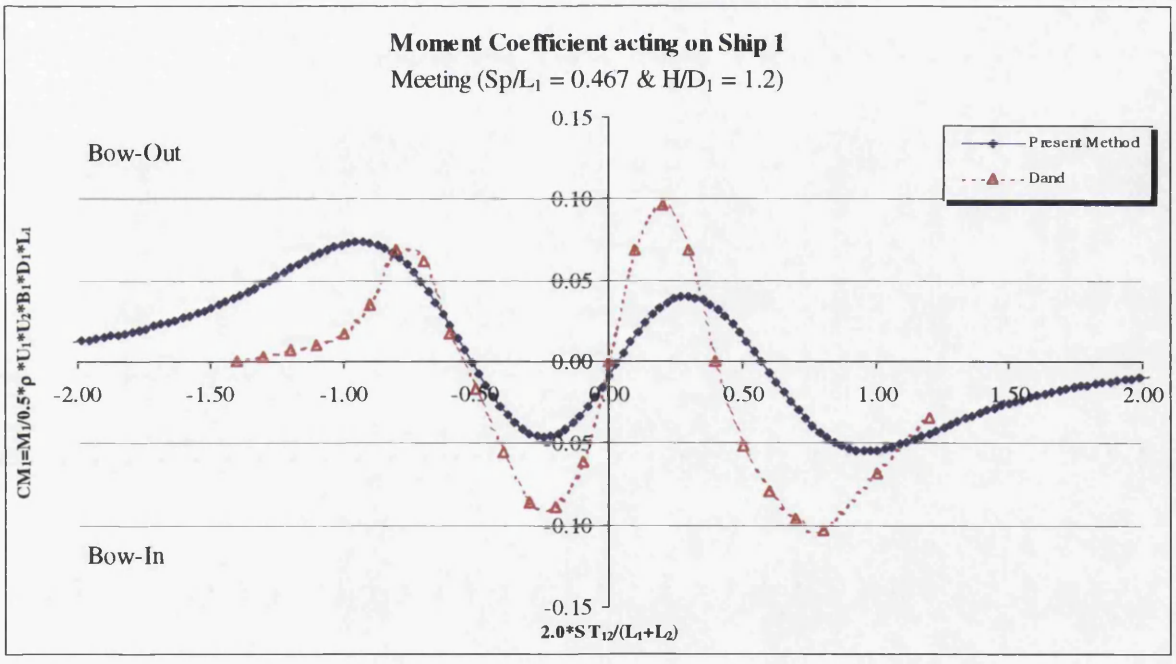

Figs 3.7a,b Comparison of the lateral force and yaw moment coefficients with Dand's experimental data. ($Sp/L_1 = 0.467$ and $H/D_1 = 1.2$, two ships meeting)

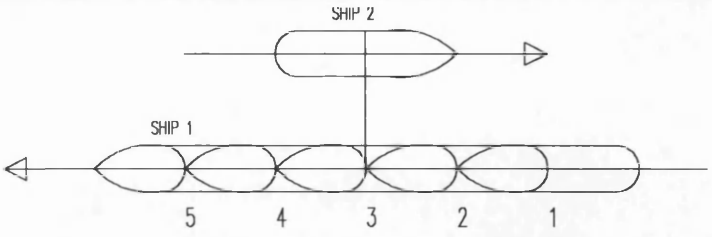

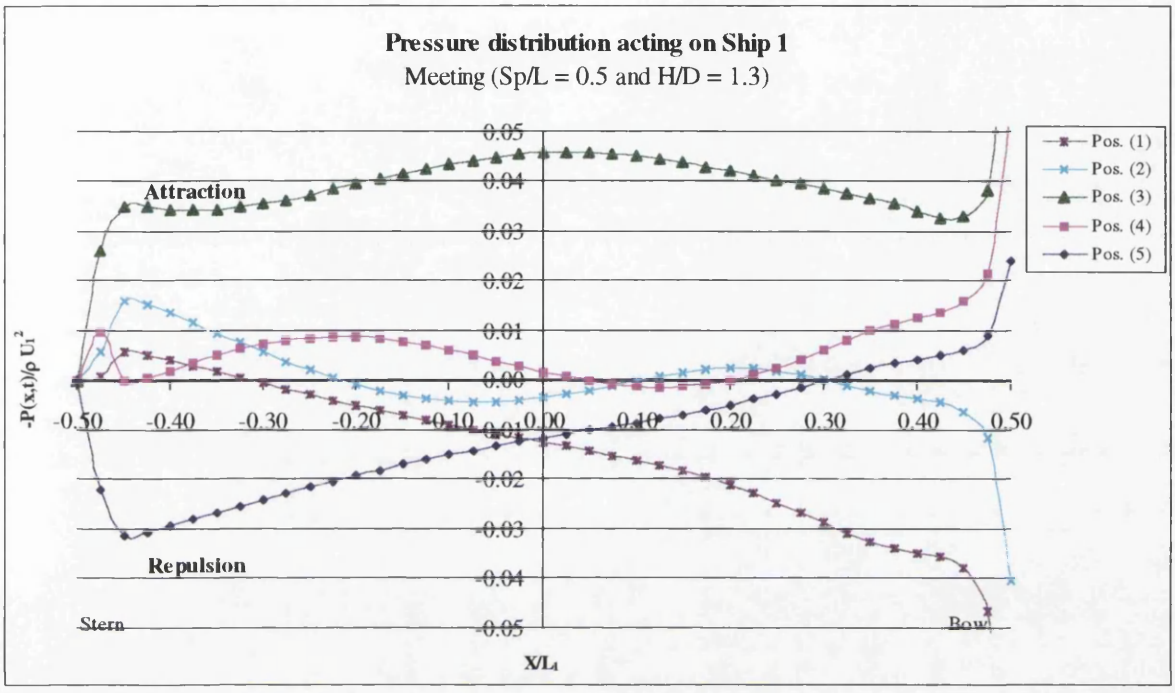

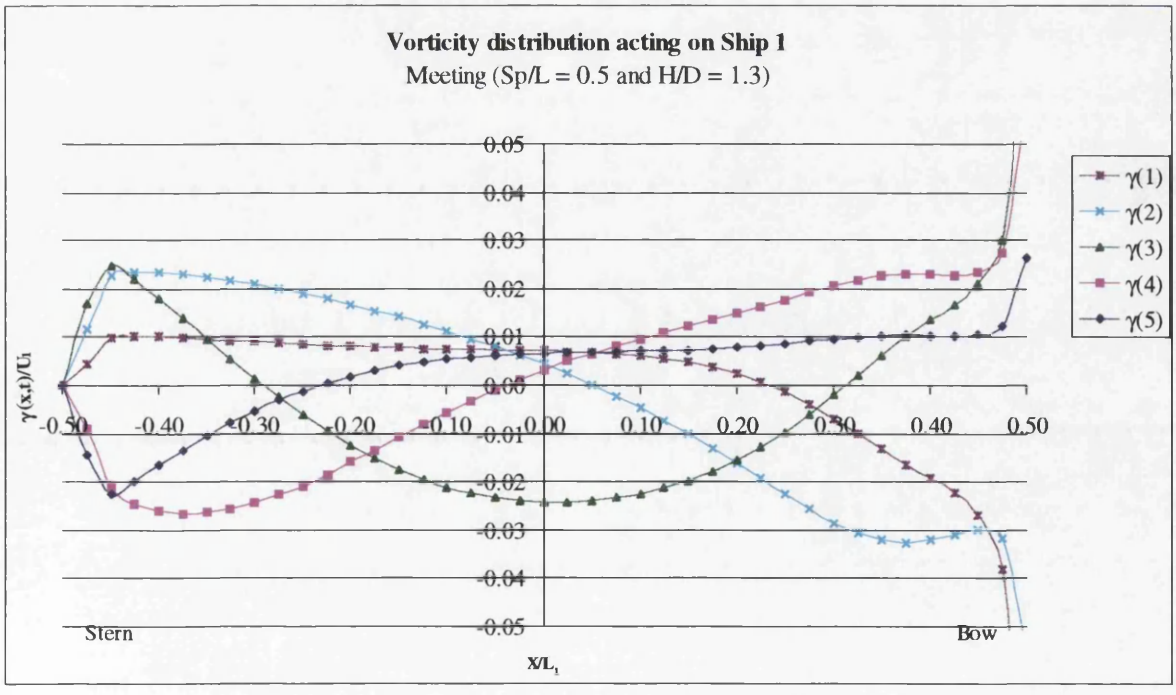

Figs 3.8a,b The pressure and vorticity distribution acting on Ship 1 for different time steps, (two ships meeting)

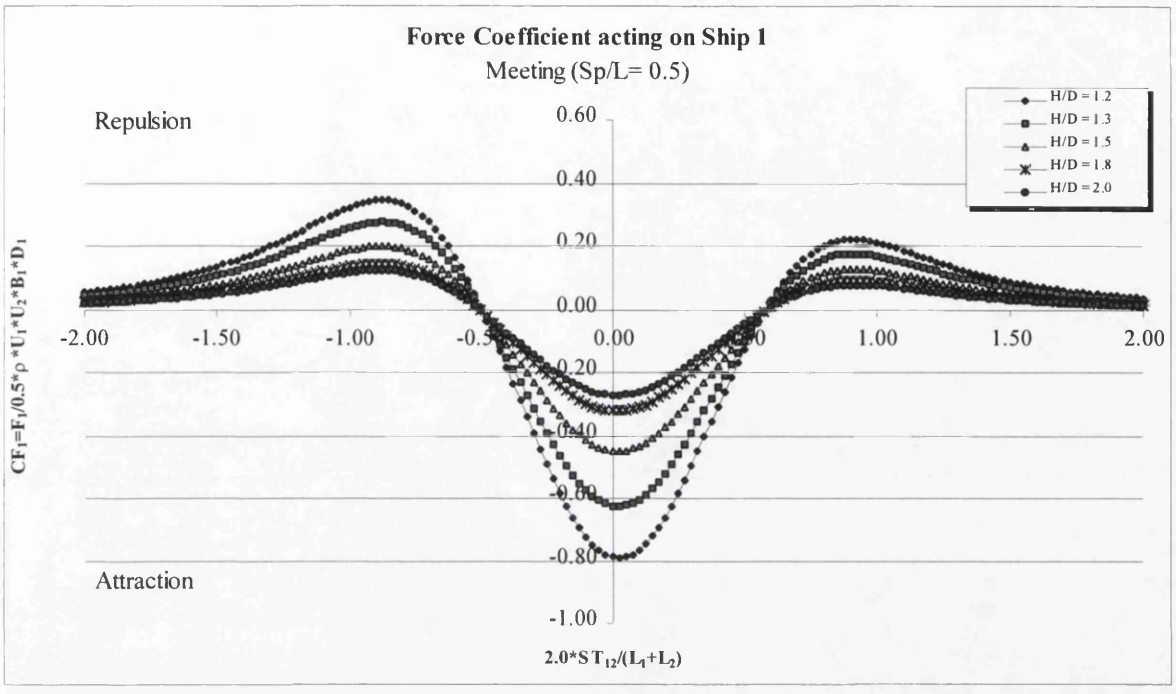

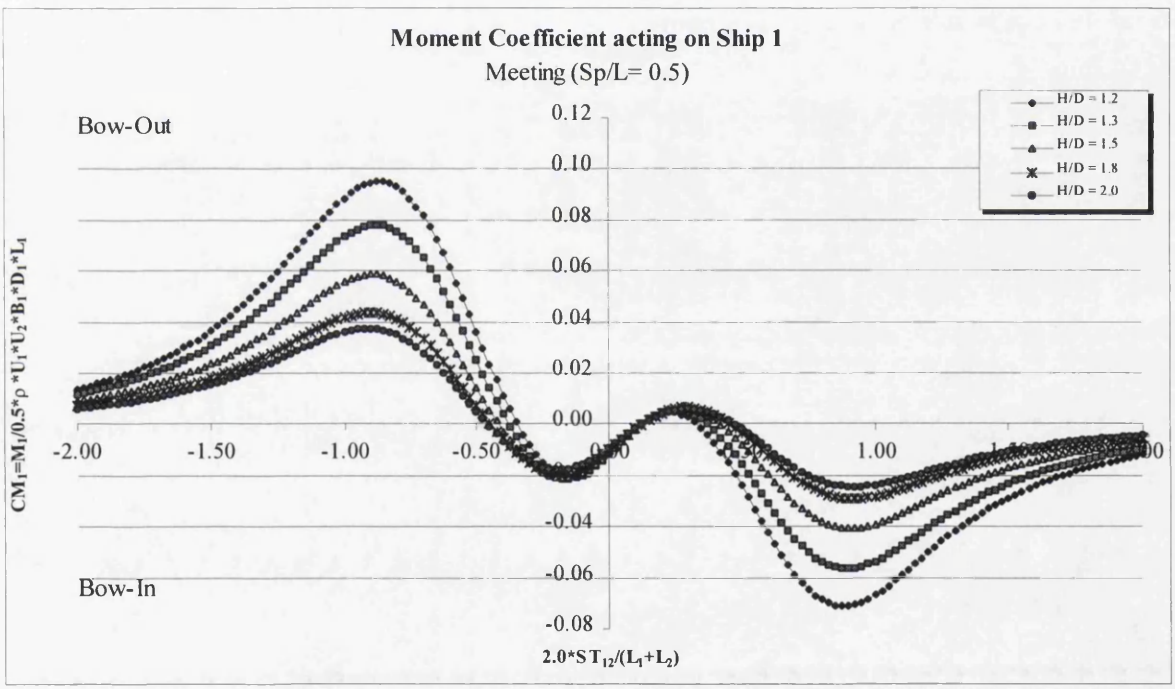

Figs 3.9a,b The lateral force and yaw moment coefficients acting on Ship 1 for various water depths, (two ships meeting)

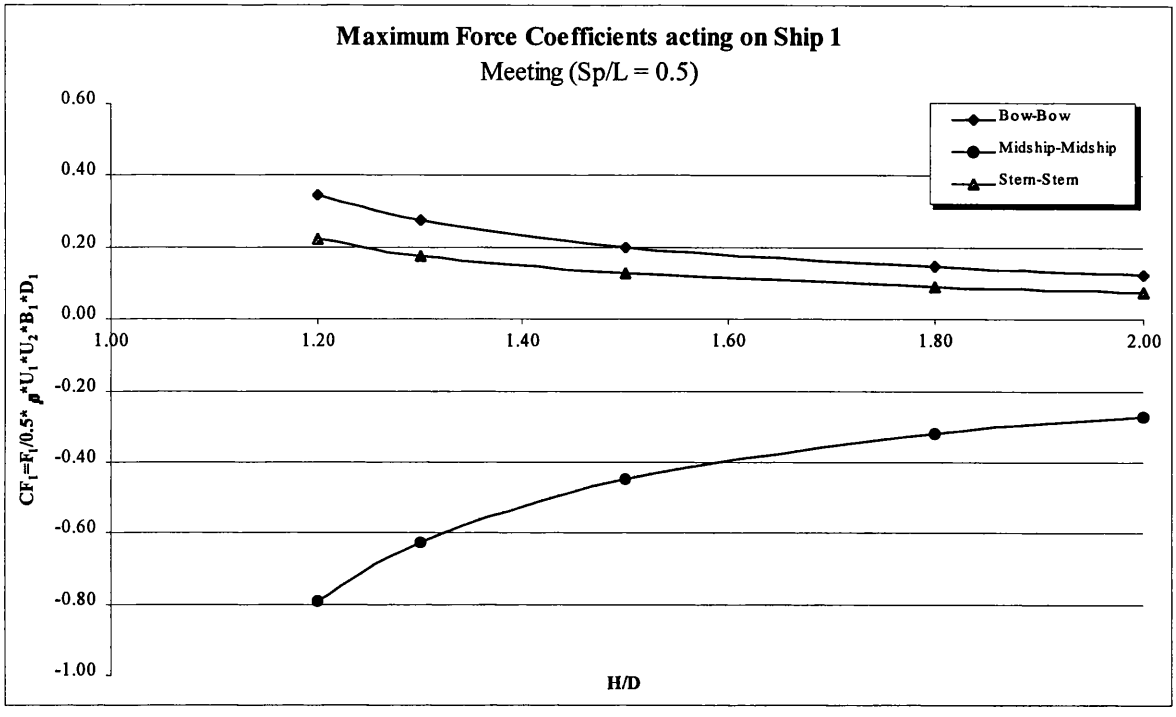

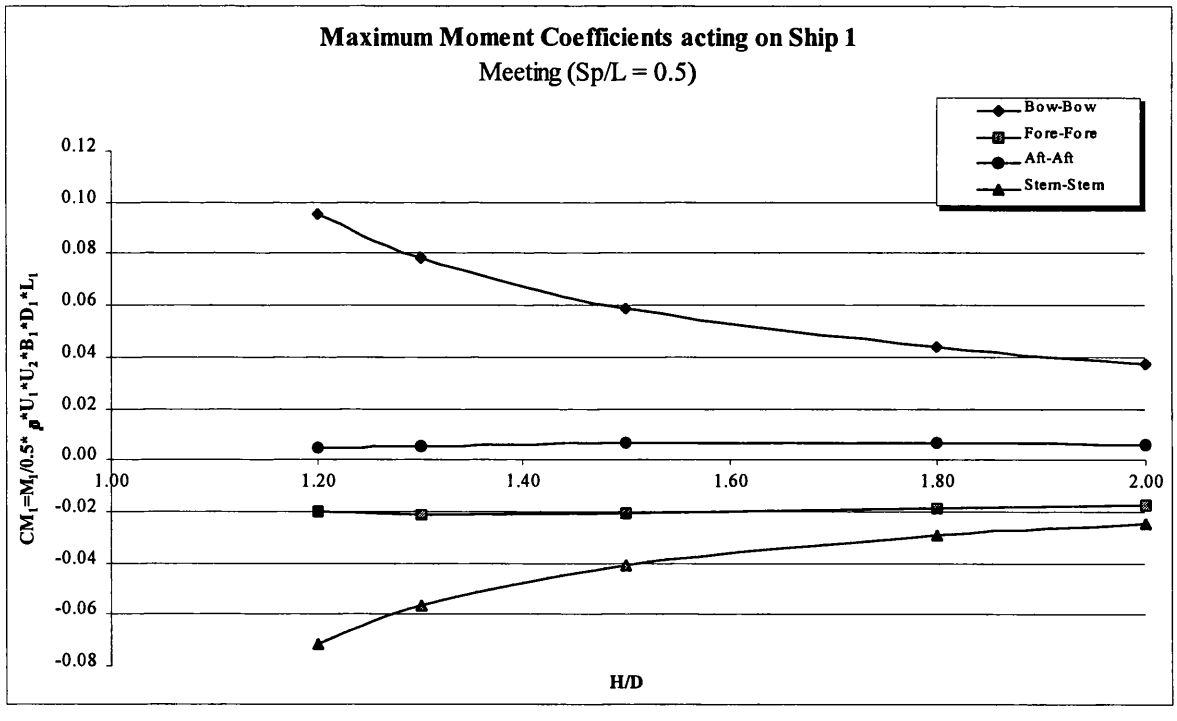

Figs 3.10a,b Maximum lateral force and yaw moment coefficients acting on Ship 1 for various water depths, (two ships meeting)

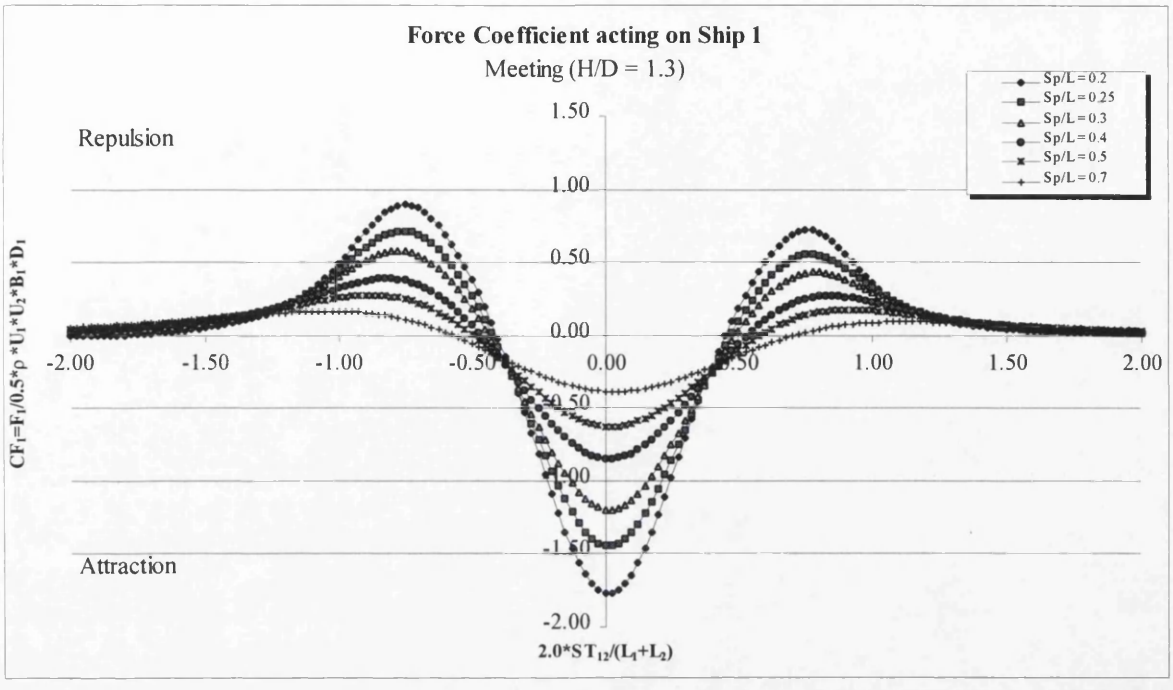

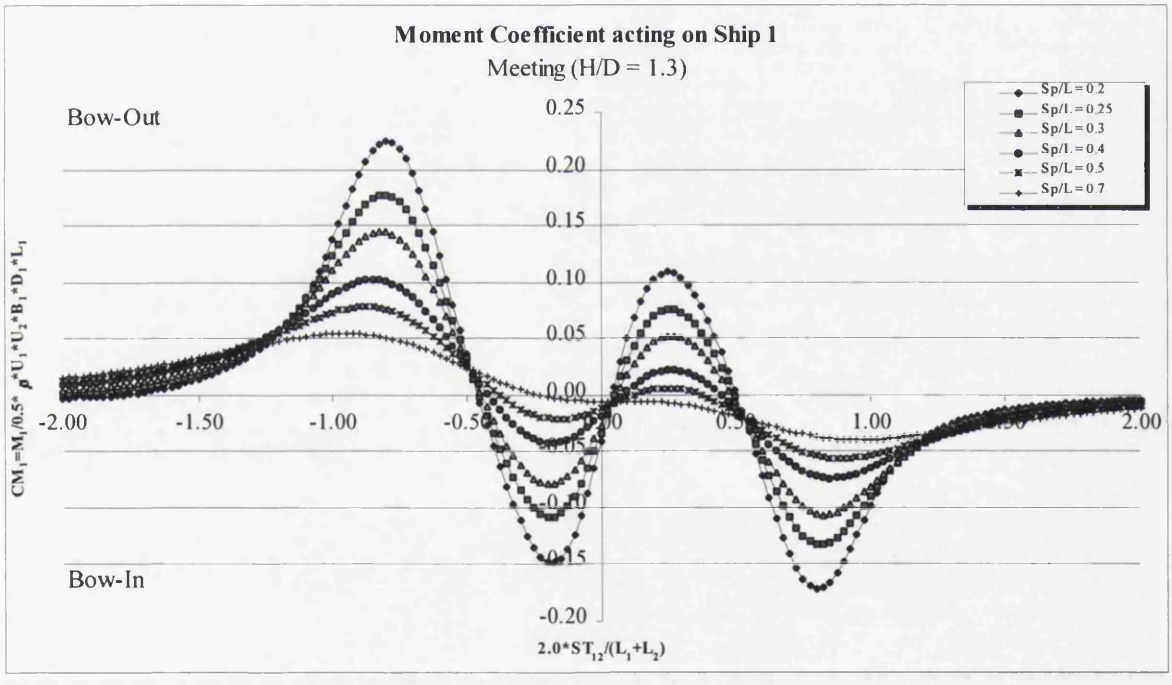

Figs 3.11a,b The lateral force and yaw moment coefficients acting on Ship 1 for various separation distances, (two ships meeting)

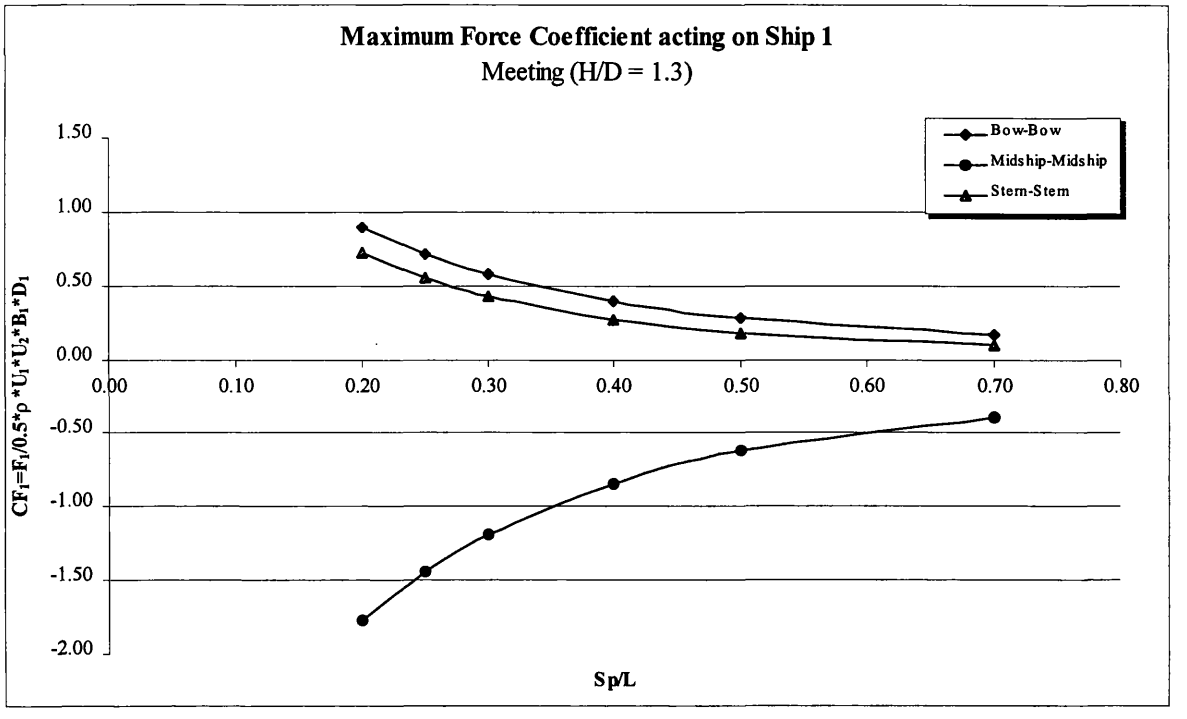

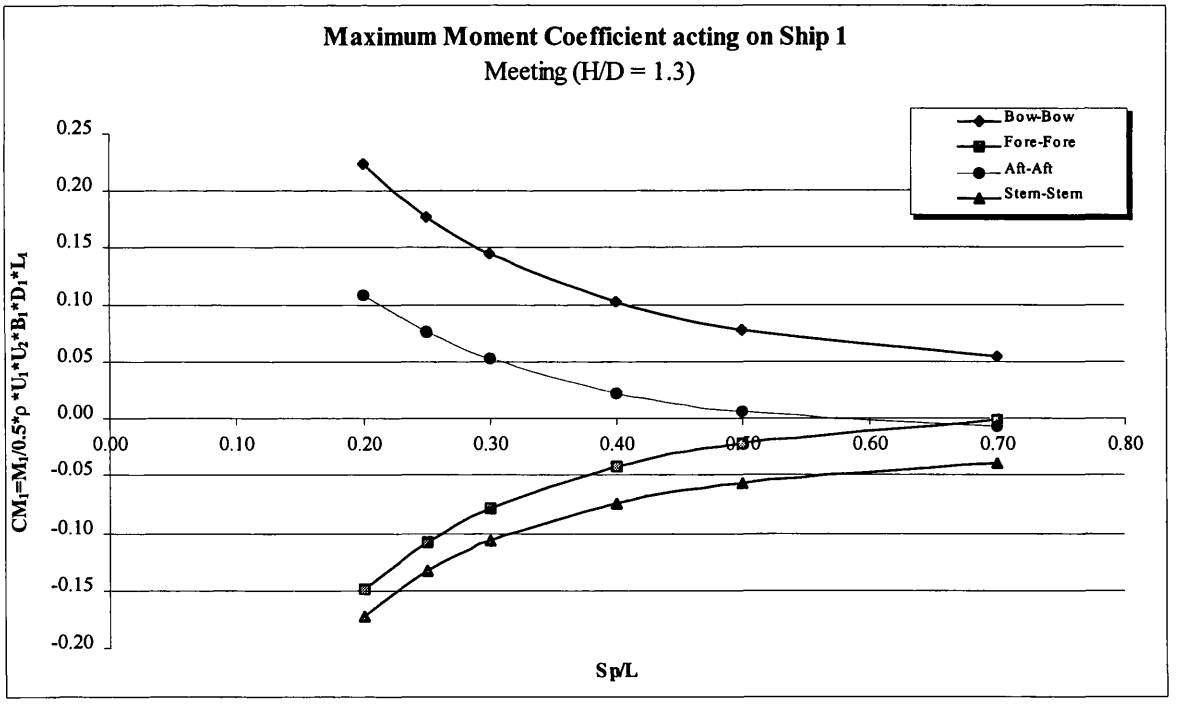

Figs 3.12a,b Maximum lateral force and yaw moment coefficients acting on Ship 1 for various separation distances, (two ships meeting)

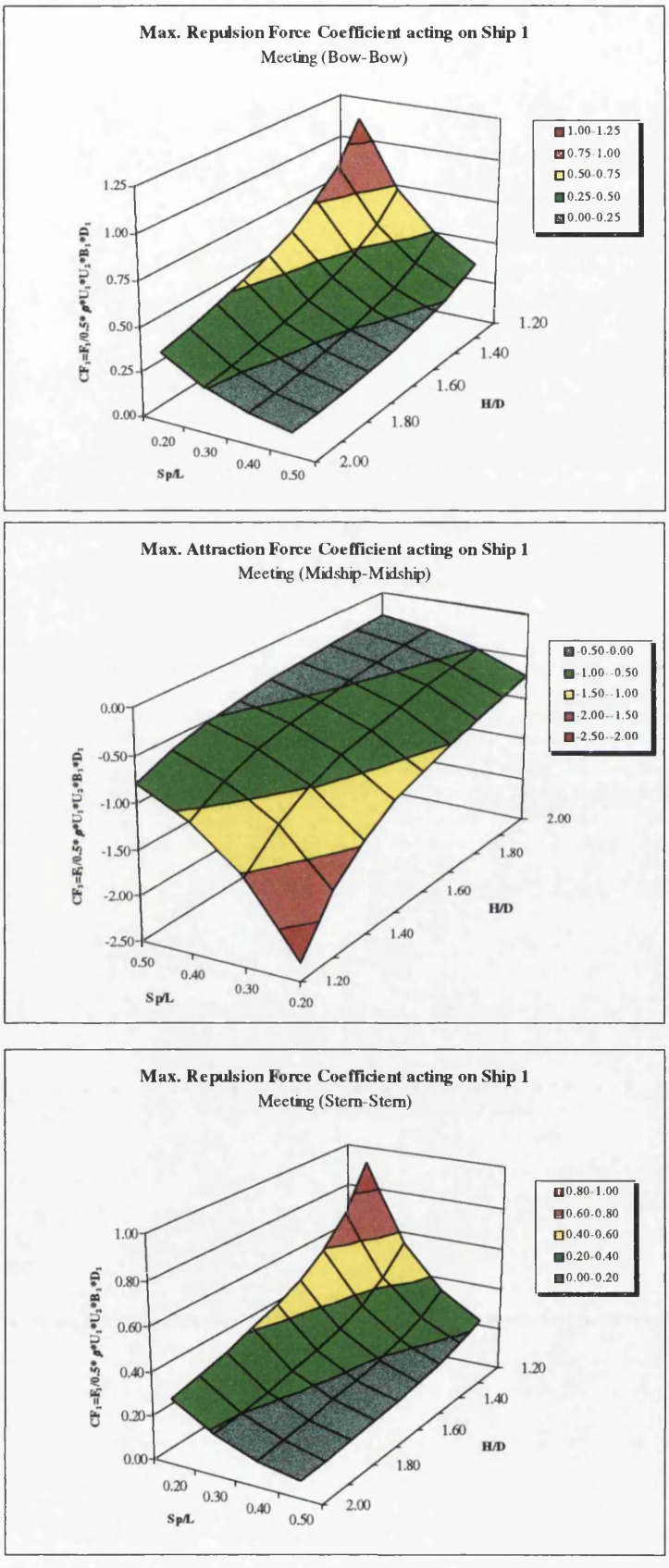

Fig 3.13 3D plots of the lateral force coefficients acting on Ship 1 for various separation distances and water depths, (two ships meeting)

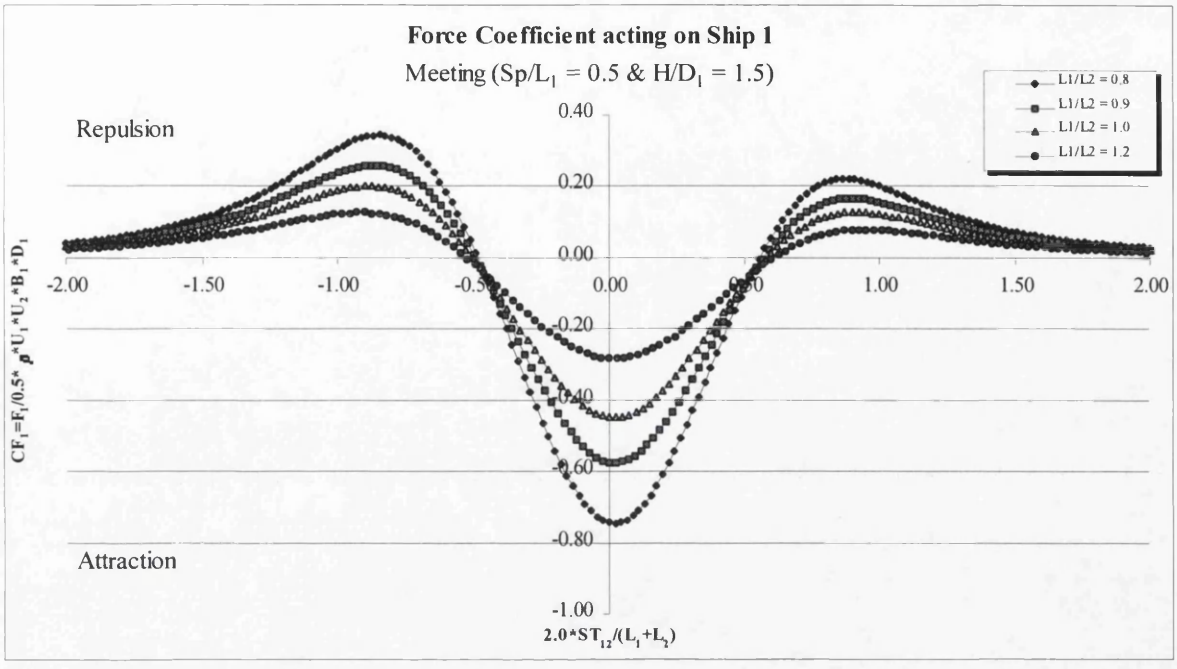

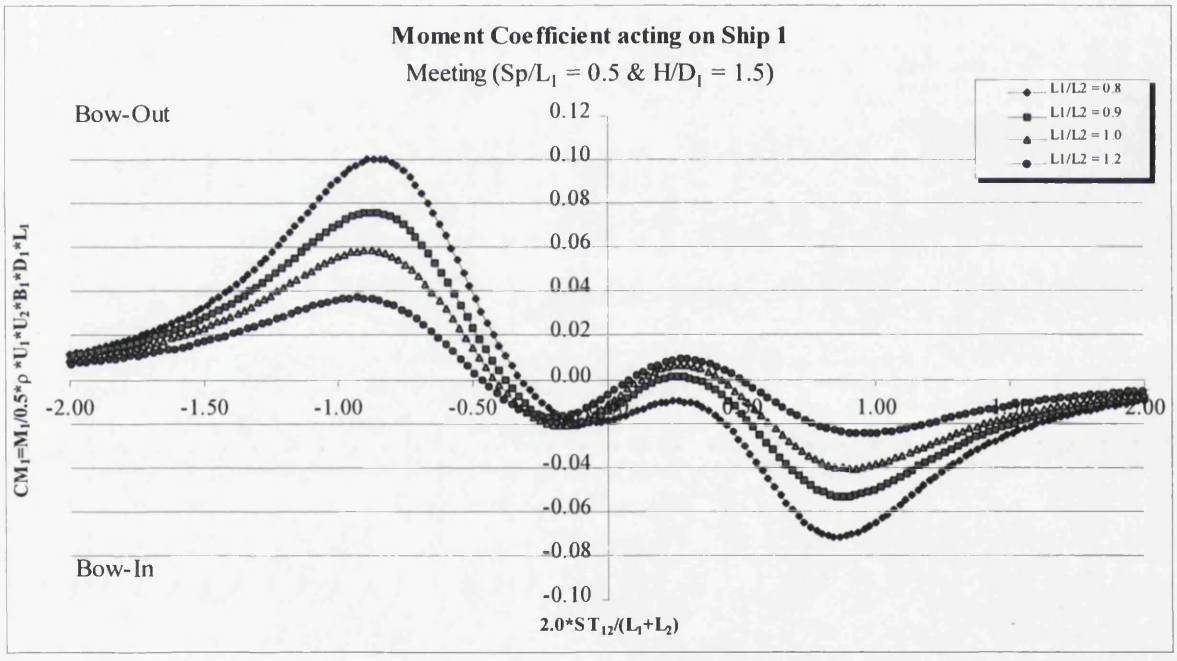

Figs 3.14a,b The lateral force and yaw moment coefficients acting on Ship 1 for various ship sizes, (two ships meeting)

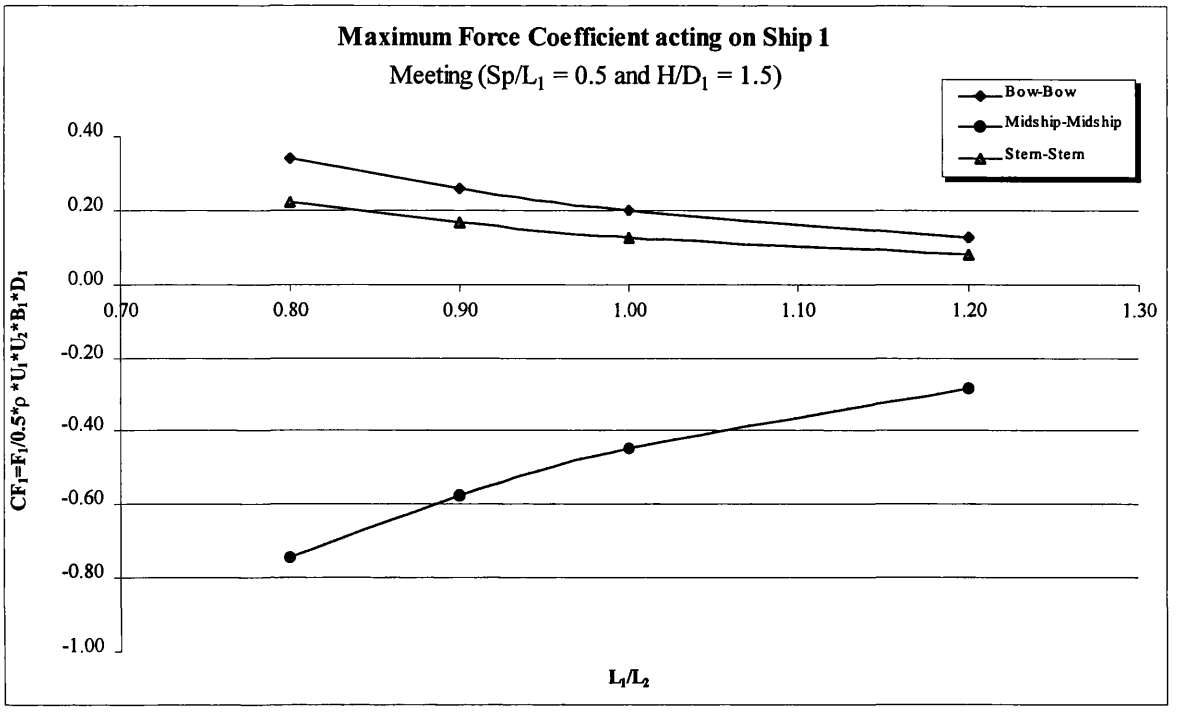

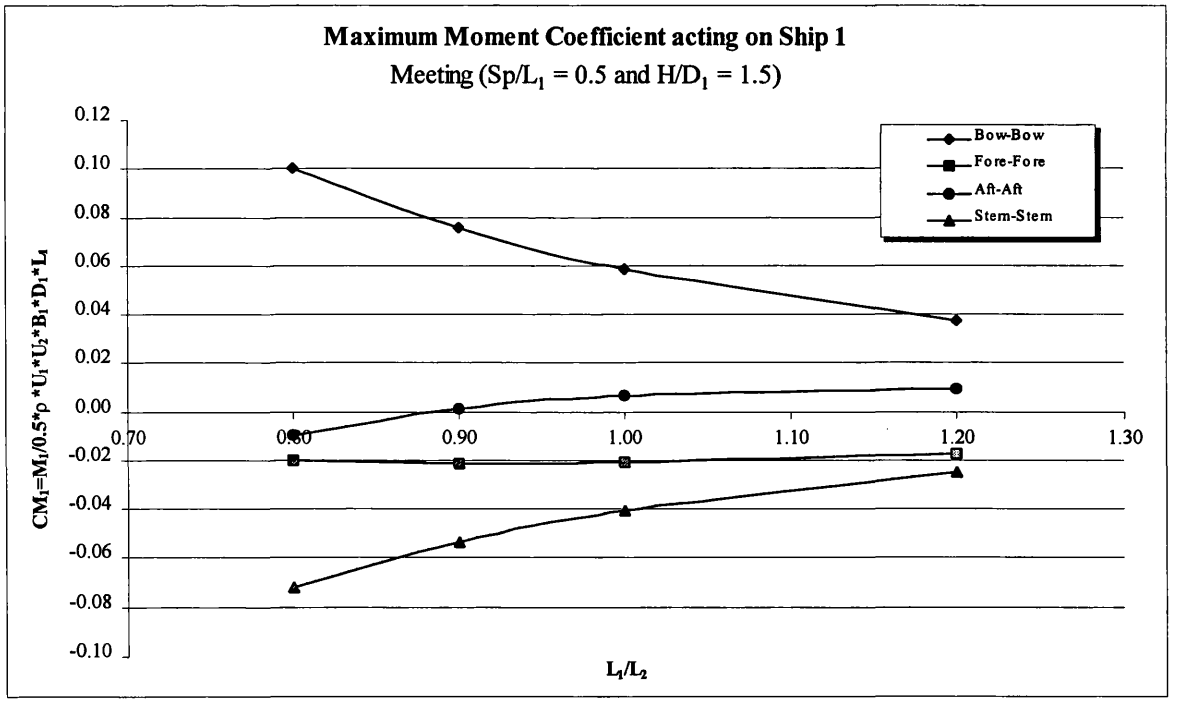

Figs 3.15a,b Maximum lateral force and yaw moment coefficients acting on Ship 1 for various ship sizes, (two ships meeting)

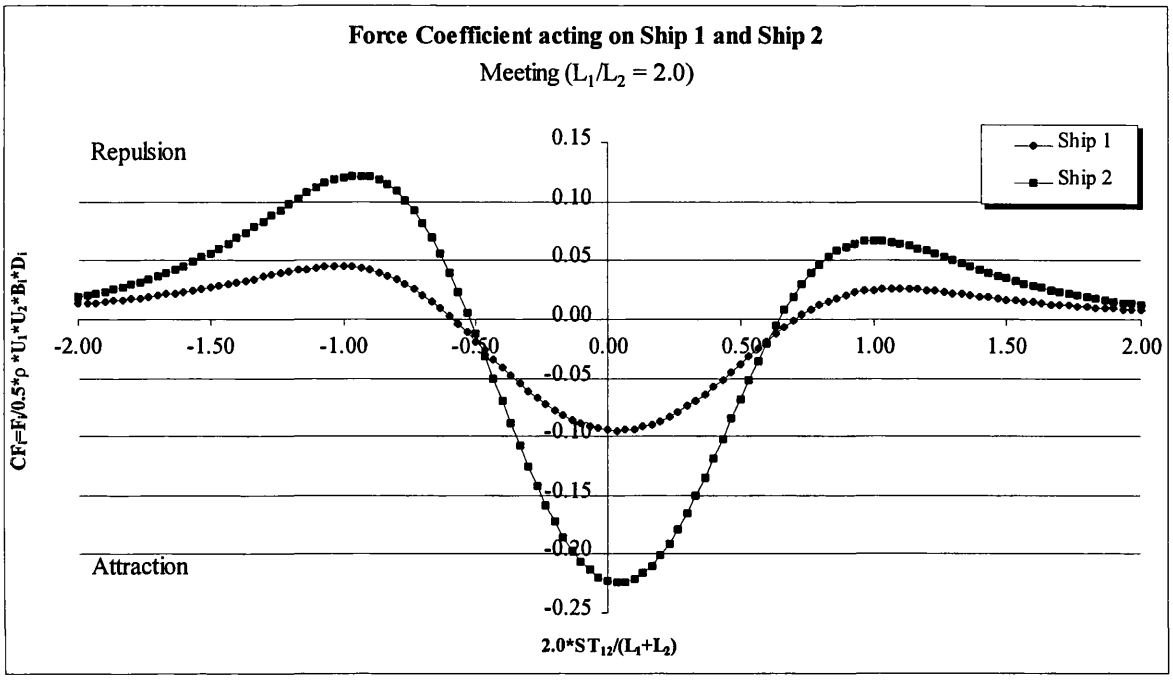

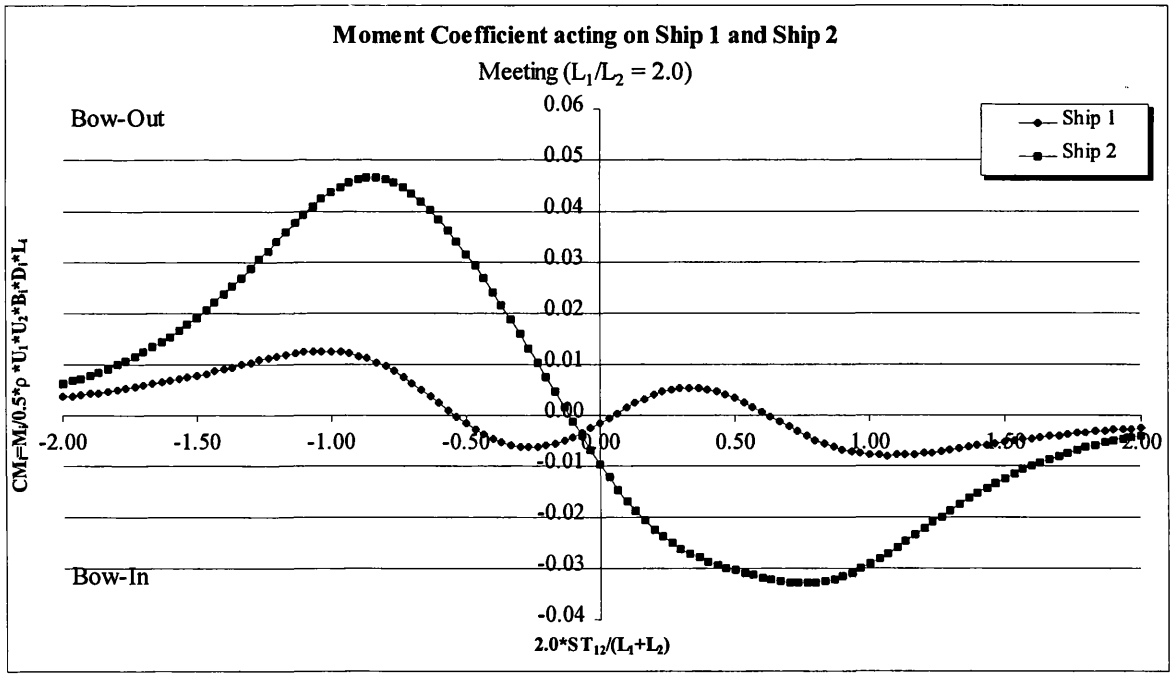

Figs 3.16a,b Comparison of the lateral force and yaw moment coefficient when Ship 1 is twice the size of Ship 2, (two ships meeting)

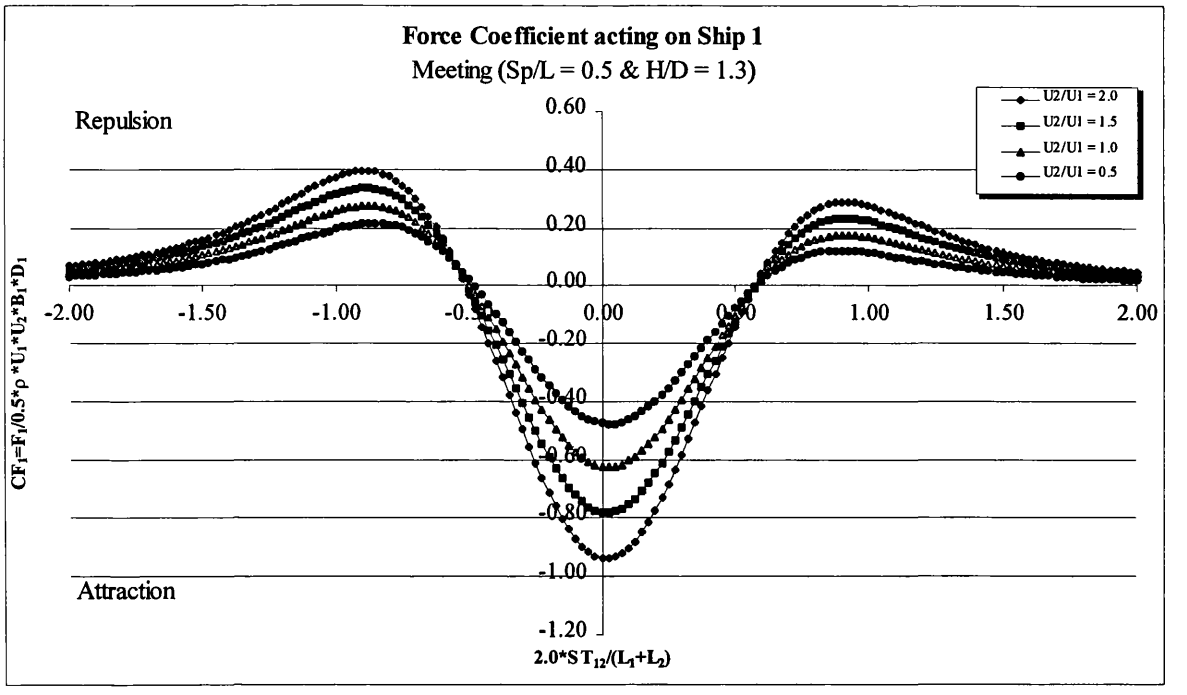

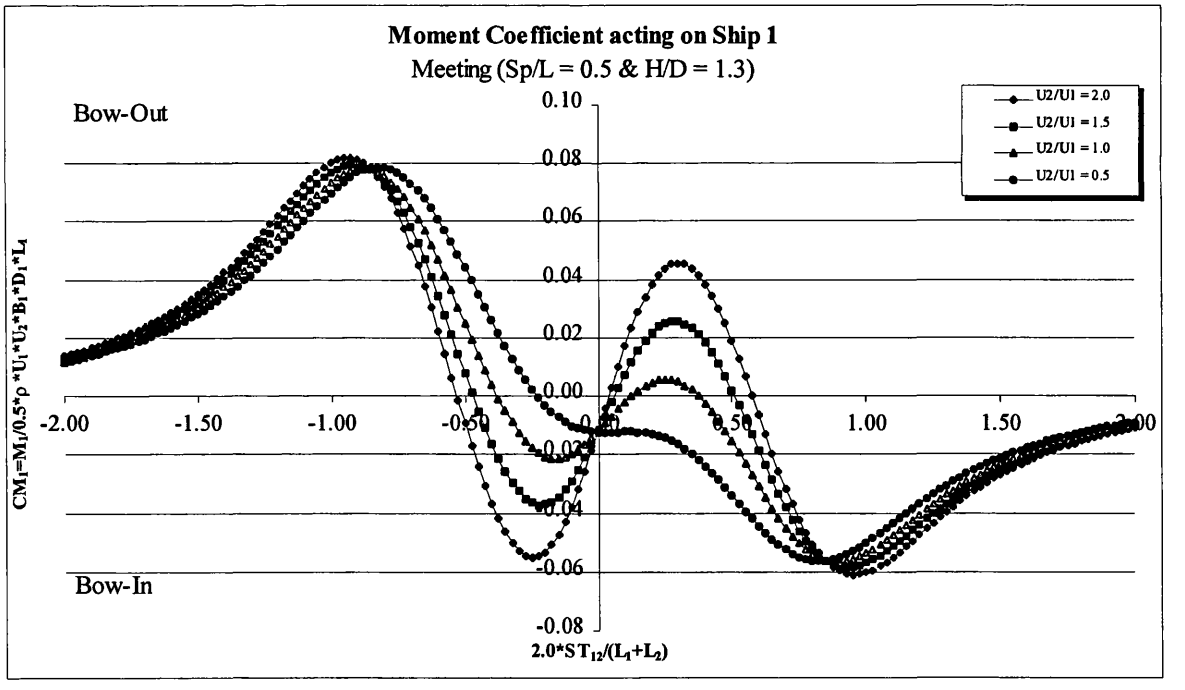

Figs 3.17a,b The lateral force and yaw moment coefficients acting on Ship 1 for various ship speeds, (two ships meeting)

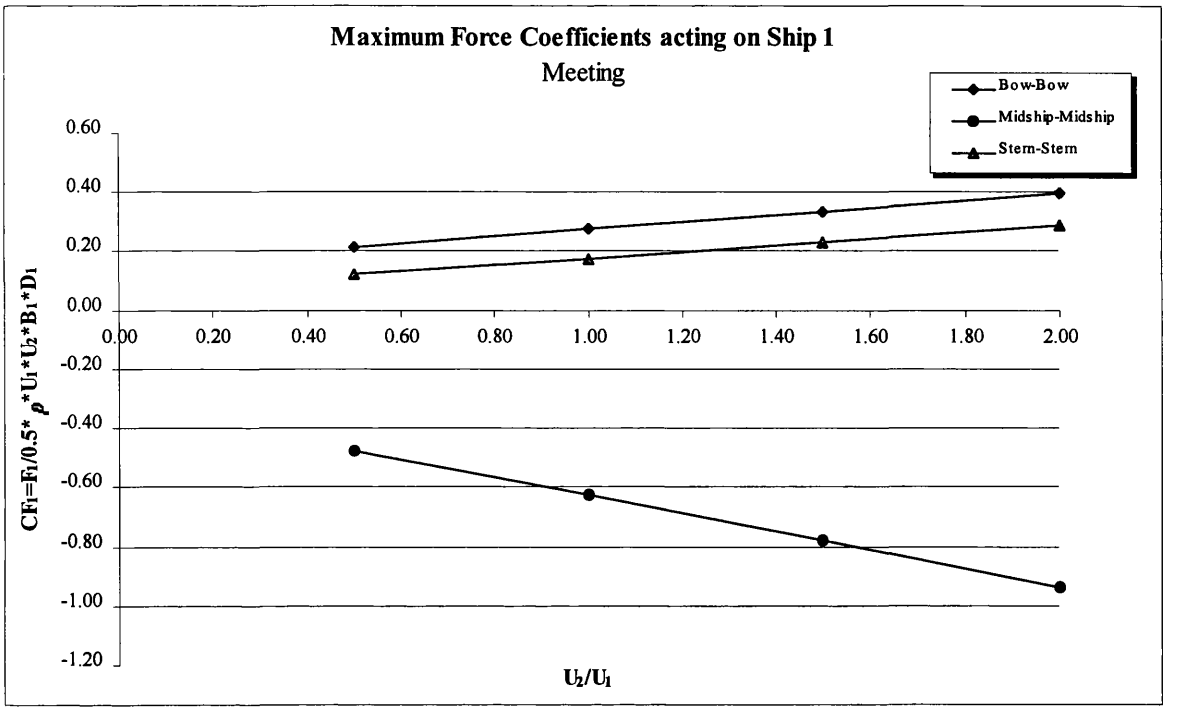

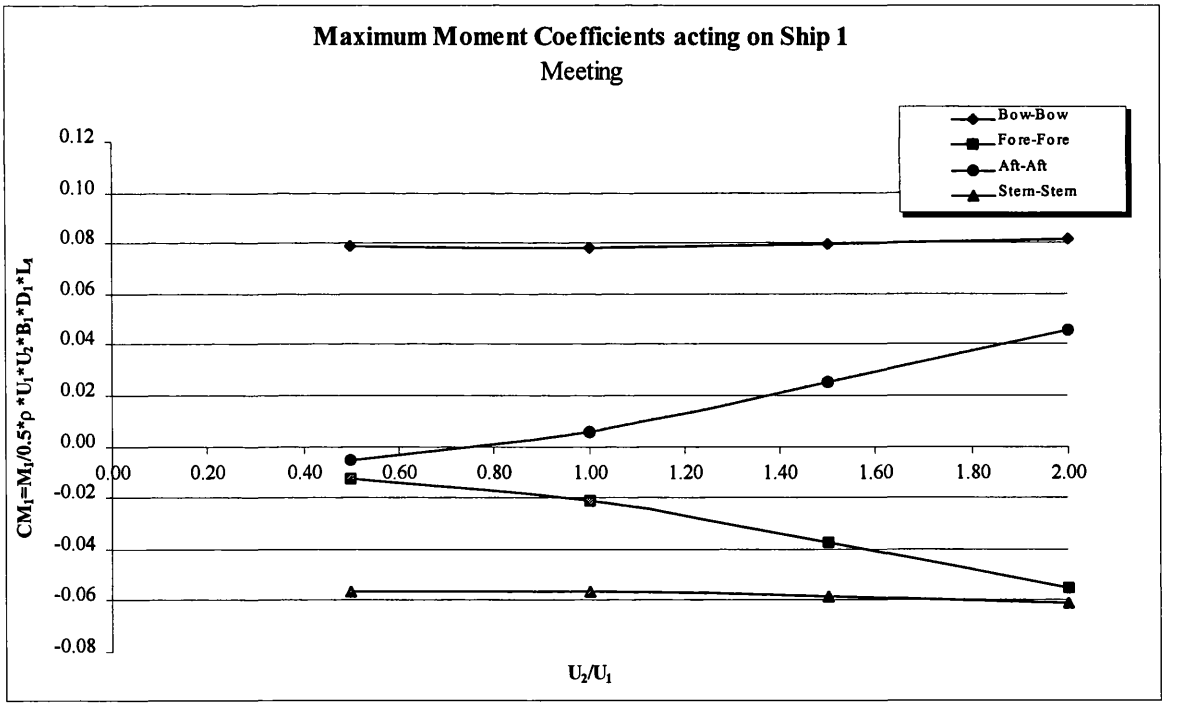

Figs 3.18a,b Maximum lateral force and yaw moment coefficients acting on Ship 1 for various ship speeds, (two ships meeting)

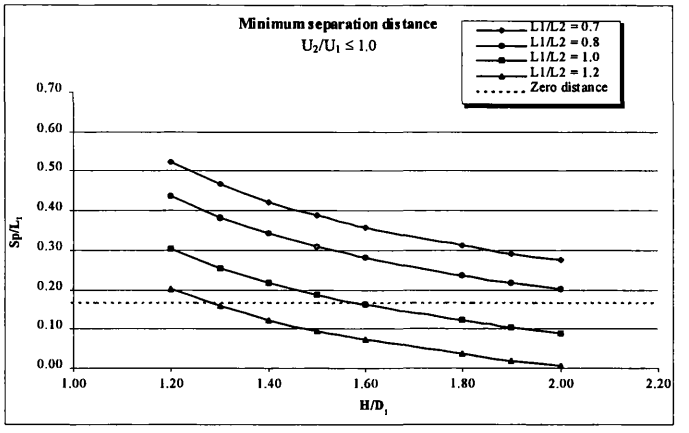

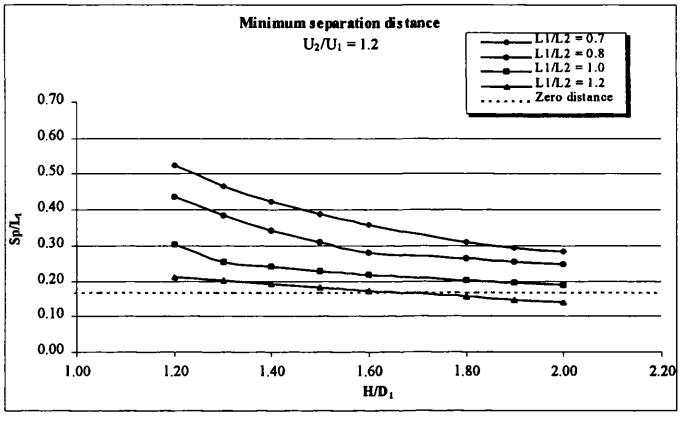

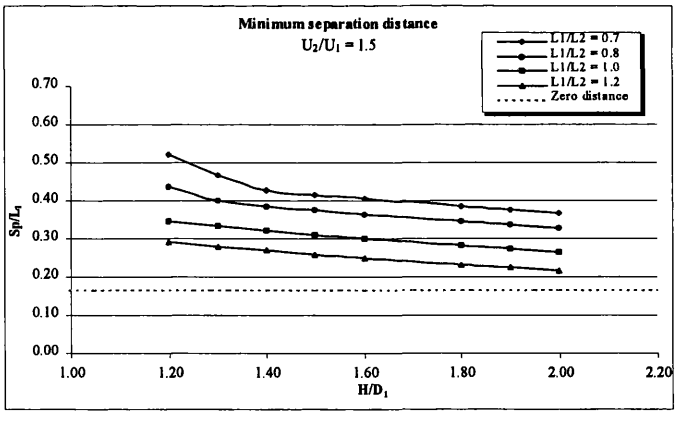

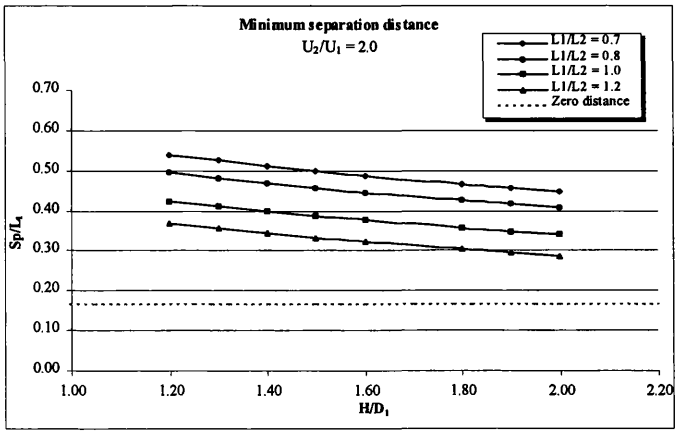

Figs 3.19a,b,c,d Minimum separation distance indicating that the rudder moment is smaller than the interaction moment, (two ships meeting)

CHAPTER 4

INTERACTION BETWEEN TWO SHIPS IN PASSING MANOEUVRE.

4.1 INTRODUCTION

In this chapter the hydrodynamic interaction forces and moments acting on two ships participating an overtaking manoeuvre in a channel are investigated. Figure 4.1 gives the plan view of such a passing situation and the sign convention for the force and moment are also indicated in the figure. Ship 1 is chosen to be the overtaking ship and the stagger, ST_{12}, is defined as follows:

$$ST_{12} = (U_1 - U_2) \times t \qquad U_1, U_2 > 0$$

where t = 0 corresponds to the instance at which the midships are aligned. The stagger, ST`{ = $2.0 \times ST_{12}/(L_1 + L_2)$}, is again non-dimensionalized such that the values –1, 0, and +1 correspond to the bow-stern, midship-midship, and stern-bow situations respectively and is used as the abscissa for the plots.

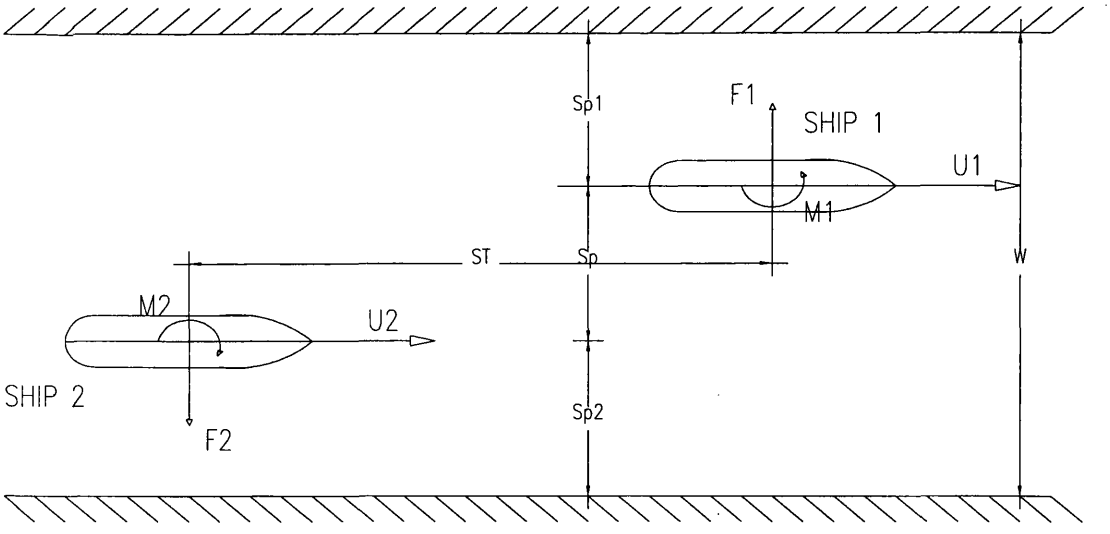

Fig 4.1 Co-ordinate system for two ships passing.

As in the parametric study for the meeting situation, here too the effects of water depth, separation distance, ship size and ship speed are also analysed. New empirical formulae for the maximum lateral force and yaw moment coefficients are then derived both for the faster and for the slower ship.

Again the separation distances and water depths are non-dimensionalized by the length and draught of Ship 1 (for principal particulars see Table 3.1), but in cases where two identical ships interacts, the subscripts are omitted.

4.2 VERIFICATION OF NUMERICAL METHOD

Again, the usefulness of any theory depends to a large extent on the agreement of its predictions with empirical data. Theoretical comparisons with Yasukawa (1983) are presented both for the faster and for the slower ship in the overtaking manoeuvre. However, the experimental measurements available in the literature were only carried out on the overtaken ship, i.e. the slower ship. Both Yasukawa (1983) and Dand (1981b) presented such experimental data, and comparisons have been made with the following results.

4.2.1 Comparisons with Yasukawa's experimental results

Results from the present calculation method are here compared to Yasukawa's (1983) measurements on a stationary model in an overtaking manoeuvre. The experimental results were carried out on the same model as used in the meeting case, and its principal particulars can be seen in Table 3.2. However, the present method cannot take ship speed equal zero as input. To simulate a stationary ship situation, the speed of Ship 2 was taken to be 0.001m/s. The magnitudes of the lateral force and yaw moment acting on Ship 2 may be incorrect because of this manipulation, and might explain the large differences in values between the experimental and the calculated results for the lateral force and yaw moment coefficients. Nonetheless, the qualitative agreement between the experimental results and the present method are very good, and Figs 4.2a,b show these non-dimensional lateral force and yaw moment obtained by the present method compared with experimental results for different separation distances. The identical ships are travelling in a 2L wide channel with water depth of 1.3 times the draught of the ships.

The overtaken Ship 2 initially experiences a repulsive lateral force as the bow of the overtaking ship approaches its stern. This repulsion force reaches maximum just as the bow of Ship 1 passes its stern. It then decreases and becomes zero as the bow of Ship 1 becomes aligned with the midship of Ship 2. Furthermore, at the midship-midship situation Ship 2 experiences a maximum attraction force. As the ships move out of this position, the attraction forces on Ship 2 decrease and are zero as its midship becomes aligned with the stern of the overtaking Ship 1. In the last quarter phase of the manoeuvre the force changes back to repulsion with a peak occurring just as the stern of Ship 1 passes the bow of Ship 2.

The yaw moment acting on Ship 2 is bow-out in nature during the first half of the transit, with a peak arising as the bow of the overtaking Ship 1 is passing the midship of Ship 2. This bow-out moment changes direction and is negligible as the midships becomes aligned. Furthermore, in the last part of the overtaking manoeuvre, Ship 2 experiences a bow-in moment that reaches its maximum when the stern of Ship 1 is passing the midship of Ship 2.

It should be noted that the phase lag, experienced from comparison with Yasukawa's experimental data for the two ships meeting situation, is absent here.

4.2.2 Comparisons with Yasukawa's theoretical results

Theoretical calculations are presented by Yasukawa (1983) for overtaking manoeuvre between two ships, where Ship 1 is the faster ship while Ship 2 is the slower ship. Yasukawa investigates the effect of water depth, separation distance, ship size and ship speed, and are in this thesis compared with results from the present method. Comparisons are presented for both.

Variation of separation distance

Figures 4.3a,b show the non-dimensional lateral force and yaw moment obtained by the present method and by Yasukawa acting on the faster Ship 1 for three different

separation distances. The depth-draught ratio is 1.3 and the two ships have same size travelling in a 2L wide channel, where Ship 1 has twice the speed of Ship 2.

Qualitatively, the results from the present method agree very well with Yasukawa's results. Ship 1 initially experiences an attractive force, which reaches maximum when its bow overtakes the stern of Ship 2. This attraction force changes to repulsion in nature as the midship of Ship 1 is about 0.3L behind the midship of Ship 2, and this repulsion force reaches its maximum when the midships becomes aligned.

Similar good agreement between the tendency for the moment coefficient curves can be seen in Fig 4.3b. In the first half of the manoeuvre, Ship 1 experiences a bow-in moment with a peak when its bow passes the midship of Ship 2. This bow-in moment changes direction and becomes zero at the midship-midship situation. During the second half of the overtaking manoeuvre, the turning moment becomes bow-out with the maximum occurring when its stern passes the midship of Ship 2.

Furthermore, the present method and Yasukawa's results also agree well for different separation distances, both for the lateral force and yaw moment coefficients. It is apparent from Figs 4.3a,b that the lateral forces and yaw moments acting on Ship 1 decrease as the separation distance increases. This is true for both methods.

A comparison between the maximum attraction and repulsion force coefficients calculated from the present method and Yasukawa in Fig 4.3a gives an approximate 6% to 13% difference in peak values for various Sp/L, where the present method is always more conservative in all cases.

Similarly small differences can be seen for the yaw moment coefficients in Fig 4.3b, where the present method calculates approximately 5% to 10% larger maximum bow-in and bow-out moment coefficients, compared to those obtained from Yasukawa.

Figures 4.3c,d show the lateral force and yaw moment coefficients acting on the overtaken Ship 2, and here too the qualitative agreement between the present method and Yasukawa is very good. Ship 2 experiences the same repulsion-attraction-repulsion force transient for both the calculation methods. In the first half of the

manoeuvre, there is a bow-out moment with a peak when the bow of Ship 1 passes its midship. During the second half of the manoeuvre, the turning moment becomes bow-in with the maximum occurring when the stern of Ship 1 passes its midship.

Again, the tendency for various separation distances is the same for the present method and Yasukawa; increasing lateral forces and yaw moments acting on Ship 2 as Sp/L decrease. In contrast to the differences between the present method and Yasukawa in peak values acting on the faster Ship 1, the maximum lateral force and yaw moment coefficients acting on Ship 2 differ only about 1% to 6% across the range of Sp/L.

Variation of water depth

From Figs 4.4a,b,c,d it is apparent that an increase in bottom clearance results in smaller hydrodynamic forces and moments on both the faster Ship 1 and the slower Ship 2. This tendency is similar both for the author's and Yasukawa's results, but there are some differences in the maximum values for the lateral force and yaw moment coefficients.

The present method produces larger peak values both for the lateral force and yaw moment coefficients compared to those of Yasukawa for the faster ship (Figs 4.4a,b). The maximum attraction and repulsion forces Ship 1 experiences when overtaking Ship 2 are approximately 10% to 20% higher using the present method. The largest disagreement occurs when the depth-draught ratio is 1.2. Similar higher peak values (11% to 15%), calculated using the present method, can be seen for the maximum yaw moment coefficients for various depth-draught ratios.

However, comparison of the maximum lateral force and yaw moment coefficients acting on the slower Ship 2 in Figs 4.4c,d demonstrated a better agreement between the results from the present method and Yasukawa. Here, the differences for various depth-draught ratios are at most 10% for the force coefficients and 4% for the moment coefficients.

4.2.3 Comparisons with Dand's experimental results

Dand (1981b) conducted model tests of one ship being overtaken by another with the same ship models as used for the experiments with two ships meeting (Tables 3.3 and 3.4). Model 1 was the slower ship model and fully instrumented, while Model 2 again simply provided the pressure distribution as the faster ship model. The experiments were again carried out in the 6.1m wide NMI number 2 tank.

Dand's experimental measurements on Model 1 are compared with calculations carried out on Ship 1, which is chosen to be the slower ship for the present method. Once more Ship 2 is scaled accordingly to give the same length Model 1 to length Model 2 ratio as for the experimental data, i.e. $L_1/L_2 = 1.19$.

However, Dand's report (1981b) does not give the speed of each model, just the relative speed. As a result assumptions regarding the speed of the overtaken ship (Ship 1) and the passing ship (Ship 2) have been made, giving $U_2/U_1 = 2.2$. Dand mentions in his report that in the experiments, the speed of the faster Model 2 was not always constant. It sometimes became trapped in the wake of Model 1. Consequently, comparisons of peak values for the non-dimensional lateral forces and yaw moments may not be correct, and Figs 4.5a,b show large differences in maximum force and yaw moment coefficients. Even though the agreement in the peak values is not so good, the similarity in the force and moment transits is recognized.

Both the present method and the experimental data give the same repulsion-attraction-repulsion transit, and the peak values appear at the bow-stern, midship-midship and stern-bow situation respectively (Fig 4.5a). It is also apparent that the increase in maximum lateral force coefficients as the separation distance reduces is comparable between the results from the present method and experimental data.

Figure 4.5b shows the comparison of yaw moment coefficients between the present method and Dand's experimental data. Also, here it is evident that the qualitative agreement is good. Ship 1 experiences a small bow-in peak just after the bow of Ship 2 passes its stern from the present method and this peak is also noticed from the experimental results. Furthermore, the results from the present method and the

experiments give a maximum bow-out moment just after the bow of Ship 2 passes its midship, and a bow-in peak when the stern of Ship 2 is moving past its midship. At the end of the overtaking manouevre the present method calculates a small maximum bow-out moment, which is also noticeable for the experimental data. Again, the agreement in peak values is not so good, and the measured maximum bow-out and bow-in moment coefficients are approximately 250% larger than the calculated ones. However, this difference is constant for the peak values for all three separation distances, indicating the same increase in yaw moments for decreasing separation distances obtained from the present method and experiments.

4.3 PRESSURE AND VORTICITY DISTRIBUTION

The pressure and vorticity distributions are derived for five different parts of the overtaking situation, and Figs 4.6a,b show the distribution on the faster Ship 1, while Figs 4.7a,b show the distribution on the slower Ship 2. The ships are chosen to be identical, and Ship 1 is travelling at twice the speed of Ship 2 in a 2L wide channel. The depth-draught ratio is 1.3 and Sp/L = 0.5.

As the bow of Ship 1 is approaching the stern of Ship 2 (position 1), the forward part of Ship 1 experiences reduced pressure, resulting in an attractive force and a bow-in moment towards Ship 2. This lowered pressure is caused by the increase in flow velocity between the forward portion of Ship 1 and the aft portion of Ship 2. As Ship 1 reaches position 2, it experiences an even lower pressure at the front half while higher pressures at the aft portion. Even though the total lateral force in this situation is negligible, this unevenly distributed pressure results in maximum bow-out moment on Ship 1. Furthermore, as the midships becomes aligned (position 3) Ship 1 experiences a different pressure distribution. The pressure at the middle portion of Ship 1 is lowered, while the pressures at the forward quarter half and aft quarters half are increased. Since these latter higher pressures are predominant, Ship 1 experiences a maximum repulsive force. However the total moment about midship is zero.

During the last part of the overtaking manoeuvre, the pressures increase at the forward portion of Ship 1, while the aft portion experiences lowered pressure, causing a maximum bow-out moment at position 4. The total lateral force is of a repulsive nature, and becomes insignificant as Ship 1 reaches position 5. However, Ship 1 still experiences a bow-out moment, caused by the low pressure at its aft portion.

The slower Ship 2 experiences a repulsive force as the bow of Ship 1 passes its stern (position 1 in Fig 4.7a). This is due to the higher pressures around the whole length of Ship 2. The yaw moment, however, is negligible. As the overtaking situation reaches position 2, the forward portion of Ship 2 experiences a higher pressure, while the pressure at the aft portion is lowered. The total lateral force acting on Ship 2 is zero in this position, while the yaw moment reaches a maximum in the bow-out direction. As described earlier, the increased flow velocity between the forward portion of Ship 1 and the aft portion of Ship 2 causes this bow-out behaviour. As the midships becomes aligned, the low pressure on Ship 2 produces a maximum attraction force while the yaw moment is zero.

Furthermore, as Ship 1 and Ship 2 leave this position, the pressure on the forward section of Ship 2 becomes lowered, while the aft portion experiences higher pressures, resulting in a maximum bow-in moment at position 4. This bow-in moment reduces as the pressure at the forward portion of Ship 2 increases, while the lateral force reaches maximum repulsion force as the stern of Ship 1 overtakes the bow of Ship 2 (position 5).

4.4 PARAMETRIC STUDY

The effect of various parameters for two ships meeting is only investigated for Ship 1 since both ships during an encounter experience the same force and moment transient. However, for the two ships passing manoeuvre the overtaking and overtaken ship experience different behaviour of the lateral forces and yaw moments. Numerical results are therefore presented both for the faster Ship 1 and the slower Ship 2. The conditions are given in tables.

This parametric study investigates the hydrodynamic forces and moments separately for the faster Ship 1 and the slower Ship 2. Figures 4.8a,b show the difference in the lateral force and yaw moment coefficients between Ship 1 and Ship 2. It is apparent that Ship 2 experiences larger lateral forces and yaw moments during the overtaking manoeuvre compared to those of Ship 1. The peak values from the force coefficient curves are as much as four times higher for Ship 2, while for the moment curves the peaks are found to be almost two times higher.

First the effect of water depth, separation distance and ship size is examined when Ship 1 is travelling at twice the speed of Ship 2. Again the subscript for the non-dimensionalized separation distance (Sp/L) and water depth (H/D) are omitted when the ships are identical. The effect of changing the passing speed of Ship 1 is then investigated.

The stagger is once more non-dimensionalized by the average ship lengths so that –1, 0 and +1 correspond to the bow-stern, midship-midship and stern-bow situations respectively.

The general trend of the force and moment variation is the same for the different overtaking configurations considered here both for the faster and for the slower ship. The overtaking Ship 1 experiences first an attraction force, which reaches a maximum as its bow passes the stern of Ship 2. This attractive force then changes direction and Ship 1 experiences a maximum repulsion force as the midships becomes aligned.

In the first half of the passing situation, Ship 1 undergoes a bow-in turning moment, which reaches a maximum as its bow passes the midship of Ship 2. This moment changes direction and is zero in the midship-midship situation. Furthermore, during the second half of the transit the turning moment acting on Ship 1 is bow-out in nature. The bow-out maximum occurs when its midship passes the stern of Ship 2.

The slower Ship 2 on the other hand experiences a different tendency for the force and moment variations. The behaviour is a repulsion-attraction-repulsion force transient during the passing situation, with the first repulsive peak occurring just after the bow of Ship 1 passes the stern of Ship 2. The attractive maximum takes place when the midships are aligned with each other. In the last part of the overtaking situation, Ship 2 experiences another repulsive force, which reaches its maximum just before the stern-bow situation.

The moment behaviour for Ship 2 is the exact opposite to that of Ship 1. During the first half of the transit Ship 2 experiences a bow-out moment, with a peak occurring when the bow of Ship 1 passes the midship of Ship 2. In the second half of the overtaking situation, the turning moment becomes bow-out in nature. The maximum bow-out moment occurs as the stern of Ship 1 travels past the midship of Ship 2.

4.4.1 The effect of water depth

Figures 4.9a,b,c,d show the effect of bottom clearance on the lateral force and moment acting on both the faster Ship 1 and the slower Ship 2 for the following conditions:

W	H/D	Sp/L	L_1/L_2	U_1/U_2
2L	Varying	0.5	1.0	2.0

Table 4.1 Condition for the effect of water depth, (two ships passing).

It is evident that the hydrodynamic forces and moments acting on Ship 1 and Ship 2 are increasing as the depth-draught ratio is decreasing.

The maximum attraction-repulsion force coefficients acting on Ship 1 is shown in Fig 4.10a. From these graphs it is apparent that the maximum lateral force coefficients are increasing rapidly as the bottom clearance decreases. The maximum attraction force coefficient is equal to the maximum repulsion force coefficient in magnitude for H/D = 1.2, while for deeper water, H/D = 2.0, the attractive peak value is 13% larger than the repulsive peak value.

Furthermore, an equivalent sharply increasing tendency of the maximum yaw moment coefficients can be seen in Fig 4.10b. Here on the other hand, the maximum bow-in moment coefficients are approximately 20% larger in magnitude than the maximum bow-out moment coefficients for various depth-draught ratios.

The maximum lateral force coefficients for the slower Ship 2 are shown in Fig 4.10c. From the graphs it is apparent that Ship 2 experiences increasing maximum repulsion–attraction-repulsion force coefficients as the bottom clearance decreases and the curves indicate a rapid increase in maximum lateral forces for low depth-draught ratios. The maximum repulsion force coefficients at the bow-stern situation have approximately 50% smaller magnitudes than the maximum attraction force coefficients for various depth-draught ratios. However, the maximum repulsion force coefficients at the end of the transit are about 60% smaller in magnitude compared to the maximum attraction force coefficients.

Figure 4.10d illustrates how the maximum yaw moment coefficients acting on the slower Ship 2 are changing for different depth-draught ratios. As expected, the maximum bow-out and bow-in moment coefficients increase more steeply as the bottom clearance decreases. Also noticeable is the similarity in magnitude of the maximum bow-out and bow-in moment coefficients, where the difference is only about 3%.

4.4.2 The effect of separation distance

The effect of how variation in the separation distance influences the lateral force and yaw moment coefficients can be seen in Figs 4.11a,b for the faster Ship 1 and in Figs 4.11c,d for the slower Ship 2 for the conditions given below:

W	H/D	Sp/L	L_1/L_2	U_1/U_2
2L	1.3	Varying	1.0	2.0

Table 4.2 Condition for the effect of separation distance, (two ships passing).

The general tendency is the same as for two ships meeting; increasing lateral force and yaw moment coefficients as the separation distance reduces. However, the force curve at the midship-midship situation seems to reach a very pointed peak as the separation distance decreases. This may indicate that Ship 1 experiences a much higher acceleration of the force in this part of the transit. Furthermore, for Sp/L less than 0.4, Ship 1 experiences a small attractive peak just before its stern passes the bow of Ship 2, which is not noticeable for larger separation distances.

The peak values for the lateral force coefficients are shown for Ship 1 in Fig 4.12a. It is apparent that the maximum attraction and repulsion force coefficients increase sharply as Sp/L decreases. The maximum attraction force coefficient is 11% smaller than the maximum repulsion force coefficient when Sp/L = 0.2, but this difference decreases to around 5% as the separation distance increases to 0.7L.

A similar increasing pattern for the maximum yaw moment coefficients acting on Ship 1 can be seen in Fig 4.12b as the separation distance reduces. Here, the maximum bow-in moment coefficients, which Ship 1 experiences during the first half of the transit, are larger compared to the maximum bow-out moment coefficients, which Ship 1 experiences in the second half of the overtaking situation. The differences grow from 8% to 25% for increasing Sp/L.

Figure 4.12c shows the various maximum non-dimensional lateral forces that Ship 2 experiences during the overtaking manoeuvre, and as the separation distance decreases we have a rapidly increasing tendency for the peak values. Similar to the effect of water depth, the maximum repulsion force coefficients, at the bow-stern situation, are approximately 50% smaller in magnitude compared to the maximum attraction force coefficients for various separation distances. The maximum repulsion force coefficients at the stern-bow situation are about 60% smaller than the attractive peak maximum, which also is an equal difference in peak values compared to the effect of the depth-draught ratio.

The maximum yaw moment coefficients, acting on Ship 2, are shown in Fig 4.12d, and as anticipated we have increasing turning moments as the separation distance reduces. Here the maximum bow-in moment coefficients are between 3% to 10% larger compared to the maximum bow-out moment coefficients.

3D plots are made to illustrate how the maximum repulsion-attraction-repulsion force coefficients acting on the slower Ship 2 tend to increase as H/D and Sp/L decrease (Figs 4.13a,b).

4.4.3 The effect of ship size

Previously, only overtaking manoeuvres of identical ships were considered. Figures 4.14a,b show the size effect on the interaction force and moment coefficients for the faster Ship 1. Ship 1 is kept constant while the overtaken Ship 2 is scaled accordingly for the following situation:

W	H/D_1	Sp/L_1	L_1/L_2	U_1/U_2
$2L_1$	1.5	0.5	Varying	2.0

Table 4.3 Condition for the effect of ship size, (two ships passing).

It is apparent that Ship 1 experiences larger hydrodynamic forces and moments if it is overtaking a bigger ship. This is expected and the same tendency as for the ship size effect in the two ship meeting case.

The peak values for the lateral force coefficients that Ship 1 experiences during transit are shown in Fig 4.15a. From the figure it can be seen that both the maximum attraction and repulsion force coefficients increase as the L_1/L_2 ratio decreases. When Ship 1 is 30% smaller than Ship 2 it experiences approximately 120% larger maximum lateral force coefficients compared to when both ships are identical. Furthermore this difference becomes 70% when Ship 1 is 20% smaller. However, if Ship 1 is 1.2 times larger than the Ship 2, it experiences around 40% less maximum attraction and repulsion force coefficients compared to the $L_1/L_2 = 1.0$ case.

The maximum yaw moment coefficients show a similar tendency for different L_1/L_2 ratios (Fig 4.15b). However, from the graphs it can be seen that the increase in maximum bow-in and bow-out moment coefficients is more profound than for the maximum force coefficients for increasing L_1/L_2. When Ship 1 is 30% smaller than the ship it passes, the maximum bow-in moment coefficients becomes 130% larger compared to the $L_2/L_1 = 1.0$ case, while the bow-out peaks becomes around 150% larger. Again, a reduction of approximately 40% in these yaw moment peaks is found when Ship 1 is 1.2 times the size of Ship 2.

Figures 4.16a,b illustrate the variation in the interaction forces and moments acting on the slower Ship 2 for different length ratios in the overtaking manoeuvre. Here, Ship 2 is kept constant, while Ship 1 is scaled geometrically. Accordingly, the water depths and separation distances are non-dimensionalized by the respective length and draught of Ship 2, and held constant for all L_2/L_1, i.e. $H/D_2 = 1.5$ and $Sp/L_2 = 0.5$. The channel width is chosen to be $2.0L_2$. Again, as Ship 2 is overtaken by bigger ships the hydrodynamic forces and moments becomes larger.

The maximum repulsion-attraction-repulsion force coefficients acting on Ship 2 can be seen in Fig 4.17a. It is apparent that as the L_2/L_1 ratio reduces the lateral forces increase. When Ship 2 is 30% smaller than the overtaking Ship 1 it experiences approximately 120% larger forces compared to the $L_2/L_1 = 1.0$ situation, while around

65% higher peak values occurs when Ship 2 is 20% smaller. This size effect is similar to that of the faster Ship 1. On the other hand, if Ship 2 is 1.2 times that of the overtaking ship, the maximum lateral forces reduces by around 35% compared to the case in which both ships are identical.

A similar pattern is noticeable for the maximum yaw moment coefficients in Fig 4.17b. Again Ship 2 is experiencing approximately 120% and 65% larger maximum bow-out and bow-in moment coefficients when Ship 2 is 30% and 20% less than Ship 1 respectively when compared to the $L_2/L_1 = 1.0$ case. As $L_2/L_1 = 1.2$, i.e. Ship 2 is 20% larger than Ship 1, Ship 2 experiences around 35% smaller peak values.

4.4.3 The effect of ship speed

In the previous parametric study the speed of the faster Ship 1 was twice that of the slower Ship 2. Here, the effect of changing the overtaking speed of Ship 1 is investigated on the lateral force and yaw moment coefficients acting on both Ship 1 and Ship 2 for the conditions given below:

W	H/D	Sp/L	L_1/L_2	U_1/U_2
2L	1.3	0.5	1.0	Varying

Table 4.4 Condition for the effect of ship speed, (two ships passing).

Figures 4.18a,b, show the lateral force and yaw moment coefficients transit acting on Ship 1 for various U_1/U_2 ratios, and it is apparent that the lateral forces increase as the relative speed increases. On the other hand, the tendency for the yaw moment coefficients is found to be somewhat differently. Ship 1 experiences larger bow-in and bow-out moments as the U_1/U_2 ratio decreases, which is opposite tendency compared to that of the lateral forces.

The maximum attraction and repulsion force coefficients can be seen in Fig 4.19a. By plotting the maximum lateral force coefficients against U_2/U_1 instead of U_1/U_2 the present method found linear behaviour for the maximum attraction force coefficients; i.e. peak values increase linearly for decreasing U_2/U_1. Similar linear tendency, although not as clearly, are also noticeable for the maximum repulsion force coefficients at the midship-midship situation.

The maximum yaw moment coefficients are shown in Fig 4.19b. Although Ship 1 experiences decreasing yaw moments for increasing U_1/U_2 ratio, the tendency is found to be linear for the maximum bow-in and bow-out peaks. However, the gradient for these curves are lower compared to the curves for the maximum lateral force coefficient.

From Figs 4.20a,b it is apparent that the overtaken Ship 2 experiences both larger hydrodynamic forces and moments when the speed of the passing Ship 1 becomes higher. For the maximum lateral force coefficients a linear tendency can be seen in Fig 4.21a when plotted against U_1/U_2. Similar increasing tendency can be seen in Fig 4.21b for the maximum yaw moment coefficients as increases, but the inclination is not as steep compared to those of the maximum lateral force coefficients.

4.5 NEW EMPIRICAL FORMULAE FOR MAXIMUM CF & CM

New empirical formulae are derived for the maximum lateral force and yaw moment coefficients for the two ship passing case, both for the faster Ship 1 and the slower Ship 2. The first set of new empirical formulae is derived from a variation in water depth and separation distance when both ships are identical travelling in a 2L wide channel, and Ship 1 has twice the speed of Ship 2. Furthermore multiplication factors are added to the new empirical formulae to take account for the ship size ratios and ship speed ratios. The empirical formulae should only be used within the ranges of data covered by the investigation.

4.5.1 Separation distance and water depth variation

Section 4.4.1 describes how the lateral forces and yaw moments increase as the bottom clearance decreases. However, this description of the depth-draught effect is only conducted for one particular separation distance (Sp/L = 0.5). A more thorough investigation has been carried out so that the new empirical formulae takes into account more separation distances and water depths. As for the two ship meeting condition, the different maximum lateral force and yaw moment coefficients are considered separately for the various parameter effects. Numerical calculations have been derived for Sp/L = 0.2, 0.25, 0.3, 0.4, 0.5 and 0.7, all for H/D = 1.2, 1.3, 1.5, 1.8 and 2.0, and the results is found in the Appendix 4.

Maximum lateral force coefficient acting on Ship 1

As the bottom clearance decreases the increase in maximum attraction force coefficient at the bow-stern situation is expressed as follows for a given Sp/L:

$$CF1_{Bow-Stern} = A\left[1-0.9\left(D/H\right)\right]^{-0.74}\left(H/D\right)^{-0.74} \tag{4.1}$$

where A is a constant which varies with the separation distance. Study shows that this constant changes for different non-dimensional separation distances in the following manner:

$$A = -0.022\left(Sp/L\right)^{-0.9} \tag{4.2}$$

The maximum attraction force coefficient at the bow-stern situation is now expressed for different separation distances and water depths by the following empirical formulae:

$$CF1_{Bow-Stern} = -0.022\left(Sp/L\right)^{-0.9}\left[1-0.9\left(D/H\right)\right]^{-0.74}\left(H/D\right)^{-0.74} \tag{4.3}$$

Similar empirical formula is obtained for the maximum repulsion force coefficients at the midship-midship situation, and is found to be on the following form:

$$CF1_{Midship-Midship} = 0.025\left(Sp/L\right)^{-1.0}\left[1-0.9\left(D/H\right)\right]^{-0.55}\left(H/D\right)^{-0.55} \quad (4.4)$$

However, eqn (4.4) is shown to calculate larger repulsive forces for depth-draught ratios below 1.3 than the present method. This is because the results from the present method do not produce a sharp increase in repulsion force coefficients for small depth-draught ratios. It also calculates higher forces for large separation distances (Sp/L = 0.7), but for such large separation distances the hydrodynamic forces and moments calculated from the present method are very small.

Maximum yaw moment coefficient acting on Ship 1

Based on the same variation of water depths and separation distances, new empirical formulae have also been derived for the maximum yaw moment coefficients. From the parameter study we have a peak in the bow-in direction as the bow of Ship 1 passes the midship of Ship 2. The following empirical formula calculates this maximum bow-in moment coefficient:

$$CM1_{Bow-Midship} = -0.041\left(Sp/L\right)^{-0.54}\left[1-0.6\left(D/H\right)\right]^{-1.0}\left(H/D\right)^{-1.0} \quad (4.5)$$

Again the tendency for the maximum bow-out moment coefficients, which occur when the stern of Ship 1 is passing the midship of Ship 2, is alike for various separation distances and water depths. Empirically this is expressed as follows:

$$CM1_{Stern-Midship} = 0.026\left(Sp/L\right)^{-0.68}\left[1-0.7\left(D/H\right)\right]^{-1.0}\left(H/D\right)^{-1.0} \quad (4.6)$$

Here too, using eqns (4.5) and (4.6) gives larger yaw moments for large separation distances compared to those of the present method.

Maximum lateral force coefficient acting on Ship 2

As described earlier, the slower ship experiences larger lateral forces in an overtaking manoeuvre. However, the increasing tendency as the bottom clearance reduces is similar compared to the faster ship, leading to the following empirical formulae for the maximum repulsion force coefficient at the bow-stern situation:

$$CF2_{Bow-Stern} = A\left[1-0.85\left(D/H\right)\right]^{-0.85}\left(H/D\right)^{-0.85} \tag{4.7}$$

where A again is a coefficient, which varies for different Sp/L. Furthermore, this constant is expressed as follows:

$$A = 0.68\left(1+Sp/L\right)^{-5.1} \tag{4.8}$$

We have now an empirical formula, which calculates the maximum repulsion force coefficients for different separation distances and water depths acting on the slower Ship 2:

$$CF2_{Bow-Stern} = 0.68\left(1+Sp/L\right)^{-5.1}\left[1-0.85\left(D/H\right)\right]^{-0.85}\left(H/D\right)^{-0.85} \tag{4.9}$$

Similar empirical formulae are derived for the maximum attraction force coefficient at the midship-midship situation, and the maximum repulsion force coefficient at the respective stern-bow situation. They are found to be as follows:

$$CF2_{Midship-Midship} = -1.12\left(1+Sp/L\right)^{-4.7}\left[1-0.85\left(D/H\right)\right]^{-0.85}\left(H/D\right)^{-0.85} \tag{4.10}$$

$$CF2_{Stern-Bow} = 0.52\left(1+Sp/L\right)^{-5.1}\left[1-0.85\left(D/H\right)\right]^{-0.85}\left(H/D\right)^{-0.85} \tag{4.11}$$

Maximum yaw moment coefficient acting on Ship 2

Ship 2 experiences also larger yaw moments compared to those of the faster Ship 1. Nevertheless, the bow-out and bow-in peaks have same increasing tendency as the depth-draught ratio decreases. Study on this increasing behaviour showed that the maximum bow-out moment coefficients, when the bow of Ship 1 passes its midship, is expressed empirically by the following formula for various water depths and separation distances:

$$CM2_{Bow-Midship} = 0.51\left(1+{}^{Sp}/_{L}\right)^{-5.0}\left[1-0.85\left({}^{D}/_{H}\right)\right]^{-0.7}\left({}^{H}/_{D}\right)^{-0.7} \quad (4.12)$$

Resembling empirical formulae are derived for the maximum bow-in moment coefficients that occur as the stern of Ship 1 passes its midship:

$$CM2_{Stern-Midship} = -0.44\left(1+{}^{Sp}/_{L}\right)^{-4.7}\left[1-0.85\left({}^{D}/_{H}\right)\right]^{-0.7}\left({}^{H}/_{D}\right)^{-0.7} \quad (4.13)$$

4.5.2 Ship size variation.

So far the new empirical formulae have not taken the size effect into account for the faster and slower ship in an overtaking manoeuvre. As described earlier, if the overtaking Ship 1 passes a larger ship it experiences larger hydrodynamic forces and moments, compared to an overtaking manoeuvre of an identical ship. Similarly, if a bigger ship overtakes Ship 2, it too experiences larger lateral forces and yaw moments. The various length ratios are investigated for a wider range of water depths and separation distances to produce a larger database from which the size effect could be included in the empirical formulae. Since the maximum lateral force and yaw moment coefficients acting on the slower Ship 2 are larger, the size effect is investigated for this ship. Numerical calculations are carried out on Ship 2, which size is kept constant, while Ship 1 is scaled geometrically. The different cases are studied for various separation distances and water depths, which are non-dimensionalized by the length and draught of Ship 2 respectively.

From the results it is apparent that the ship size effect for the overtaking manoeuvre is the same as for the two ship meeting manouevre; the increase in maximum lateral force coefficients for different L_2/L_1 ratios have similar increasing trend for decreasing Sp/L_2. This is the case for all H/D_2 ratios of 1.3, 1.5 and 2.0. However, the actual water depth for the two first depth-draught ratios limit the size of Ship 1, and as a result the range of L_2/L_1 ratios.

It became clear from the investigation that the ship size effect could be expressed with the same multiplication factor as obtained from two ship meeting situation. The empirical formulae for the maximum lateral force and yaw moment coefficients, derived from the $L_2/L_1 = 1.0$ case, are modified with an addition of the following factor to take account for the ship size effect:

$$\left(L_2/L_1\right)^{-2.19} \tag{4.14}$$

The present method assumes similar ship size effect for the maximum lateral force and yaw moment coefficients acting on the faster Ship 1. As a result the same multiplication factor described in eqn (4.14) is added to the respectively $L_1/L_2 = 1.0$ case. This is then on the following form.

$$\left(L_1/L_2\right)^{-2.19} \tag{4.15}$$

4.5.3 Ship speed variation

Previously, the present method has only considered the overtaking situation where Ship 1 has twice the speed of Ship 2. Here empirical multiplication factors are derived to take into account the effect of various relative speeds. These multiplication factors are added to the already derived empirical formulae for the maximum lateral force and yaw moment coefficients where Ship 1 has twice the speed of Ship 2. The speed effect is only examined for one particular situation; $Sp/L = 0.5$, $H/D = 1.0$ and $L_1/L_2 = 1.0$. The present method assumes equal ship speed effect for all separation distances,

water depths and ship sizes, because of the linear tendencies for the maximum lateral force coefficients and yaw moment coefficients.

Maximum lateral force coefficient acting on Ship 1

From the parametric study of the ship speed effect (section 4.4.4) it is apparent that the maximum lateral forces and yaw moments acting on the faster Ship 1 in general increases linearly as the U_2/U_1 ratio decreases. At the bow-stern situation we add a multiplication factor to the empirical formula to take the speed effect into account for the maximum attraction force coefficient, derived from the $U_2/U_1 = 0.5$ case (Equal $U_1/U_2 = 2.0$):

$$M.CF1_{Bow-Stern} = 1 - {1.333}/{2} - 1.333\left({\Delta U}/{U_1}\right) \tag{4.16}$$

where $\Delta U = U_2 - U_1$

A similar factor is derived for the maximum repulsion force coefficient at the midship-midship situation and is found to be on the following form:

$$M.CF1_{Midship-Midship} = 1 - {2.842}/{2} - 2.842\left({\Delta U}/{U_1}\right) \tag{4.17}$$

Since Ship 1 does not experience a fully linear increase in repulsion forces at the midship-midship situation for decreasing U_2/U_1, the multiplication factor in eqn (4.17) does not give maximum repulsion force coefficients as accurate as for the maximum attraction force coefficients.

Maximum yaw moment coefficient acting on Ship 1

For the maximum yaw moment coefficients the tendency is found to be somewhat different. As U_2/U_1 decreases, i.e. the relative speed between Ship 1 and Ship 2 enlarges, Ship 1 experiences larger yaw moments. However, the tendency for the maximum yaw moment coefficient is linear, and hence the ship speed effect is

expressed empirically. The multiplication factor to be added to the empirical formulae for maximum bow-in moment coefficients derived for the $U_2/U_1 = 0.5$ case is as follows:

$$M.CM1_{Bow-Stern} = 1 + 0.315/2 + 0.315\left(\Delta U/U_1\right) \tag{4.18}$$

and the multiplication factor for the maximum bow-in moment coefficients at the stern-midship situation is found to be:

$$M.CM1_{Stern-Midship} = 1 + 0.593/2 + 0.593\left(U_2/U_1\right) \tag{4.19}$$

Maximum lateral force coefficient acting on Ship 2

As described earlier, the maximum lateral force coefficients increase linearly as U_1/U_2 increases. Again the empirical formulae from the $U_1/U_2 = 2.0$ case takes the ship speed effect into account by adding a multiplication factor, and is found to be as follows for the maximum repulsion force coefficients at the bow-stern situation:

$$M.CF2_{Bow-Stern} = 1 - 0.645 - 0.645\left(\Delta U/U_2\right) \tag{4.20}$$

Furthermore we have for the maximum attraction force coefficients at the midship-midship situation the following multiplication factor:

$$M.CF2_{Midship-Midship} = 1 - 0.884 - 0.884\left(\Delta U/U_2\right) \tag{4.21}$$

Finally the empirical formulae, for the maximum repulsion force coefficients at the stern-midship situation, takes the ship speed effect into account by adding the following linear factor:

$$M.CF2_{Stern-Midship} = 1 - 0.978 - 0.978\left(\Delta U / U_2\right) \tag{4.22}$$

Maximum yaw moment coefficient acting on Ship 2

The multiplication factor to the empirical formulae for the maximum yaw moment coefficients is very similar and is found to be:

$$M.CM2_{Bow-Midship} = 1 - 0.337 - 0.337\left(\Delta U / U_2\right) \tag{4.23}$$

for the maximum bow-out moment coefficients acting on Ship 2 as the bow of Ship 1 passes the midship of Ship 2, and

$$M.CM2_{Stern-Midship} = 1 - 0.318 - 0.318\left(\Delta U / U_2\right) \tag{4.24}$$

for the maximum bow-in moment coefficients at the stern-midship situation. Both these linear factors in eqns (4.23) and (4.24) are added to the earlier derived empirical formulae for the situation of Ship 1 having twice the speed of Ship 2.

4.5.4 Overall new empirical formulae

By gathering the various empirical formulae for the different peak values the maximum lateral force and yaw moment coefficients are expressed by the following overall formulae both for the faster Ship 1 and for the slower Ship 2.

Faster Ship 1

For the faster ship in an overtaking manoeuvre, the following new empirical formula can be used to calculate the maximum lateral force coefficients:

$$CF1_i = Y1_i^{ps}\left(Sp/L_1\right)^{\kappa_i}\left[1+Y1_i^{pd}\left(D_1/H\right)\right]^{\lambda_i}\left(H/D_1\right)^{\lambda_i}\left(L_1/L_2\right)^{\delta}\left[1+Y1_i^{pu}/2+Y1_i^{pu}\left(\Delta U/U_1\right)\right] \qquad i = 1,2$$

where p denotes the passing manoeuvre and
i = 1 denotes the bow-stern situation
i = 2 denotes the midship-midship situation

and $\Delta U = U_2 - U_1$

The different constants for maximum lateral force coefficients can be seen in Table 4.5 below:

	Bow-Stern	Midship-Midship
$Y1^{ps}$	-0.022	0.025
$Y1^{pd}$	-0.90	-0.90
$Y1^{pu}$	-1.333	-2.842
κ	-0.90	-1.00
λ	-0.74	-0.55
δ	-2.19	-2.19

Table 4.5 Coefficients for the maximum lateral force coefficients acting on the faster Ship 1, (two ships passing).

Similarly, the new empirical formula for the maximum yaw moment coefficients is found to be:

$$CM1_i = N1_i^{ps}\left(Sp/L_1\right)^{\mu_i}\left[1+N1_i^{pd}\left(D_1/H\right)\right]^{\nu_i}\left(H/D_1\right)^{\nu_i}\left(L_1/L_2\right)^{\delta}\left[1+N1_i^{pu}/2+N1_i^{pu}\left(\Delta U/U_1\right)\right] \qquad i = 1,2$$

where p denotes the passing manoeuvre and
i = 1 denotes the bow-midship situation
i = 2 denotes the stern-midship situation

and $\Delta U = U_2 - U_1$

The constants for the maximum yaw moment coefficients are given in Table 4.6 below:

	Bow-Midship	Stern-Midship
$N1^{ps}$	-0.041	0.026
$N1^{pd}$	-0.60	-0.70
$N1^{pu}$	0.315	0.593
μ	-0.54	-0.68
ν	-1.00	-1.00
δ	-2.19	-2.19

Table 4.6 Coefficients for the maximum yaw moment coefficients acting on the faster Ship 1, (two ships passing).

Slower Ship 2

The new empirical formula for the maximum lateral force coefficients acting on the slower ship in an overtaking manoeuvre is found to be:

$$CF2_i = Y2_i^{ps}\left(1+Sp/L_2\right)^{\tau_i}\left[1+Y2_i^{pd}\left(D_1/H\right)\right]^{\upsilon_i}\left(H/D_1\right)^{\upsilon_i}\left(L_2/L_1\right)^{\delta}\left[1+Y2_i^{pu}+Y2_i^{pu}\left(\Delta U/U_2\right)\right] \qquad i = 1,2,3$$

where p denotes the passing manoeuvre and
i = 1 denotes the bow-stern situation
i = 2 denotes the midship-midship situation
i = 3 denotes the stern-bow situation

and $\Delta U = U_2 - U_1$

The different constants for maximum lateral force coefficients can be seen in Table 4.7 below:

	Bow-Stern	Midship-Midship	Stern-Bow
$Y2^{ps}$	0.68	-1.12	0.52
$Y2^{pd}$	-0.85	-0.85	-0.85
$Y2^{pu}$	-0.645	-0.884	-0.978
τ	-5.10	-4.70	-5.10
υ	-0.85	-0.85	-0.85
δ	-2.19	-2.19	-2.19

Table 4.7 Coefficients for the maximum lateral force coefficients acting on the slower Ship 2, (two ships passing).

The new empirical formula for the maximum yaw moment coefficients is on the following form:

$$CM2_i = N2_i^{ps}\left(1+{Sp}/{L_2}\right)^{\omega_i}\left[1+N2_i^{pd}\left({D_2}/{H}\right)\right]^{\psi_i}\left({H}/{D_2}\right)^{\psi_i}\left({L_2}/{L_1}\right)^{\delta}\left[1+N2_i^{pu}+N2_i^{pu}\left({\Delta U}/{U_2}\right)\right] \qquad i = 1,2$$

where and p denotes the passing manoeuvre and
i = 1 denotes the bow-midship situation
i = 2 denotes the stern-midship situation

and $\Delta U = U_2 - U_1$

The constants for the maximum yaw moment coefficients are given in the Table 4.8 below:

	Bow-Midship	Stern-Midship
$N2^{ps}$	0.51	-0.44
$N2^{pd}$	-0.85	-0.85
$N2^{pu}$	-0.337	-0.318
ω	-5.00	-4.70
ψ	-0.70	-0.70
δ	-2.19	-2.19

Table 4.8 Coefficients for the maximum yaw moment coefficients acting on the slower Ship 2, (two ships passing).

4.6 PRACTICAL APPLICATION

Similar to the two ships meeting manoeuvre, graphs are made to identify safe and unsafe operations for the two ships passing manoeuvre. The yaw moments acting on the faster Ship 1 are small and hence the rudder can withstand the interaction moments and keep it travelling at a straight line for all conditions. However, the slower Ship 2 experiences much larger yaw moments, resulting in the regions for unsafe operations.

Again, the area of the rudder on Ship 2 is taken as 2% of the product L times D. The situations where the hydrodynamic moments are larger than the rudder moments can now be found by utilizing Clark's formulae (see the Appendix 2).

Figures 4.22a,b,c show which regions are below the point of rudder adequacy. Once more, if Ship 2 is travelling in conditions under the curves, unsafe operations occur. In all cases the maximum bow-out moments at the bow-midship situation are larger than the maximum bow-in moments at the stern-midship situation. It is apparent that when Ship 2 is overtaken by a bigger and a much faster Ship 1, the regions of unsafe operations becomes larger (i.e. the area below the curves becomes larger). However, since the separation distances are non-dimensionalized by the length of Ship 2, we have zero distance between the ship-sides when Sp/L = 0.17, which are drawn as a dotted line denoted "Zero distance". Furthermore, the minimum separation distance can be found for different speed ratios, other than plotted in the figures, by linear interpolation.

Even if the rudder moment is smaller than the hydrodynamic moments, it is not certain that Ship 2 will collide, either with Ship 1 or the channel wall. However, when the rudder moment can not oppose the interaction moments, Ship 2 will experience difficulties when trying to keep a straight course. Again, a simulation study where the ships where free to move in the horizontal plane, would show if the ships were to collide. Such simulation investigations should be studied further.

4.7 CONCLUDING REMARKS

- The comparison with experimental data shows good qualitatively agreement, but quantitatively the result are not so good. However there are many uncertainties such as the width of test tank, ship speed etc.

- The comparisons with Yasukawa (1983) theoretical predictions of the lateral force and yaw moment coefficients, shows good tendency and value agreement, both for the faster ship (Ship 1) and the slower ship (Ship 2).

- Comparisons with Dand (1981b) show also good agreement of tendencies, but the peak values from the experimental data are much higher compared to those derived from the present method. However, there are many uncertainties involved with these comparisons. Dand's report do not give the exact speed of the ship models used in the test runs, only the relative speed. As a result, the speeds used by the present method are assumed.

- Parametric studies show that the interactive forces and moments increase as the separation distance and depth-draught ratio decrease. It is also evident that a slower and smaller ship experiences larger lateral forces and yaw moments.

- New empirical formulae are derived based on the peak values from the non-dimensionalized force and moment curves, which describe the force and moment transits the ships experience during an overtaking manoeuvre. These new empirical formulae for the maximum lateral force and yaw moment coefficients takes into account the effect of separation distance, water depth, ship size and speed.

- Graphs are produced to illustrate the regions where safe and unsafe operations are identified (i.e. when the rudder moment is smaller than the interaction moments).

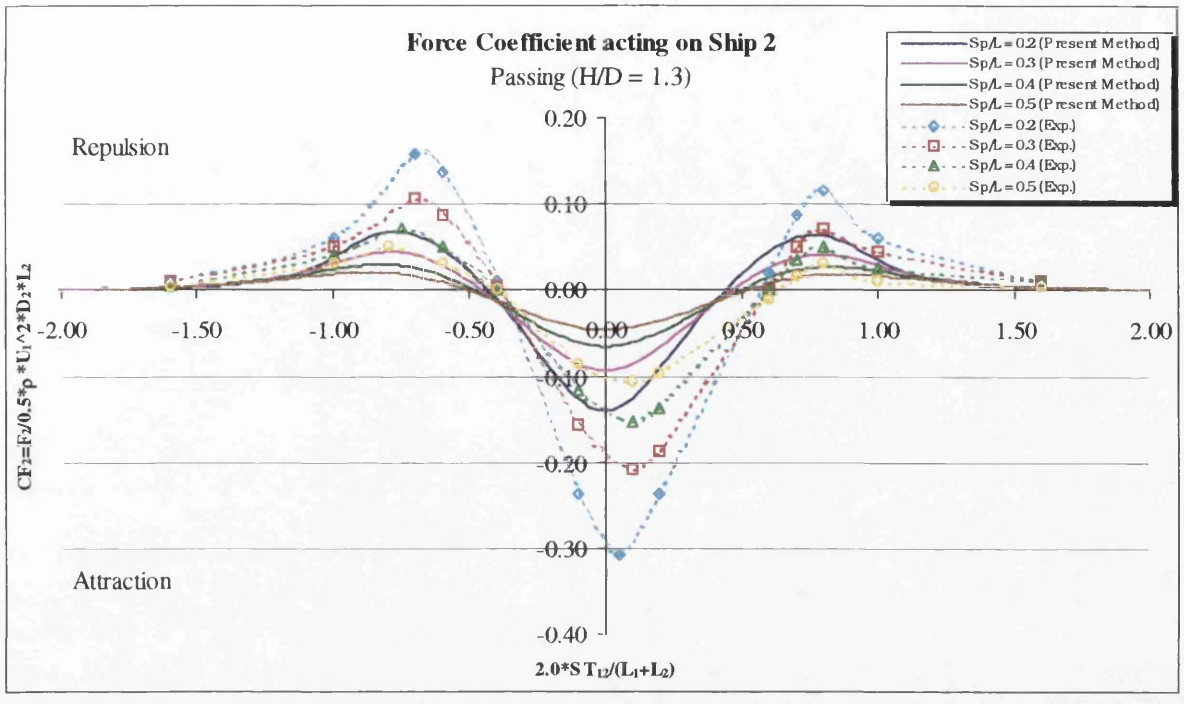

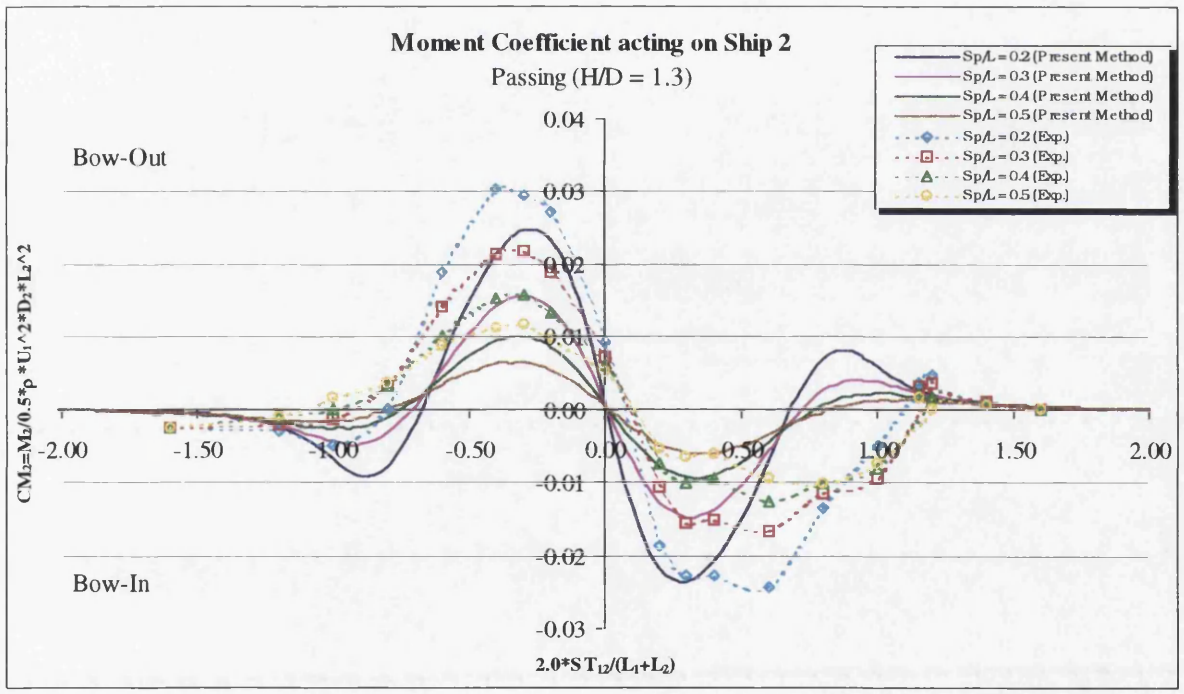

Figs 4.2a,b Comparison of the lateral force and yaw moment coefficients with Yasukawa's experimental data for various separation distances, (two ships passing)

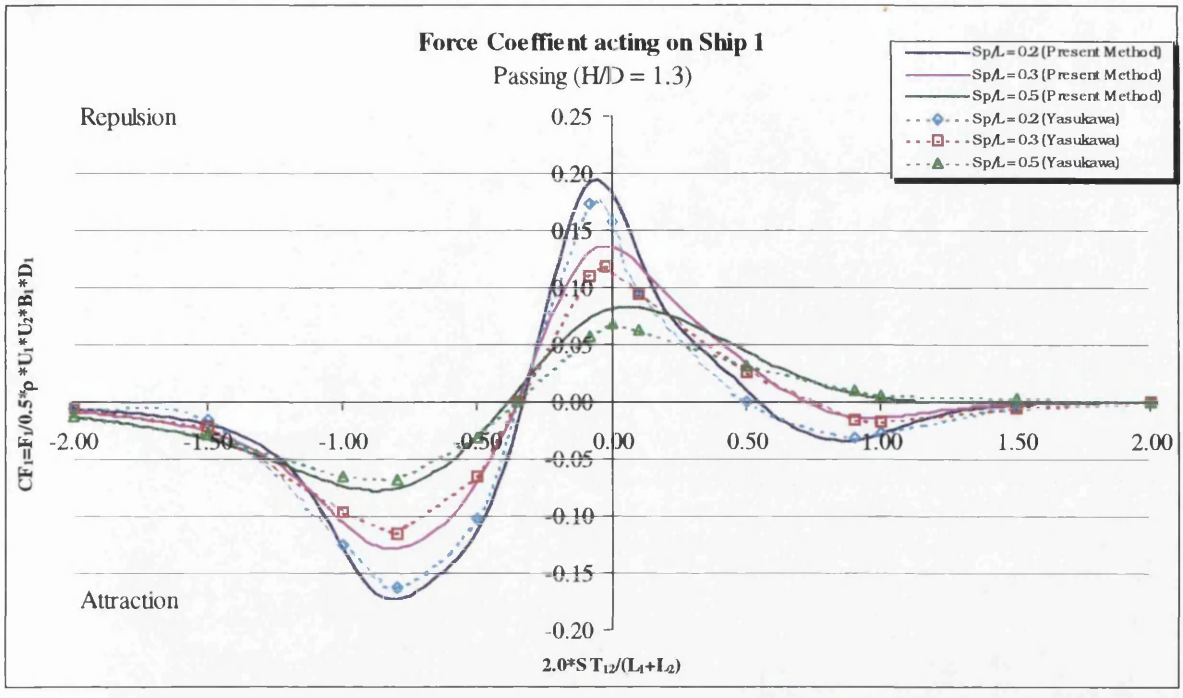

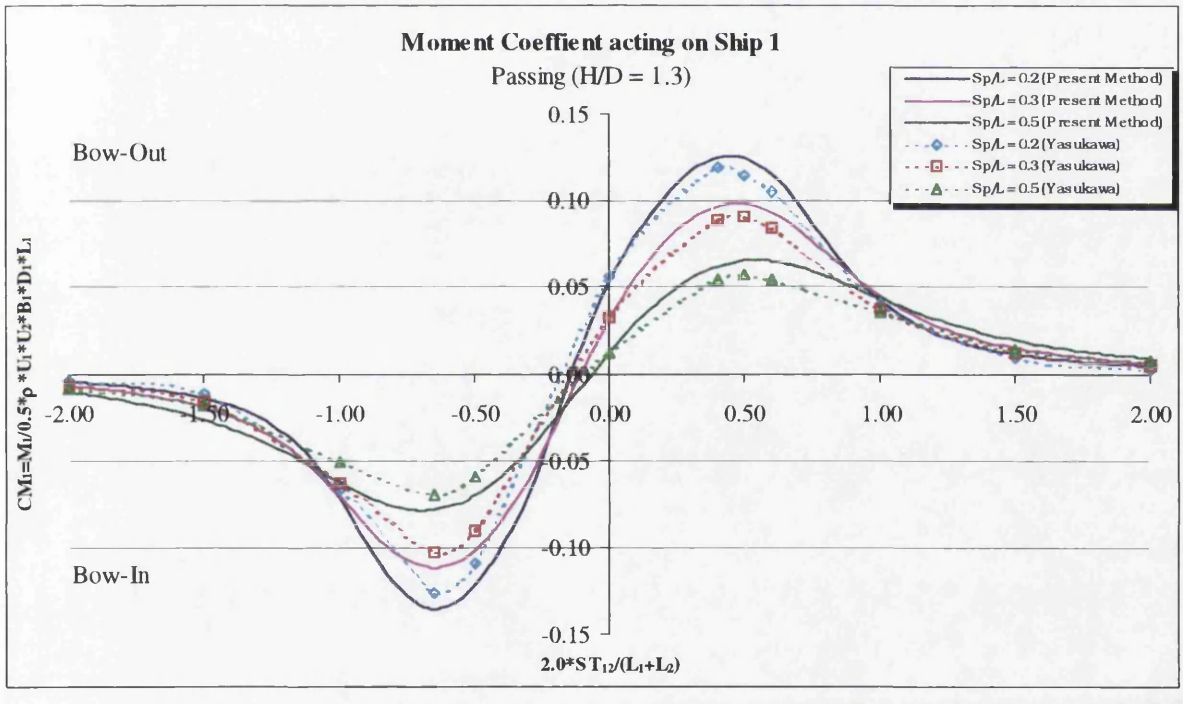

Figs 4.3a,b Comparison of the lateral force and yaw moment coefficients acting on the faster Ship 1 with Yasukawa's theoretical data for various separation distances, (two ships passing)

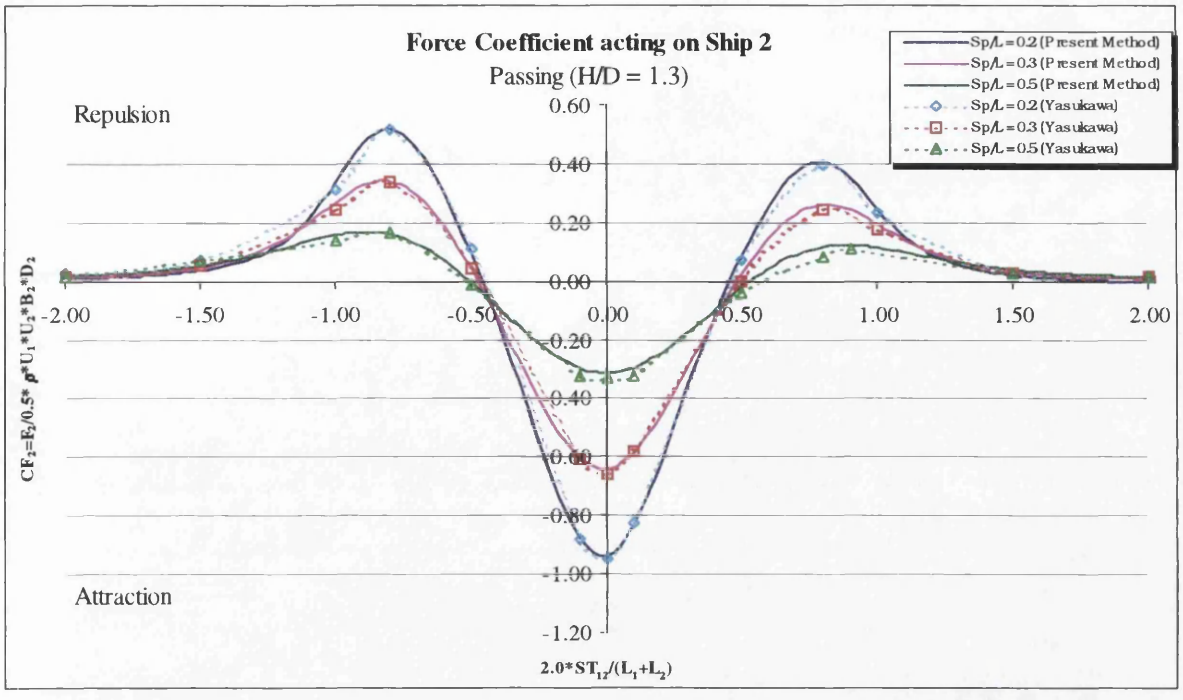

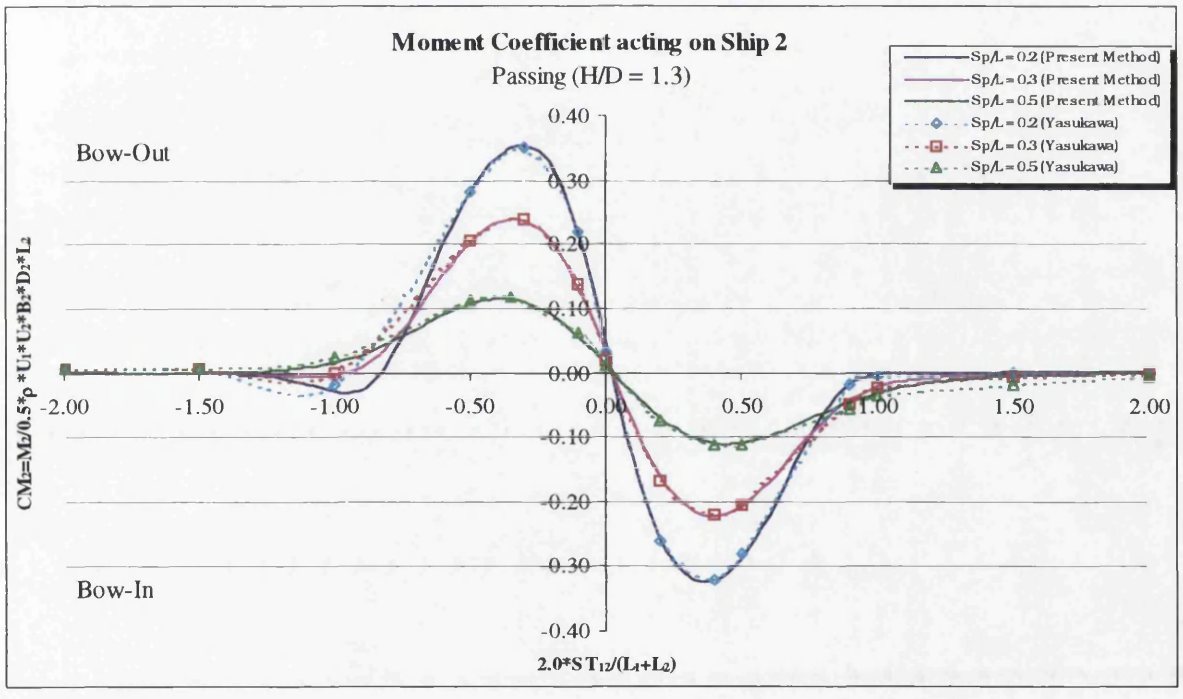

Figs 4.3c,d Comparison of the lateral force and yaw moment coefficients acting on the slower Ship 2 with Yasukawa's theoretical data for various separation distances, (two ships passing)

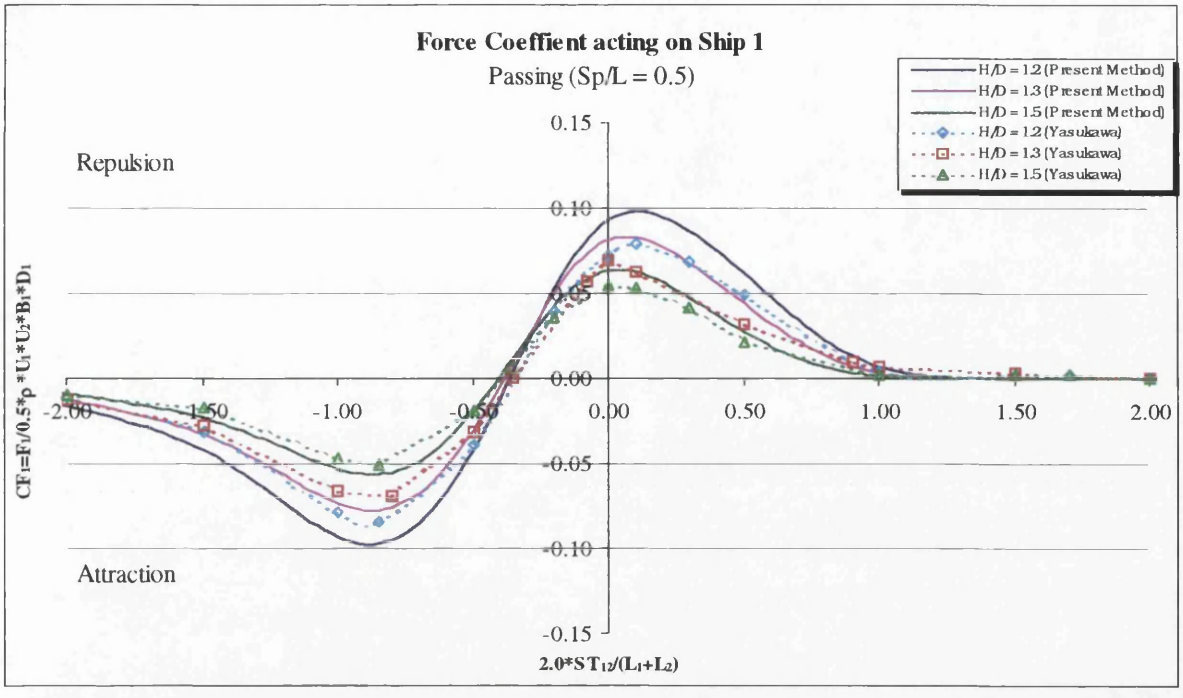

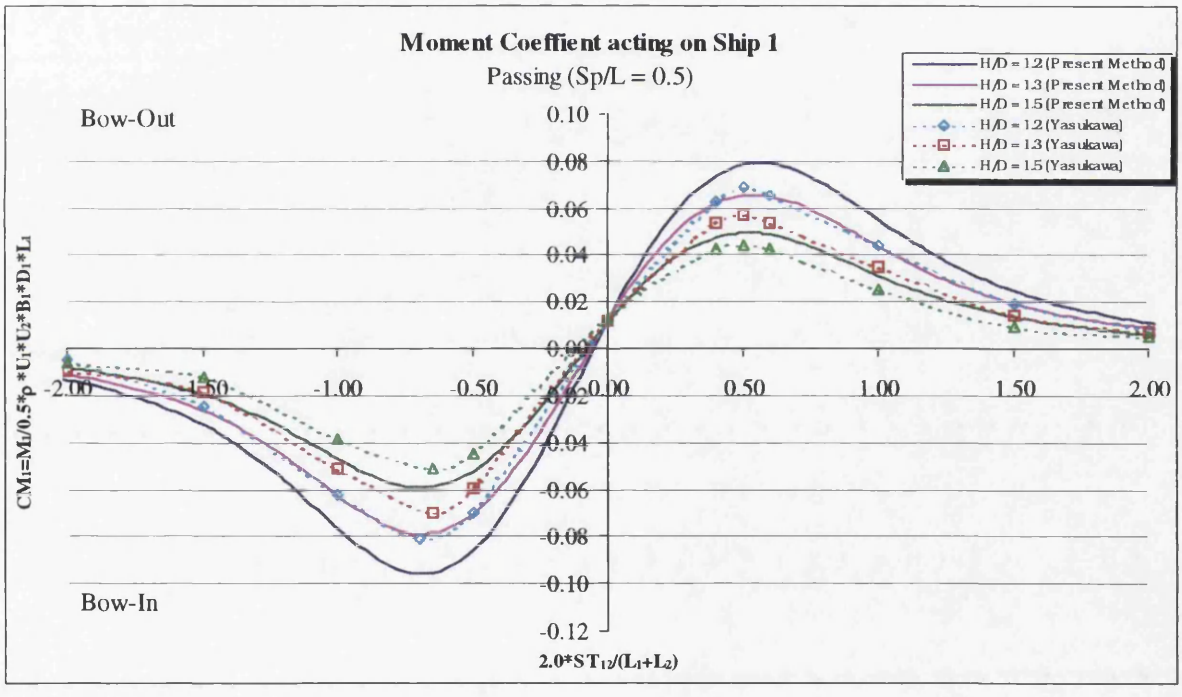

Figs 4.4a,b Comparison of the lateral force and yaw moment coefficients acting on the faster Ship 1 with Yasukawa's theoretical data for various water depths, (two ships passing)

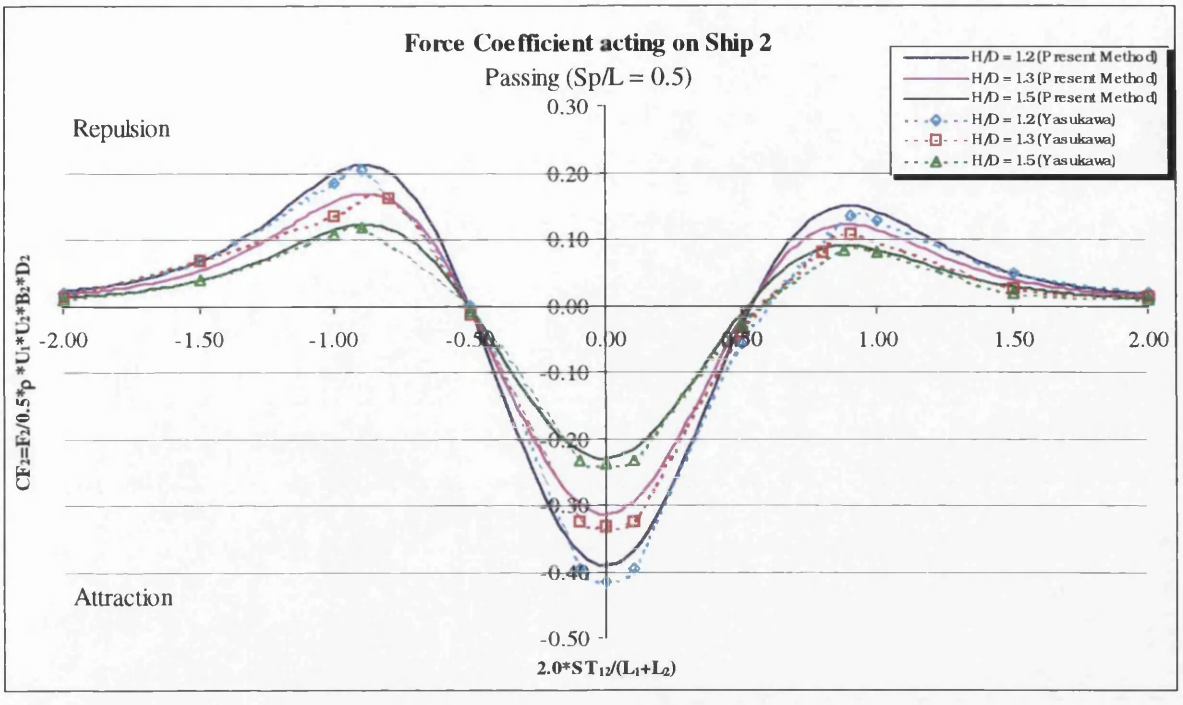

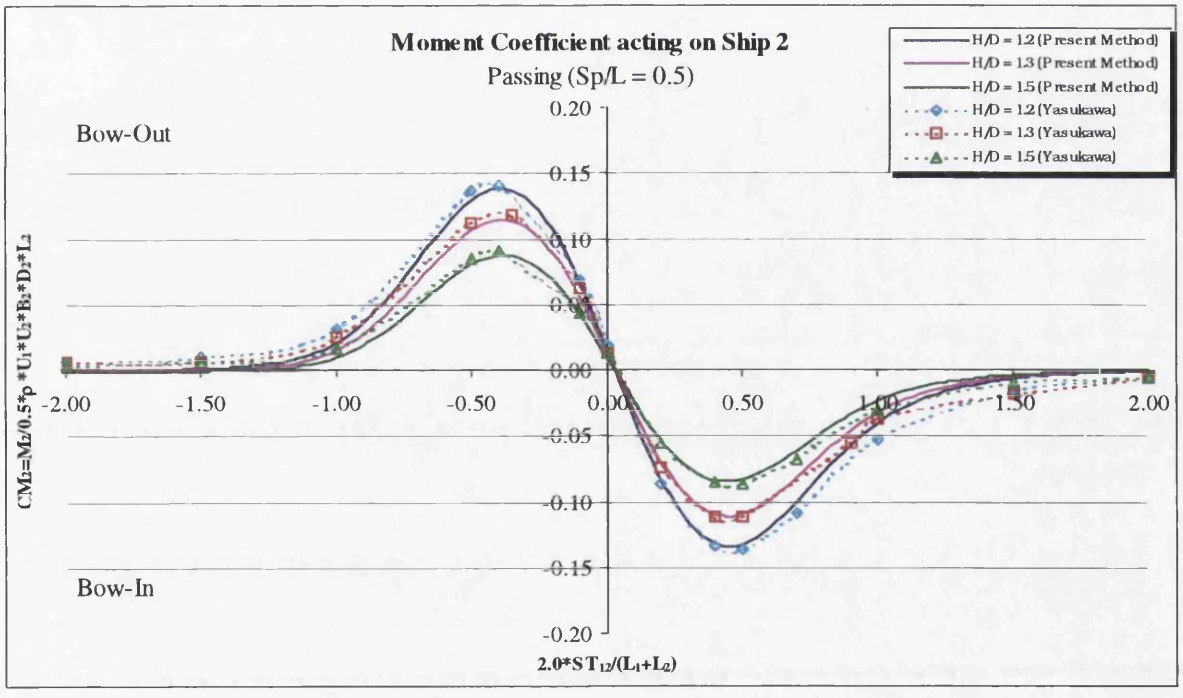

Figs 4.4c,d Comparison of the lateral force and yaw moment coefficients acting on the slower Ship 2 with Yasukawa's theoretical data for various water depths, (two ships passing)

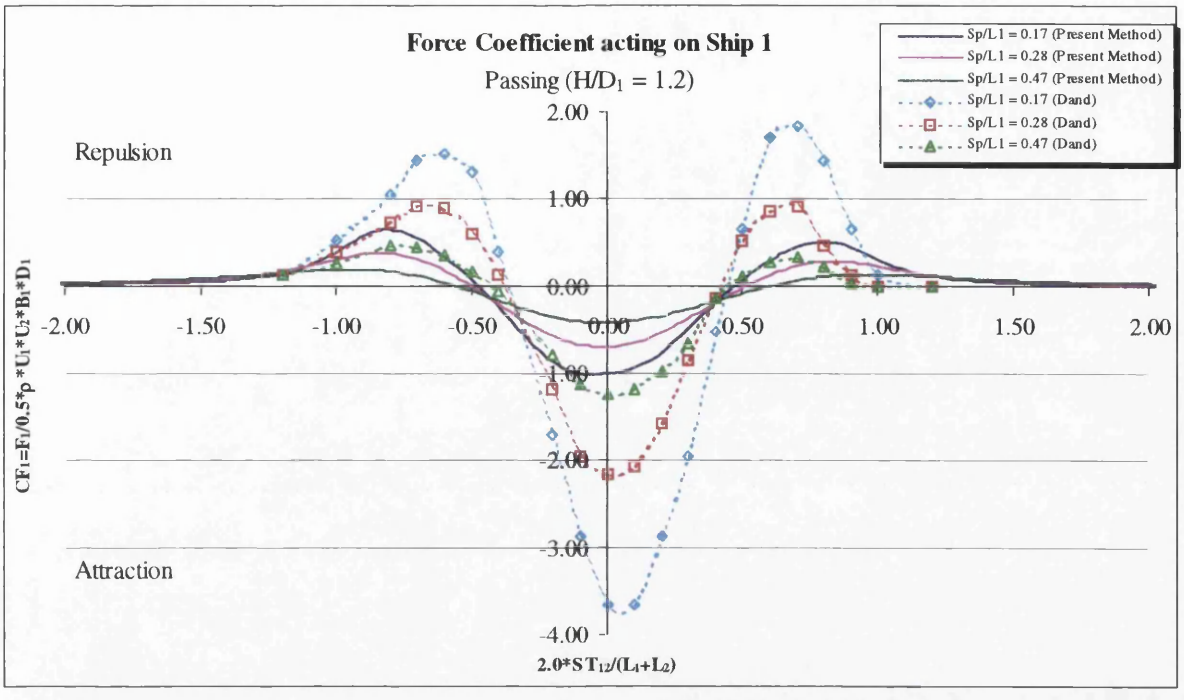

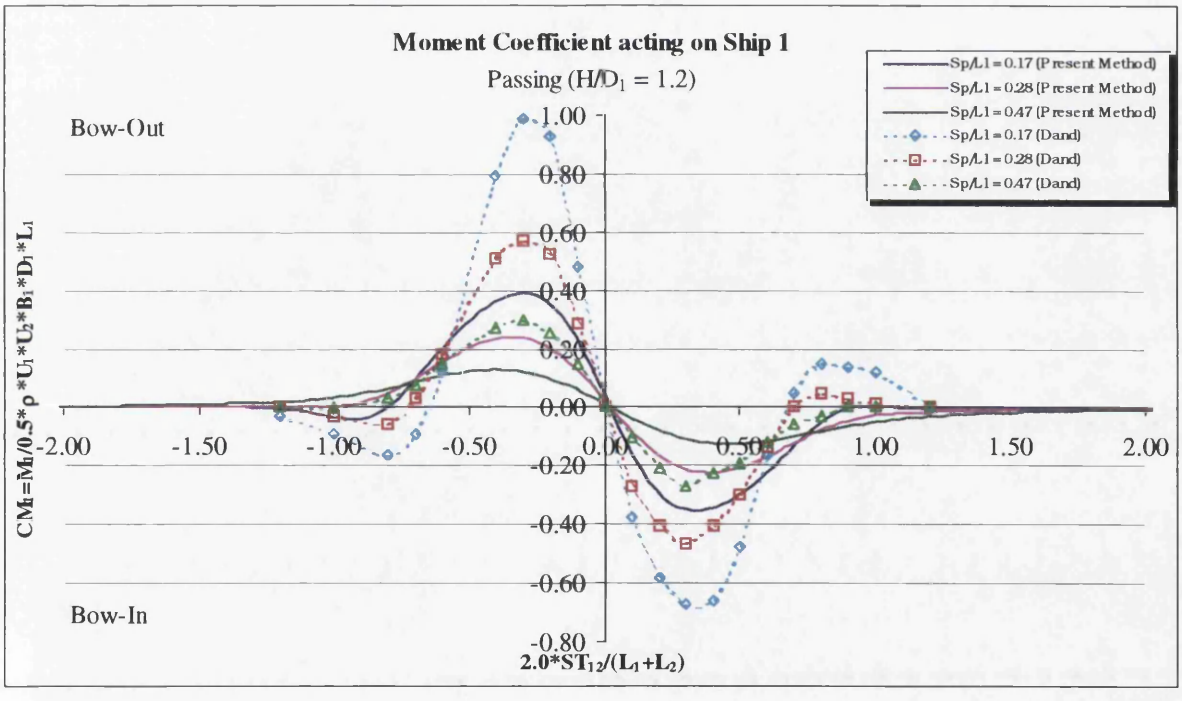

Figs 4.5a,b Comparison of the lateral force and yaw moment coefficients with Dand's experimental data, (two ships passing)

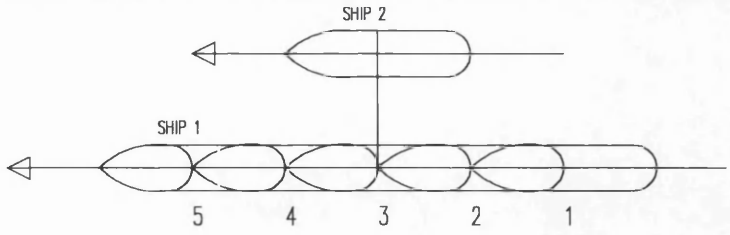

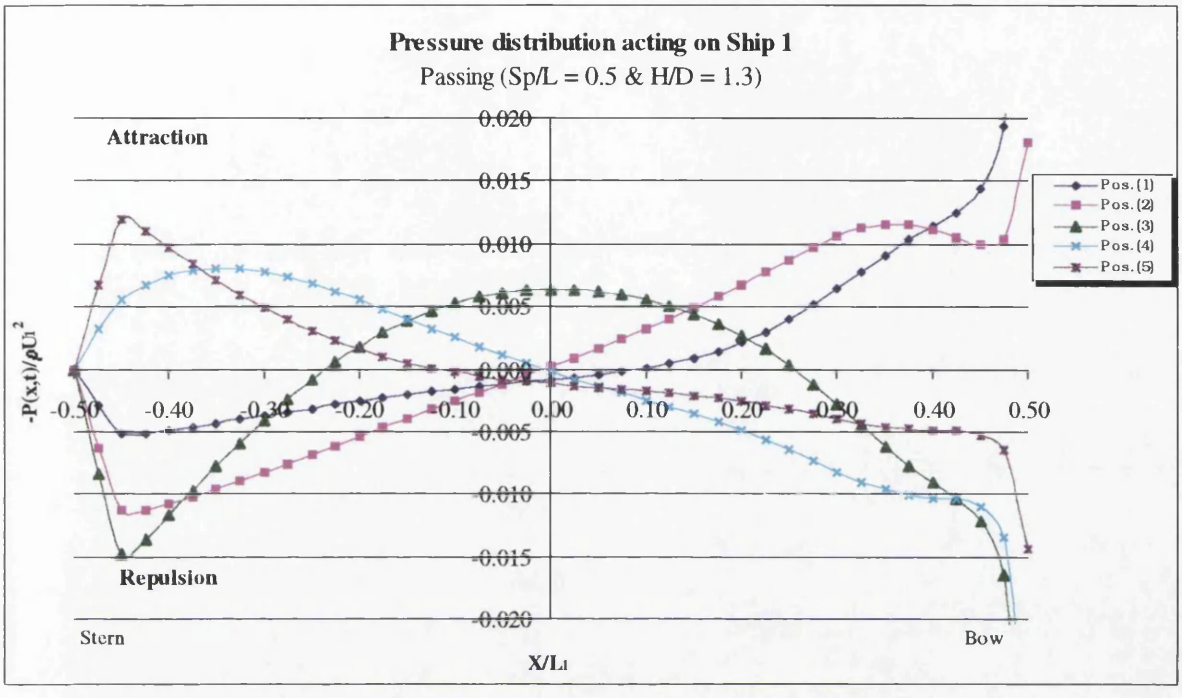

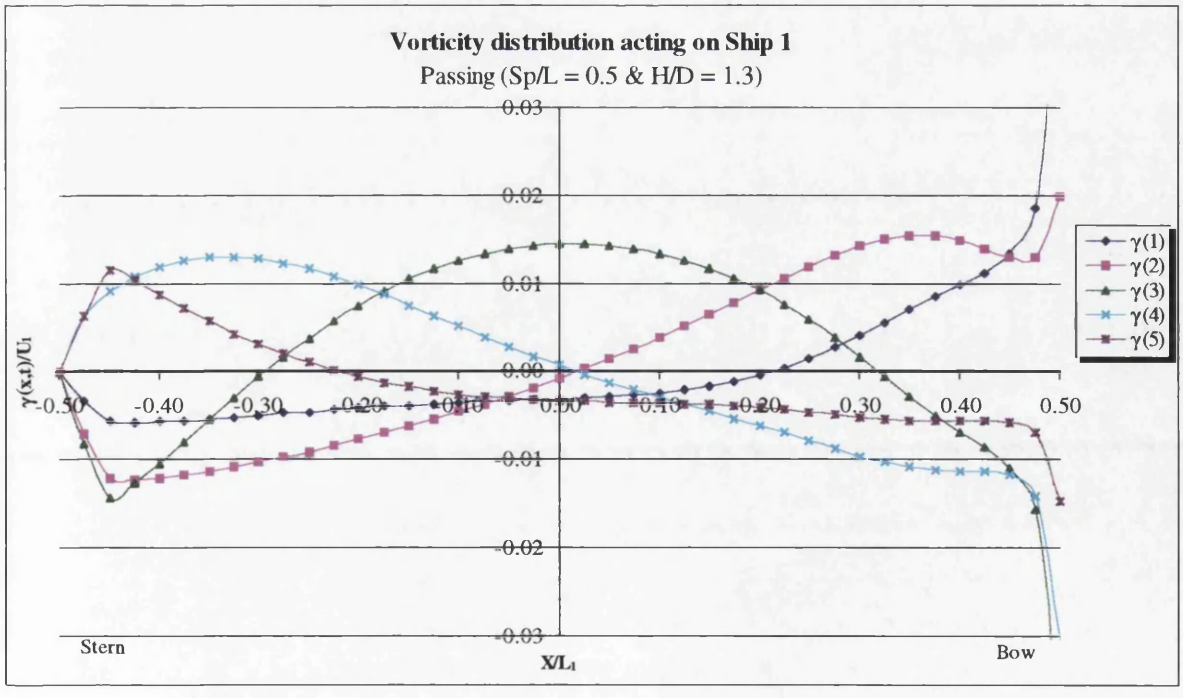

Figs 4.6a,b The pressure and vorticity distribution acting on the faster Ship 1 for different time steps, (two ships passing)

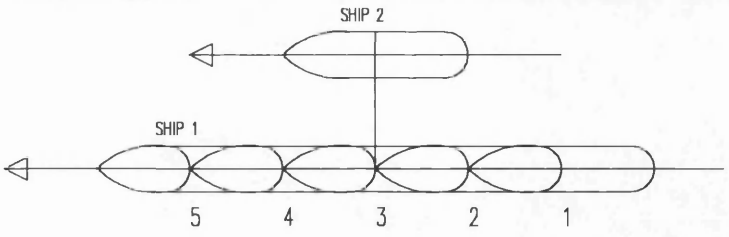

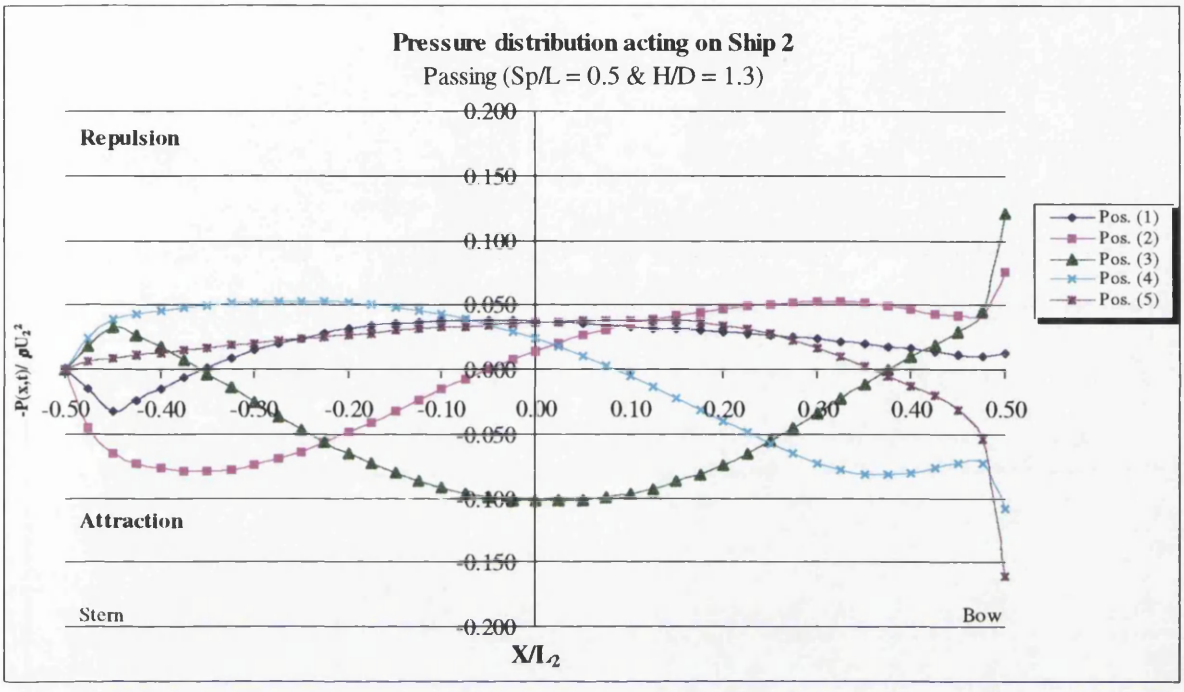

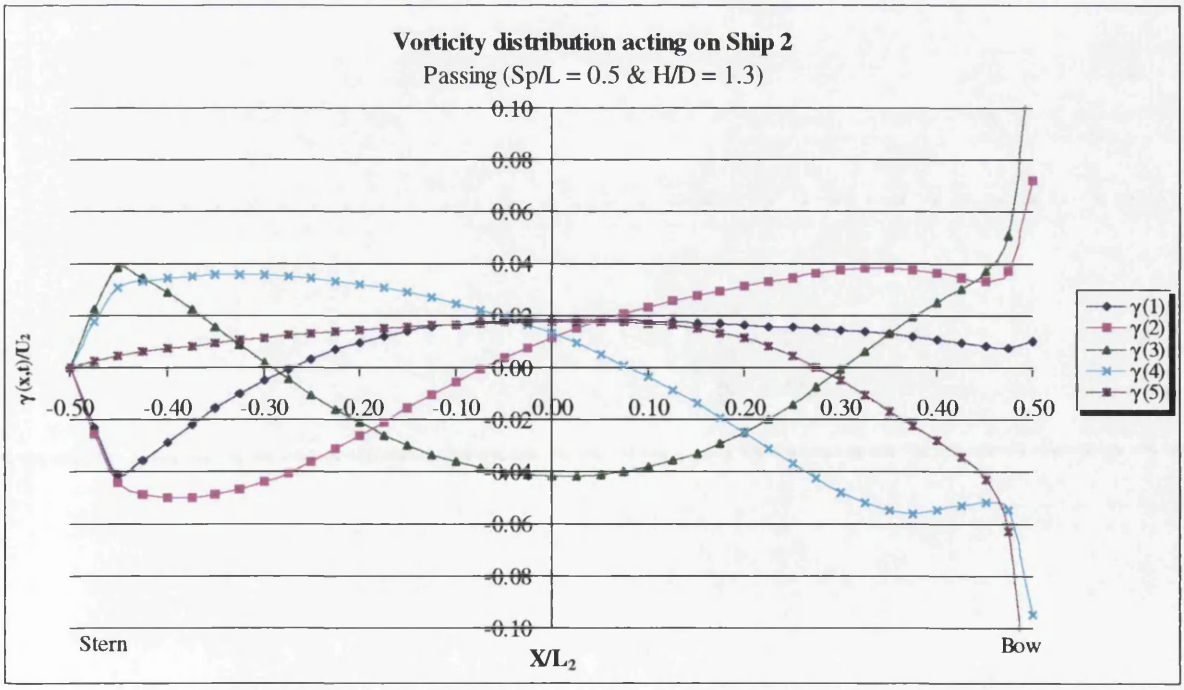

Figs 4.7a,b The pressure and vorticity distribution acting on the slower Ship 2 for different time steps, (two ships passing)

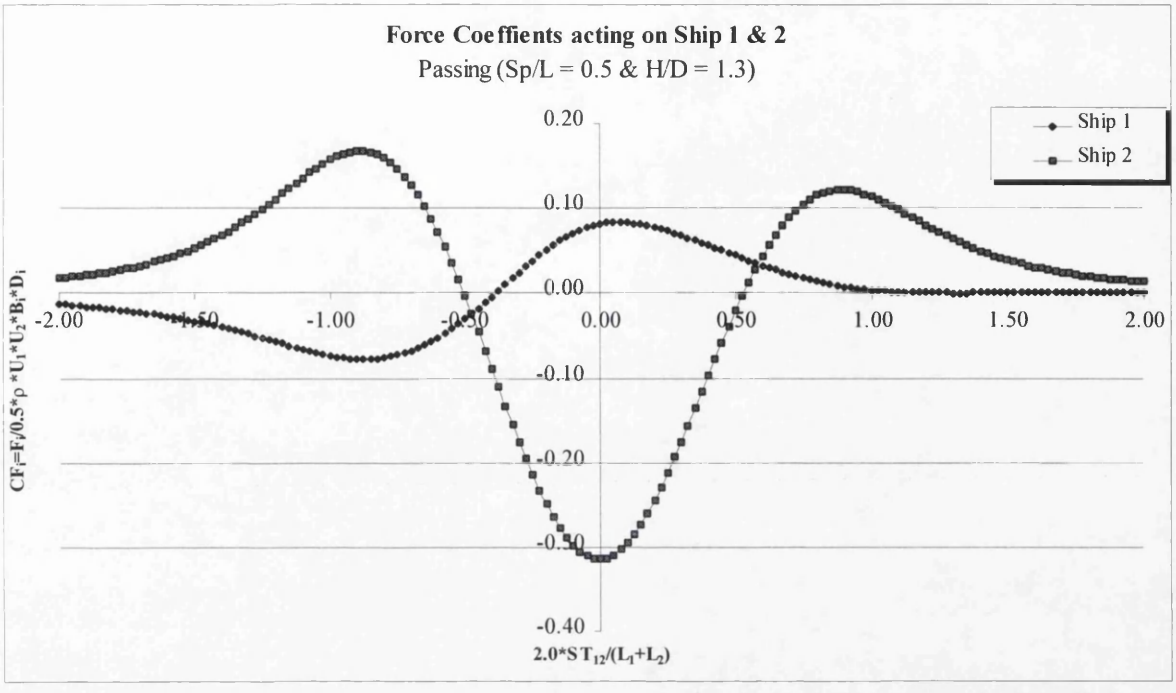

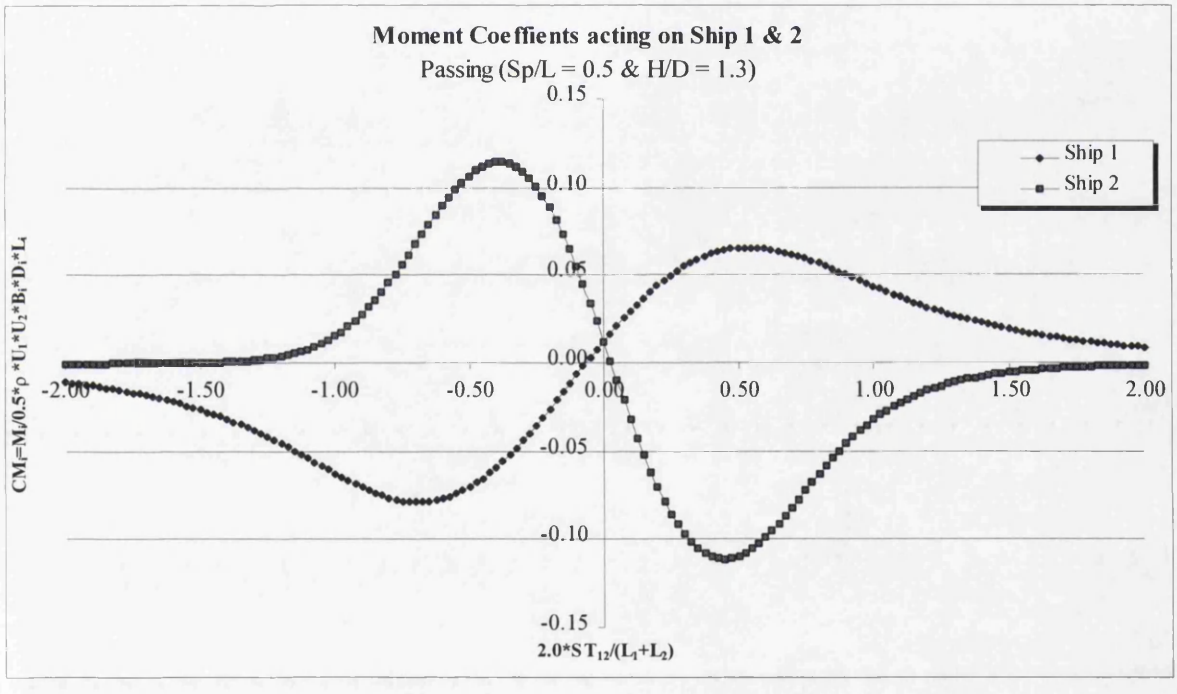

Figs 4.8a,b Comparison of the lateral force and yaw moment coefficients acting on the faster Ship 1 and the slower Ship 2, (two ships passing)

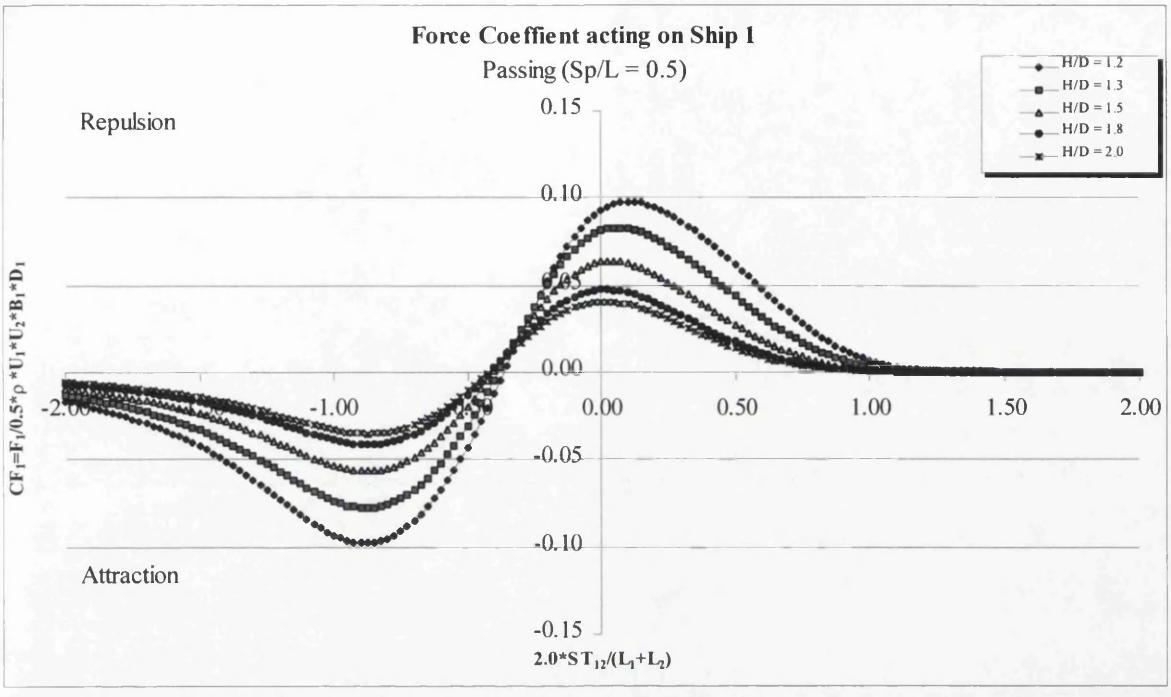

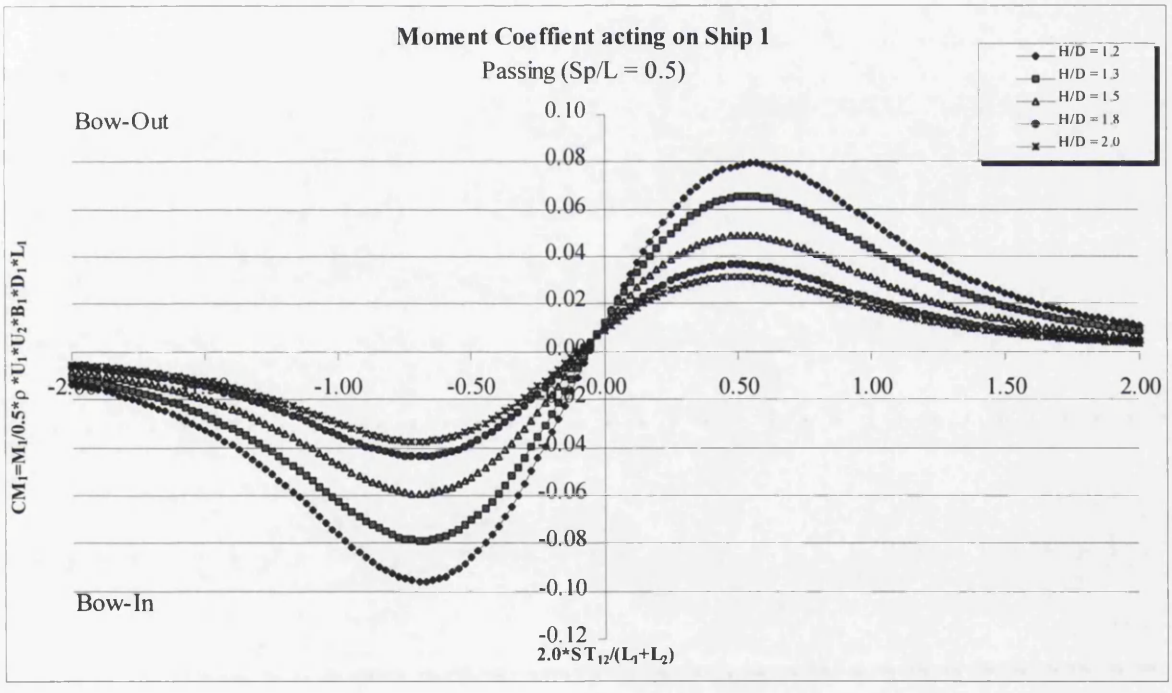

Figs 4.9a,b The lateral force and yaw moment coefficients acting on the faster Ship 1 for various water depths, (two ships passing)

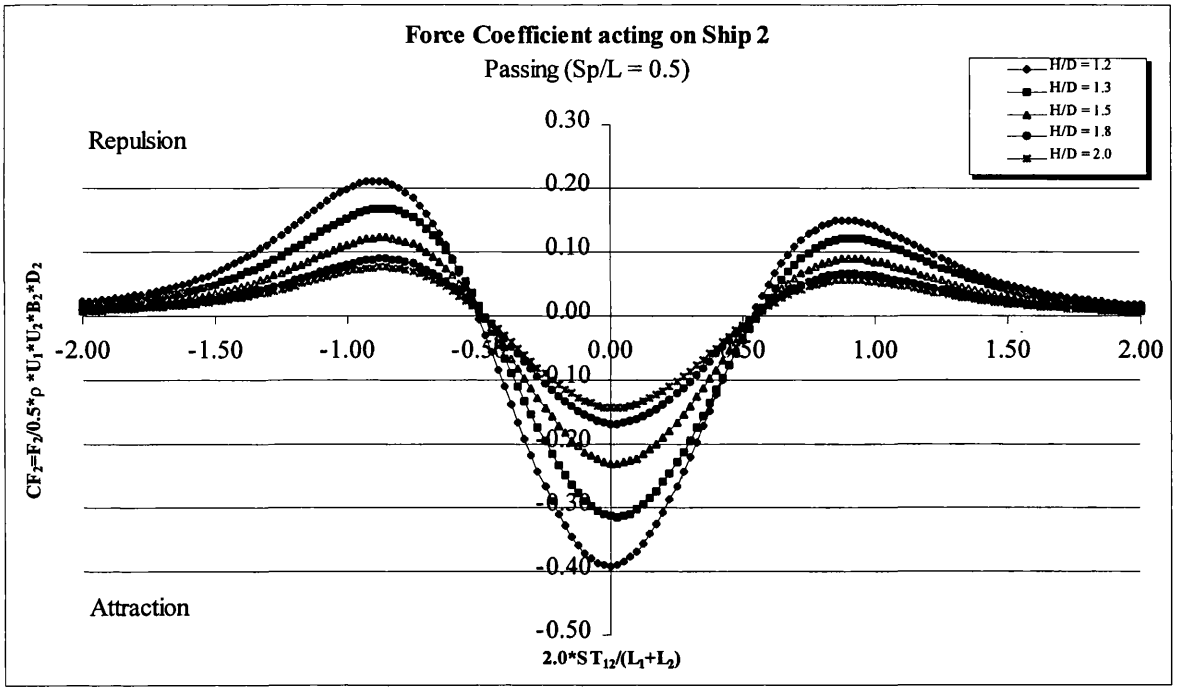

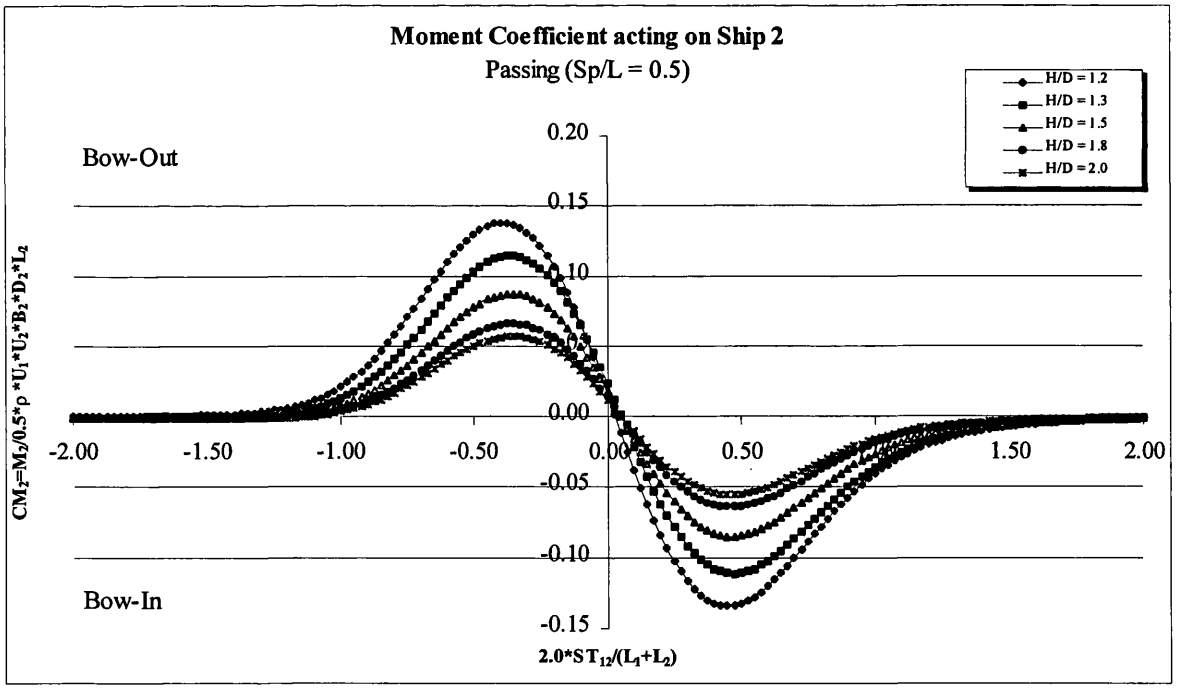

Figs 4.9c,d The lateral force and yaw moment coefficients acting on the slower Ship 2 for various water depths, (two ships passing)

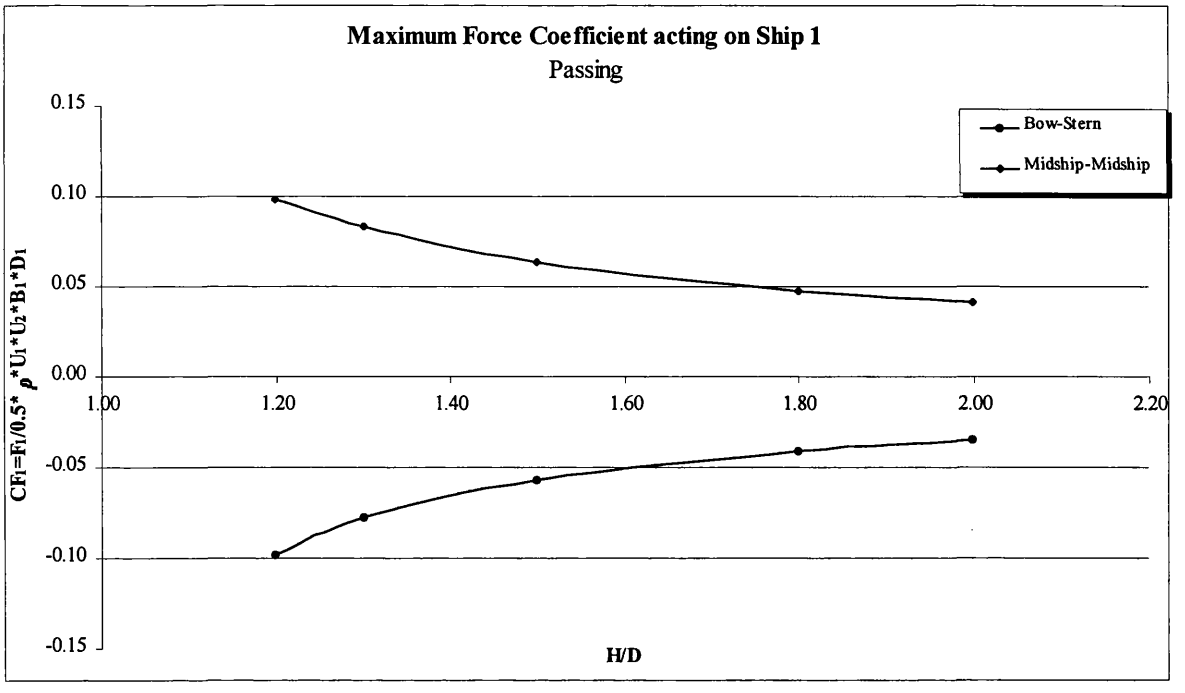

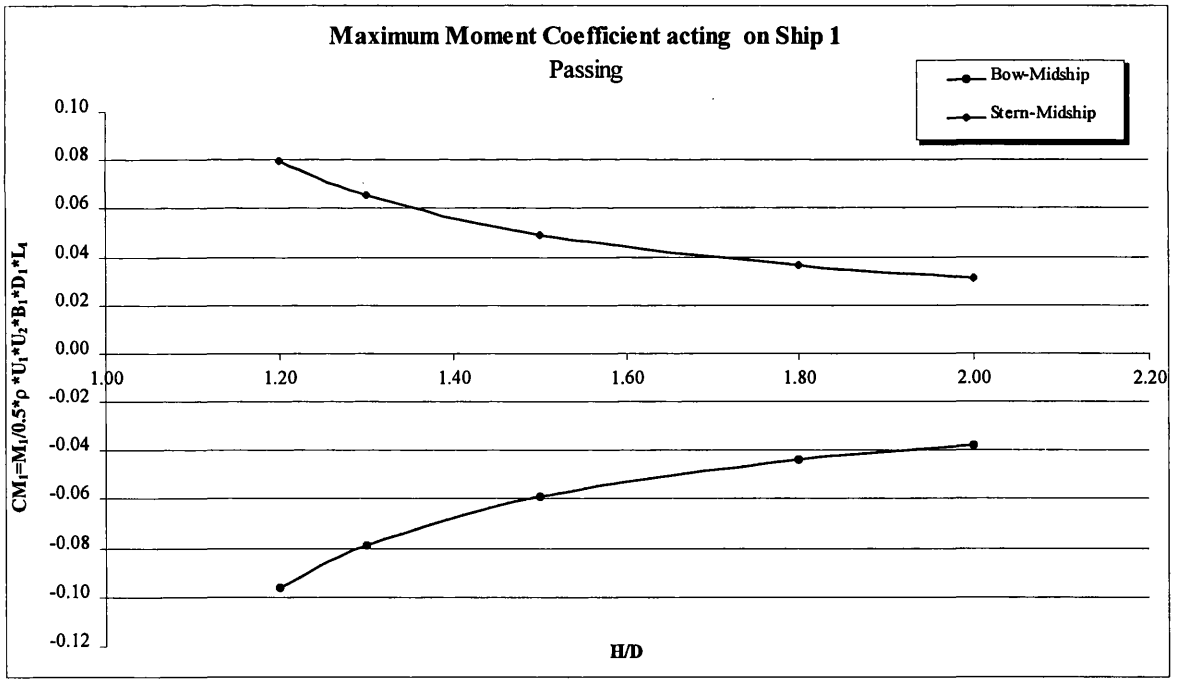

Figs 4.10a,b Maximum lateral force and yaw moment coefficients acting on the faster Ship 1 for various water depths, (two ships passing)

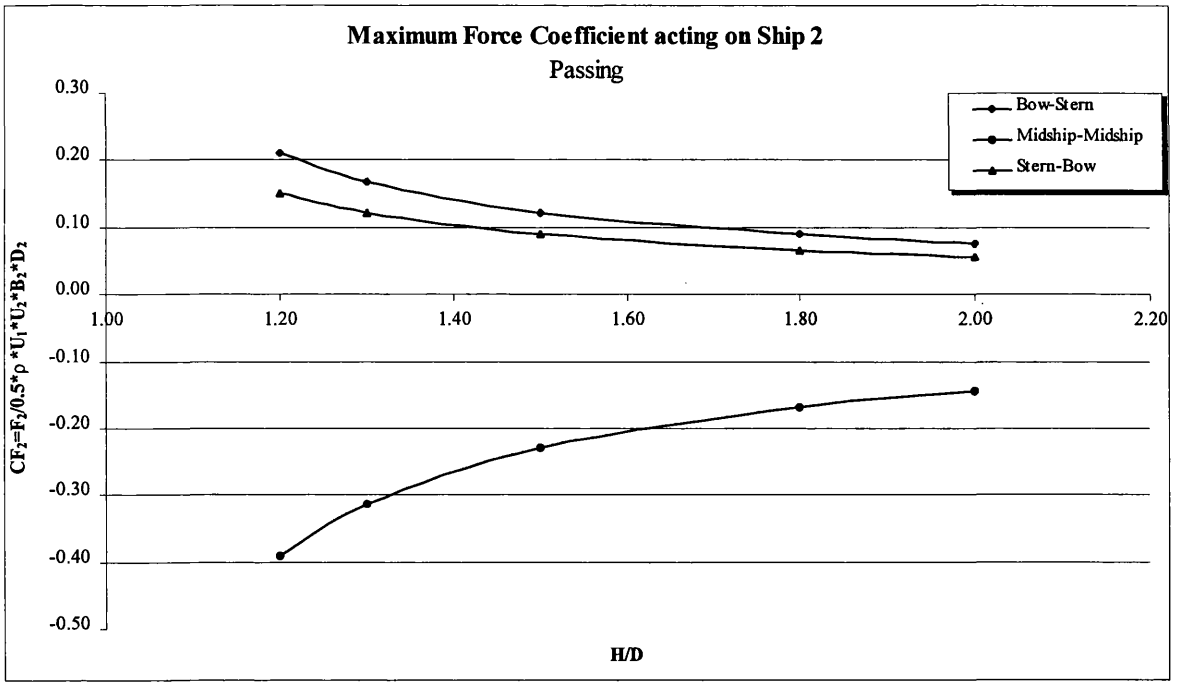

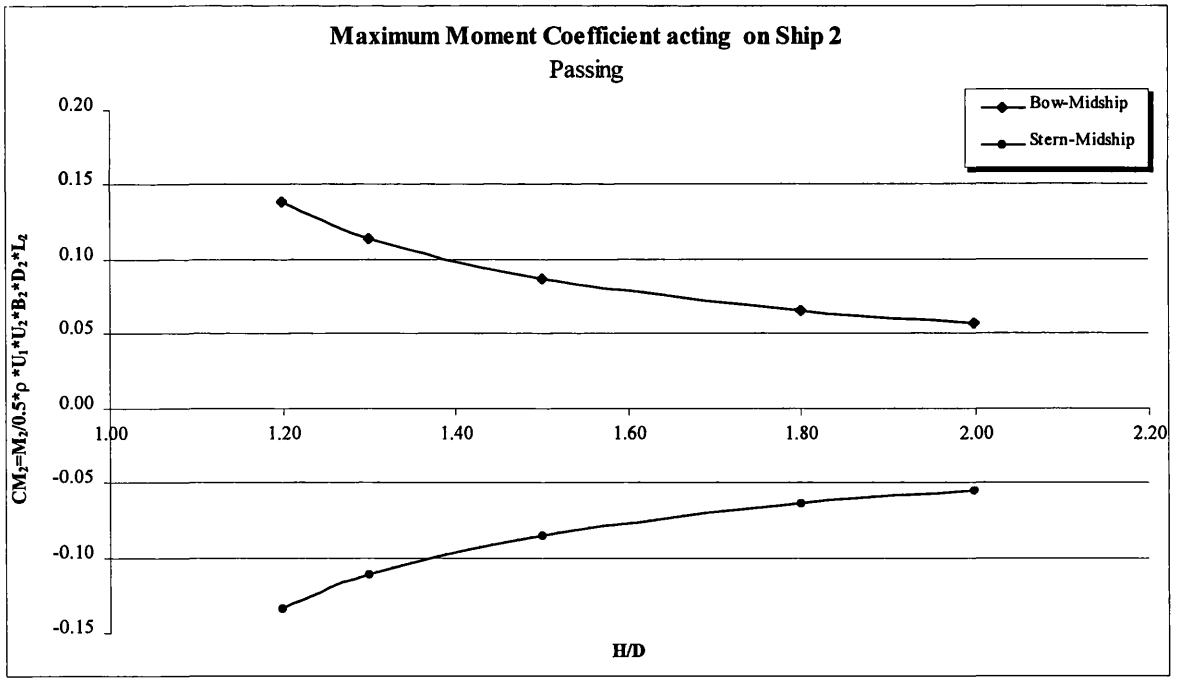

Figs 4.10c,d Maximum lateral force and yaw moment coefficients acting on the slower Ship 2 for various water depths, (two ships passing)

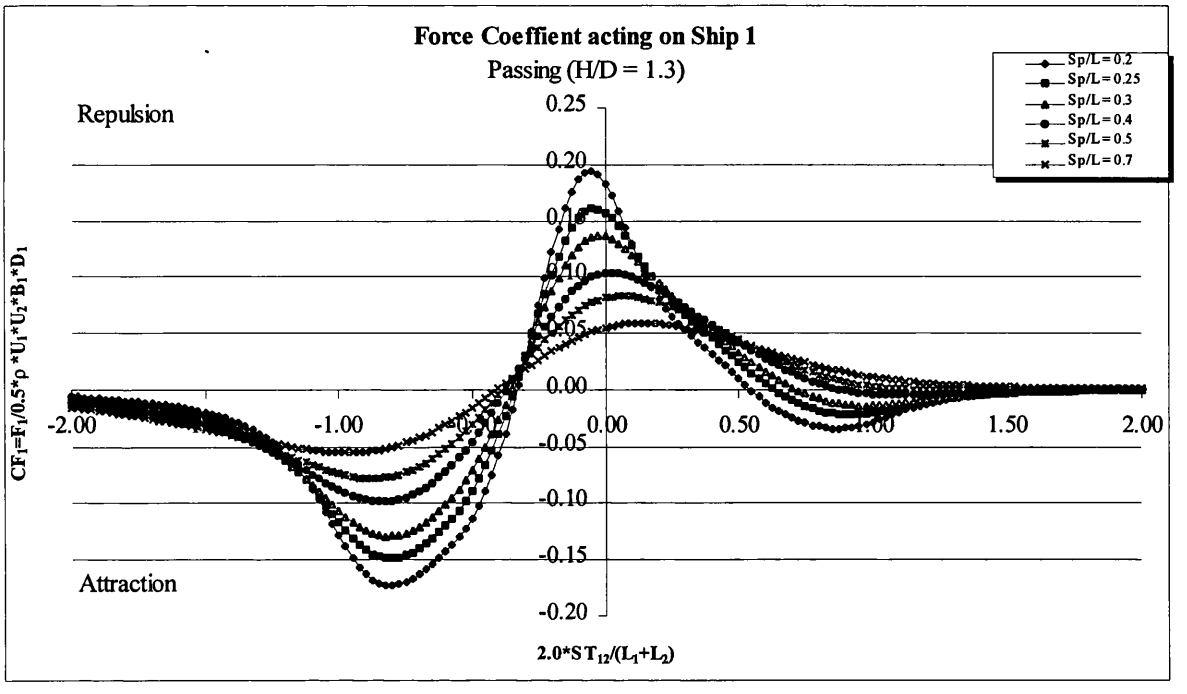

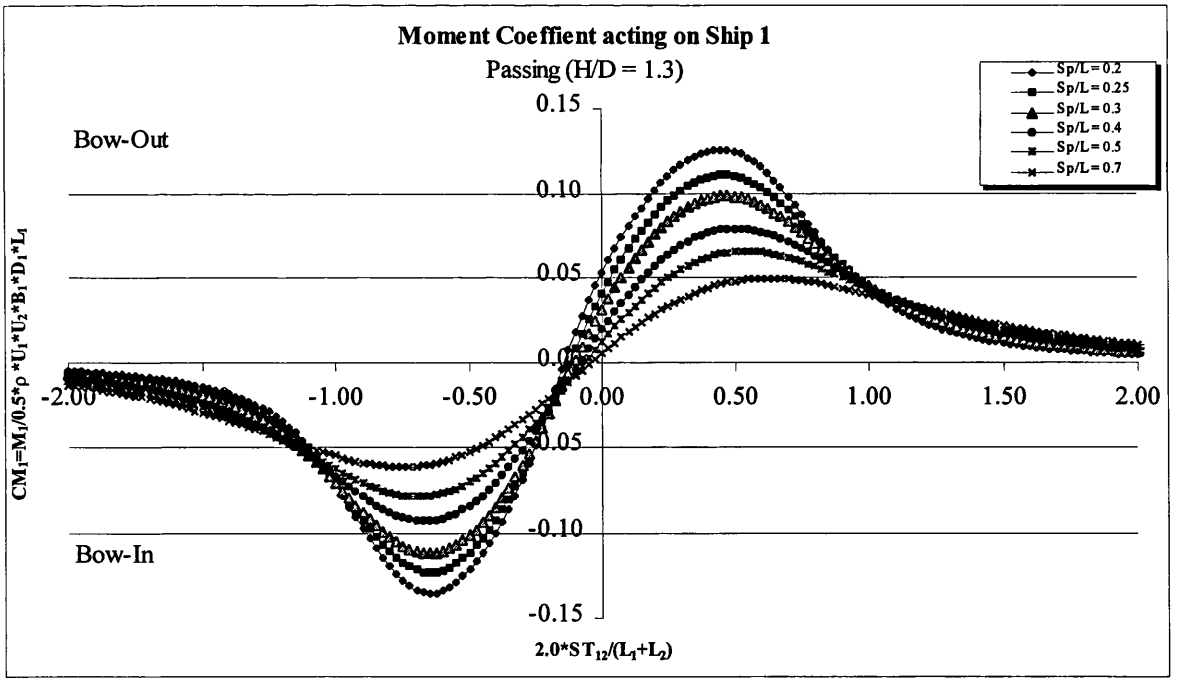

Figs 4.11a,b The lateral force and yaw moment coefficients acting on the faster Ship 1 for various separation distances, (two ships passing)

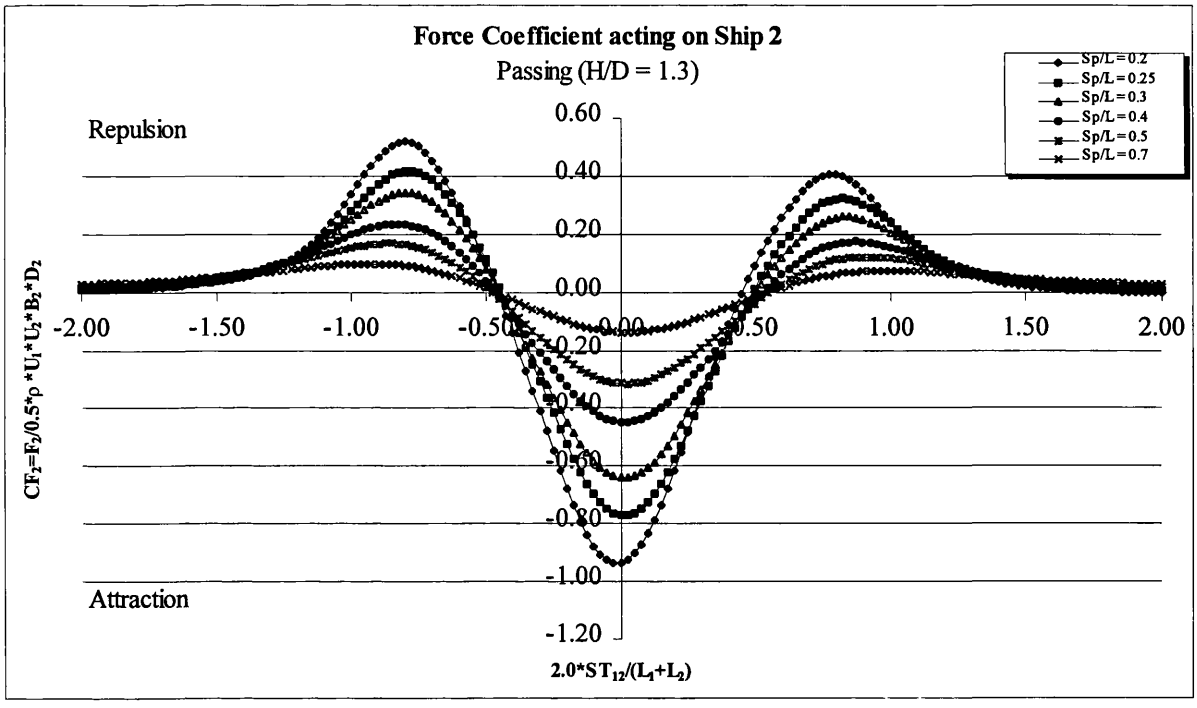

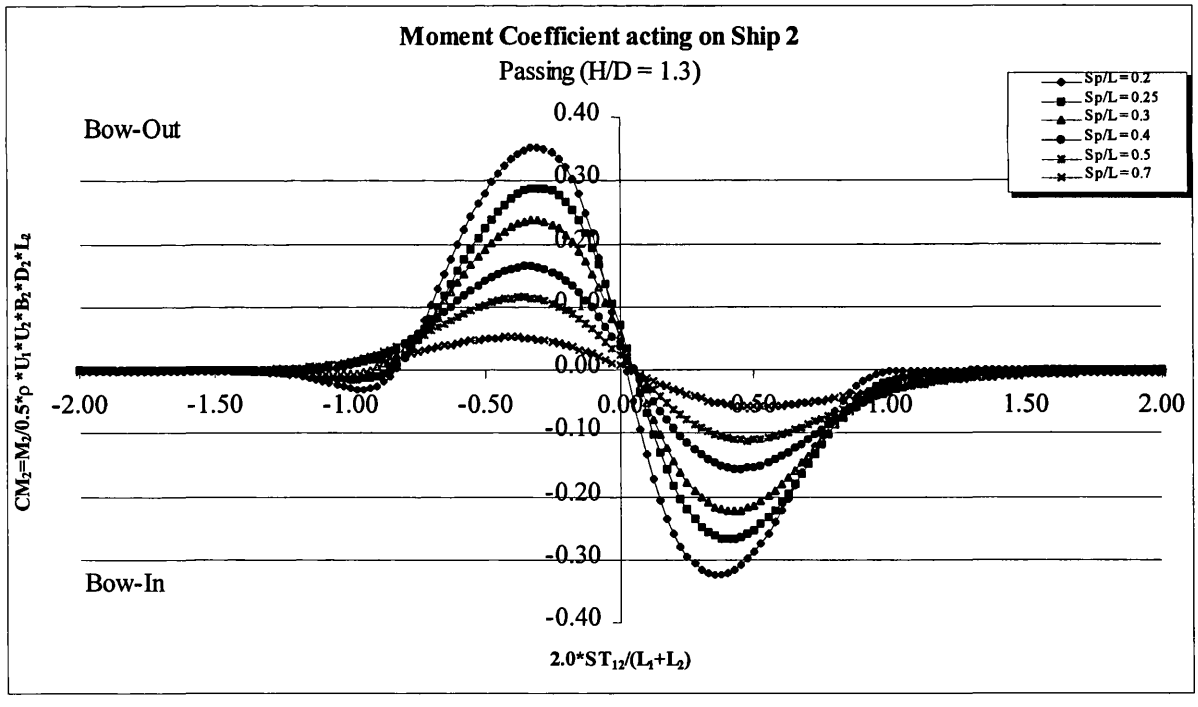

Figs 4.11c,d The lateral force and yaw moment coefficients acting on the slower Ship 2 for various separation distances, (two ships passing)

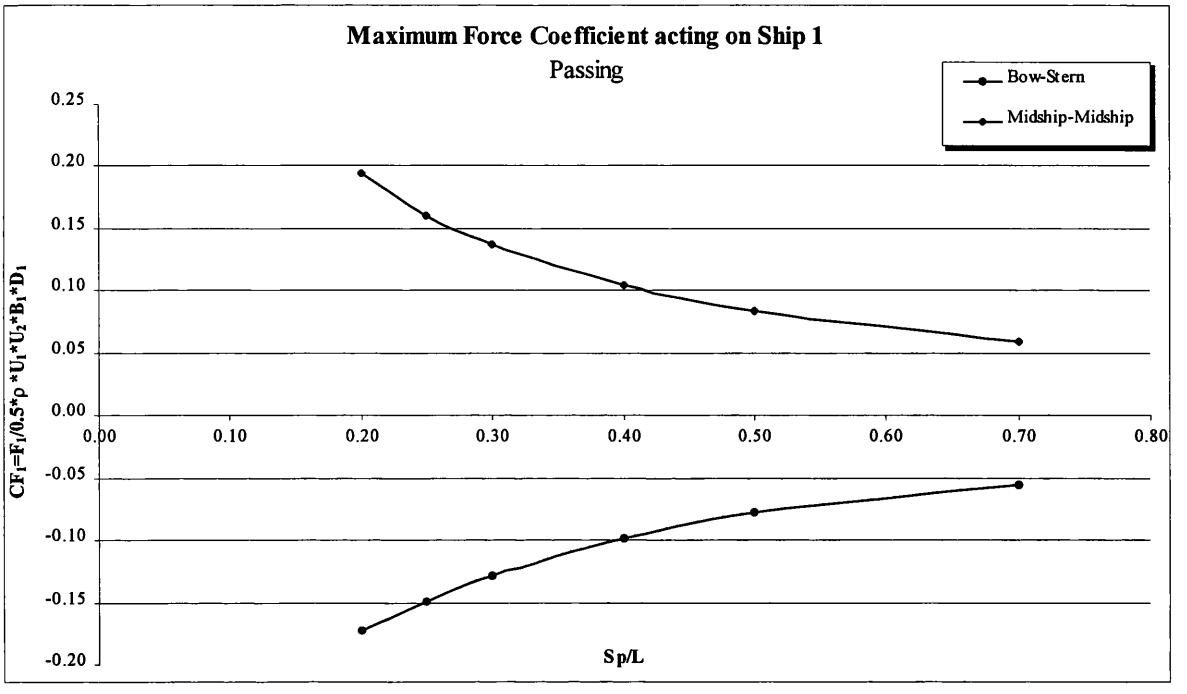

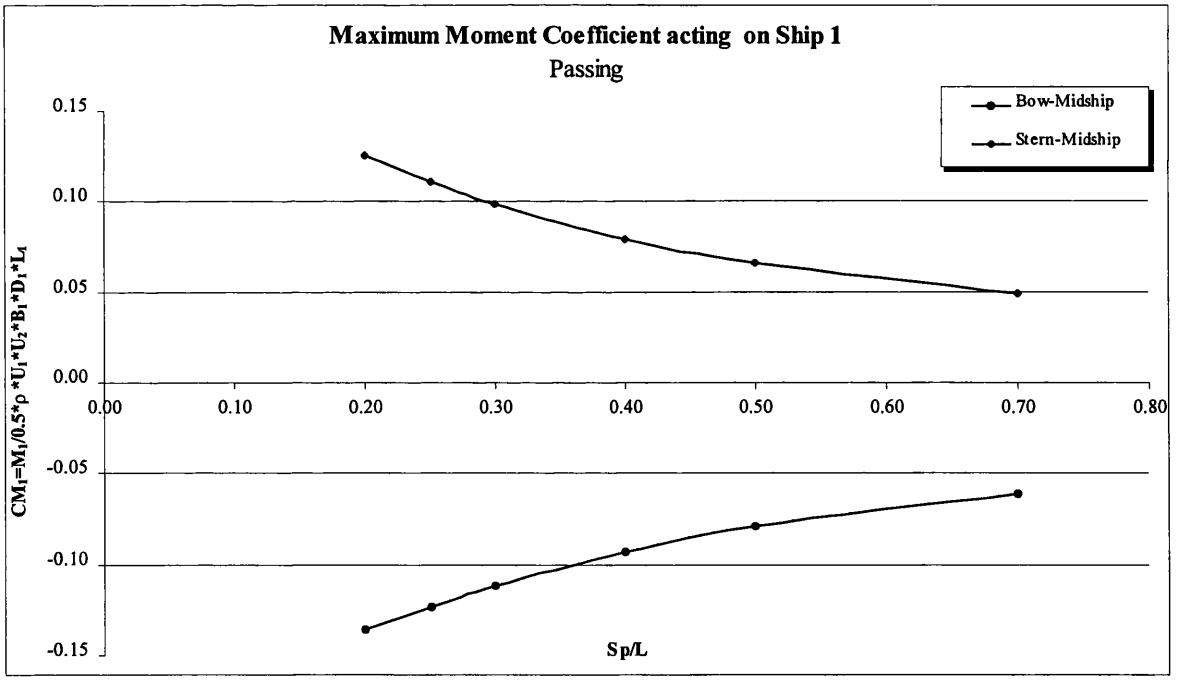

Figs 4.12a,b Maximum lateral force and yaw moment coefficients acting on the faster Ship 1 for various separation distances, (two ships passing)

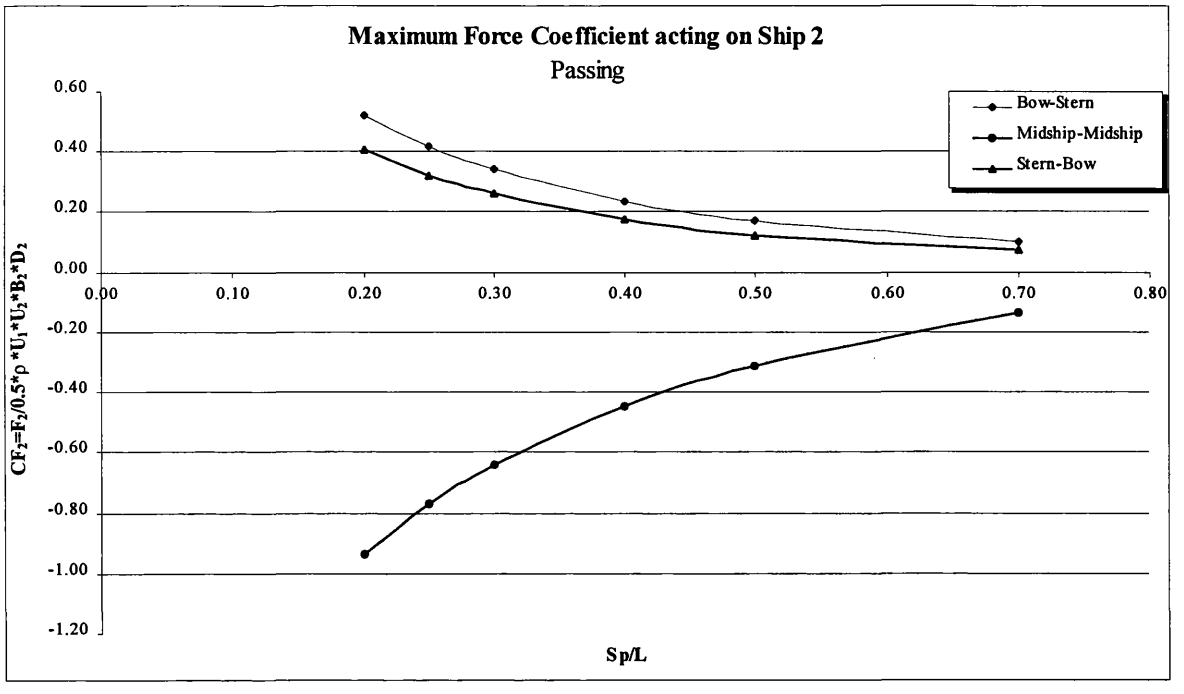

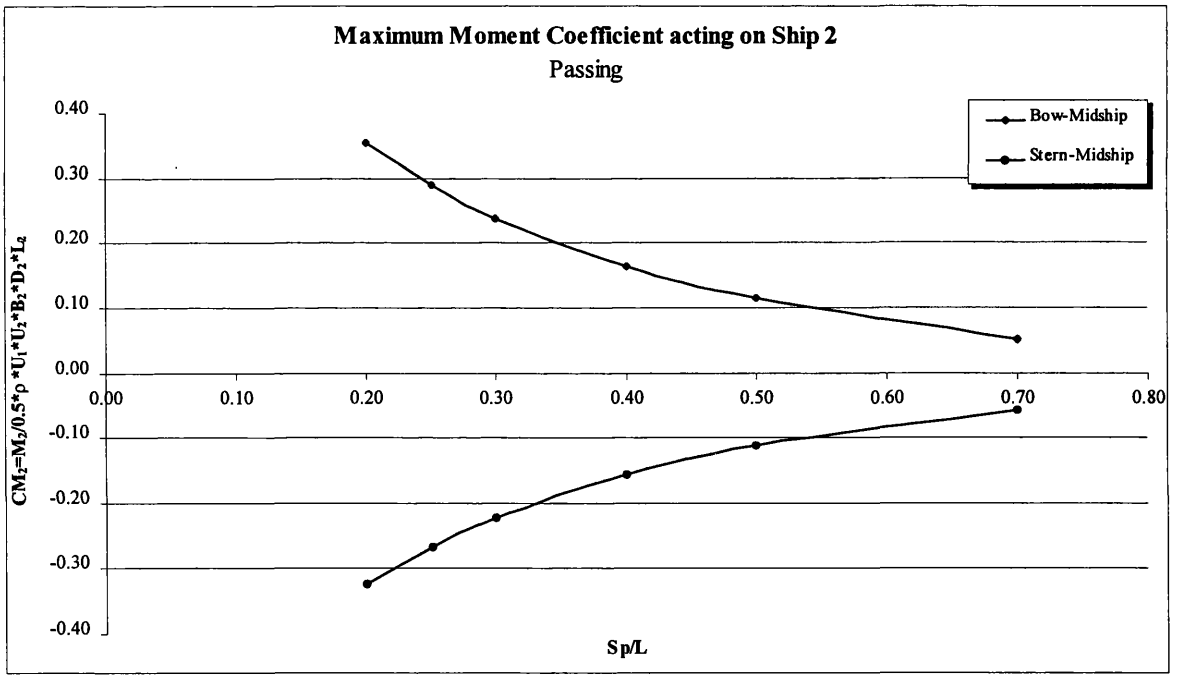

Figs 4.12c,d Maximum lateral force and yaw moment coefficients acting on the slower Ship 2 for various separation distances, (two ships passing)

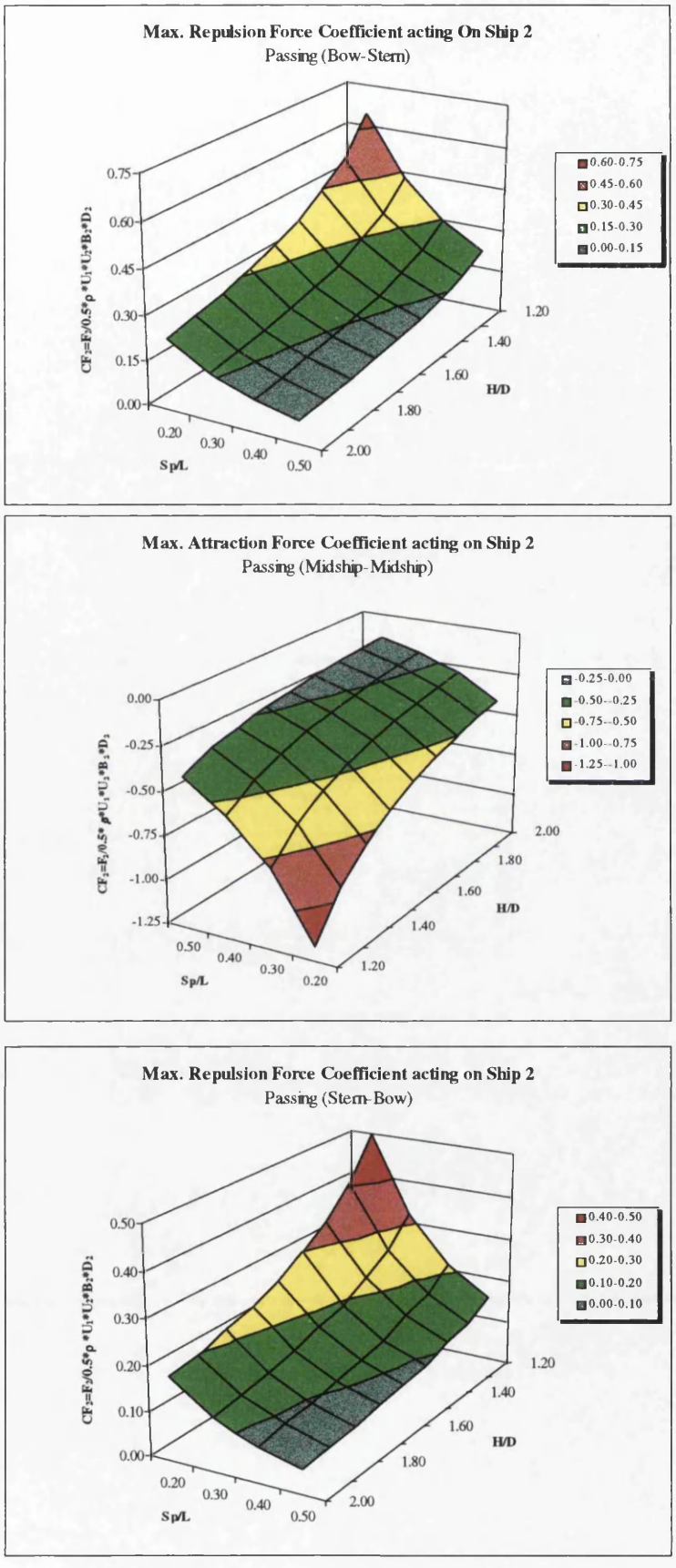

Fig 4.13 3D plots of the lateral force coefficients acting on the slower Ship 2 for various separation distances and water depths, (two ships passing)

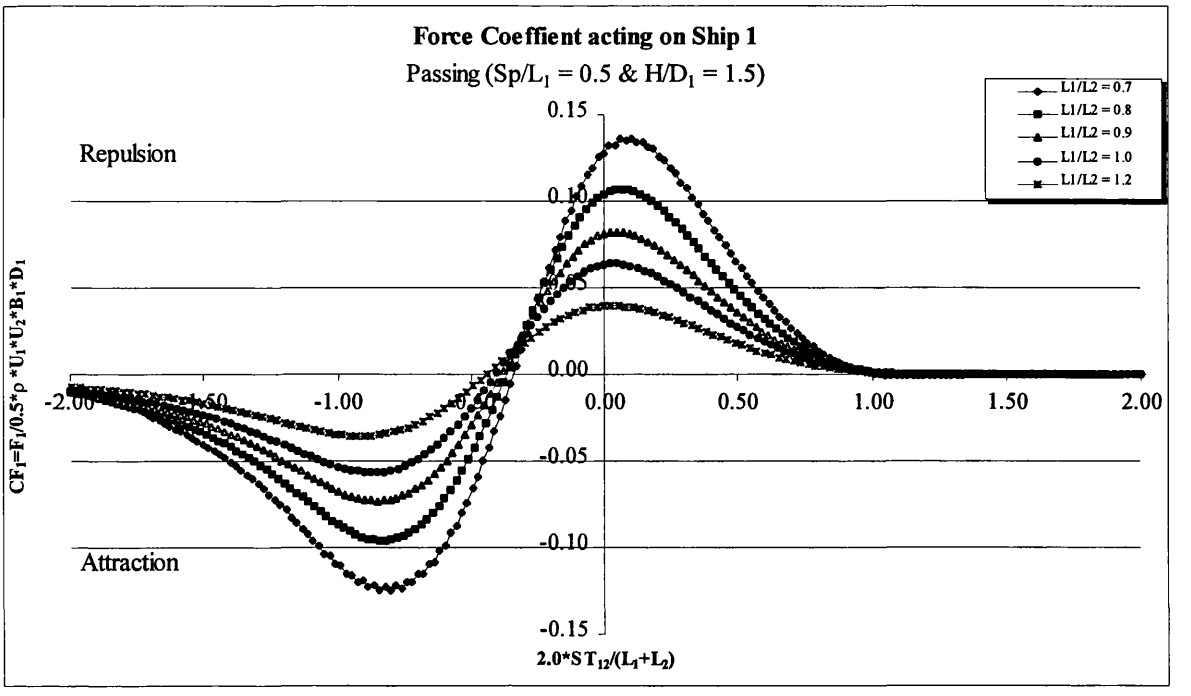

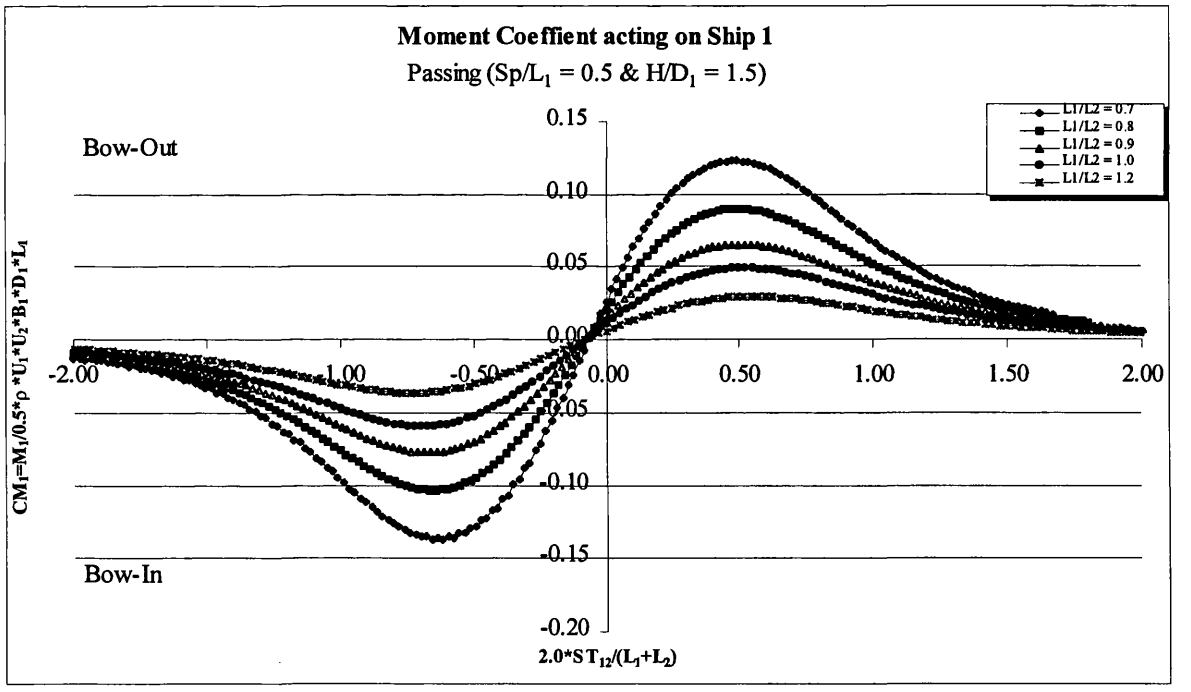

Figs 4.14a,b The lateral force and yaw moment coefficients acting on the faster Ship 1 for various ship sizes, (two ships passing)

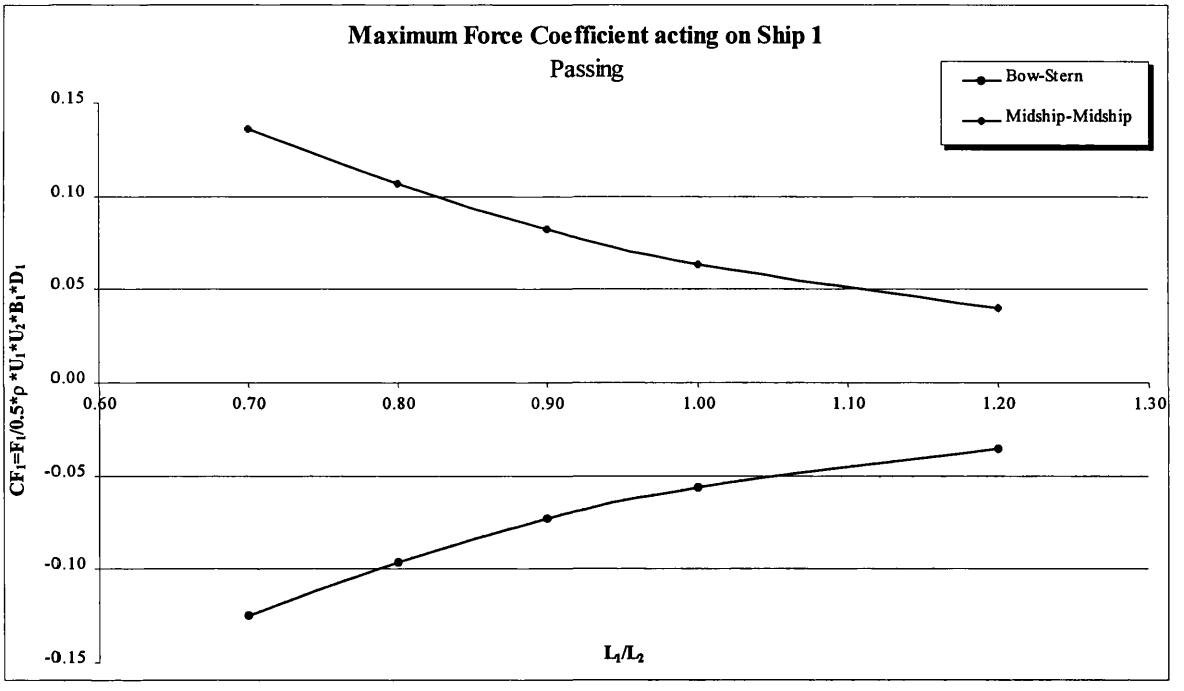

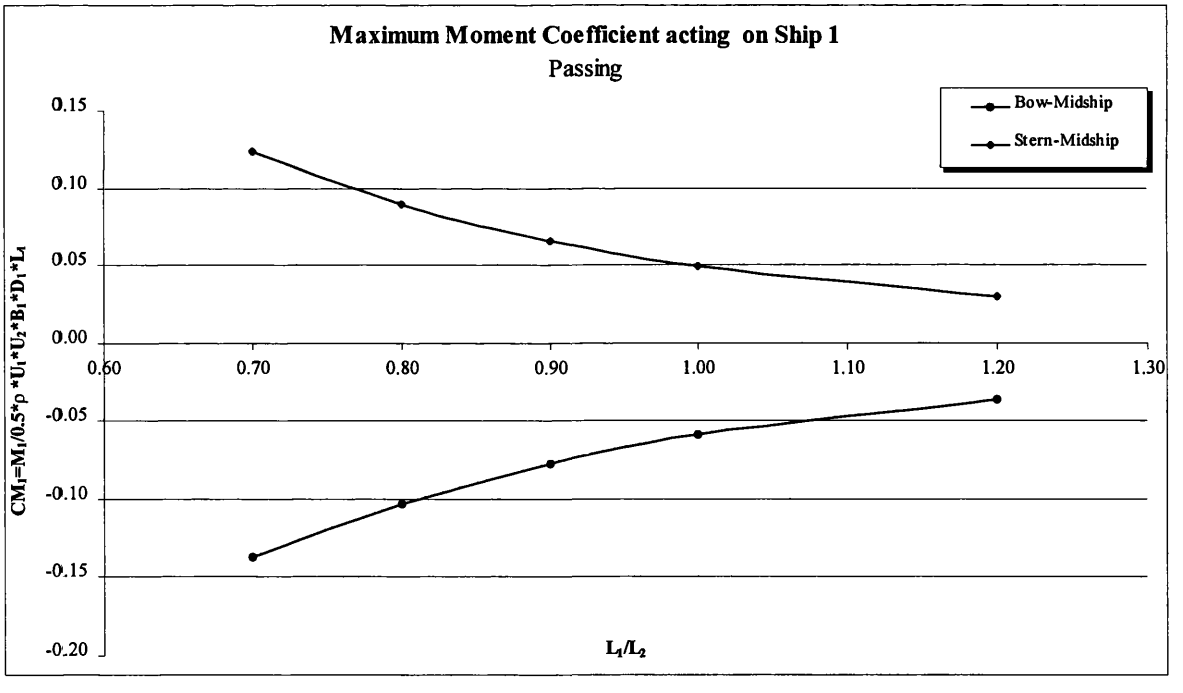

Figs 4.15a,b Maximum lateral force and yaw moment coefficients acting on the faster Ship 1 for various ship sizes, (two ships passing)

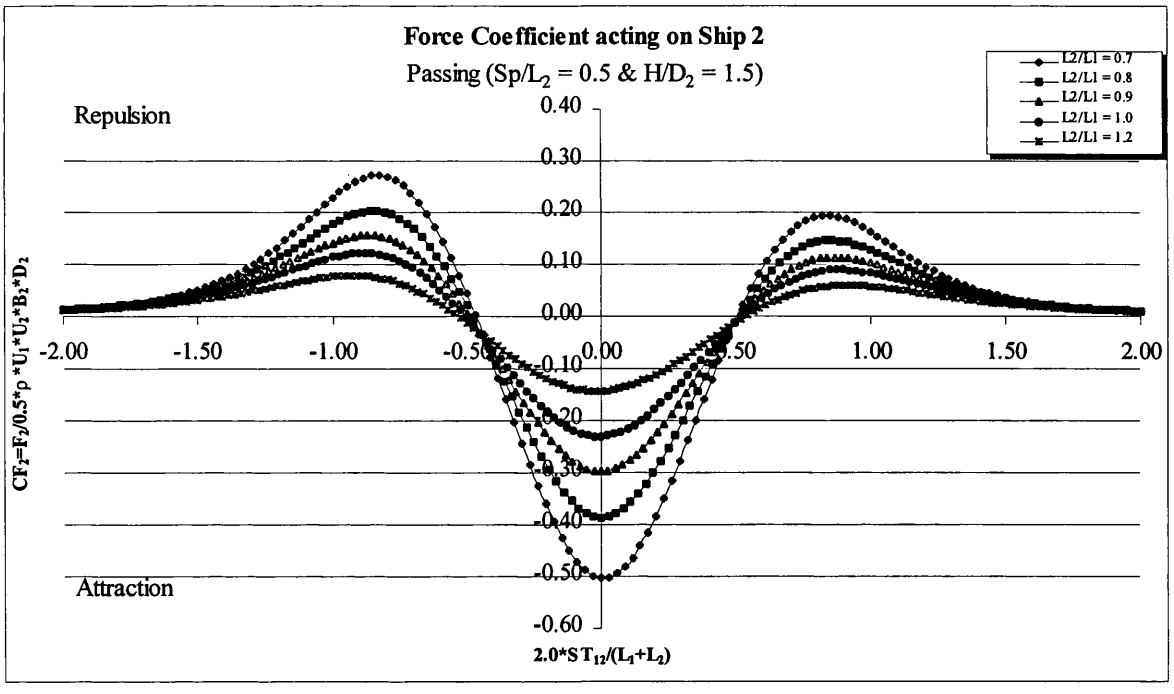

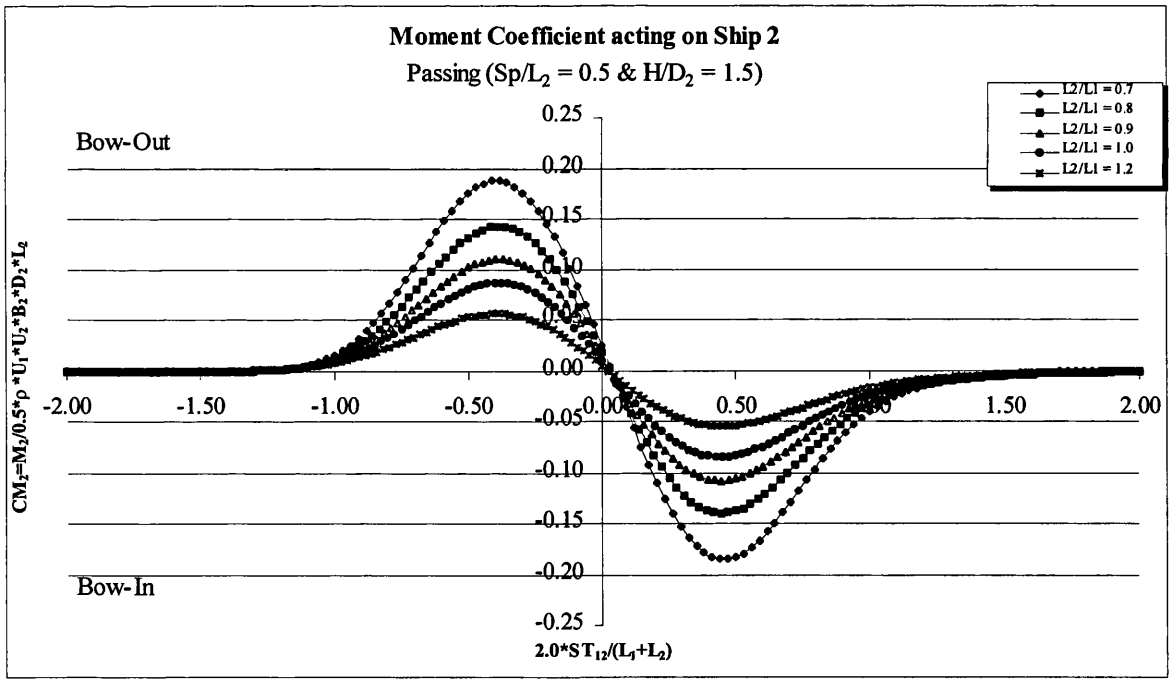

Figs 4.16a,b The lateral force and yaw moment coefficients acting on the slower Ship 2 for various ship sizes, (two ships passing)

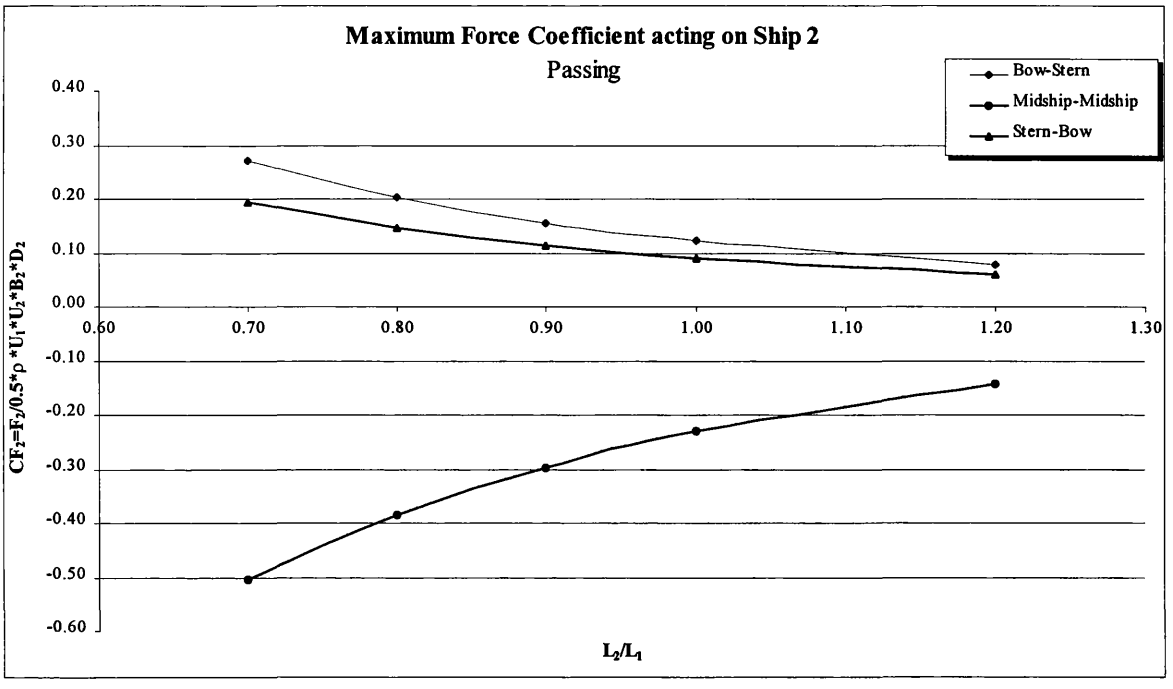

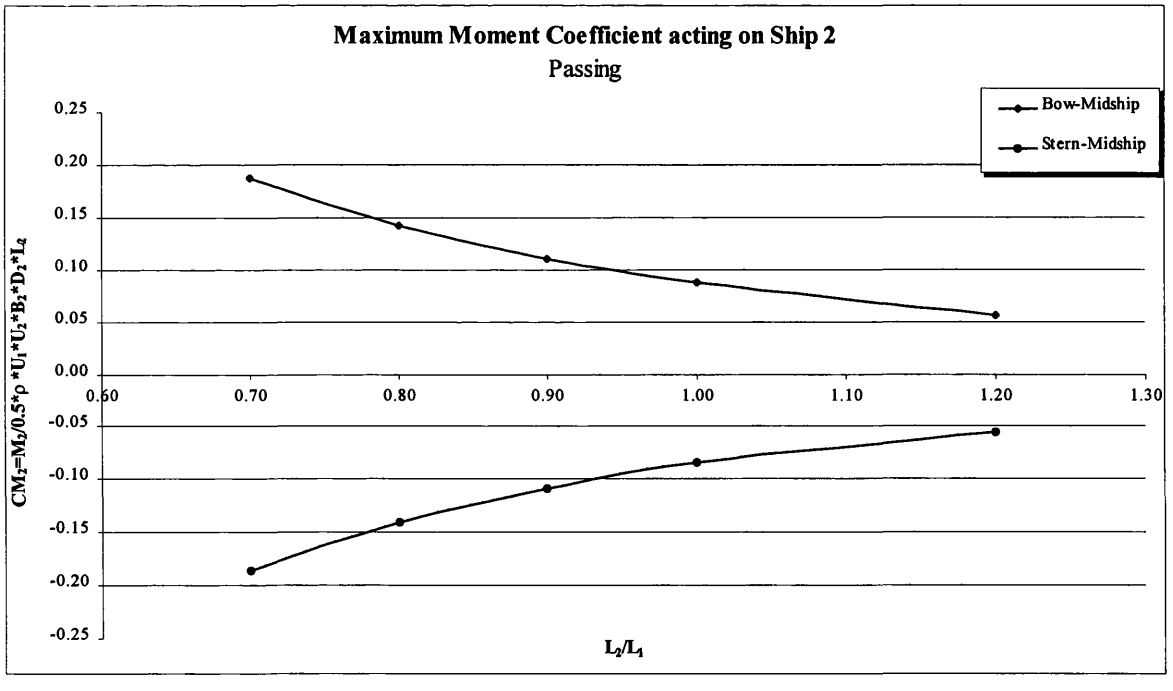

Figs 4.17a,b Maximum lateral force and yaw moment coefficients acting on the slower Ship 2 for various ship sizes, (two ships passing)

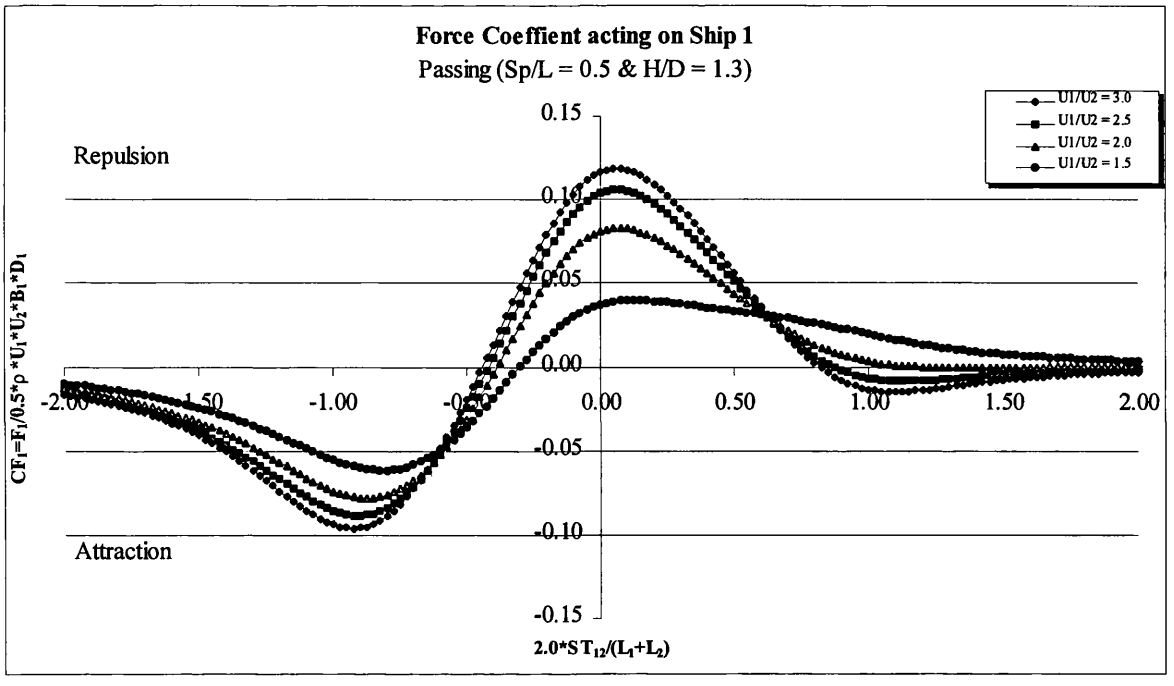

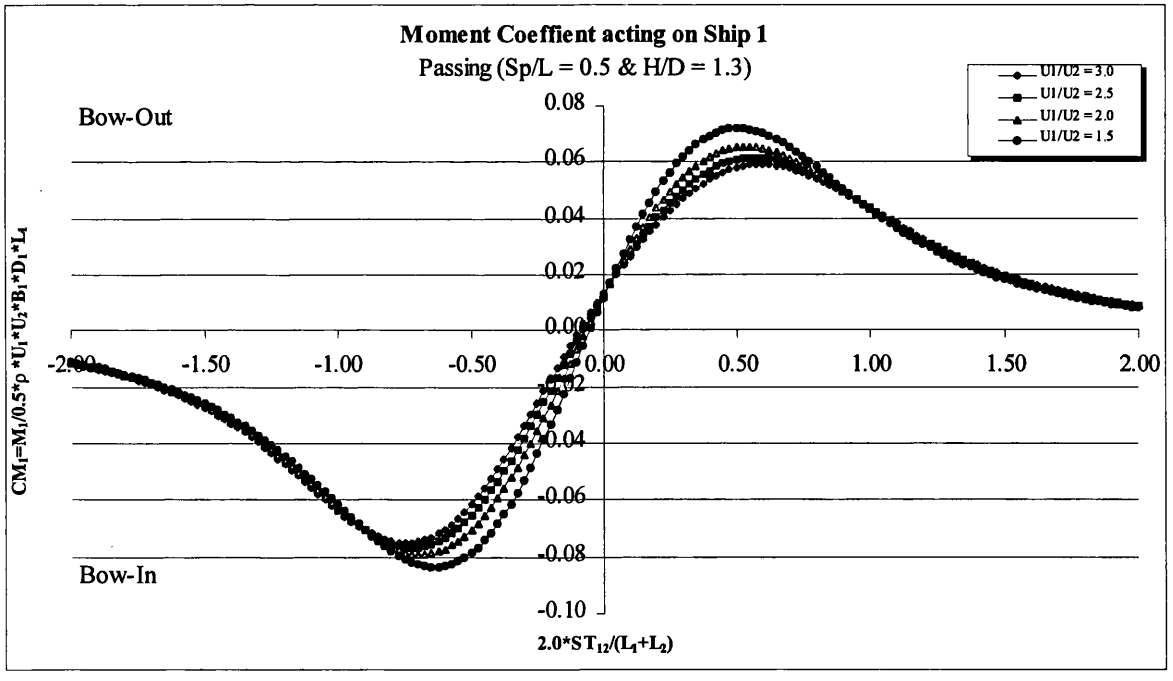

Figs 4.18a,b The lateral force and yaw moment coefficients acting on the faster Ship 1 for various ship speeds, (two ships passing)

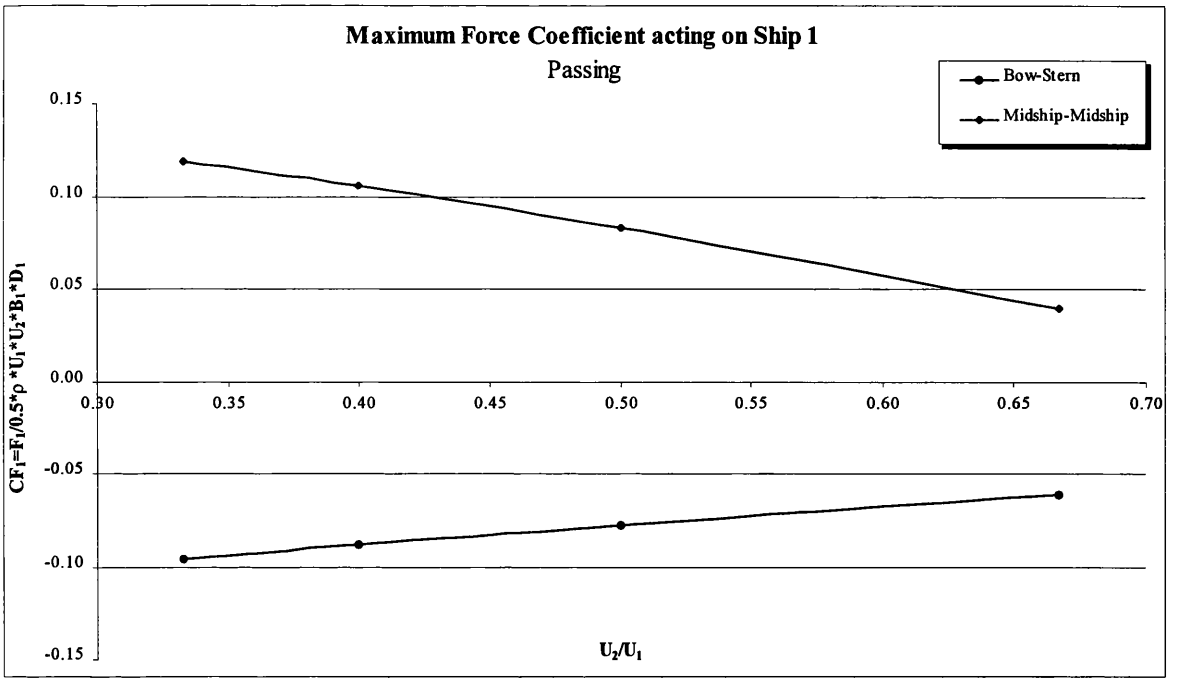

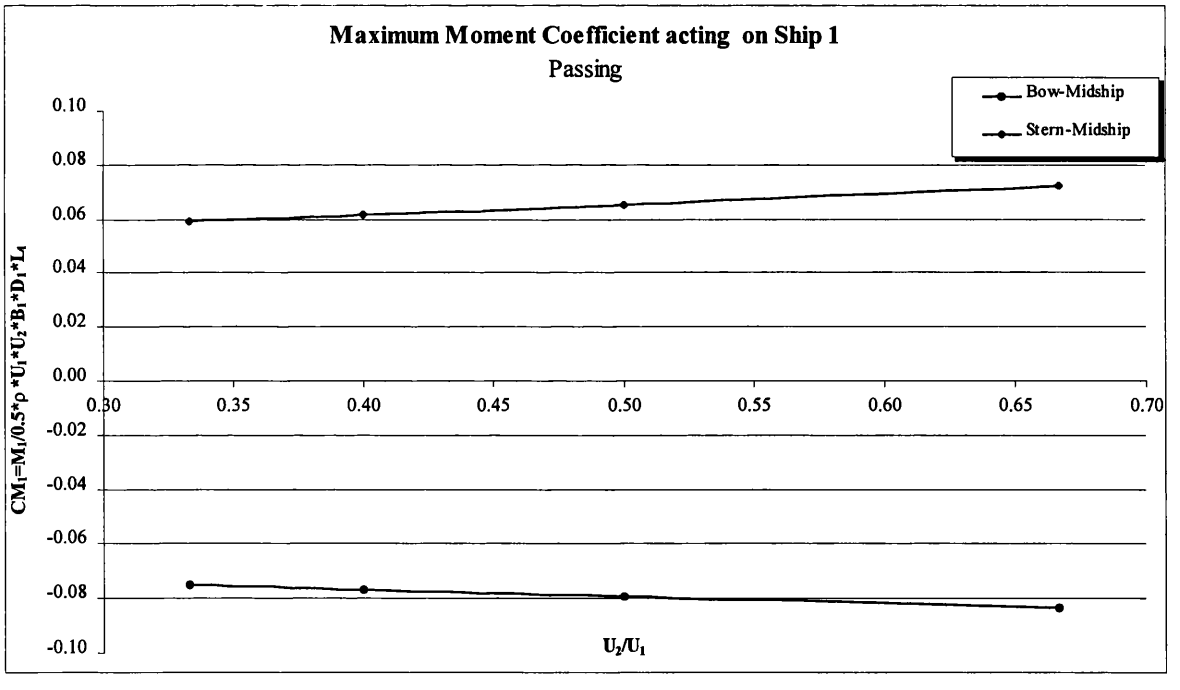

Figs 4.19a,b Maximum lateral force and yaw moment coefficients acting on the faster Ship 1 for various ship speeds, (two ships passing)

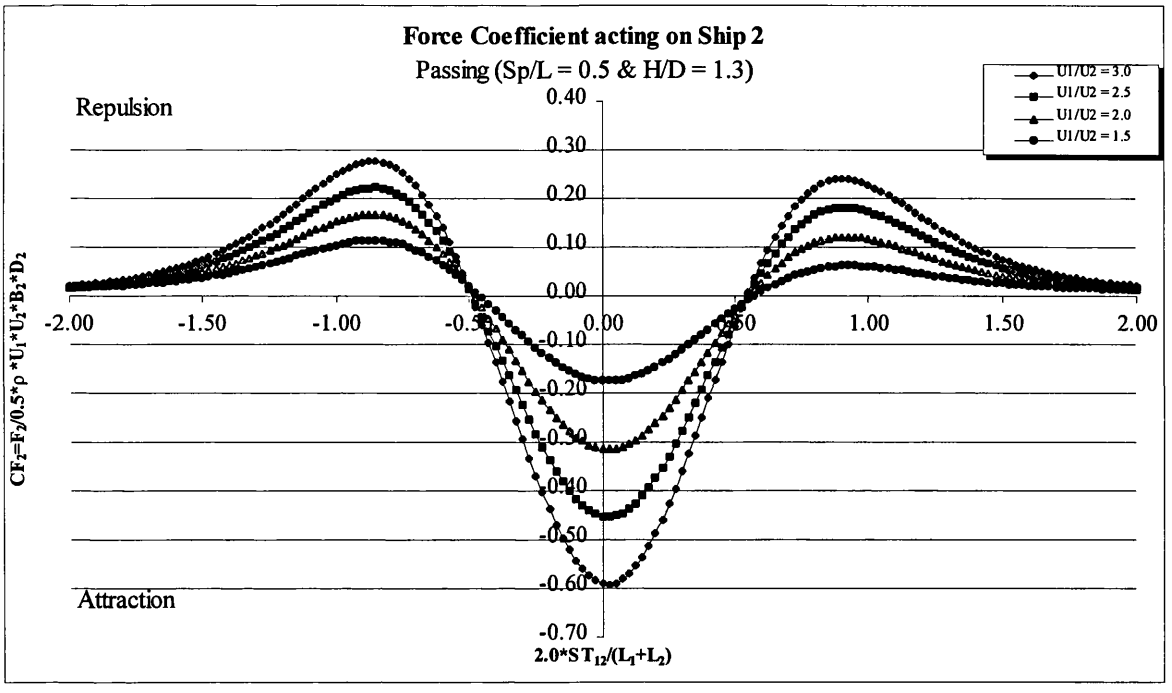

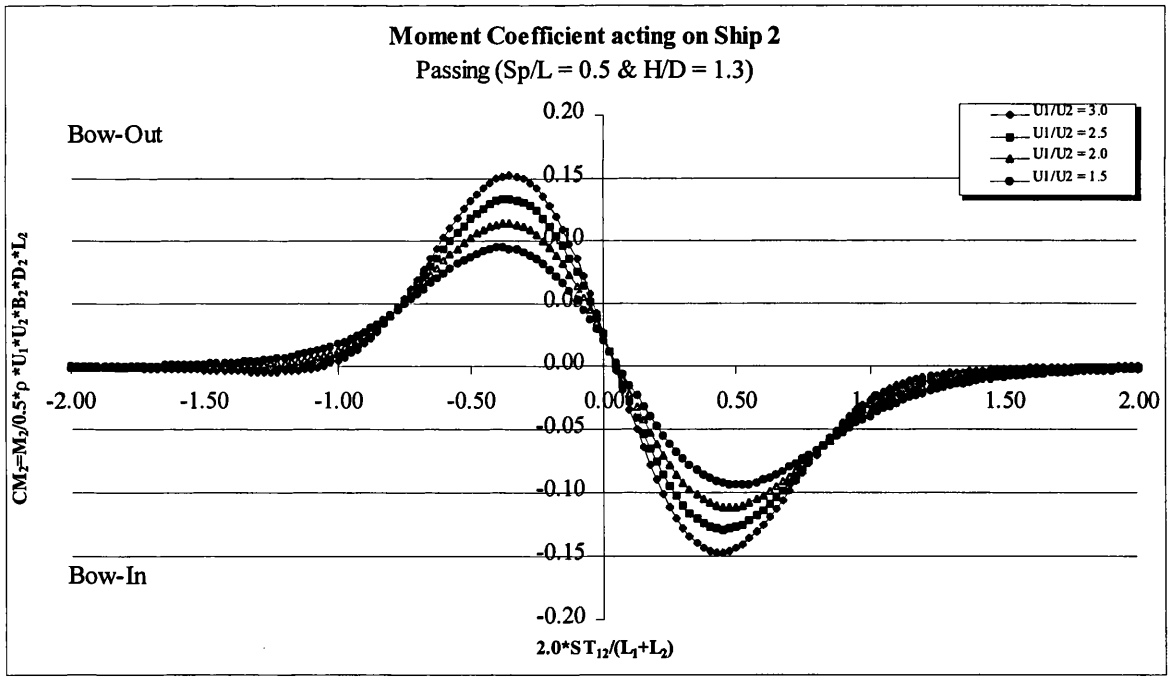

Figs 4.20a,b The lateral force and yaw moment coefficients acting on the slower Ship 2 for various ship speeds, (two ships passing)

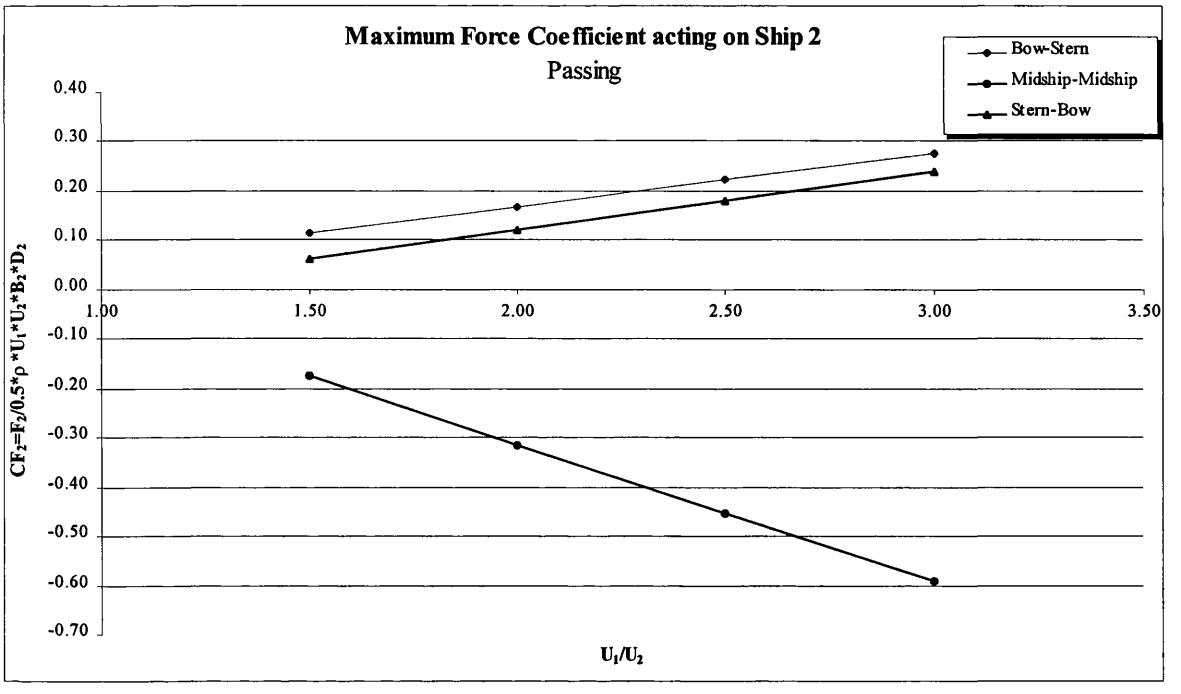

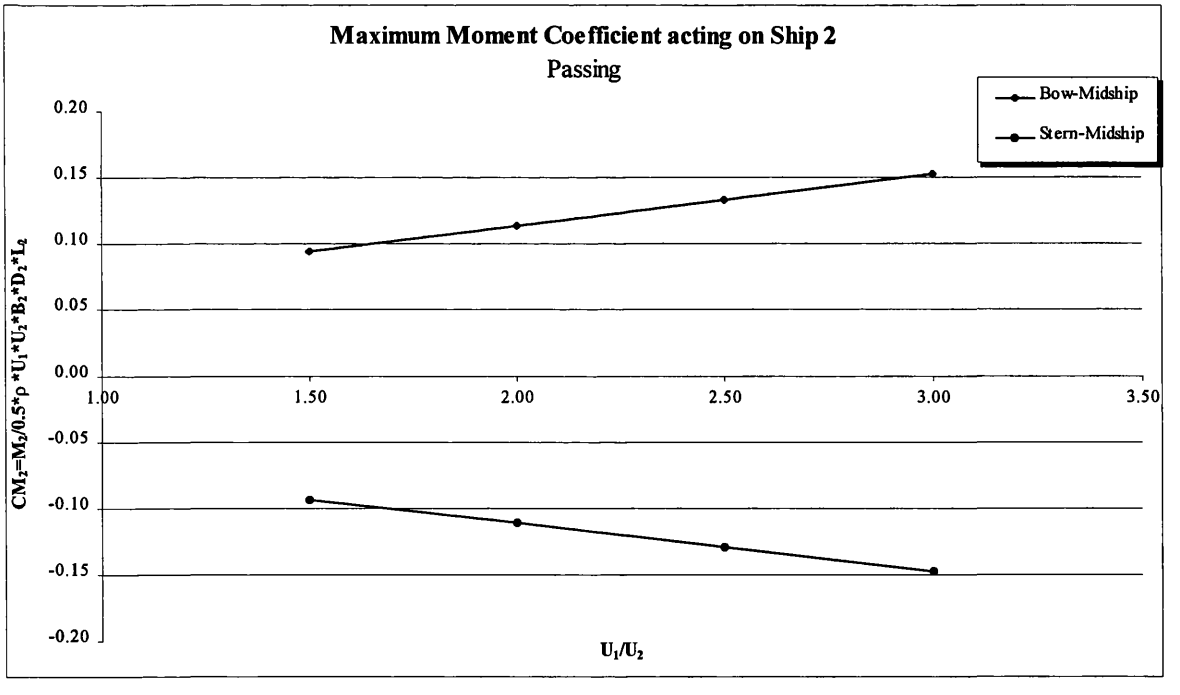

Figs 4.21a,b Maximum lateral force and yaw moment coefficients acting on the slower Ship 2 for various ship speeds, (two ships passing)

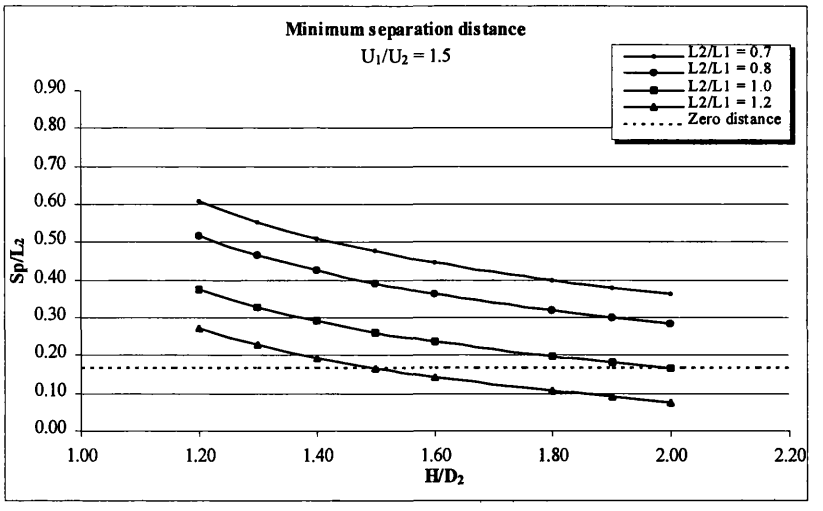

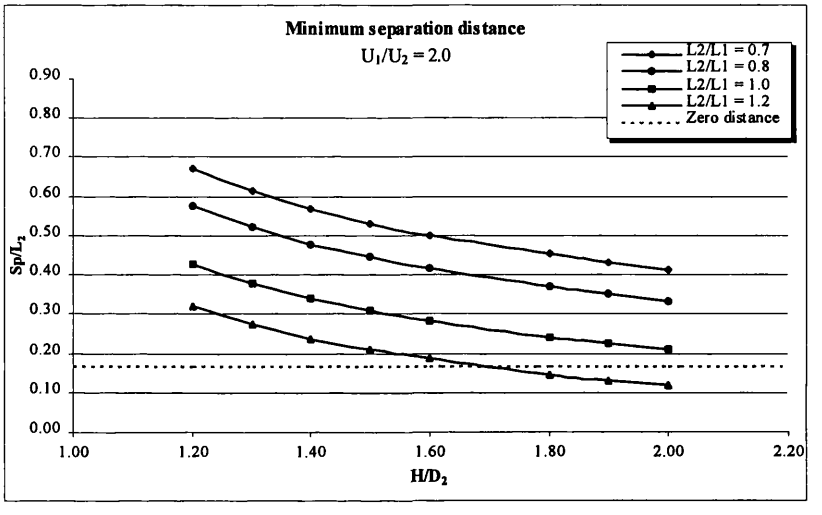

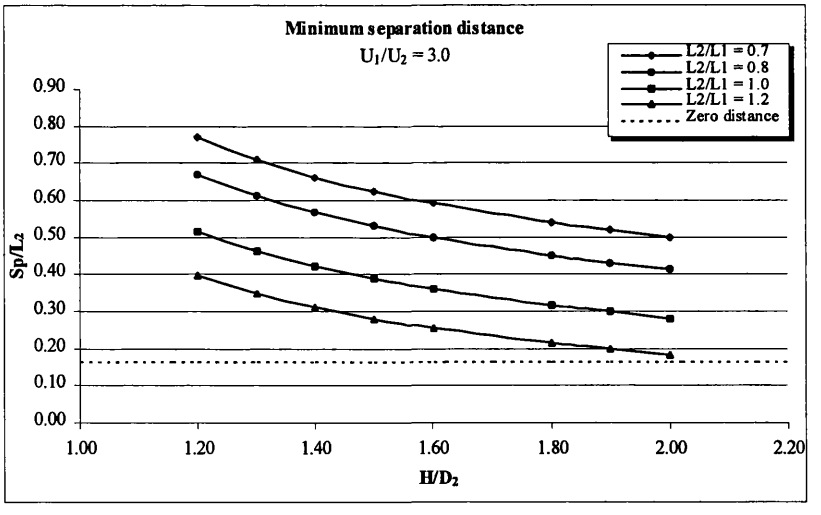

Figs 4.22a,b,c Minimum separation distance indicating that the rudder moment is smaller than the interaction moment, (two ships passing)

CHAPTER 5

INTERACTION BETWEEN THREE SHIPS IN MEETING MANOEUVRE.

5.1 INTRODUCTION

In the two previous chapters the present method was used to deal only with two ships in configuration. Here, a more complicated study has been carried out in order to investigate the hydrodynamic interaction forces and moments between three ships in a meeting situation. Ship 1 first encounters Ship 3 followed by Ship 2, where the longitudinal distance between Ship 2 and Ship 3, ST_{23}, is constant throughout the transit and defined as negative. The plan view of such an encountering manoeuvre can be seen in Fig 5.1, in which the sign convention for the lateral forces and yaw moments are denoted.

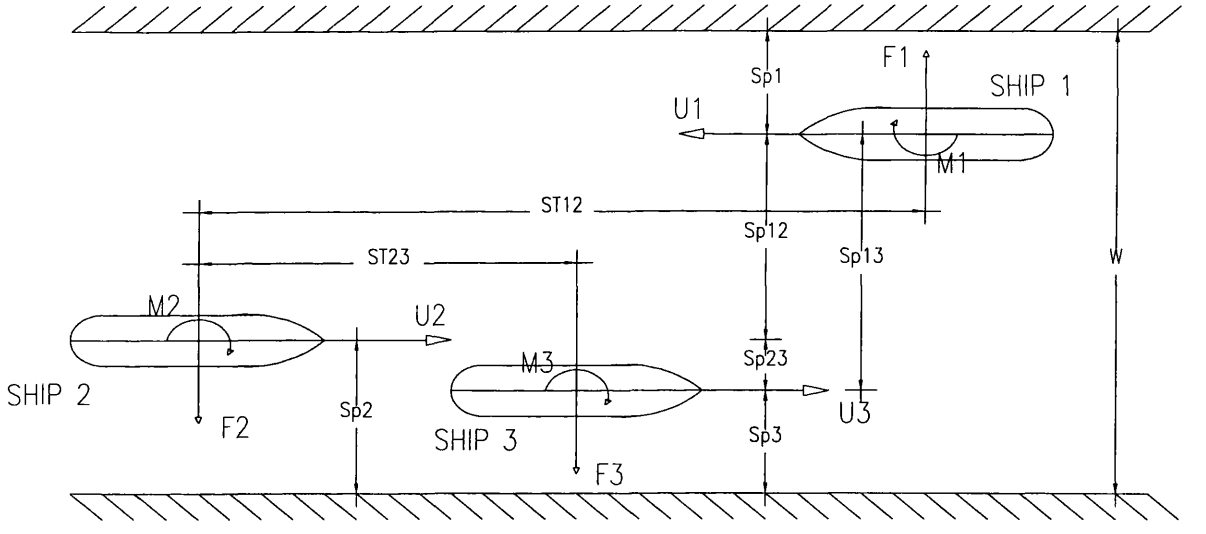

Fig 5.1 Co-ordinate system for three ships meeting.

Numerical results are presented only for Ship 1, since both Ship 2 and Ship 3 experience the same force and moment transit as for two ships meeting. Again, the stagger, ST_{12}, is defined as the longitudinal distance between the midships of Ship 1 and Ship 2:

$$ST_{12} = (U_1 + U_2) \times t \qquad U_1, U_2 > 0$$

where t = 0 corresponds to the situation in which the midships are aligned.

The stagger, ST`{ = $2.0 \times ST_{12}/(L_1 + L_2)$}, is non-dimensionalized such that the values –1, 0, and +1 correspond to the bow-bow, midship-midship, and stern-stern situations respectively with Ship 2, and is used as the abscissa for the plots.

Again, the effect of several parameters is investigated, (such as that of water depth, separation distance, ship size, ship speed and the longitudinal distance, or the stagger, between Ship 2 and Ship 3.)

The principal particulars for Ship 1 are shown in Table 3.1 The separation distances and the stagger between the midships of Ship 2 and Ship 3 are non-dimensionalized by the length of Ship 1, while the water depth is non-dimensionalized by the draught of Ship 1. However, in the cases where all three ships are identical, the subscripts are omitted for these non-dimensionals.

5.2 VERIFICATION OF NUMERICAL METHOD

Previous research into the three ships meeting problem is limited. The only available data, to which the results from the present method can be compared, are theoretical predictions by Yasukawa (1983). Yasukawa presented the lateral forces and yaw moments acting on one ship, non-dimensionalized, when encountering two identical ships in a 2L wide channel. (Here, this ship is referred as Ship 1). The depth-draught ratio was to be 1.3, while the separation distance between Ship 1 and Ship 2 was 0.5L and the separation distance between Ship 1 and Ship 3 was 0.6L. All ships in the encountering manoeuvre were travelling at an equal speed, and the constant longitudinal distance between the midships of Ship 2 and Ship 3 was taken as -1.5L. As a result, non-dimensionalized stagger values (ST_{12}) of -2.5, -1.5 and -0.5 correspond to bow-bow, midship-midship and stern-stern situations between Ship 1 and Ship 3 respectively.

Figures 5.2a,b show a comparison of the lateral force and yaw moment coefficients acting on Ship 1, and qualitatively, the results from the present method agree well with Yasukawa's theoretical data. Initially, Ship 1 experiences a repulsion force as its

bow passes the bow of Ship 3 (ST` = -2.5), followed by an attraction peak at the midship-midship situation (ST` = -1.5). This is the same force transit as for the two ships in a meeting manoeuvre. However, as Ship 1 moves out of this position the presence of Ship 2 begins to influence the interaction forces. As a result, a large repulsion force appears, that reaches its maximum just after the stern of Ship 1 passes the midship of Ship 3 at the same time as the bow of Ship 1 is slightly ahead of the bow of Ship 2 (ST`= -0.8). The repulsion experienced by Ship 1 from the stern of Ship 3 plus that from the bow of Ship 2 generates this large peak value. The rest of the encountering manoeuvre gives a force transit that corresponds to a two ships meeting condition; a maximum attraction force as the midships of Ship 1 and Ship 2 become aligned (ST` = 0.0), and a maximum repulsion force as the stern of Ship 1 passes the stern of Ship 2 (ST` = 0.8).

There is only a small difference between the present method and Yasukawa when comparing the peak values for the non-dimensionalized repulsion and attraction lateral forces. The disagreements vary only between approximately 3% to 8%.

Similarly good qualitative agreement is found for the yaw moments between the present method and Yasukawa. Ship 1 first experiences a bow-out moment that reaches its maximum as the bow of Ship 1 encounters the bow of Ship 3 (ST` = -2.5). This tendency is common to the two ships meeting manoeuvre. Although this bow-out moment decreases as Ship 1 moves out of this position, it does not change direction immediately before the midships of Ship 1 and Ship 3 become aligned (ST` = -1.7), while it does in the case of two ships meeting. However, for smaller separation distances between Ship 1 and Ship 3, this bow-out moment does become a bow-in turning moment, as discussed further in the parametric study, chapter 4.4.

Furthermore, Ship 1 experiences a maximum bow-out moment again as the stern of Ship 1 reaches the midship of Ship 3 at the same time as the bow of Ship 1 passes the bow of Ship 2 (ST` = -1.0). This peak appears because its interaction with the bow of Ship 2, which produces a bow-out moment on Ship 1, is predominant. This turning moment decreases and becomes negligible around the point when the stern of Ship 1 passes the midship of Ship 3 and the bow of Ship 1 moves past the midship of Ship 2 (ST` = -0.5). Once more, the last part of the encountering manoeuvre gives a similar

moment transit as for the two ships meeting situation with a maximum bow-in peak as the stern of Ship 1 passes the stern of Ship 2.

Quantitatively, the agreement is also fairly good, where the maximum bow-out and bow-in moment coefficients are approximately 8% to 14% larger for the present method compared to Yasukawa's peak values.

5.3 PRESSURE AND VORTICITY DISTRIBUTION

In chapter 2.3 the pressure and vorticity distribution acting on Ship 1 for two ships meeting are derived for positions along the whole part of the encountering manoeuvre. The pressure and vorticity distribution are here presented only for when Ship 1 occupies positions between Ship 3 and Ship 2, since the distributions at the beginning and end of the transit are the same as for two ships meeting. Figures 5.3a,b show these pressure and vorticity distributions acting on Ship 1 while travelling in a 2L wide channel. The separation distance from Ship 3 is 0.6L while the separation distance from Ship 2 is 0.5L. The depth-draught ratio is chosen to be 1.3. All ships are travelling at the same speed.

Figure 5.3a shows that as the midships of Ship 1 and Ship 2 become aligned (position 1), Ship 1 experiences low pressures around the hull facing Ship 2, causing a maximum attraction force. From the pressure distribution it is also worth noting that the aft portion of Ship 1 endures lower pressures than the forward part, resulting in a small bow-out moment. Furthermore, at position 2 there is more unevenly distributed pressures where the stern of Ship 1 passes the midship of Ship 3 at the same time as the bow of Ship 1 reaches the bow of Ship 2. The pressures at the aft portion of Ship 1 are attractive in nature, while the forward pressures are of a repulsive nature. As a result, Ship 1 experiences a maximum bow-out moment in this position. The total lateral force acting on Ship 1 is repulsive in nature. When Ship 1 travels only a stagger distance of 0.25L further (position 3), the pressures become higher around the hull of Ship 1, resulting in a maximum repulsion force. This portion tends to veer

away from Ship 2 since the pressures are higher at the forward sections of the hull, causing a bow-out turning moment

Furthermore, as the stern of Ship 1 moves past the stern of Ship 3 at the same time as the bow of Ship 1 passes the midship of Ship 2 (position 4), the pressures around the forward portion are negligible, while the pressures at the aft end are higher. Consequently, Ship 1 experiences a repulsive force and a bow-in moment. When the midships of Ship 1 and Ship 2 are aligned (position 5), the repulsion force changes direction and becomes a maximum attraction force because of the low pressure around the hull of Ship 1 facing Ship 2. Since the pressures are lowest at the forward part, the turning moment is of a bow-in nature.

5.4 PARAMETRIC STUDY

This section presents a parametric study of the lateral forces and yaw moments acting on three ships in meeting manoeuvres. As described previously, Ship 1 first encounters Ship 3 followed by Ship 2. Again, only the results from Ship 1 are presented here since both Ship 2 and Ship 3 experience the same lateral force and yaw moment transit as for two ships meeting. First the effect of separation distance, water depth and ship size is investigated for the cases in which all three ships are travelling at an equal speed. The ship speed effect is then examined. In addition, a study is carried out into how a variation in the longitudinal distance, or stagger, between Ship 2 and Ship 3 influences the hydrodynamic forces and moments acting on Ship 1. All the various conditions are stated in tables.

The general trend of the force and moment transit is similar for the various meeting manoeuvres considered here. Ship 1 first experiences a repulsion-attraction transit when encountering Ship 3, in which the peak values occur at the bow-bow ($ST` = -2.5$), and midship-midship ($ST` = -1.5$) respectively. However, immediately before the stern-stern situation with Ship 3, the interaction forces acting on Ship 1 are already strongly influenced by the presence of the bow of Ship 2, resulting in a large maximum repulsion force ($ST` = -0.8$). During the last part of the manoeuvre, Ship 1

experiences an attraction-repulsion force transit with peak values when in midship-midship (ST` = 0.0) and stern-stern (ST` = 1.0) situations respectively with Ship 2.

Ship 1 experiences first a bow-out moment that reaches a peak as its bow passes the bow of Ship 3 (ST` = -2.5). This turning moment decreases as Ship 1 moves out of this position. Ship 1 again experiences a maximum bow-out moment as its stern is aligned with the midship of Ship 3 at the same time as its bow reaches the bow of Ship 2 (ST` = -1.0). This turning moment then changes direction and becomes a maximum bow-in moment immediately before the midships of Ship 1 and Ship 2 are side by side (ST` = -0.2). Finally, a bow-in peak appears as the stern of Ship 1 passes the stern of Ship 2 (ST` = 1.0).

5.4.1 The effect of water depth

Figures 5.4a,b show how a variation of the depth-draught ratio affects the lateral force and yaw moment coefficients acting on Ship 1. Ship 1 first encounters Ship 3 followed by Ship 2 for the condition given below:

W	H/D	Sp_{12}/L	Sp_{13}/L	$L_1/L_{2,3}$	$U_{2,3}/U_1$	ST_{23}
2L	Varying	0.5	0.6	1.0	1.0	-1.5L

Table 5.1 Condition for the effect of water depth, (three ships meeting).

It is apparent from Figs 5.4a,b that the lateral forces and yaw moments increase as the bottom clearance decreases. This increasing tendency is what would be expected since Ship 1 experiences a similar increasing pattern for the hydrodynamic forces and moments when encountering only one ship.

The maximum lateral force coefficients are shown in Fig 5.5a for different water depths, where it can be seen that Ship 1 experiences a sharp increase in force coefficients for small bottom clearances. The largest repulsion forces occur when ST` = -0.8 (i.e. when Ship 1 is positioned between Ship 2 and Ship 3). For various depth-draught ratios these peak values are approximately 40% larger compared to the

maximum repulsion force coefficients appearing when the bow of Ship 1 passes the bow of Ship 3 (ST` = -2.5). However, the maximum repulsion forces when ST` = -0.8 are 43% smaller in magnitude compared to the attraction peaks appearing when its midship is aligned with the midship of Ship 2 (ST` = 0.0).

Figure 5.5b shows the maximum yaw moment coefficients for various depth-draught ratios, and as the bottom clearance reduces, Ship 1 experiences a rapid increase in maximum bow-out and bow-in moment coefficients. For a depth draught ratio of 1.2, Ship 1 experiences the largest bow-out moment coefficient when its bow meets the bow of Ship 3 (ST` = -2.5). This bow-out maximum is 32% larger compared to the bow-out peak appearing when Ship 1 is in a stern-midship situation with Ship 3 and a bow-bow situation with Ship 2 (ST` = -1.0). However, in deeper water, H/D = 2.0, the difference between these two bow-out peaks is reduced to about 5%.

The largest bow-in moment coefficient acting on Ship 1 appears as its stern passes the stern of Ship 2 (ST` = 1.0) for a depth-draught ratio of 1.2. This peak value is approximately 25% larger than the bow-in maximum occurring immediately before a midship-midship situation with Ship 2 (ST` = -0.2). Again, the difference becomes smaller as the depth-draught ratio decreases and is negligible when H/D = 1.5. For deeper waters the maximum bow-in moment coefficients when ST` = -0.2 become larger compared to the peak values when ST` = 0.8, and the difference increases to 21% for H/D = 2.0.

The disagreements are found to be small when comparing the magnitudes of the maximum bow-out coefficients when ST` = -1.0 with the maximum bow-in moment coefficients when ST` = -0.2 for various bottom clearances.

(Diagrams of the effect of water depth for different separation distances are shown in the Appendix 5.)

5.4.2 The effect of separation distance

In the case of three ships travelling in a channel, the separation distance from Ship 1 to both Ship 2 (Sp_{12}) and Ship 3 (Sp_{13}) can be varied, giving several possible manoeuvre configurations. However, in this thesis the separation distance between Ship 2 and Ship 3 (Sp_{23}) is chosen to constant and 0.1L, while varying the lateral distance between these ships and Ship 1. Figures 5.6a,b show how variations of the separation distance influences the lateral force and yaw moment coefficients, where the condition is shown below:

W	H/D	Sp_{12}/L	Sp_{13}/L	$L_1/L_{2,3}$	$U_{2,3}/U_1$	ST_{23}
2L	1.3	Varying	Varying	1.0	1.0	-1.5L

Table 5.2 Condition for the effect of separation distance, (three ships meeting).

where Ship 1 first meets Ship 3 followed by Ship 2. The separation distance between Ship 2 and Ship 3 is 0.1L, i.e. $Sp_{23} = 0.1L$.

From Figs 5.6a,b it can be seen that as the separation distance between Ships 1 and both Ship 2 and Ship 3 decreases the lateral forces and yaw moments increase. This is anticipated since the same tendency is the same for two ships meeting.

Figure 5.7a shows the maximum lateral force coefficients acting on Ship 1 during the encountering manoeuvre plotted against the non-dimensionalized separation distance between Ship 1 and Ship 2, i.e. Sp_{12}/L. The curves highlight the fact that the force coefficients tend to increase more rapidly as the lateral distance between the ships becomes smaller. This tendency is common to the two ships meeting situation. However, a higher gradient is clearly noticed for the curve representing the maximum repulsion force coefficients when ST` = -0.8 (i.e. when Ship 1 is positioned between Ship 2 and Ship 3). As a result, this peak value is approximately 130% larger for $Sp_{12}/L = 0.2$ than the maximum repulsion force coefficient experienced by Ship 1 in a bow-bow situation with Ship 3 (ST` = -2.5). The difference reduces as the separation distance increases and for $Sp_{12}/L = 0.6$ these peaks have equal magnitude.

It is found that the magnitudes of the maximum repulsion force coefficients when ST` = -0.8 are smaller for all separation distances when compared to the maximum attraction peaks when ST` = 0.0, (i.e. when the midship of Ship 1 is aligned with the midship of Ship 2). For $Sp_{12}/L = 0.2$ the difference is around 22% and it increases to approximately 67% for $Sp_{12}/L = 0.7$.

The maximum yaw moment coefficients acting on Ship 1 are shown in Fig 5.7b for various non-dimensionalized separation distances, and it is once more evident that the peak values increase sharply for small separation distances. This tendency is especially noticeable for the yaw moments when ST` = -1.7 (i.e. immediately before the midship-midship situation with Ship 3), and ST` = 0.3, (i.e. just prior to the midship-midship situation with Ship 2). As the separation distances increase, the bow-in maximums that Ship 1 experiences when ST` = -1.7 decrease and become zero for a $Sp_{12}/L$ ratio of 0.41. Furthermore, for larger separation distances the yaw moment changes direction and becomes bow-out in nature. An identical tendency can be seen for the yaw moment coefficients when ST` = 0.3 where Sp_{12}/L ratios above 0.41 give bow-out peaks while for larger separation distances Ship 1 experiences small bow-in moments.

For small Sp_{12}/L ratios, Ship 1 experiences similar maximum bow-out moment coefficients when ST` = -2.5 (i.e. the bow-bow situation with Ship 3), compared to when ST` = -1.0 (i.e. the stern-midship situation with Ship 3 and the bow-bow situation with Ship 2). However, as the Sp_{12}/L ratio increases from 0.3 to 0.7, the difference in bow-out peaks grows from 5% to approximately 50%, where the maximum bow-out moment coefficients when ST` = -1.0 are largest.

Small differences in peak values are also found for the bow-in peaks acting on Ship 1 immediately before the midship-midship situation (ST` = -0.2) and the stern-stern situation (ST` = 1.0) with Ship 2, when the separation distances are small. For separation distances beyond 0.4L the bow-out peaks when ST` = 0.8 decrease more slowly than the bow-out peaks when ST` = -0.2, resulting in a difference of approximately 47% for a Sp_{12}/L ratio of 0.7.

The maximum bow-out moment coefficient when ST` = -1.0 is found to be approximately 20% smaller in magnitude than the bow-in peak when ST` = -0.2 for a Sp_{12}/L ratio of 0.2. This difference decreases and becomes negligible for $Sp_{12}/L = 0.45$. Furthermore, the bow-out peaks, when ST` = -1.0, become larger than the bow-in moment coefficients for larger separation distances.

5.4.3 The effect of ship size

An investigation into the effect of ship sizes on the lateral forces and yaw moments acting on Ship 1 is also carried out for the three ships meeting situation. Again, many manoeuvre configurations are possible, since the size of all three ships can be changed individually. This thesis limits the examination of the size effect by keeping the size of Ship 1 constant while geometrically scaling both Ship 2 and Ship 3 equally, i.e. the size of Ship 2 equals the size of Ship 3 for all the results presented. Once more, only the numerical calculations carried out on Ship 1 are shown here, where it first meets Ship 3 followed by Ship 2 for the following situation:

W	H/D_1	Sp_{12}/L_1	Sp_{13}/L_1	$L_1/L_{2,3}$	$U_{2,3}/U_1$	$ST_{23} - L_{2,3}$
$2L_1$	1.5	0.5	0.6	Varying	1.0	$-0.5L_1$

Table 5.3 Condition for the effect of ship size, (three ships meeting).

The longitudinal distance between the stern of Ship 3 and the bow of Ship 2 is chosen to be constant and taken as $0.5L_1$ for all length ratios (i.e. $ST_{23} - L_{2,3} = -0.5L_1$)

Figures 5.8a,b show the size effect on the lateral force and yaw moment coefficients acting on Ship 1, where it is found that Ship 1 experiences larger hydrodynamic forces and moments when encountering bigger ships. This tendency is common to two ships meeting situations.

The maximum lateral force coefficients, shown in Figs 5.9a, are plotted against the $L_1/L_{2,3}$ ratio. It is apparent that as the $L_1/L_{2,3}$ ratio decreases the peak values increase sharply. The maximum repulsion peaks acting on Ship 1 when ST` = -2.5, (i.e. when

its bow passes the bow of Ship 3), behave in a similar way to the maximums appearing at the bow-bow situation for two ships meeting. When Ship 1 is 20% smaller than both Ship 2 and Ship 3 it experiences approximately 70% larger peak values for this repulsion force coefficient compared to the situation where all three ships are identical. Again, when Ship 1 is 1.2 times larger than Ship 2 and Ship 3 the result is around 37% smaller lateral force peaks for Ship 1 when compared to the $L_1/L_{2,3} = 1.0$ case.

Similar percentage differences are also found for various $L_1/L_{2,3}$ ratios for the maximum attraction and repulsion force coefficients when ST` = 0.0 and ST` = 0.8 (i.e. when Ship 1 is in a midship-midship and stern-stern situation respectively with Ship 2.)

However, the maximum attraction force coefficients acting on Ship1 when ST` = -1.5 (i.e. when Ship 1 is in a midship-midship situation with Ship 3) increase by approximately 80% for a $L_1/L_{2,3}$ ratio of 0.8 compared to the $L_1/L_{2,3} = 1.0$ case. As Ship 1 becomes 1.2 times the size of Ship 2 and Ship 3 the reduction in peak values is about 42%. Furthermore, when ST` = -0.8 (i.e. when positioned between Ship 2 and Ship 3) the maximum repulsion force coefficients increase by around 100% if Ship 1 is 20% smaller than Ships 2 and 3 compared to the $L_1/L_{2,3} = 1.0$ case. Once more, Ship 1 experiences a reduction in peak value as Ship 1 gets 1.2 times bigger than Ship 2 and Ship 3, and the lessening of the repulsion maximum is found to be approximately 50%.

The maximum yaw moment coefficients acting on Ship 1 are shown in Fig 5.9b for various $L_1/L_{2,3}$ ratios. The bow-out and bow-in peaks at the beginning (ST` = -2.5) and end (ST` = 1.0) of the encountering transit respectively, increase sharply as the $L_1/L_{2,3}$ ratio decreases. This is as anticipated since Ship 1 experiences a similar tendency for these moment peaks when meeting only one ship. When Ship 1 is 20% smaller than Ships 2 and 3, it experiences approximately 70% smaller peak values compared to when all three ships are identical for both the bow-out moment coefficients when ST` = -2.5, and for the bow-in moment coefficients when ST` = 1.0. On the other hand, when Ship 1 is 1.2 times larger than Ship 2, the result is around 37% smaller yaw moment peaks.

The maximum bow-out moment coefficients when ST` = -1.0 (i.e. the stern-midship situation with Ship 3 and the bow-bow situation with Ship 2) have a linear increase in peak values for a decreasing $L_1/L_{2,3}$ ratio. When Ship 1 is 20% larger than Ship 2 and Ship 3 it experiences approximately 20% higher bow-out peaks compared to the $L_1/L_{2,3}$ case, and when Ship 1 is 1.2 times the size of Ships 2 and 3 the peak values decrease with around 20%.

However, the maximum bow-in moment coefficients, when ST` = -0.2 (i.e. immediately before the midship-midship situation with Ship 2), do not have a sharp increase in peak values for a decreasing $L_1/L_{2,3}$ ratio. A 20% size reduction of Ship 1 compared to Ship 2 and Ship 3 produces only about 9% larger peak values, while increasing the size of Ship 1 by 1.2 times that of Ships 2 and 3 generates approximately 23% smaller maximums.

5.4.4 The effect of ship speed

So far only encounters by ships travelling at the same speed has been considered. In this section the effect of ship speed on the lateral forces and yaw moments acting on Ship 1 is investigated. However, the present method must take the equal speed of Ships 2 and 3 as input, i.e. the longitudinal distance between these two ships has to be constant during transit. The condition is given below:

W	H/D	Sp_{12}/L	Sp_{13}/L	$L_1/L_{2,3}$	$U_{2,3}/U_1$	ST_{23}
2L	1.3	0.5	0.6	1.0	Varying	-1.5L

Table 5.4 Condition for the effect of ship speed, (three ships meeting).

Figures 5.10a,b show the effect of a change in relative speed on the lateral force and yaw moment coefficients acting on Ship 1. When $U_{2,3}/U_1 < 1.0$, Ship 1 is travelling faster than the two ships it encounters and when $U_{2,3}/U_1 > 1.0$ it is the slower ship. It is apparent from Figs 5.10a,b that Ship 1 experiences greater lateral forces and yaw moments when travelling more slowly than Ship 2 and Ship 3. As expected, this is the

same tendency that Ship 1 experiences when meeting only one faster ship. On the other hand, when moving faster than the two ships it encounters, the hydrodynamic forces and moments become smaller.

The peak values for the lateral force coefficients, plotted against $U_{2,3}/U_1$, are shown in Fig 5.11a. It is evident from the graph that the repulsion and attraction peaks acting on Ship 1 increase linearly when the speeds of Ship 2 and Ship 3 are gradually increased. This tendency is again common to the two ships meeting manoeuvre. When Ship 1 is travelling at half the speed of both Ship 2 and Ship 3 it experiences between 44% to 63% larger maximum lateral force coefficients than when all three ships have the same speed. Furthermore, if we increase the speed of Ship 1 to twice the speed of Ship 2 and Ship 3 the force peaks decrease by approximately 21% to 32% compared to the same $U_{2,3}/U_1 = 1.0$ case.

Figure 5.11b illustrates the variation of the maximum yaw moment coefficients acting on Ship 1 for different $U_{2,3}/U_1$ ratios. The bow-out and bow-in peak values at the beginning (ST` = -2.5) and end (ST` = 1.0) of the transit respectively do not change significantly for different $U_{2,3}/U_1$ ratios. Once again, this tendency is common to the two ships meeting manoeuvre.

However, the maximum bow-out moment coefficients when ST` = -1.0 (i.e. the stern-midship situation with Ship 3 and the bow-bow situation with Ship 2), increase linearly for the growing $U_{2,3}/U_1$ ratio. As a result, Ship 1 experiences approximately 63% larger peak values when it travels at half the speed of Ship 2 and Ship 3 and 31% smaller peak values when travelling at twice the speed of Ships 2 and 3 compared to $U_{2,3}/U_1 = 1.0$. Because of this growth in peak values for increasing speed ratios, Ship 1 experiences larger maximum bow-out moment coefficients when ST` = -1.0 compared to the bow-out peaks when ST` = -2.5 for $U_{2,3}/U_1$ ratios above 1.35. Furthermore, this difference in bow-out peak values is found to be around 31% for a $U_{2,3}/U_1$ ratio of 2.0.

The maximum bow-in moment coefficients, appearing immediately before the midship-midship situation with Ship 2 (ST` = -0.2), increase linearly for $U_{2,3}/U_1$ ratios above 1.0. However, for $U_{2,3}/U_1 = 1.0$ there is a discontinuity in the curve, and the

reduction in bow-in peaks, as Ship 1 is the faster ship, becomes less steep. Ship 1 experiences about 80% larger peak values for a $U_{2,3}/U_1$ ratio of 2.0 compared to the $U_{2,3}/U_1 = 1.0$ situation and approximately 32% smaller peak values when Ship 1 travels with twice the speed of Ship 2 and Ship 3. Furthermore, Ship 1 experiences larger maximum bow-in moment coefficients for $U_{2,3}/U_1$ ratios above 1.25, resulting in a difference of approximately 42% when $U_{2,3}/U_1 = 2.0$.

5.4.5 The effect of longitudinal distance between Ship 2 and Ship 3

Previously, the longitudinal distance between Ship 2 and Ship 3 has been kept constant (ST_{23} = -1.5L). In this section the present method is used to examine the effect of changing the longitudinal distance, or the stagger, between the midships of Ship 2 and Ship 3. However, in order to describe this effect, one '3 ships interaction' problem is shown together with two '2 ships interaction' manoeuvres in Figs 5.12a,b. For the three ships meeting configuration, Ship 1 first encounters Ship 3 followed by Ship 2 for the following condition:

W	H/D	Sp_{12}/L	Sp_{13}/L	$L_1/L_{2,3}$	$U_{2,3}/U_1$	ST_{23}
2L	1.3	0.5	0.6	1.0	1.0	-1.5L

Table 5.5 Condition for comparison of a '3 ships interaction' problem with two '2 ships interaction' problem.

The two '2 ships interaction' conditions represent the presence of Ship 2 and Ship 3 in the three ships meeting manoeuvre separately with separation distances of 0.5L and 0.6L to Ship 1 respectively.

It is apparent from Fig 5.12a that the stern-stern repulsion peak from Ship 3 (ST` = -0.5) plus the bow-bow repulsion from Ship 2 (ST` = -1.0) gives a large repulsion force acting on Ship 1 for the 3 ships interaction manoeuvre (ST` = -0.8). This repulsion peak value grows and becomes largest when the ST_{23}/L ratio becomes −1.8L since Ship 1 then experiences maximum repulsion from both the stern of Ship 3 and the bow of Ship 2.

Comparison of the yaw moment coefficients acting on Ship 1 between a '3 ships interaction' manoeuvre and two '2 ships interaction' manoeuvre can be seen in Fig 5.12b. Again, the moment transit varies with a changing stagger between Ship 2 and Ship 3.

Figures 5.13a,b show how these variations of the stagger between Ship 2 and Ship 3 effects the lateral force and yaw moment coefficients acting on Ship 1 for the following condition:

W	H/D	Sp_{12}/L	Sp_{13}/L	$L_1/L_{2,3}$	$U_{2,3}/U_1$	ST_{23}
2L	1.3	0.5	0.6	1.0	1.0	Varying

Table 5.6 Condition for the effect of longitudinal distance between Ship 2 and Ship 3, (three ships meeting).

The stagger, as described in the introduction, is non-dimensionalized such that –1, 0 and +1 corresponds to the bow-bow, midship-midship and stern-stern situation with Ship 2 respectively, and is used as the abscissa for the plots. However, the stagger values representing the bow-bow, midship-midship and stern-stern situation with Ship 3 vary with the longitudinal distance between Ship 2 and Ship 3 respectively. That is, for a ST_{23}/L ratio of -1.0, Ship 1 is in a bow-bow situation with Ship 3 when ST` = -2.0 and for $ST_{23}/L$ = -2.0 the bows meet when ST` = -3.0.

It is apparent from Figs 5.13a,b that Ship 1 experiences a different force and moment transit during the encountering manoeuvre when changing the longitudinal spacing between Ship 2 and Ship 3. The alteration can be seen particularly in the maximum lateral force and yaw moment coefficients when Ship 1 occupies positions between Ship 2 and Ship 3.

The variation in the peak values can be seen in Figs 5.14a for the lateral force coefficients. Ship 1 is found to have approximately 25% larger repulsion forces for a ST_{23}/L ratio of -1.8, compared to the previous ST_{23}/L = -1.5 case when ST`= -0.8 (i.e.

when Ship 1 is in a stern-stern situation with Ship 3 at the same time as it is in a bow-bow situation with Ship 2.)

Furthermore, the most noticeable feature of the maximum yaw moment coefficient variation in Fig 5.14b is that Ship 1 experiences larger bow-out and bow-in peaks for a ST_{23}/L ratio of –1.0. The largest difference compared to the ST_{23}/L = -1.5 case is found when ST` = -1.0 (i.e. when Ship 1 is in a midship-midship situation with Ship 3 and a bow-bow situation with Ship 2.)

5.4 CONCLUDING REMARKS

- Good agreement is found when comparing the lateral force and yaw moment coefficients acting on Ship 1 in three ships meeting manoeuvre with Yasukawa's predicted data. This is true both for the force and moment transits and for the calculated maximum hydrodynamic forces and moments.

- From the parametric studies it is apparent that the interaction forces and moments increase as the separation distance and water depth decreases. Furthermore, the present method also found that Ship 1 experiences larger lateral forces and yaw moments when reducing its size and speed compared to those of the encountering Ship 2 and Ship 3.

- An investigation into the effect of the longitudinal distance, or stagger, between Ship 2 and Ship 3 (ST_{23}), reveals that Ship 1, when situated between these ships, experiences largest repulsion forces when this longitudinal distance between the midships is –1.8L. However, largest yaw moments are found when ST_{23} = -1.0L, i.e. when there are zero distance between the stern of Ship 2 and the bow of Ship 3.

- The three ships meeting manoeuvre is more potentially dangerous compared to the two ships meeting manoeuvre. This is due to the large interaction forces and moments Ship 1 experiences when positioned between Ship 2 and Ship 3 and hence interacting with both ships.

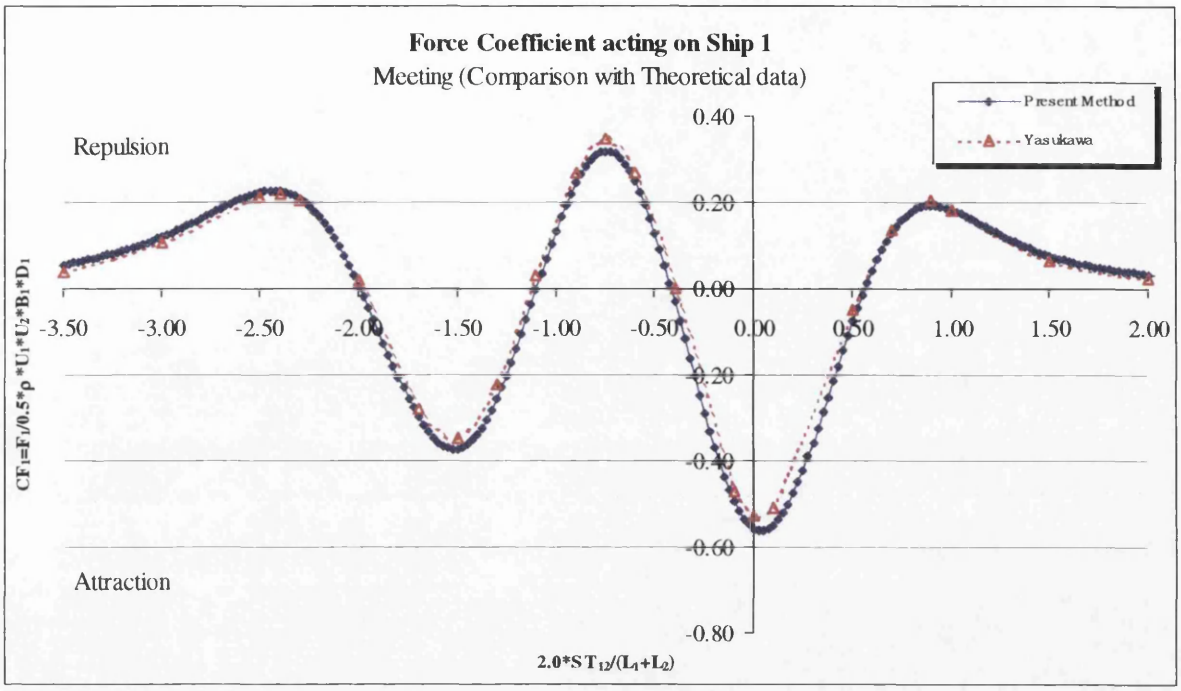

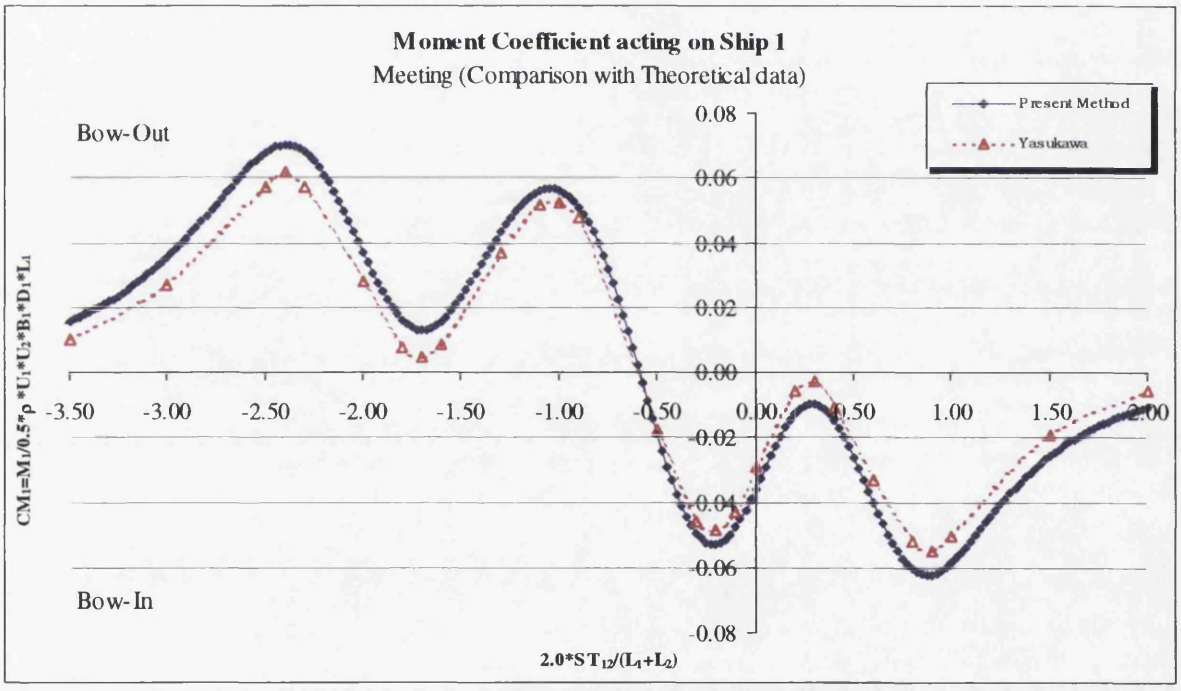

Figs 5.2a,b Comparison of the lateral force and yaw moment coefficients with Yasukawa's experimental data, (three ships meeting)

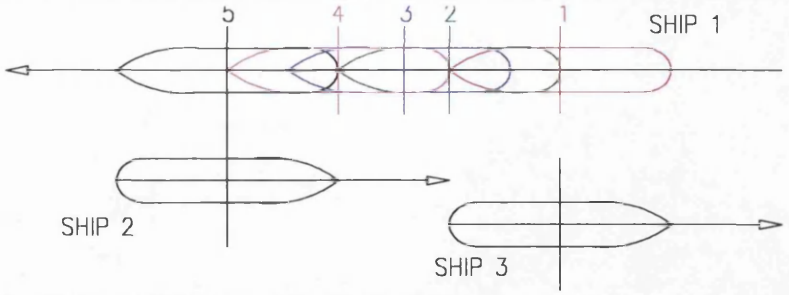

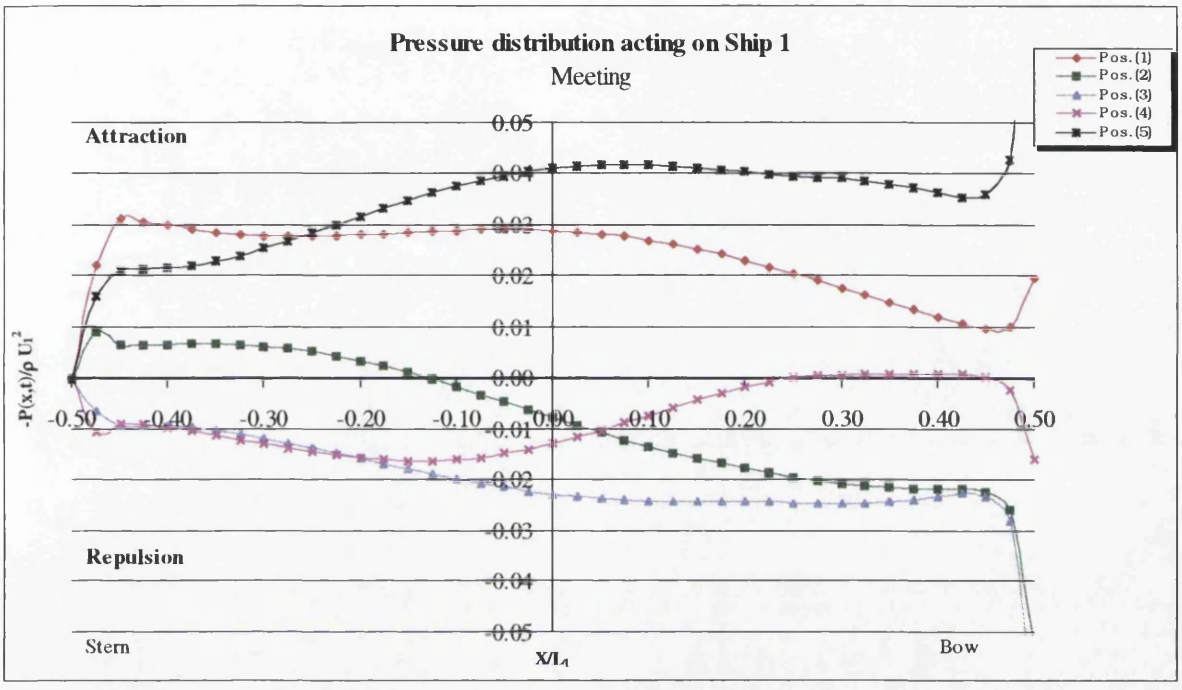

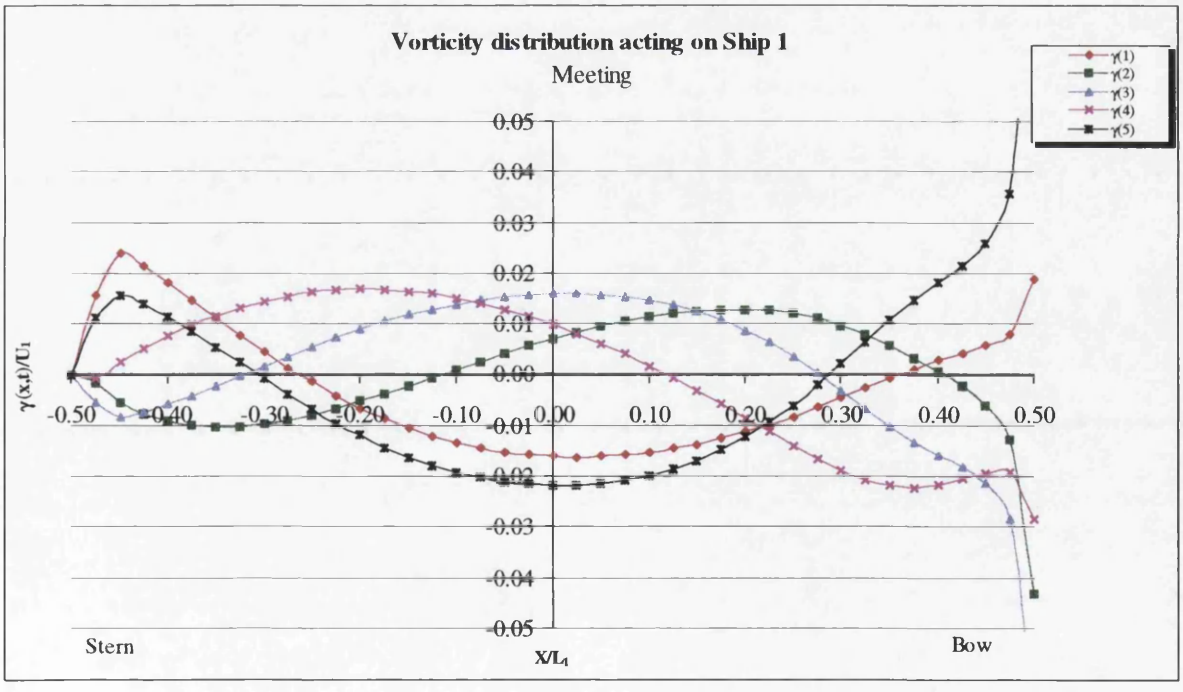

Figs 5.3a,b The pressure and vorticity distribution acting on Ship 1 for different time steps, (three ships meeting)

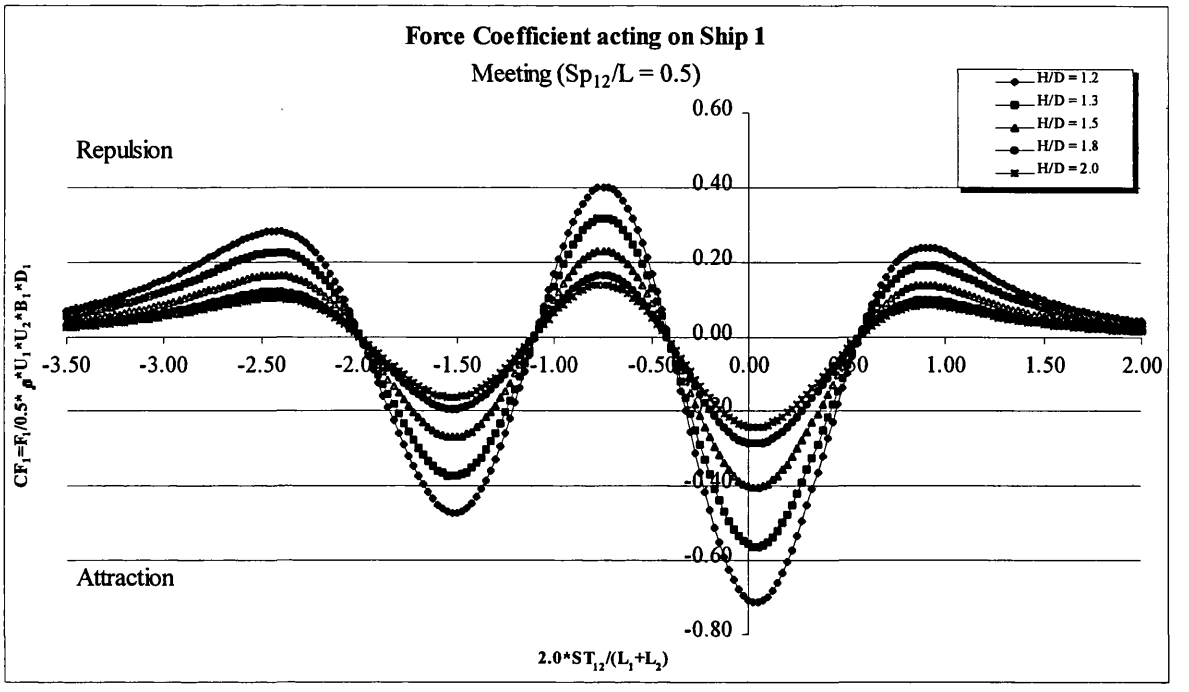

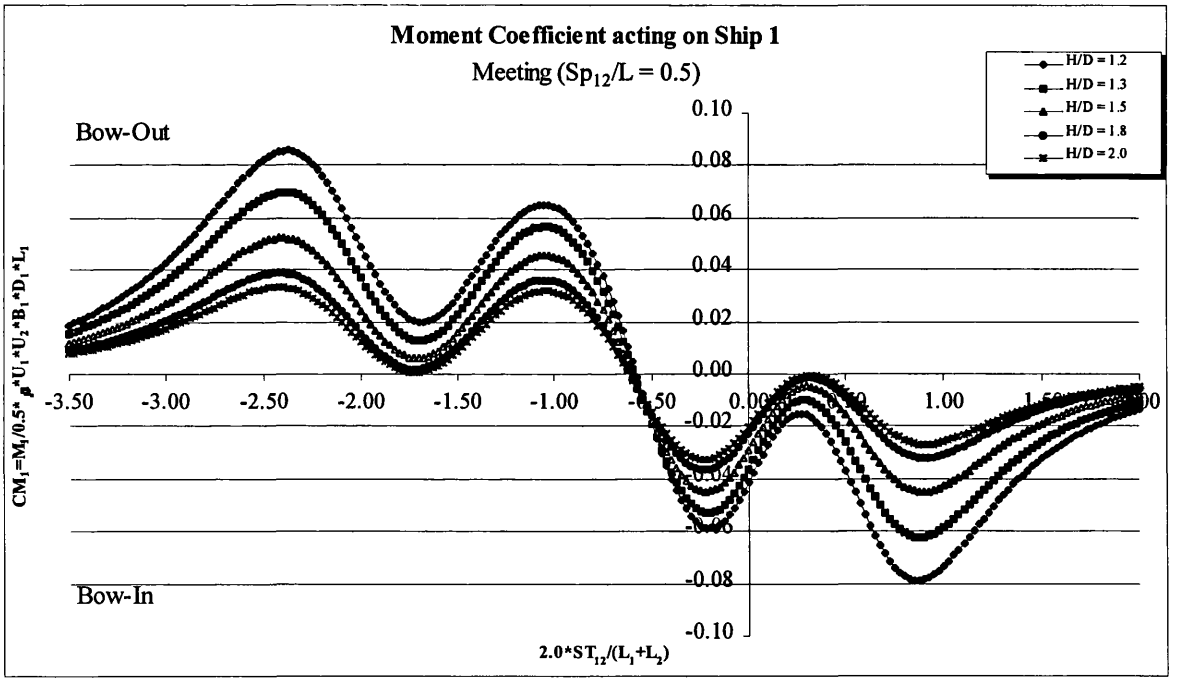

Figs 5.4a,b The lateral force and yaw moment coefficients acting on Ship 1 for various water depths, (three ships meeting)

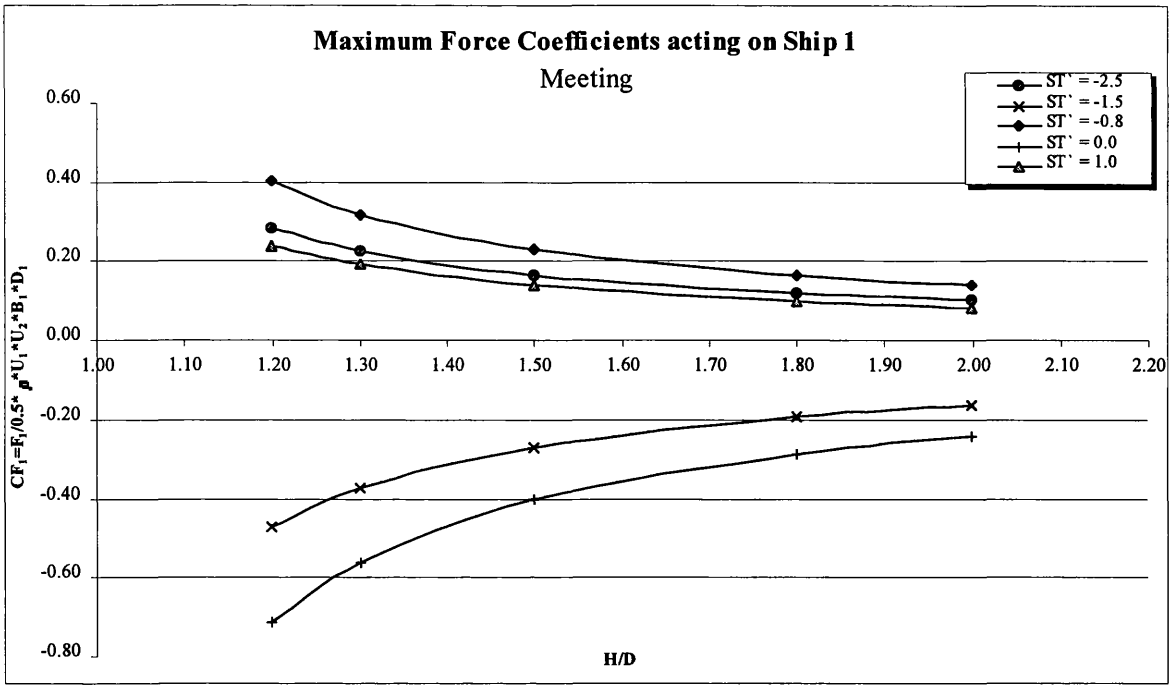

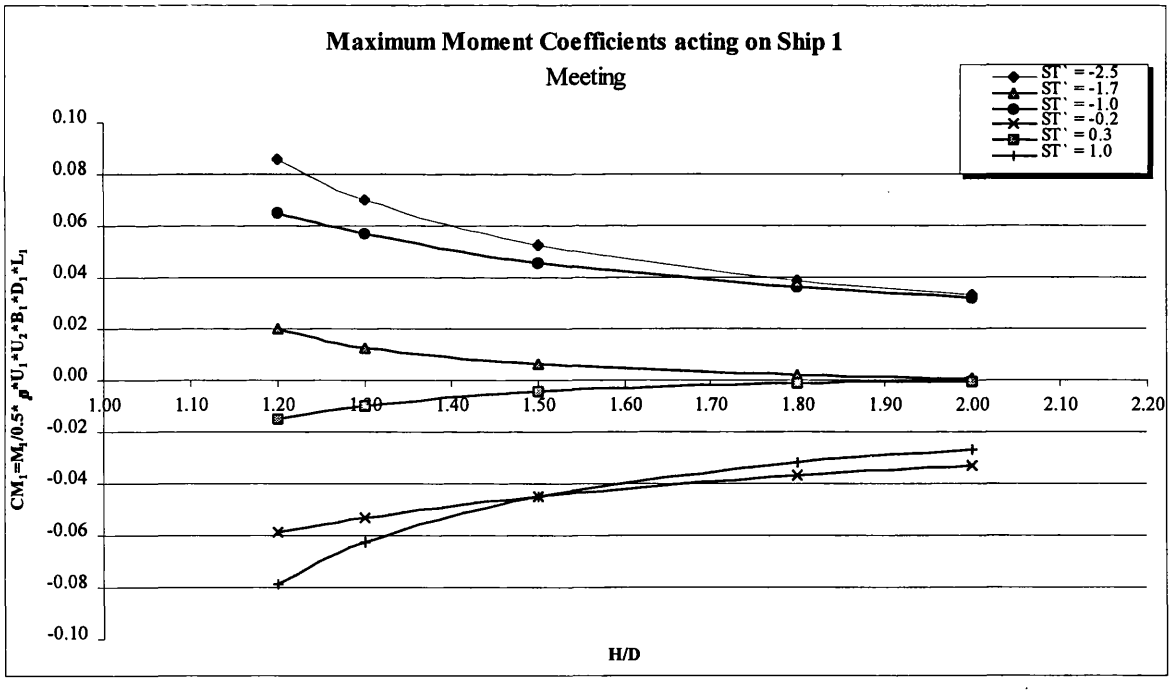

Figs 5.5a,b Maximum lateral force and yaw moment coefficients acting on Ship 1 for various water depths, (three ships meeting)

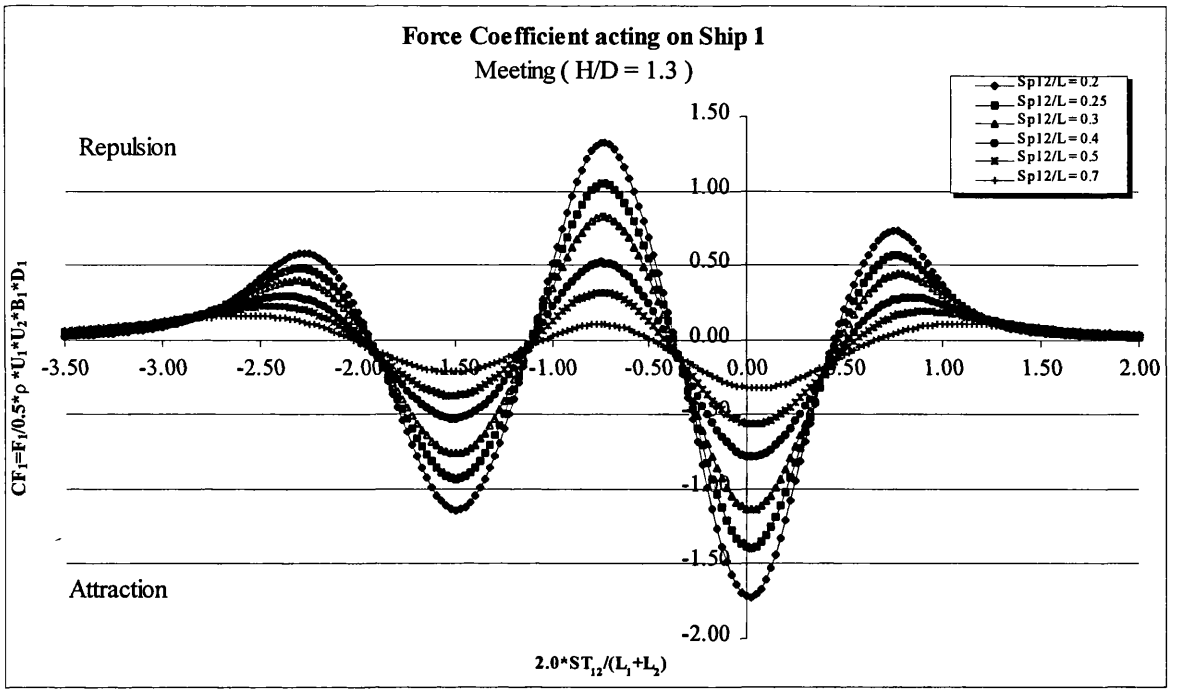

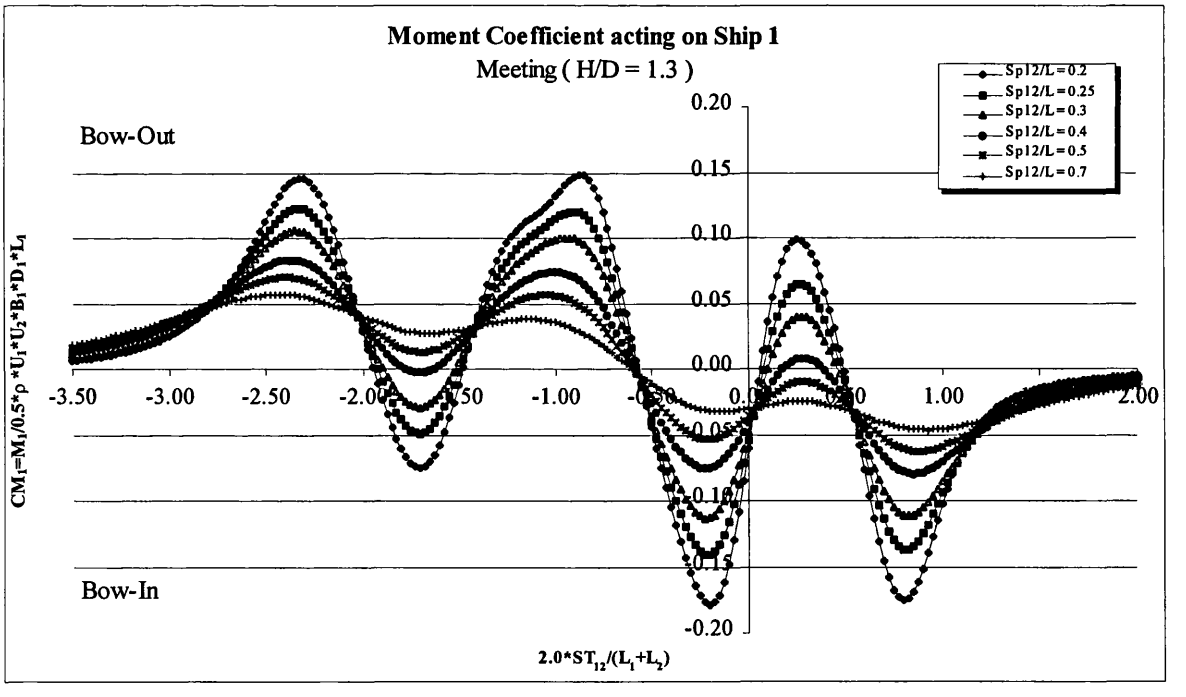

Figs 5.6a,b The lateral force and yaw moment coefficients acting on Ship 1 for various separation distances, (three ships meeting)

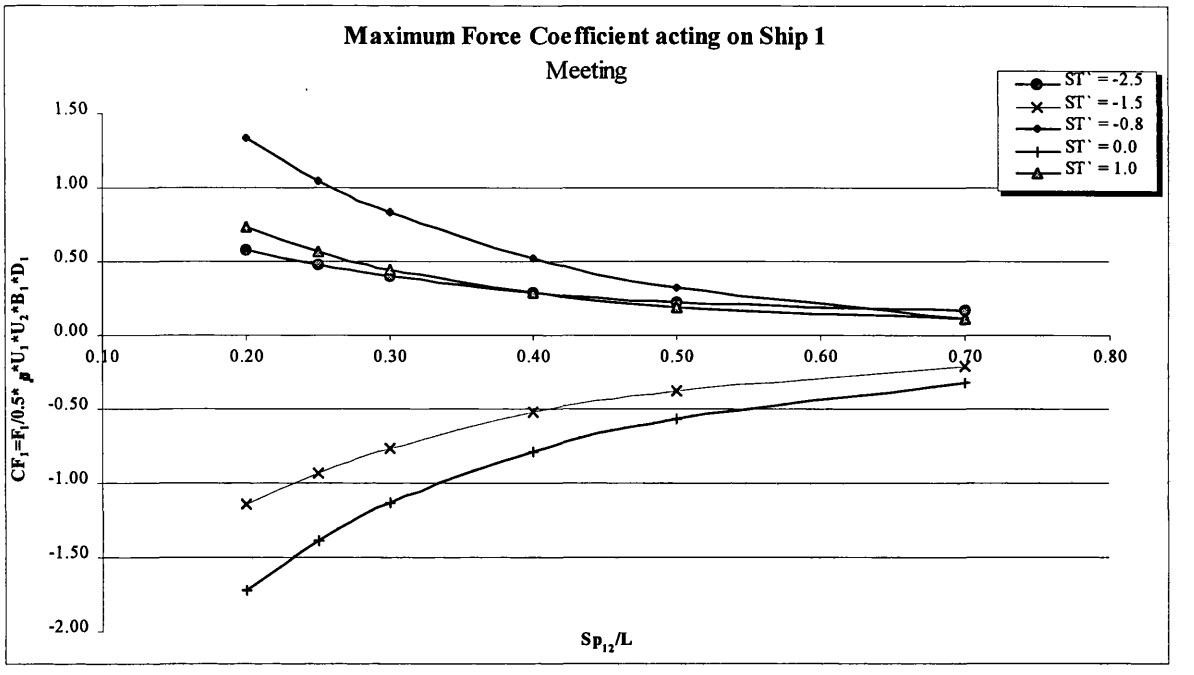

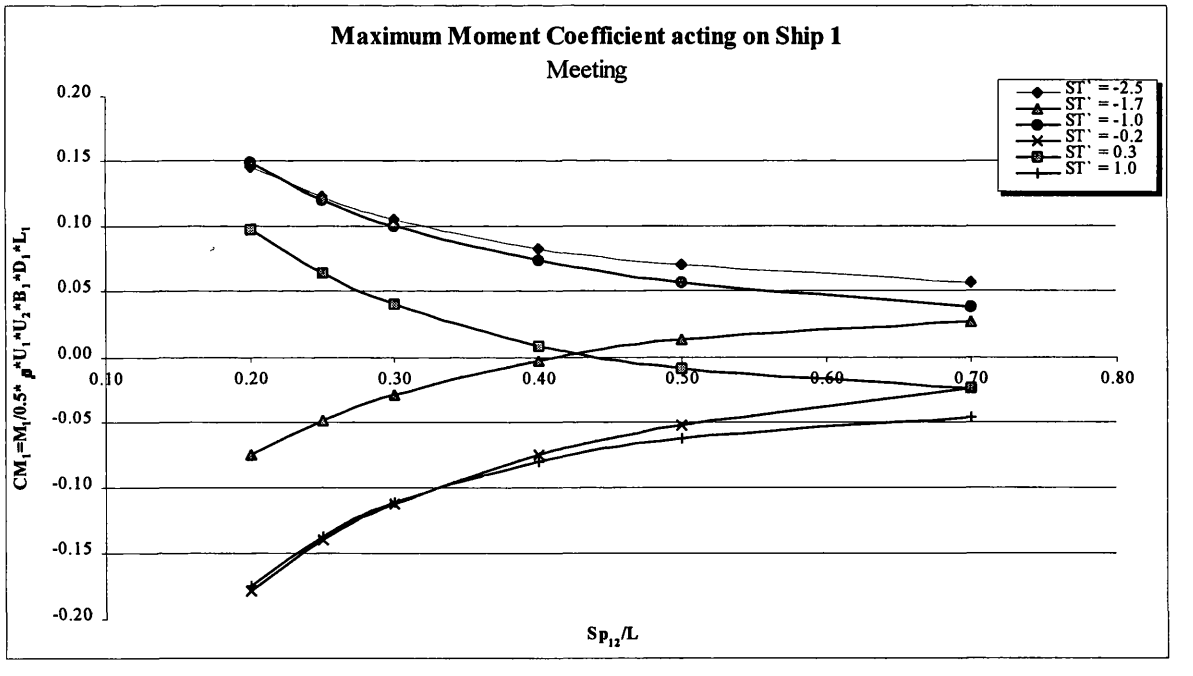

Figs 5.7a,b Maximum lateral force and yaw moment coefficients acting on Ship 1 for various separation distances, (three ships meeting)

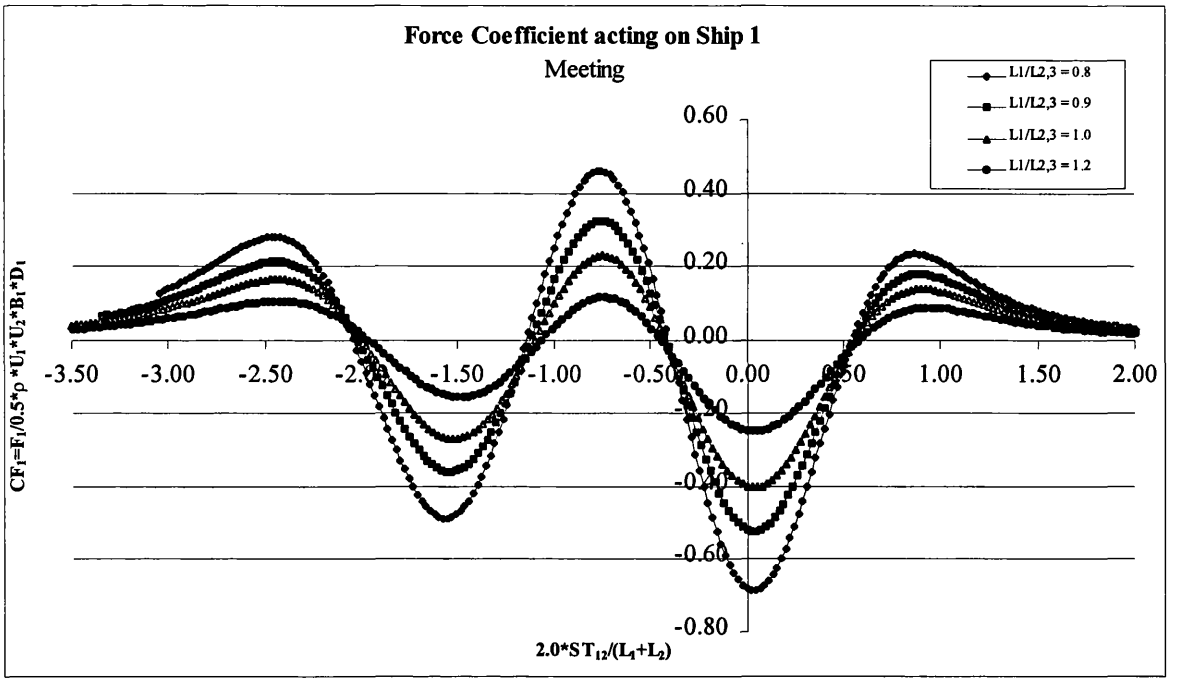

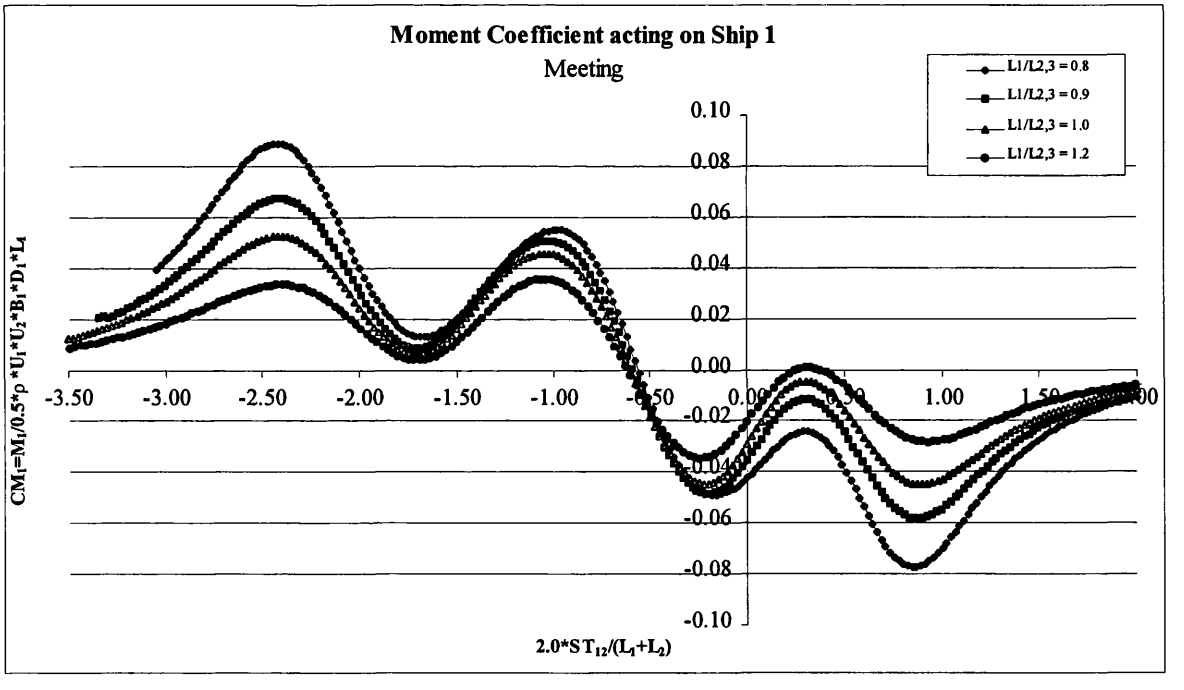

Figs 5.8a,b The lateral force and yaw moment coefficients acting on Ship 1 for various ship sizes, (three ships meeting)

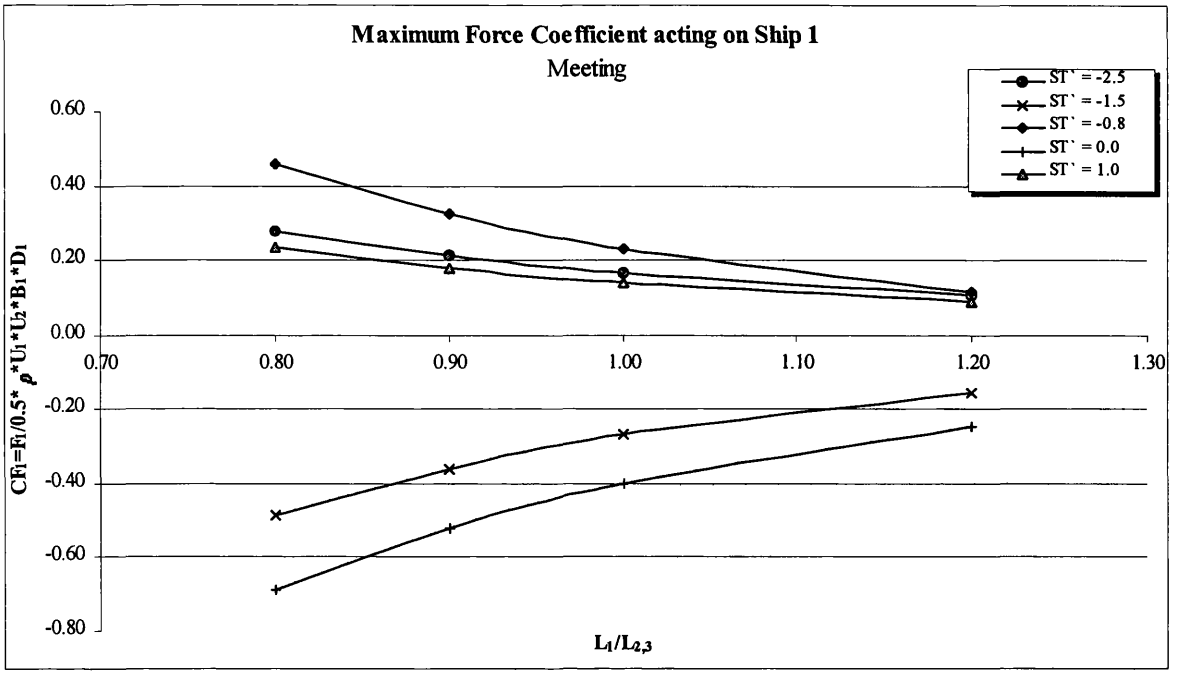

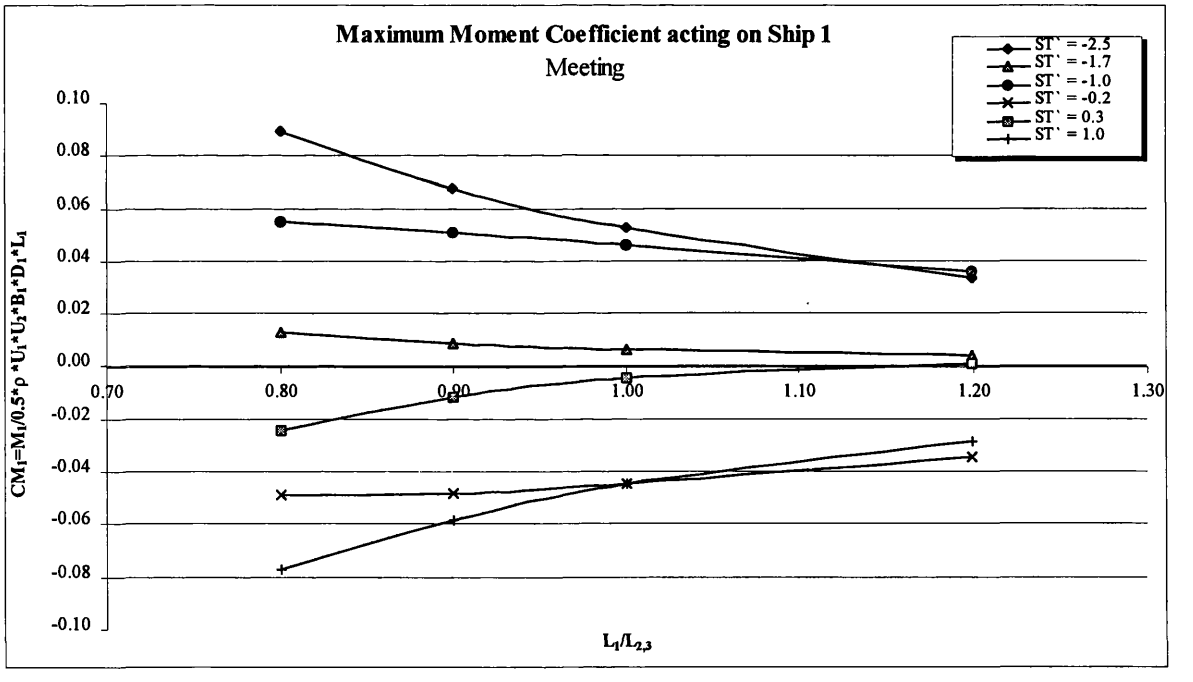

Figs 5.9a,b Maximum lateral force and yaw moment coefficients acting on Ship 1 for various ship sizes, (three ships meeting)

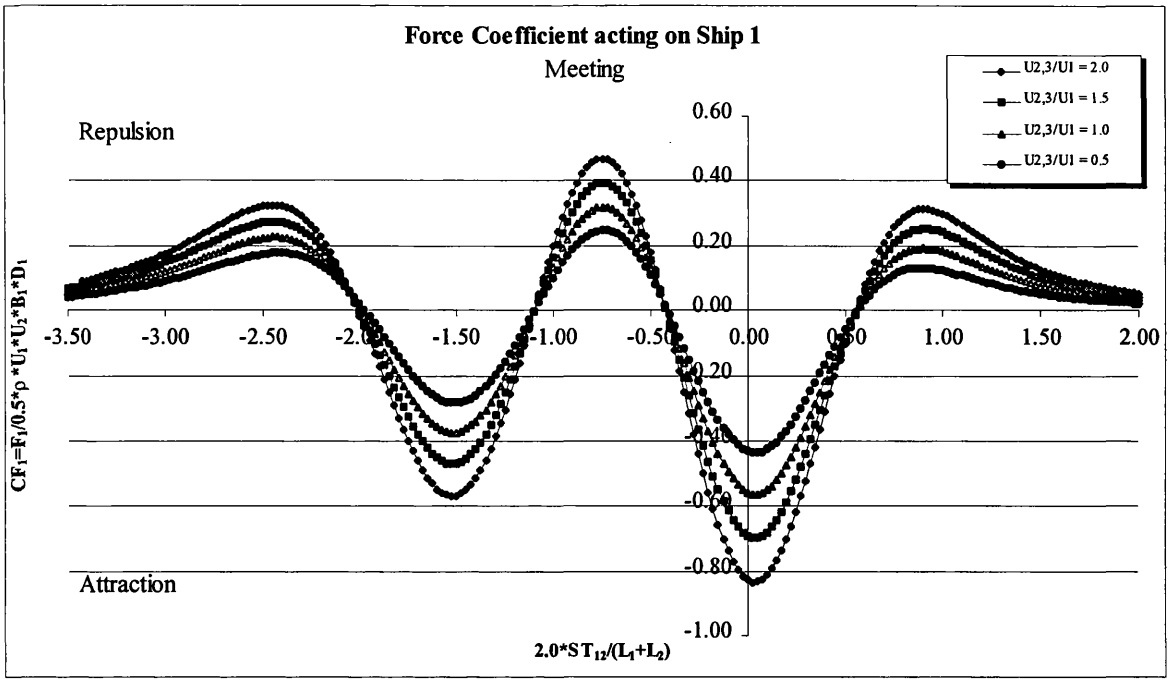

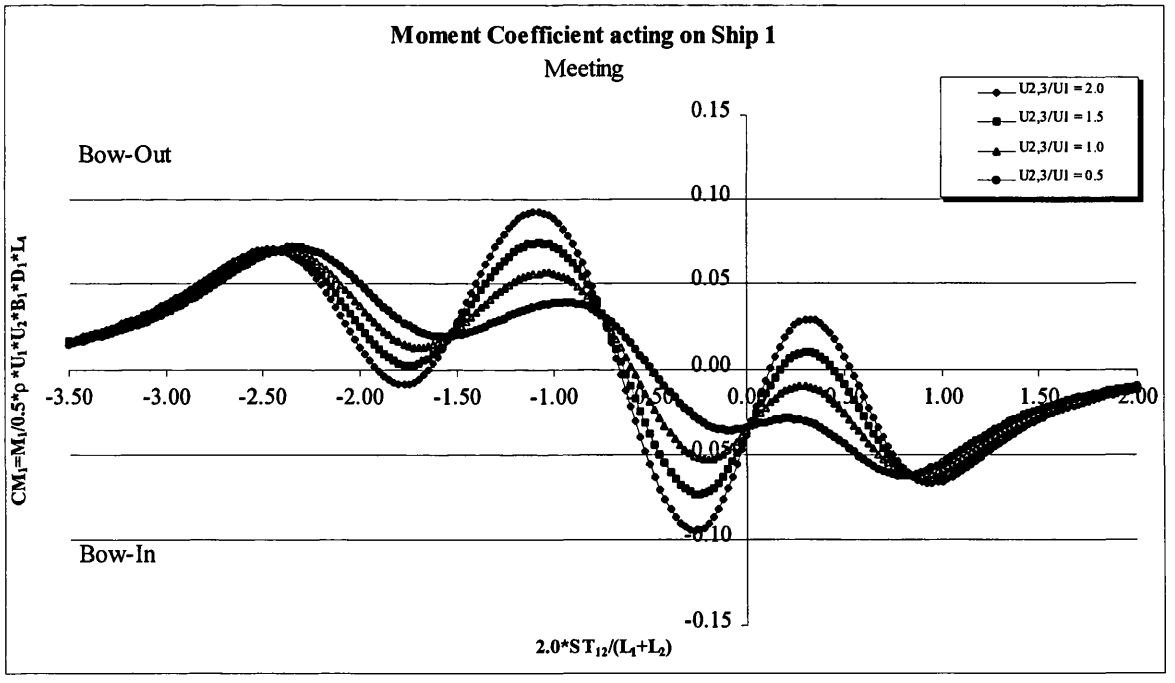

Figs 5.10a,b The lateral force and yaw moment coefficients acting on Ship 1 for various ship speeds, (three ships meeting)

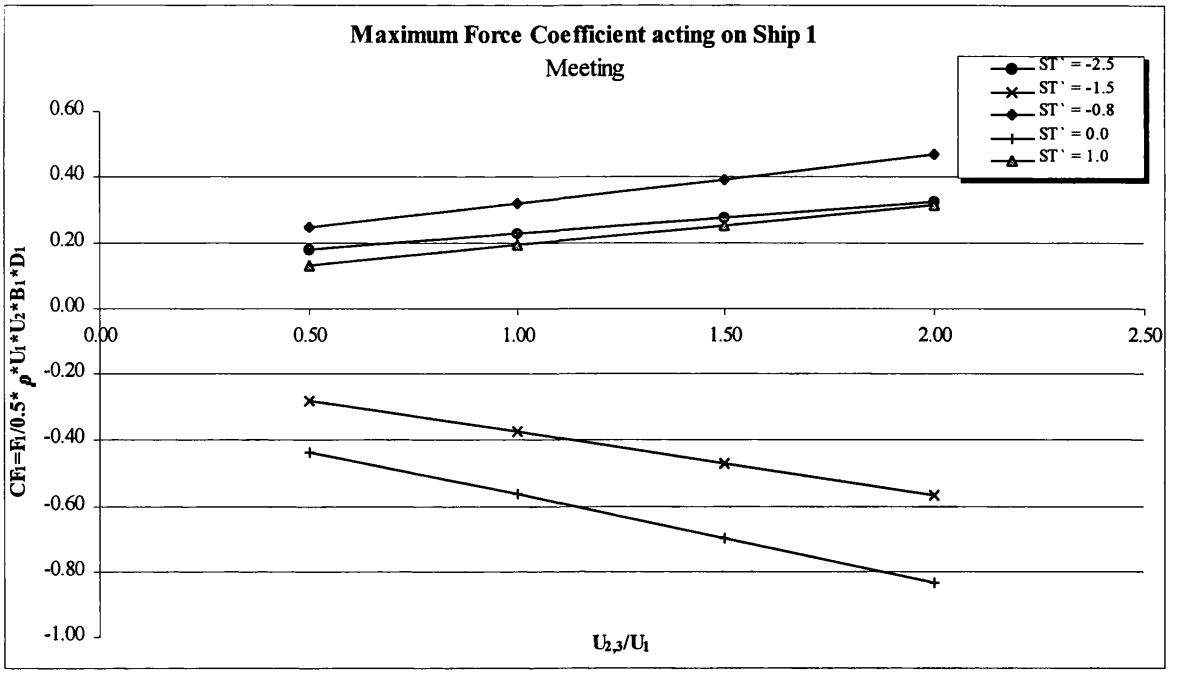

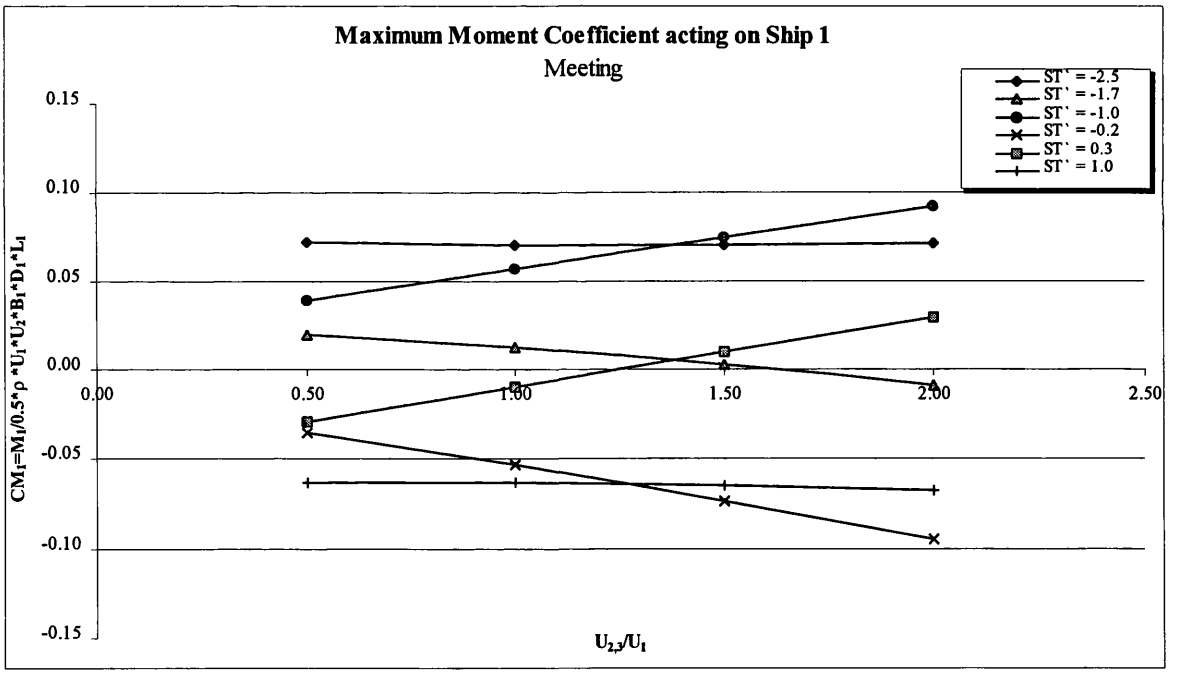

Figs 5.11a,b Maximum lateral force and yaw moment coefficients acting on Ship 1 for various ship speeds, (three ships meeting)

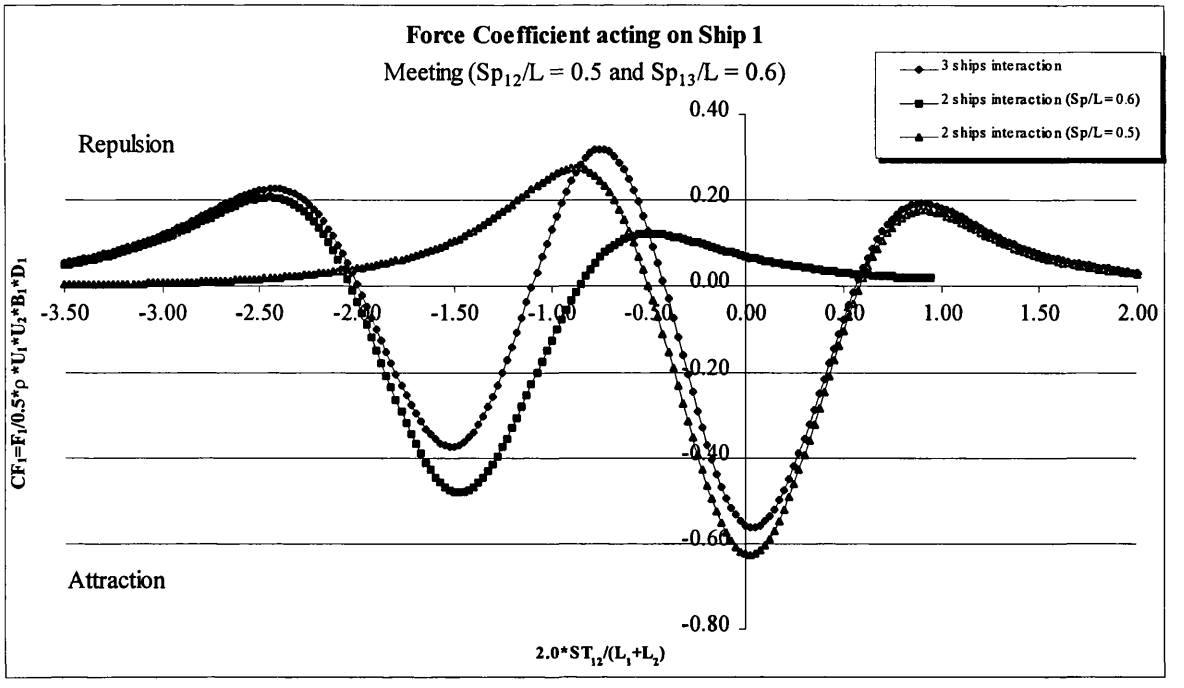

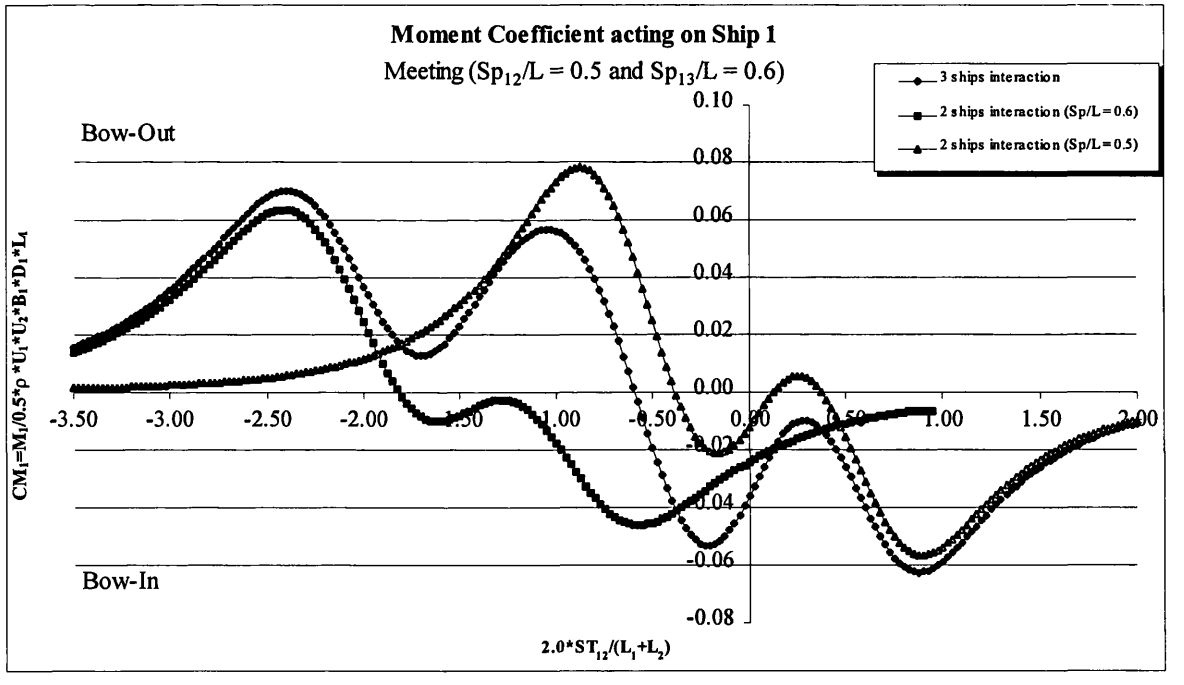

Figs 5.12a,b Comparisons of the lateral force and yaw moment coefficients acting on Ship 1 between two and three ships meeting manoeuvre.

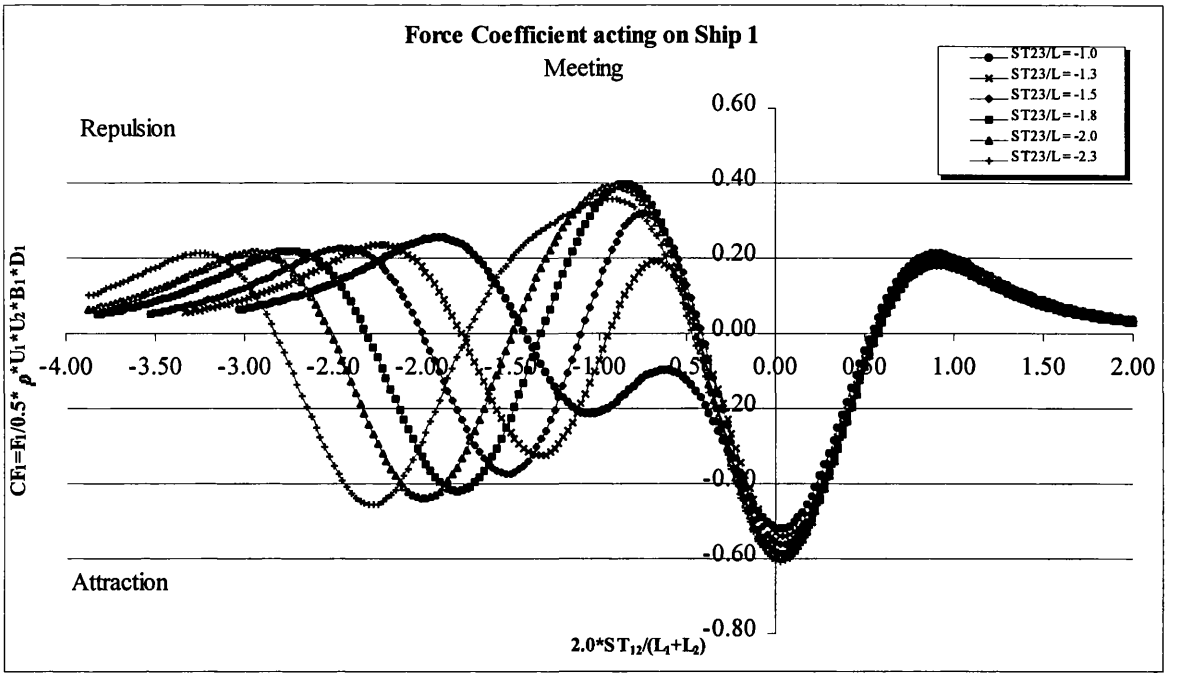

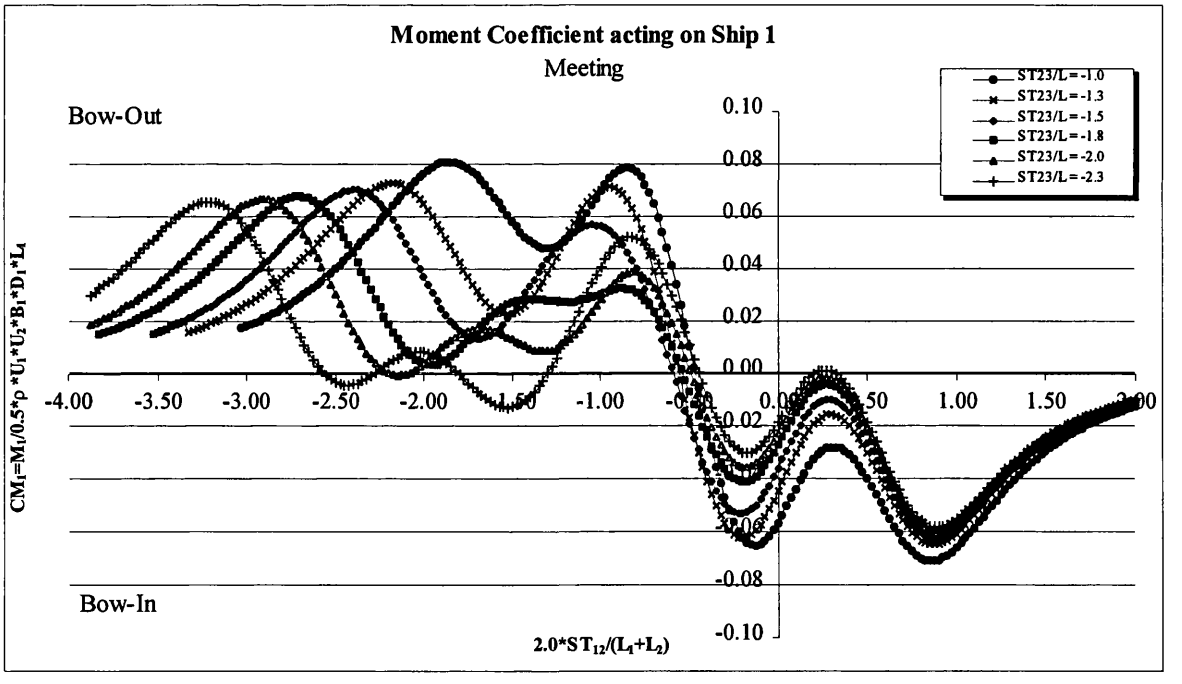

Figs 5.13a,b The lateral force and yaw moment coefficients acting on Ship 1 for various longitudinal distances between Ship 2 and Ship 3, (three ships meeting)

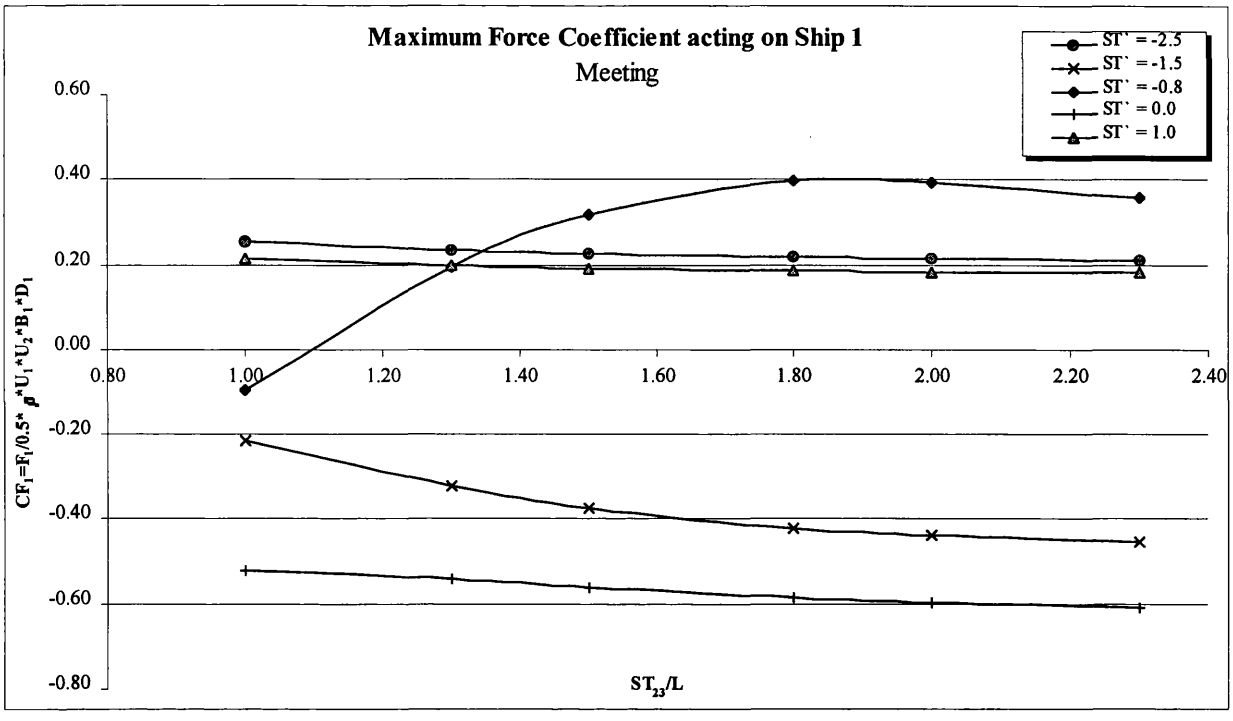

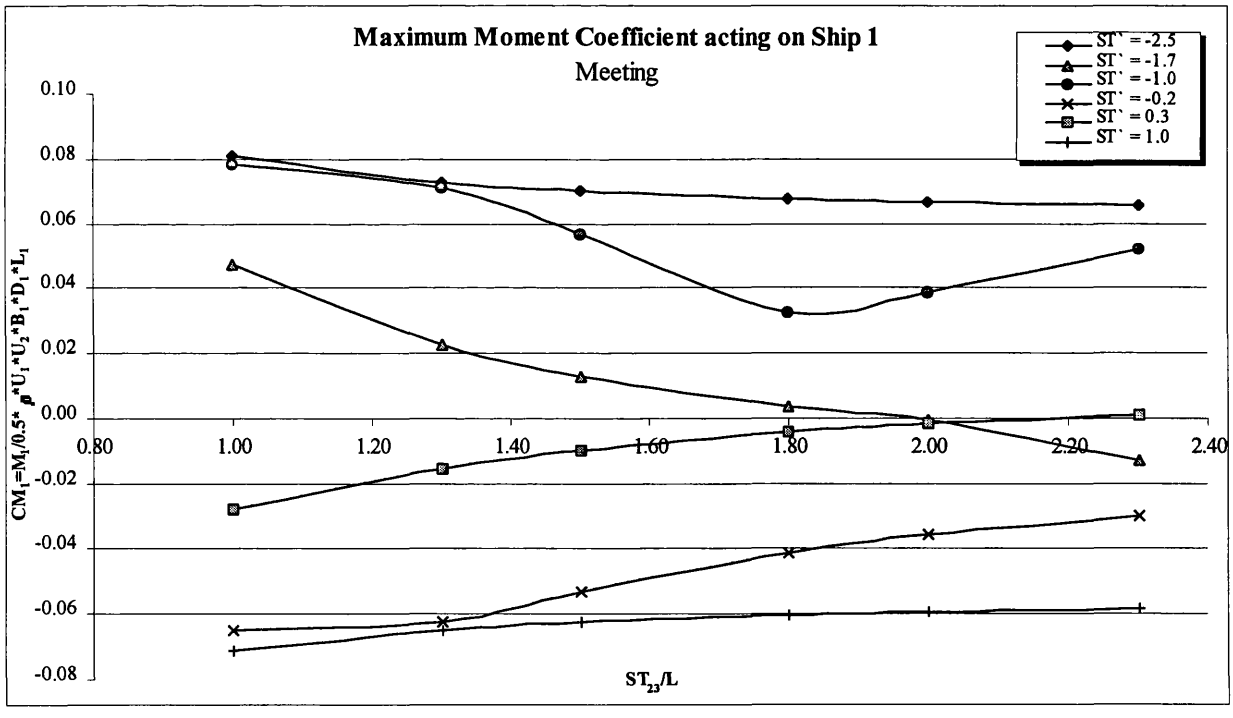

Figs 5.14a,b Maximum lateral force and yaw moment coefficients acting on Ship 1 for various longitudinal distances between Ship 2 and Ship 3, (three ships meeting)

CHAPTER 6

INTERACTION BETWEEN THREE SHIPS IN PASSING MANOEUVRE.

6.1 INTRODUCTION

An investigation into the problem concerning three ships in a passing manoeuvre is carried out in this chapter. From the situations involving only two ships in the overtaking manoeuvre (chapter 4) it is discovered that the slower ship experiences much larger lateral forces and yaw moments. As a result, the present method looks only into the problems where one ship is being overtaken by two other ships. Ship 1 is chosen to be the slower ship and is overtaken by Ship 2 followed by Ship 3. Again, the longitudinal distance between Ship 2 and Ship 3, ST_{23}, must be constant throughout the transit and is defined as a negative value. Fig 6.1 shows the plan view and the sign convention for such a three ships passing condition.

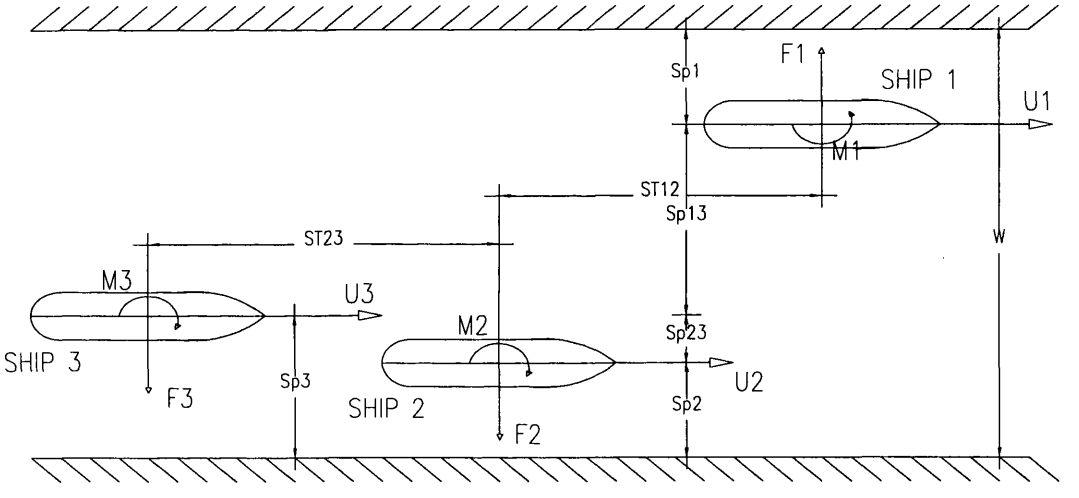

Fig 6.1 Co-ordinate system for three ships passing.

As for the two ships passing manoeuvre, the stagger is defined as follows:

$$ST_{12} = (U_1 - U_2) \times t \qquad U_1, U_2 > 0$$

where t = 0 corresponds to the situation in which the midships of Ship 1 and Ship 2 are aligned. Furthermore, the stagger, ST`{ $= 2.0 \times ST_{12}/(L_1 + L_2)$ }, is non-dimensionalized such that the values –1, 0, and +1 correspond to the stern-bow, midship-midship, and bow-stern situations respectively with Ship 2, and is used as the abscissa for the plots.

As before, only numerical results from Ship 1 (for principal particulars see Table 3.1) are presented when investigating the effect of water depth, separation distance, ship size, ship speed and the stagger between Ship 2 and Ship 3 (ST_{23}). Furthermore, the separation distances and water depths are non-dimensionalized by the length and draught respectively of Ship 1, and the stagger between Ship 2 and Ship 3 is non-dimensionalized by the length of Ship 1. Again, when all three ships in the passing manoeuvre are identical, the subscript is omitted for these non-dimensionals.

6.2 VERIFICATION OF NUMERICAL METHOD

Existing results for the case of three ships passing are limited to the theoretical predictions produced by Yasukawa (1983) for one ship being overtaken by two faster ships. Yasukawa's data are here compared to the lateral force and yaw moment coefficients calculated using the present method when Ship 2 and Ship 3 overtake Ship 1. All three ships are identical and travelling in a 2L wide and 1.3D deep channel. The separation distance between Ship 1 and Ship 2 is 0.6L while the separation distance between Ship 1 and Ship 3 is 0.5L. Both Ship 2 and Ship 3 are moving at the same speed, which again is twice the speed of Ship 1. The longitudinal distance between the midships of Ships 2 and 3 is -1.5L, and as a result non-dimensionalized stagger values (ST`) of +0.5, +1.5 and +2.5 correspond to the stern-bow, midship-midship and bow-stern situations respectively between Ship 1 and Ship 3.

Figures 6.2a,b show the comparison between the present method and that of Yasukawa of the lateral force and yaw moment coefficients acting on the slower Ship 1. The qualitatively agreement is very good where Ship 1 initially experiences a repulsion force that reaches its maxima as the bow of Ship 2 passes the stern of Ship 1 (ST` = -1.0). As the overtaking manoeuvre proceeds, the repulsion force changes direction and we have maximum attraction force as the midships of Ship 1 and Ship 2 become aligned (ST` = 0.0). So far, the force transit is common to the two ships passing situation. Furthermore, the lateral force shifts direction again as Ship 1 becomes situated between Ship 2 and Ship 3. Another repulsion force peak appears

when the bow of Ship 1 is 0.2L behind the midship of Ship 2 at the same time as the stern of Ship 1 is 0.3L behind the bow of Ship 3 (ST` = 0.8). This maximum repulsion force is larger than the first repulsion peak, i.e. when ST` = -1.0.

The last part of the overtaking manoeuvre is the same as for two ships passing. Ship 1 experiences a maximum attraction force as the midships of Ship 1 and Ship 3 become aligned (ST` = 1.5) and a maximum repulsion force as the stern of Ship 3 passes the bow of Ship 1 (ST` = 2.5)

The differences in maximum repulsion and attraction force coefficients are found to be small when the results from the present method are compared with Yasukawa's data, and they vary from only about 2 to 6 percent.

Similar good agreement for the yaw moments is found between the present method and Yasukawa (see Fig 6.2b). At the beginning of the transit Ship 1 experiences a bow-out moment with a peak appearing as the midship of Ship 2 reaches the stern of Ship 1 (ST` = -0.5). As for the two ships passing condition, the turning moment changes direction to bow-in around the midship-midship situation between Ship 1 and Ship 2 (ST` = 0.0). A bow-in peak occurs as Ship 1 is in a bow-midship situation with Ship 2 and a stern-bow situation with Ship 3 (ST` = 0.5).

Furthermore, as the overtaking manoeuvre proceeds, Ship 1 interacts heavily with both Ship 2 and Ship 3 resulting in a maximum bow-out moment. This peak appears as the bow of Ship 1 is 0.2L behind the stern of Ship 2 at the same time as the midship of Ship 1 is 0.2L behind the midship of Ship 3 (ST` = 1.2). For the remainder of the overtaking manoeuvre, Ship 1 is mostly influenced by the presence of Ship 3, resulting in a maximum bow-in moment as the midship of Ship 3 reaches the bow of Ship 1 (ST` = 2.0).

Quantitatively, the agreement is also good where the differences in maximum bow-out and bow-in moment coefficients obtained by the present method and those produced by Yasukawa's predictions are between 2 to 9 percent.

6.3 PRESSURE AND VORTICITY DISTRIBUTION

The pressure and vorticity distribution are presented only for the part of the overtaking manoeuvre where Ship 1 is situated between Ship 2 and Ship 3 as in the three ships meeting situation. Five different time steps are chosen to cover this part of the transit, and they are placed at positions where Ship 1 experiences the maximum lateral forces and yaw moments. Figures 6.3a,b show the pressure and vorticity distribution acting on Ship 1 when overtaken by Ship 2 followed by Ship 3, both travelling at twice the speed of Ship 1. Again, all three ships are identical and moving in a 2L wide and 1.3D deep channel. The separation distance between Ship 1 and Ship 2 is taken as 0.6L while the separation distance between Ship 1 and Ship 3 is 0.5L. The stagger between Ship 2 and Ship 3 is chosen to be –1.5L.

It is apparent from Fig 6.3a that as the midships of Ship 1 and Ship 2 become aligned (position 1), Ship 1 experiences lower pressures around its middle sections resulting in a maximum attraction force. Since the pressures at the fore portions and the aft portions are of a similarly low magnitude, the yaw moment is negligible. However, the pressure distribution acting on Ship 1 becomes more uneven as the midship of Ship 2 reaches the bow of Ship 1 at the same time as the bow of Ship 3 reaches the stern of Ship 1 (position 2). The aft portions of Ship 1 experience increased pressures while the fore parts experience decreased pressures, which result in a maximum bow-in moment. The lateral force is repulsive in nature since the increased pressures over the aft portions are predominant.

Furthermore, Fig 6.3a shows greater pressures over the middle sections of Ship 1 at position 3, where the bow of Ship 1 is 0.3L behind the midship of Ship 2 and its stern is 0.3L behind the bow of Ship 3. This results in a maximum repulsion force. Again, the pressure distribution is similar for the fore and aft parts of the hull of Ship 1, causing the yaw moment to be negligible. As the overtaking manoeuvre proceeds to position 4, where the bow of Ship 1 is 0.2L behind the stern of Ship 2 and the midship of Ship 1 is 0.2L behind the stern of Ship 3, the pressure distribution becomes different for the fore and aft parts of Ship 1. The pressures are lower over the aft sections while they are higher for the fore parts, resulting in a maximum bow-out

moment. Here, the lateral force is of an attractive nature since the lower pressures over the aft portions of Ship 1 are predominant.

When the midships of Ship 1 and Ship 3 become aligned (position 5) the pressure distribution becomes similar to the that found when Ship 1 is in a midship-midship situation with Ship 2 (position 1). However, since the separation distance between Ship 1 and Ship 2 is smaller (Sp_{12} = 0.6L) than that of Ship 1 and Ship 3 (Sp_{13} = 0.5L), the pressures are lower over the middle sections. This results in a maximum attraction force that is larger than the attraction peak appearing at position 1.

6.4 PARAMETRIC STUDY

This section investigates the effect of changing various parameters for the lateral forces and yaw moments acting on Ship 1 when situated in a three ships passing manoeuvre. Again, Ship 1 is overtaken by Ship 2 followed by Ship 3. The effect of altering the water depth, separation distance and ship size where both Ship 2 and Ship 3 are travelling at twice the speed of Ship 1 is examined. Furthermore, the effect of varying the overtaking speed of Ship 2 and Ship 3 is investigated. Once more, the different conditions for the overtaking manoeuvre is given in tables.

Ship 1 experiences a similar lateral force and yaw moment transit during the overtaking situations for this parametric study. Firstly, a maximum repulsion force followed by an attraction force peak when Ship 1 is in a stern-bow and a midship-midship situation respectively with Ship 2. Furthermore, when Ship 1 is in a position between Ship 2 and Ship 3 it again experiences a maximum repulsion force. During the last part of the transit, a maximum attraction force occurs as the midships of Ship 1 and Ship 3 become aligned and a repulsion peak value appears as the stern of Ship 3 passes the bow of Ship 1.

Initially, Ship 1 experiences a bow-out moment as the bow of Ship 2 approaches its stern, and the yaw moment reaches a maximum when Ship 1 is in a stern-midship

situation with Ship 2. As the overtaking manoeuvre proceeds, the yaw moment changes direction and a bow-in peak appears when the bow of Ship 1 is passed by the midship of Ship 2 at the same time as its stern becomes aligned with the bow of Ship 3. Furthermore, a maximum bow-out moment occurs as the bow of Ship 1 is 0.2L behind the stern of Ship 2, and the stern is 0.2L behind the midship of Ship 3. Finally, Ship 1 experiences a bow-in moment peak as its bow is passed by the midship of Ship 3.

6.4.1 The effect of water depth

The effect of water depth is shown in Figs 6.4a,b for the lateral force and yaw moment coefficients acting on the slower Ship 1. Ship 1 is first passed by Ship 2 and then by Ship 3 for the following condition:

W	H/D	Sp_{12}/L	Sp_{13}/L	$L_1/L_{2,3}$	$U_{2,3}/U_1$	ST_{23}/L
2L	Varying	0.6	0.5	1.0	2.0	-1.5

Table 6.1 Condition for the effect of water depth, (three ships passing).

It is apparent from Figs 6.4a,b that as the bottom clearance decreases the lateral forces and yaw moments acting on Ship 1 increase. This tendency is common to that experienced by the slower ship for the two ships passing manoeuvre.

The maximum lateral force coefficients for different depth-draught ratios are shown in Fig 6.5a, where it can clearly be seen that Ship 1 experiences a sharp increase in force coefficients for small water depths. The largest repulsion force coefficients appear when ST` = 0.8, the point at which the bow of Ship 1 is 0.2L forward of the stern of Ship 2 at the same time as its stern is 0.2L ahead of the midship of Ship 3). For various depth-draught ratios, these peak values are approximately 37% larger than the repulsion peaks occurring as Ship 1 and Ship 2 are in a stern-bow situation (ST` = -1.0). However, the maximum repulsion force coefficients when ST` = 0.8 are

about 47% smaller in magnitude than the maximum attraction force coefficients appearing when the midships of Ship 1 and Ship 3 become aligned (ST` = 1.5).

Figure 6.5b illustrates how the maximum yaw moment coefficients acting on Ship 1 vary for different water depths, and again a rapid growth in peak values is found for small bottom clearances. Ship 1 experiences its largest bow-out moment when its stern is being passed by the midship of Ship 2 (ST` = -0.5). For a depth-draught ratio of 1.2 this peak is around 28% larger than the bow-out peak appearing when ST` = 1.2 (i.e. when the midship of Ship 1 is 0.2L behind the bow of Ship 3). However, this variance reduces for deeper waters and for H/D = 2.0 the difference is approximately 17%.

For various depth-draught ratios, the largest bow-in moment coefficients occur as the midship of Ship 3 passes the bow of Ship 1 (ST` = 2.0). When H/D = 1.2, the bow-in peak at this position is about 96% larger than the maximum bow-in moment coefficient occurring as the bow of Ship 1 is overtaken by the midship of Ship 2 at the same time as its stern is passed by the bow of Ship 3 (ST` = 0.5). Once more, the variance in peak values decreases and becomes approximately 80% for a depth-draught ratio of 2.0.

The difference between the maximum bow-out moment coefficients when ST` = 1.2 and the maximum bow-in moment coefficients when ST` = 0.5 is found to be constant and about 17% in magnitude, the latter peak values being the smallest.

(Diagrams of the effect of water depth for various separation distances are shown in the Appendix 6.)

6.4.2 The effect of separation distance

As for the three ships meeting manoeuvre, the lateral distances between Ship 1 and both Ships 2 and 3 can be changed separately, resulting in several possible configurations from which the effect of separation distance can be studied. However, in this thesis the separation distance between Ship 2 and Ship 3 is kept constant, and taken as 0.1L (Sp_{23} = 0.1L) where Ship 3 passes closest to Ship 1 for all cases. Figures 6.6a,b show the lateral force and yaw moment coefficients acting on the slower Ship 1 where the non-dimensionalized lateral distance between Ship 1 and Ship 3 (Sp_{13}/L) denotes the various separation distances in the graph. The condition is given in the table below:

W	H/D	Sp_{12}/L	Sp_{13}/L	$L_1/L_{2,3}$	$U_{2,3}/U_1$	ST_{23}/L
2L	1.3	Varying	Varying	1.0	2.0	-1.5

Table 6.2 Condition for the effect of separation distance, (three ships passing).

It is apparent from Figs 6.6a,b that Ship 1 experiences larger lateral forces and yaw moments as the separation distance decreases. This tendency is common to the two ships passing manoeuvre.

The maximum lateral force coefficients acting on Ship 1 are shown in Fig 6.7a where they are plotted against the non-dimensionalized separation distance between Ship 1 and Ship 3 (Sp_{13}/L). Again, a sharply increasing tendency can be seen for the different repulsion and attraction peaks for small separation distances. In particular, the curve representing the maximum repulsion force coefficient when ST` = 0.8 (i.e. when the bow of Ship 1 is positioned 0.2L ahead of the stern of Ship 2 at the same time as the stern of Ship 1 is 0.2L ahead of the midship of Ship 3) shows just such a rapidly increasing trend. For Sp_{13}/L = 0.2 this repulsion peak value is approximately 116% larger than the maximum repulsion force coefficient appearing when Ship 1 is in a stern-bow situation with Ship 2 (ST` = -1.0). However, as the separation distance increases the difference reduces, resulting in an equal magnitude of these peak values for a Sp_{13}/L ratio of 0.6.

However, if the peak magnitudes of the repulsion force coefficients when ST` = 0.8 are compare with the maximum attraction force coefficients when ST` = 1.5 (i.e. when the midships of Ship 1 and Ship 3 are aligned), we find that the attraction peak values are greater for all separation distances. For $Sp_{13}/L = 0.2$ the difference in peak size is about 20%, increasing to approximately 73% for a Sp_{13}/L ratio of 0.7.

The maximum yaw moment coefficients acting on Ship 1 are shown in Figs 5.7a,b for various separation distances. Again, the curves highlight the fact that the moment coefficients tend to increase more rapidly as the lateral distance between the ships becomes smaller. The bow-out peaks in particular increase sharply when ST` = 1.2 (i.e. when the midship of Ship 1 is 0.2L behind the bow of Ship 3). For a $Sp_{13}/L$ ratio of 0.2 this bow-out peak is approximately 36% larger than the maximum bow-out moment coefficients experienced by Ship 1 when its midship is passed by the bow of Ship 2 (ST` = -0.5). However, the difference in peak values decreases for the growing separation distance, and for $Sp_{13}/L = 0.4$ these bow-out maximums are equal. For Sp_{13}/L ratios above 0.4 the bow-out peaks when ST` = -0.5 become highest.

Ship 1 experiences larger bow-in peak values when ST` = 2.0 (i.e. when its bow is passed by the midship of Ship 3) compared to the bow-in maximums when ST` = 0.5 (i.e. when Ship 1 is in a bow-midship situation with Ship 2 and a stern-bow situation with Ship 3) for various separation distances. For $Sp_{13}/L = 0.2$ the difference between these bow-in peaks is approximately 38%, and despite the fact that the percentage variance increases, the curves are found to descend in a similar way.

The maximum bow-out moment coefficients when ST` = 1.2 are found to have larger magnitudes than the bow-in maximums when ST` = 0.5 for Sp_{13}/L ratios above 0.6. The difference increases to 38% as the Sp_{13}/L ratio reduces to 0.2.

6.4.3 The effect of ship size

This section examines the effect on the lateral forces and yaw moments of changing the ship sizes for the three ships passing manoeuvre. Again, Ship 1 has been chosen to be the slower ship while being overtaken by Ship 2 followed by Ship 3. The size of Ship 1 is kept constant while scaling both Ship 2 and Ship 3 geometrically, resulting in equal sizes of the two latter ships for all case studies. The condition for the overtaking manoeuvre is shown below:

W	H/D_1	Sp_{12}/L_1	Sp_{13}/L_1	$L_1/L_{2,3}$	$U_{2,3}/U_1$	ST_{23}-$L_{2,3}$
$2L_1$	1.3	0.6	0.5	Varying	2.0	$-0.5L_1$

Table 6.3 Condition for the effect of ship size, (three ships passing).

As for the three ships meeting manoeuvre, the longitudinal distance between the stern of Ship 2 and the bow of Ship 3 is kept constant with a value of $0.5L_1$ for all length ratios (i.e. $ST_{23} - L_{2,3} = 0.5L_1$)

As anticipated, Ship 1 experiences greater lateral forces and yaw moments when the overtaking ships (Ships 2 and 3) are bigger and, accordingly, smaller hydrodynamic forces and moments when Ship 2 and Ship 3 are smaller (illustrated in Figs 6.8a,b).

The maximum lateral force coefficients acting on Ship 1 are shown in Fig 6.9a where they are plotted against the $L_1/L_{2,3}$ ratio. As the size of Ships 2 and 3 increases, the repulsion and attraction peaks tend to increase more rapidly, a tendency that is common to the two ships passing manoeuvre. When Ship 1 is 20% smaller than Ships 2 and 3 it experiences between 65% to 72% larger maximum lateral force coefficients compared to the $L_1/L_{2,3} = 1.0$ case for all peak positions except when $ST` = 0.8$. The maximum attraction force coefficients achieved a higher gradient when $ST` = 0.8$ (i.e. when the bow of Ship 1 is positioned 0.2L ahead of the stern of Ship 2 at the same time as the stern of Ship 1 is 0.2L ahead of the midship of Ship 3). As a result, a $L_1/L_{2,3}$ ratio of 0.8 gives 108% larger peak values compared to the $L_1/L_{2,3} = 1.0$ case when Ship 1 is at this stagger position.

For the passing manoeuvres in which Ship 1 is 1.2 times bigger than the overtaking ships, it experiences about 35 to 41 percent smaller repulsion and attraction peak values compared to the situations where all three ships are identical. This is true for all peak locations, except when ST` = 0.8 where the reduction is about 53%.

In Fig 6.9b it is found that Ship 1, when 20% smaller than Ship 2 and Ship 3, experiences an increase of 65 to 69 percent in the maximum bow-out and bow-in moment coefficients appearing during the beginning (ST` = -0.5) and end (ST` = 2.0) of the transit respectively. On the other hand, when Ship 1 is 1.2 times the size of Ships 2 and 3 it experiences about 36 percent smaller yaw moment coefficients when ST` = -0.5 and ST` = 2.0 compared to the $L_1/L_{2,3} = 1.0$ case.

The maximum bow-in and bow-out moment coefficients acting on Ship 1 when it occupies positions between Ship 2 and Ship 3, i.e. when ST` = 0.5 and ST` = 1.2, increase by 80 to 85 percent when Ship 1 is 20% smaller than the passing ships. When Ship 1 is 1.2 times bigger than Ships 2 and 3 it experiences a reduction of approximately 42 percent in peak magnitudes.

6.4.4 The effect of ship speed

In the previous sections involving three ships passing manoeuvres, the overtaking speed of Ship 2 and Ship 3 was twice that of Ship 1. Here, an investigation into the effect of changing the relative passing speed of these two vessels on the lateral forces and yaw moments acting on Ship 1 is carried out. However, as described earlier, the present method is limited to take the equal speed of Ships 2 and 3 as input. Consequently, the longitudinal distance, or stagger, between Ship 2 and Ship 3 (ST_{23}) must be constant during transit. The condition is given in the table below:

W	H/D	Sp_{12}/L	Sp_{13}/L	$L_1/L_{2,3}$	$U_{2,3}/U_1$	ST_{23}/L
2L	1.3	0.6	0.5	1.0	Varying	-1.5

Table 6.4 Condition for the effect of ship speed, (three ships passing).

where Ship 1 is overtaken by Ship 2, followed by Ship 3.

Figures 6.10a,b show how changes in the overtaking speed of Ship 2 and Ship 3 influences the lateral force and yaw moment coefficients acting on Ship 1. As for the two ships passing manoeuvre, the hydrodynamic forces and moments grow as the ratio of the overtaking speed to the overtaken speed ($U_{2,3}/U_1$) increases.

The maximum lateral force coefficients acting on Ship 1 are shown in Fig 6.11a where they are plotted against the $U_{2,3}/U_1$ ratio. It can be seen that the attraction force peaks tend to increase linearly with a higher gradient than the repulsion peaks. Also noticeable is that the repulsion maximums when ST` = 0.8 (i.e. when Ship 1 is situated between Ships 2 and 3) incline more rapidly, compared to the growth of the two other maximum repulsion force coefficients (i.e. when ST` = -1.0 and ST` = 2.5).

Figure 6.11b illustrates how the maximum yaw moment coefficients increase linearly for the increasing $U_{2,3}/U_1$ ratio. The bow-out peaks appearing when ST` = 1.2 (i.e. when the midship of Ship 1 is 0.2L behind the bow of Ship 3) are found to produce a steeper curve than the bow-out maximums when ST` = -0.5 (i.e. when Ship 1 is in a stern-midship situation with Ship 3). As a result, these peaks are of similar magnitude for a $U_{2,3}/U_1$ ratio of 3.0. The graphs representing the bow-in peak values (i.e. when ST` = 0.5 and ST` = -2.0) are found to have a similar gradient.

6.4.5 The effect of longitudinal distance between Ship 2 and Ship 3

The longitudinal distance, or stagger, between Ships 2 and 3 was kept constant throughout the previous calculations on Ship 1 (ST_{23} = -1.5L). However, the hydrodynamic forces and moments acting on Ship 1, when positioned between Ship 2 and Ship 3, vary as this stagger changes. A '3 ships interaction' problem is plotted together with two '2 ships interaction' problems to explain this behaviour of the lateral force and yaw moment coefficients acting on Ship 1 (see Figs 6.12a,b).

For the three ships passing manoeuvre, Ship 1 is first overtaken by Ship 2 followed by Ship 3 for the condition as follows:

W	H/D	Sp_{12}/L	Sp_{13}/L	$L_1/L_{2,3}$	$U_{2,3}/U_1$	ST_{23}/L
2L	1.3	0.6	0.5	1.0	2.0	-1.5

Table 6.5 Condition for comparison of a '3 ships interaction' problem with two '2 ships interaction' problem.

The two '2 ships interaction' conditions represent the presence of Ship 2 and Ship 3 in the three ships passing manoeuvre separately, i.e. with a separation distance of 0.6L and 0.5L respectively from Ship 1.

It is apparent from Fig 6.12a that the maximum repulsion force coefficient when ST` = 0.8 for the '3 ships interaction' condition is a result of the stern repulsion from Ship 2 plus the bow repulsion from Ship 3. However, this peak becomes largest when $ST_{23}$ is increased from –1.5L to –2.0L because then the stern repulsion peak from Ship 2 (ST` = 0.5) becomes aligned with the repulsion peak from Ship 3 (ST` = 1.0).

Comparison of the yaw moment coefficients acting on Ship 1 between a '3 ships interaction' manoeuvre and two '2 ships interaction' manoeuvres can be seen in Fig 6.12b. When Ship 1 is situated between Ship 2 and Ship 3 in the '3 ships interaction' problem, the maximum bow-in (ST` = 0.5) and bow-out (ST` = 1.2) moments are smaller than the two '2 ships interaction' peaks at the same staggers. The bow-in peak when ST` = 0.5 is reduced because Ship 1 also experiences a moment of bow-out nature from Ship 3, despite the fact that the induced bow-in moment from Ship 2 is predominant. A similar reducing tendency is found for the inflicted bow-out maximum from Ship 3 when ST` = 1.2. Here, this bow-out peak value is smaller since Ship 2 causes a moment of bow-in nature to Ship 1 during this part of the transit.

Figs 6.13a,b show the lateral force and yaw moment coefficients acting on Ship 1 for various non-dimensionalized staggers between Ship 2 and Ship 3 (ST_{23}/L) where the condition is shown in the table below:

W	H/D	Sp_{12}/L	Sp_{13}/L	$L_1/L_{2,3}$	$U_{2,3}/U_1$	ST_{23}
2L	1.3	0.6	0.5	1.0	2.0	Varying

Table 6.6 Condition for the effect of longitudinal distance between Ship 2 and Ship 3, (three ships passing).

As described previously, the stagger is non-dimensionalized such that the values of –1, 0 and +1 correspond to the stern-bow, midship-midship and stern-stern situations between Ship 1 and Ship 2. However, the stagger values representing the stern-bow, midship-midship and bow-stern situations between Ship 1 and Ship 3 change for different ST_{23}. For example, a ST_{23}/L ratio of –1.0 gives a stern-bow situation between Ship 1 and Ship 3 when ST` = 0.5. Furthermore, this stern-bow situation occurs when ST` = 1.5 for ST_{23}/L = -2.0.

As for the three ships meeting manoeuvre, Ship 1 experiences changes in the force and moment transit when varying the ST_{23}/L ratio.

The different maximum lateral force coefficients are shown in Fig 6.14a where they are plotted against the ST_{23}/L ratio. It is found that Ship 1 experiences approximately 35% larger repulsion forces for a ST_{23}/L ratio of –2.0 compared to the previous calculations where ST_{23}/L = -1.5 when ST` = 0.8.

Fig 6.14b shows the maximum yaw moment coefficients experienced by Ship 1 when changing the stagger between Ship 2 and Ship 3. It is apparent that the bow-in and bow-out peaks that appear when Ship 1 is positioned between Ship 2 and Ship 3, (i.e. when ST` = 0.5 and ST` = 1.2 respectively), increase as the ST_{23}/L ratio increases.

6.6 CONCLUDING REMARKS

- The comparison with Yasukawa's (1983) theoretical calculation carried out on the slower Ship 1 in a three ships passing manoeuvre shows a good level of agreement, both for the lateral force and yaw moment coefficients.

- The parametric studies show that the interaction forces and moments increase as the separation distance and water depth decreases. Furthermore, the present method also found that when the size and speed of the overtaken Ship 1 is reduced by comparison to those of the passing Ships 2 and 3, it experiences larger lateral forces and yaw moments. These tendencies are common to what the slower ship (Ship 2) for the two ships passing manoeuvre is experiencing. However, even though a growth in the relative speed creates larger interaction forces, a situation in which the relative speed is lower may cause a more hazardous condition. This is because the overtaking manoeuvre then takes a longer time.

- An investigation into the effect of the longitudinal distance, or stagger, between the faster Ships 2 and 3 (ST_{23}), reveals that Ship 1, when situated between these ships, experiences the largest repulsion forces when the longitudinal distance between the midships is –1.8L. The largest yaw moments are found when ST_{23} = -1.0L, i.e. when the stern of Ship 2 is aligned with the bow of Ship 3.

- The three ships passing manoeuvre is potentially more dangerous than the two ships passing manoeuvre. This is due to the large interaction forces and moments Ship 1 experiences when positioned between Ship 2 and Ship 3 and hence interacting with both ships.

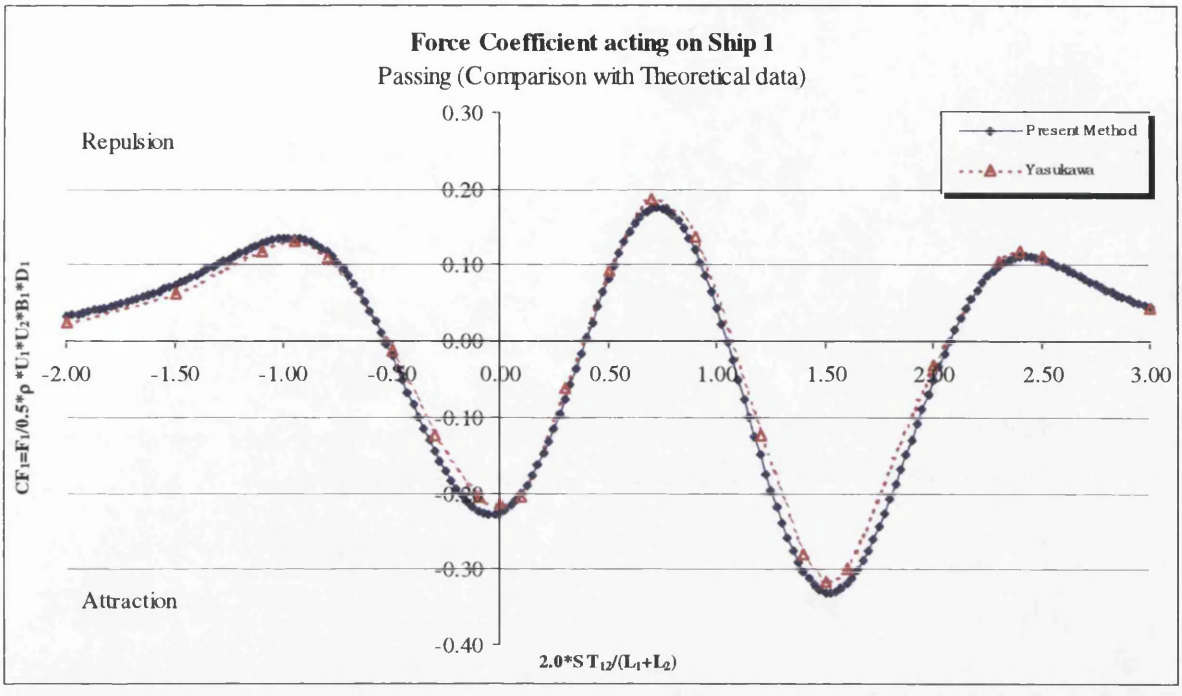

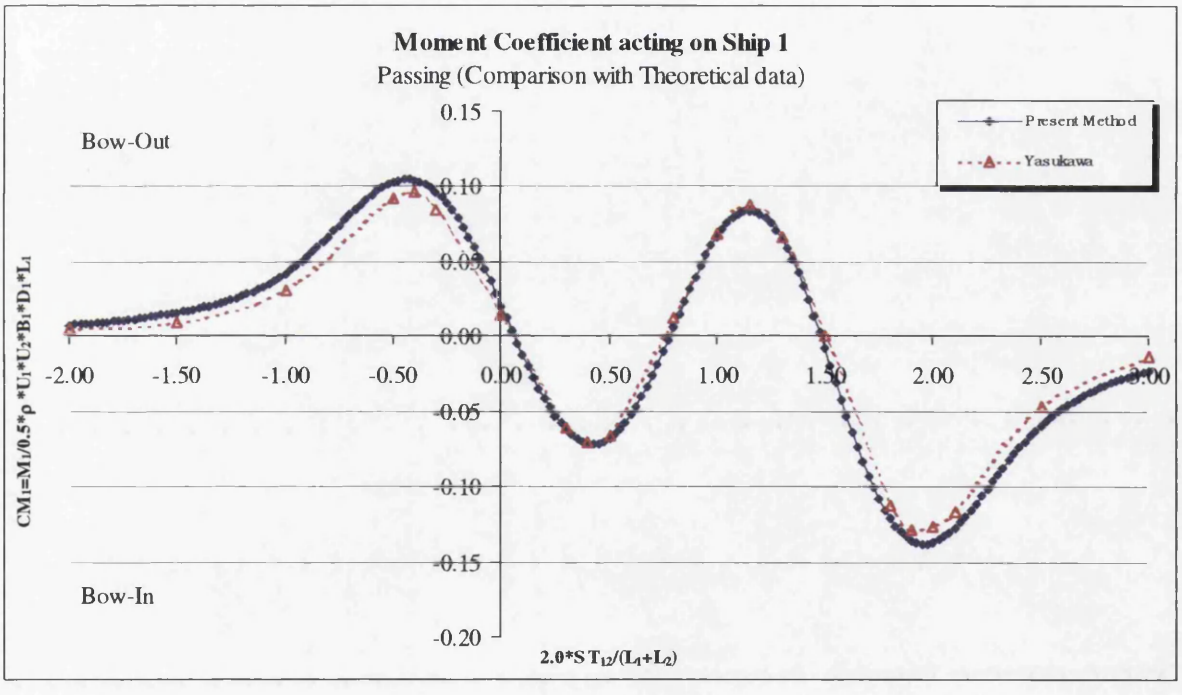

Figs 6.2a,b Comparison of the lateral force and yaw moment coefficients with Yasukawa's experimental data, (three ships passing)

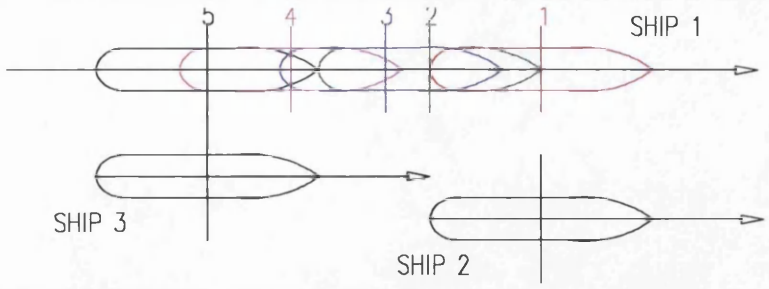

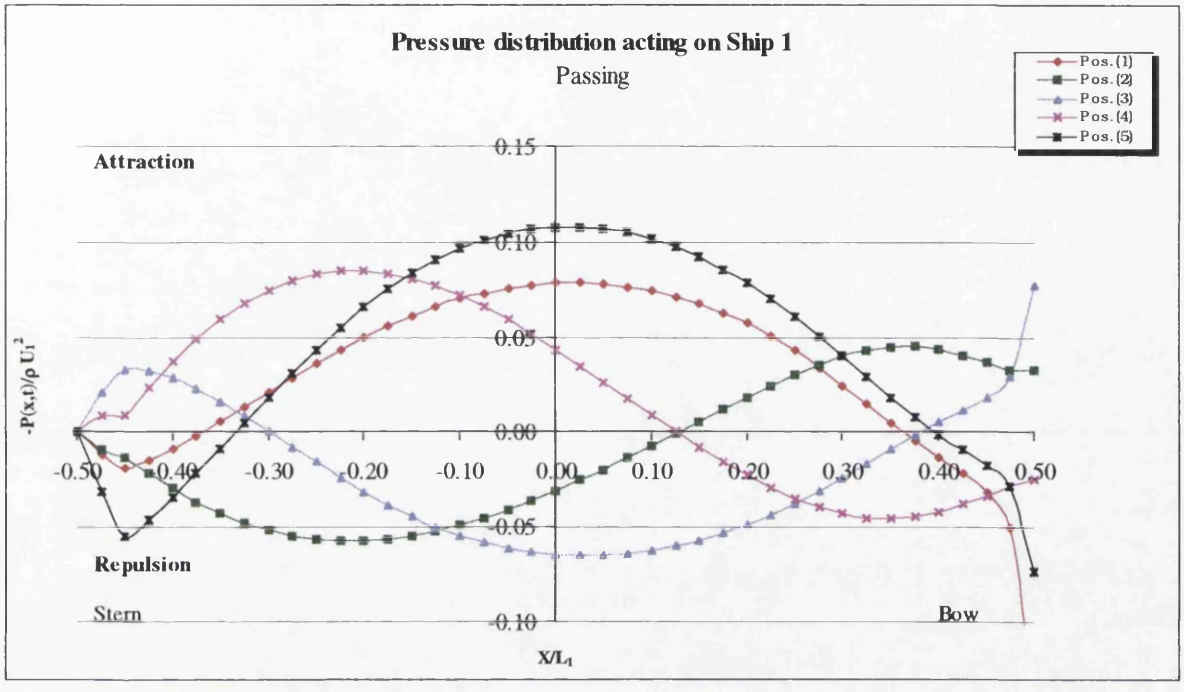

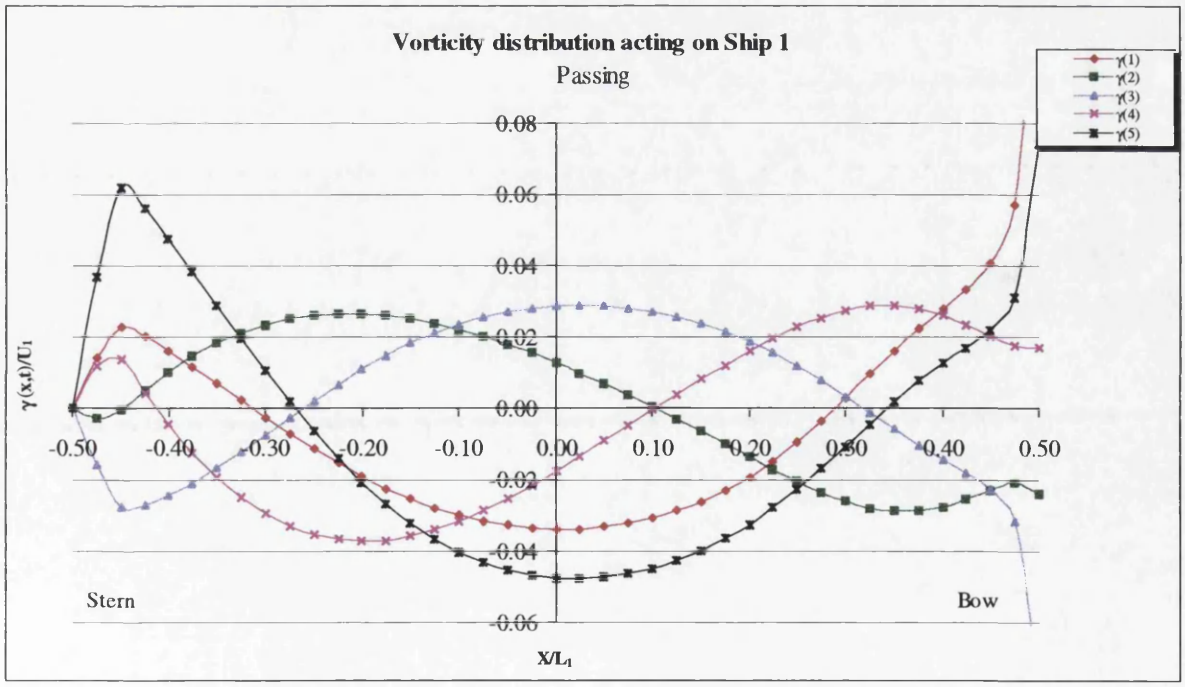

Figs 6.3a,b The pressure and vorticity distribution acting on Ship 1 for different time steps, (three ships passing)

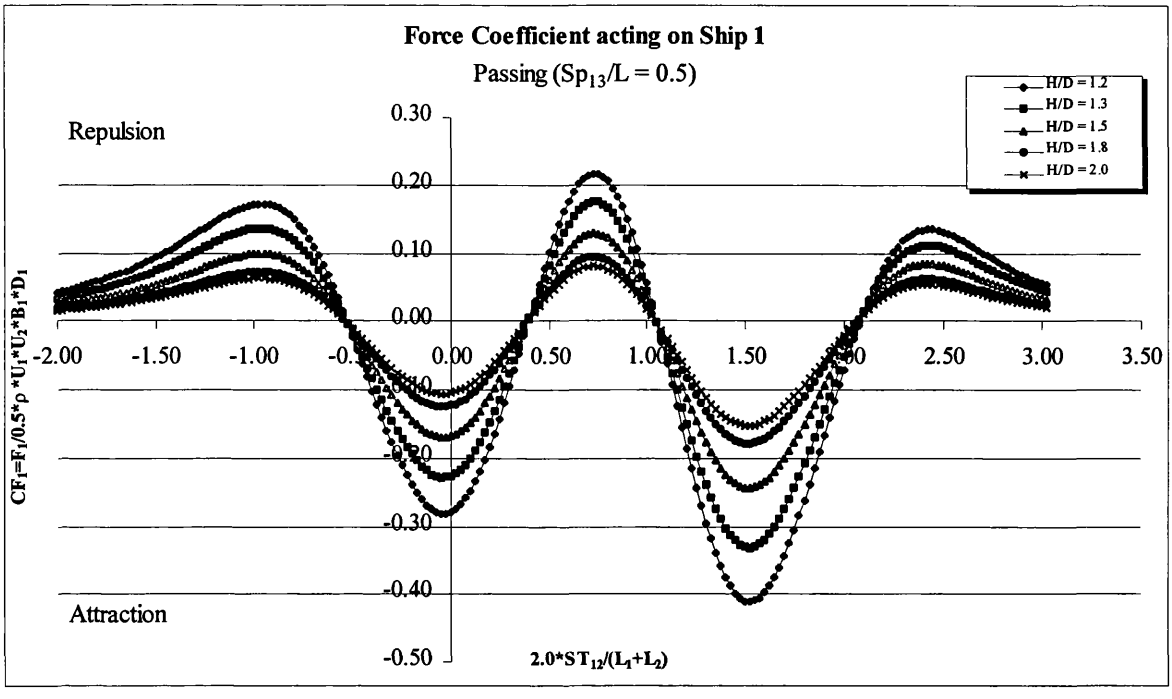

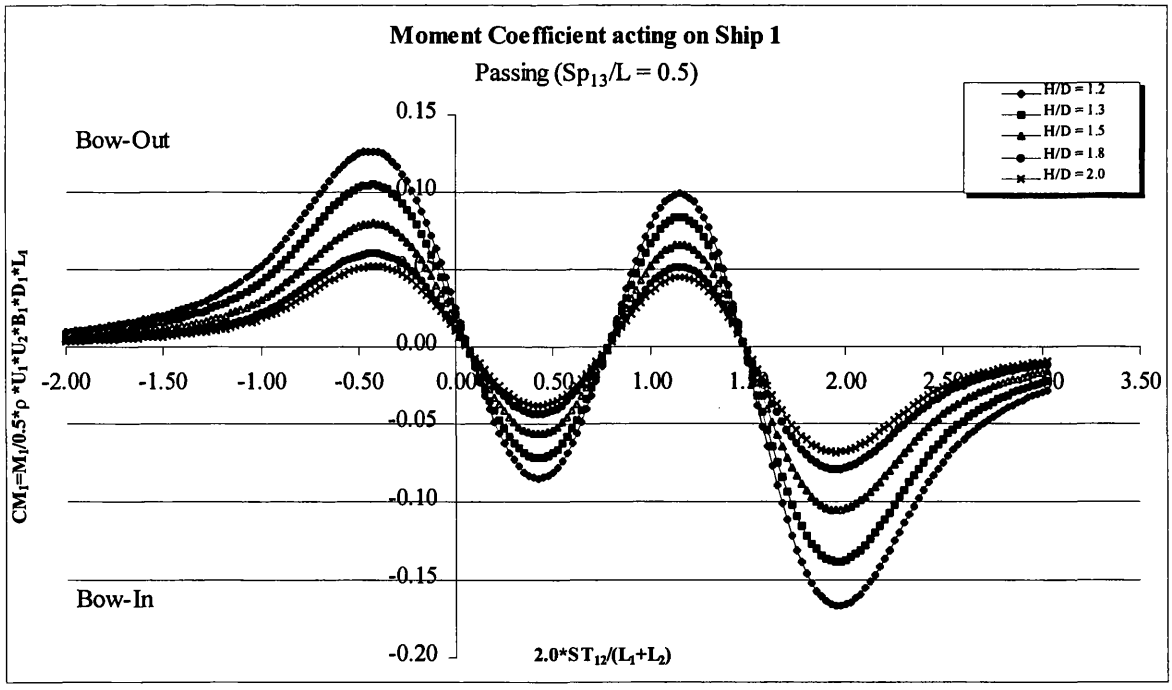

Figs 6.4a,b The lateral force and yaw moment coefficients acting on Ship 1 for various water depths, (three ships passing)

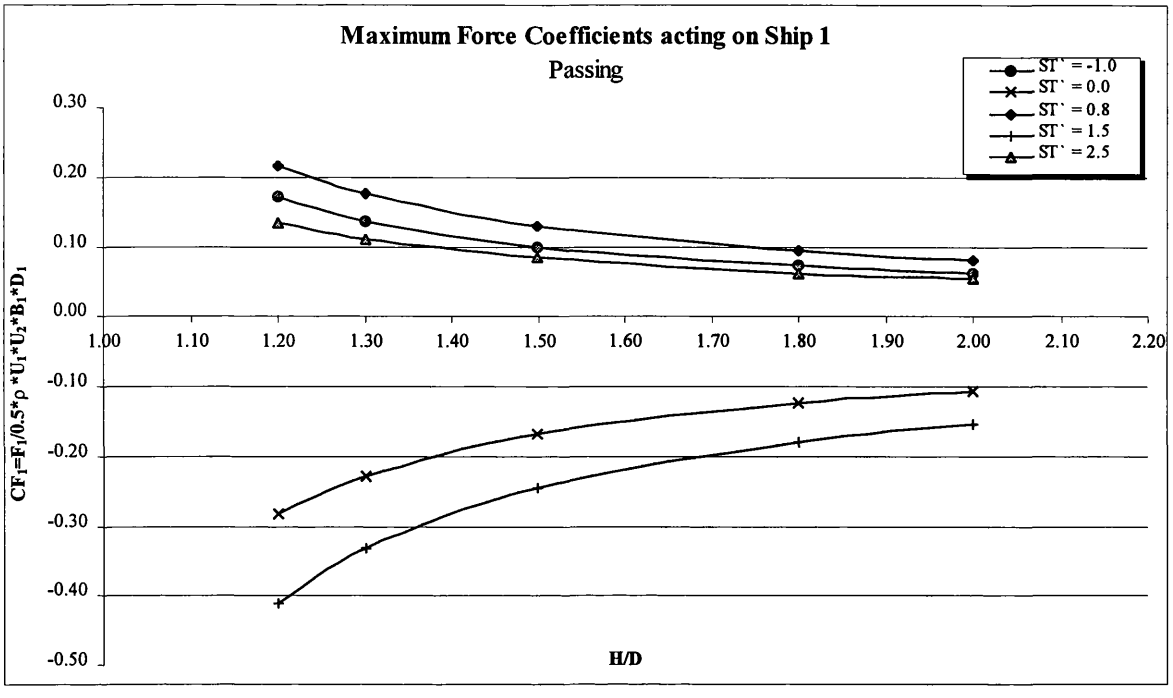

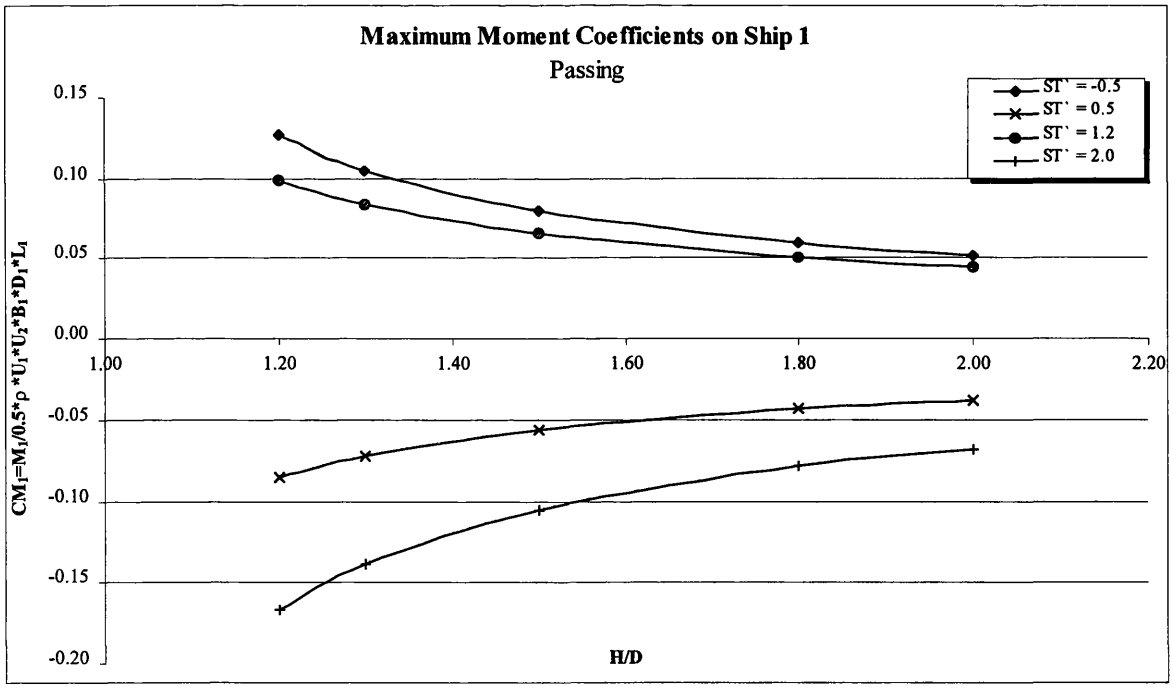

Figs 6.5a,b Maximum lateral force and yaw moment coefficients acting on Ship 1 for various water depths, (three ships passing)

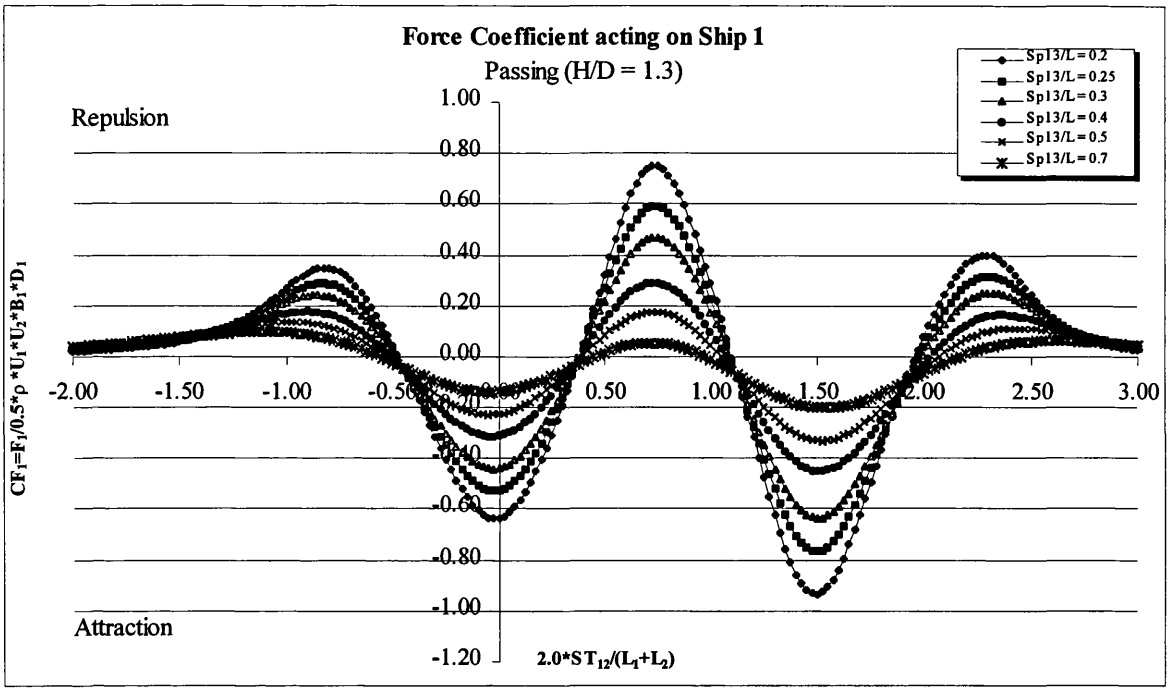

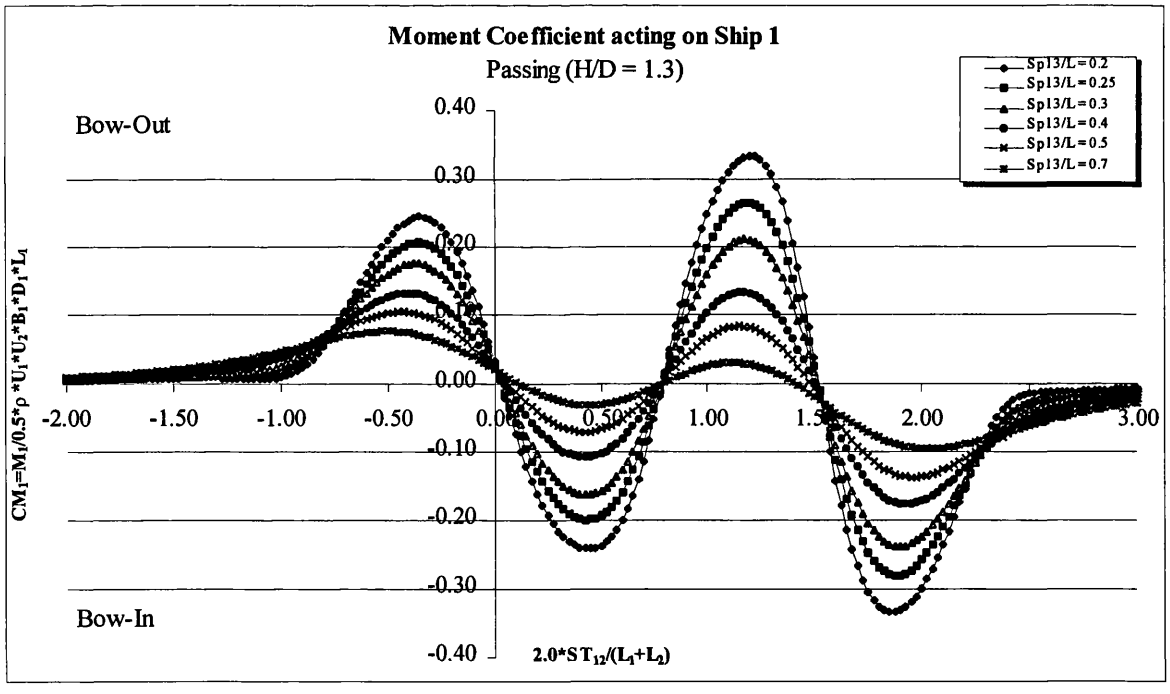

Figs 6.6a,b The lateral force and yaw moment coefficients acting on Ship 1 for various separation distances, (three ships passing)

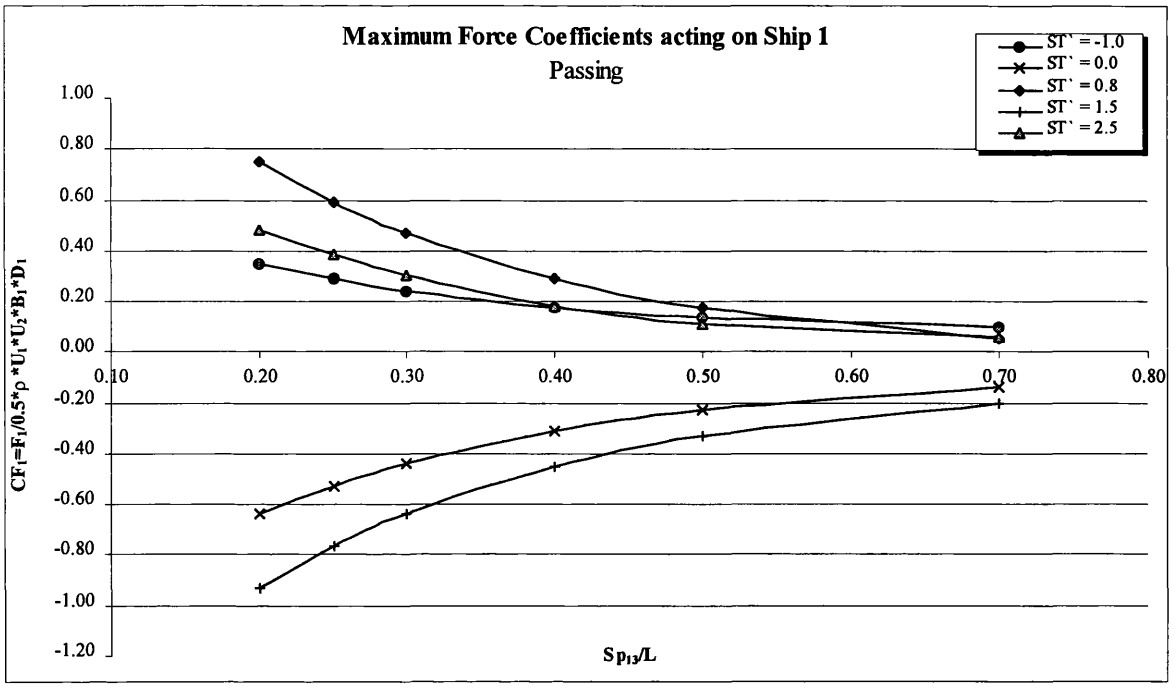

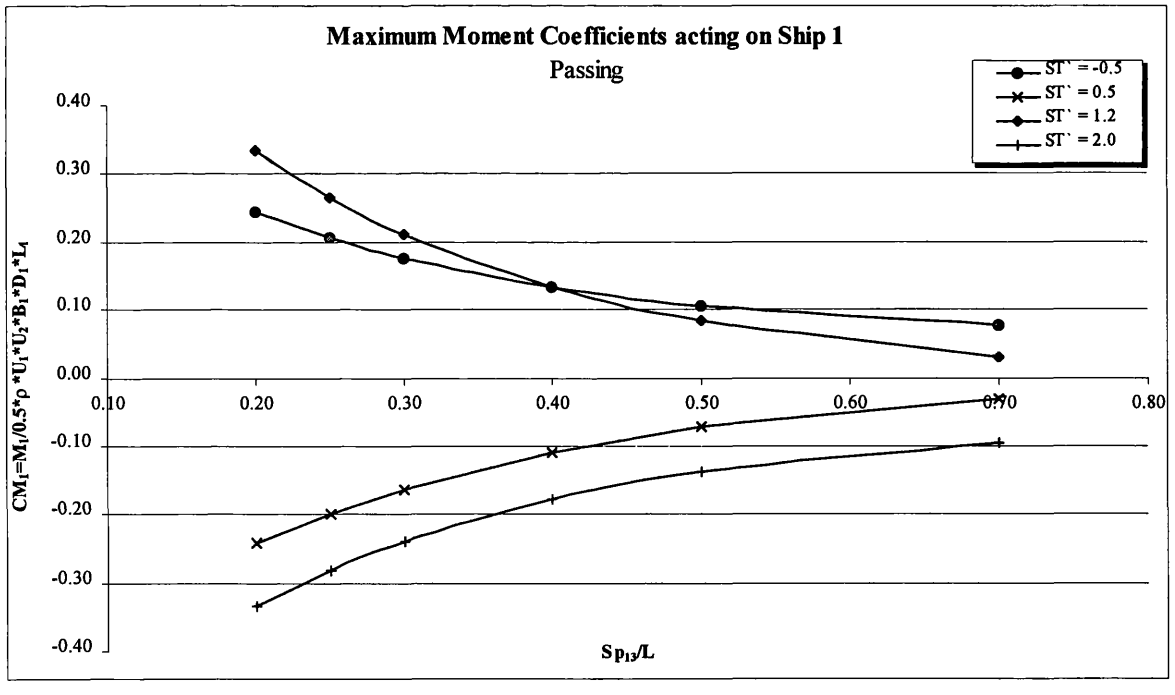

Figs 6.7a,b Maximum lateral force and yaw moment coefficients acting on Ship 1 for various separation distances, (three ships passing)

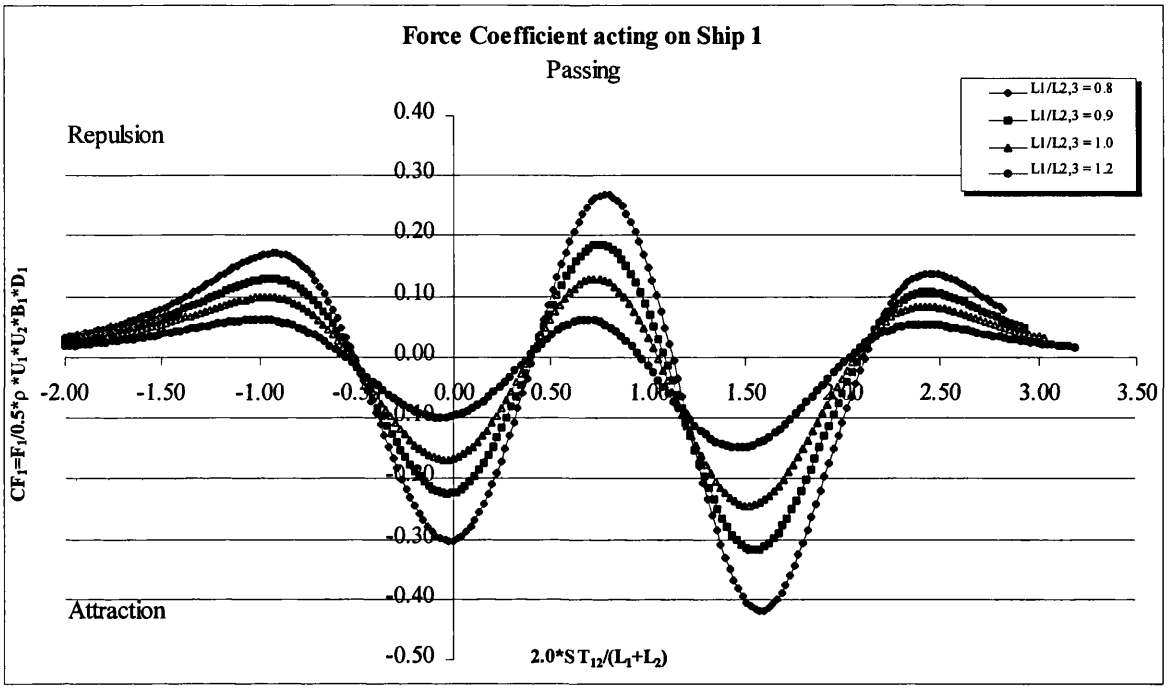

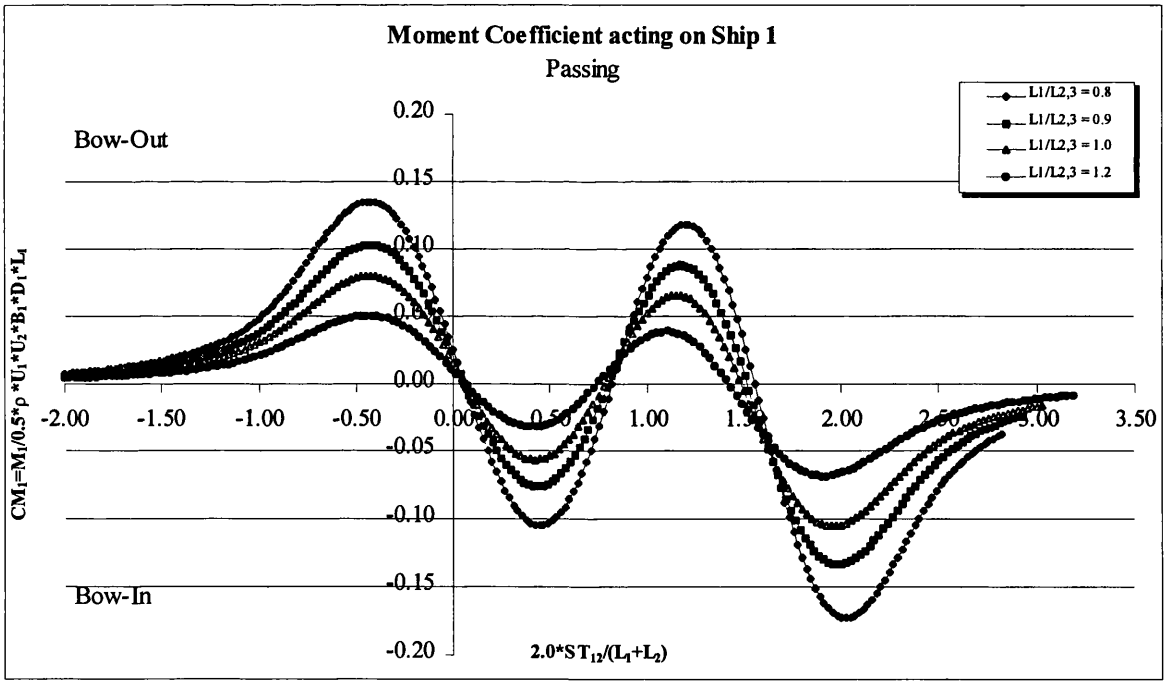

Figs 6.8a,b The lateral force and yaw moment coefficients acting on Ship 1 for various ship sizes, (three ships passing)

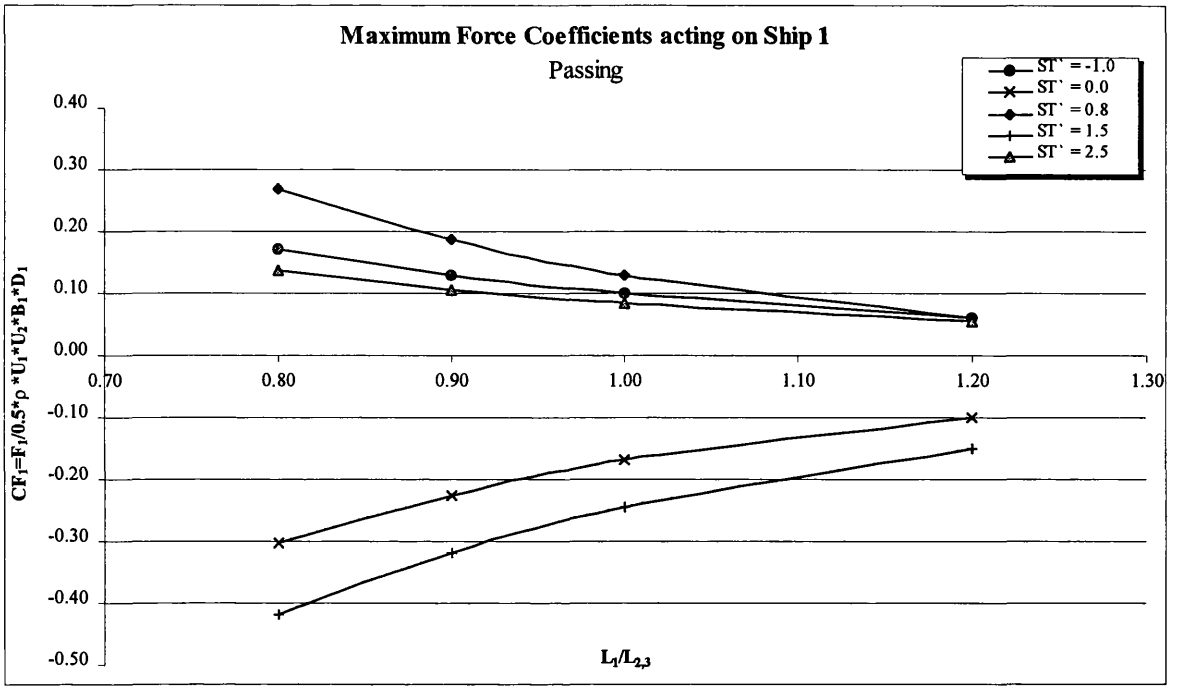

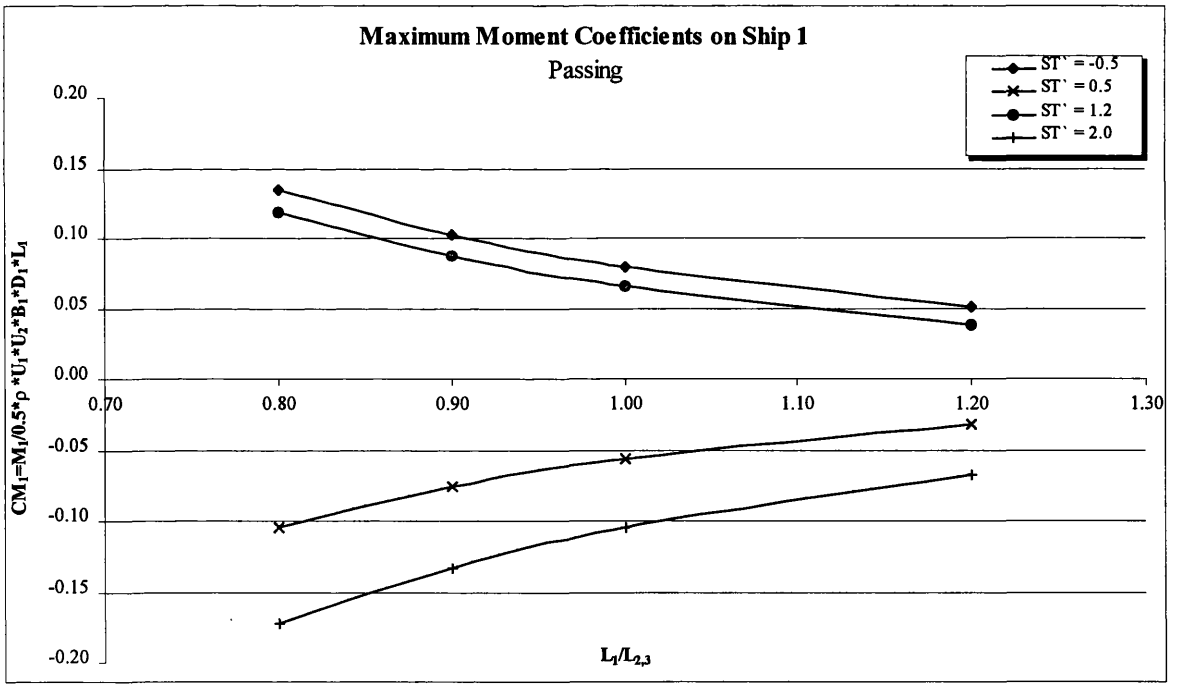

Figs 6.9a,b Maximum lateral force and yaw moment coefficients acting on Ship 1 for various ship sizes, (three ships passing)

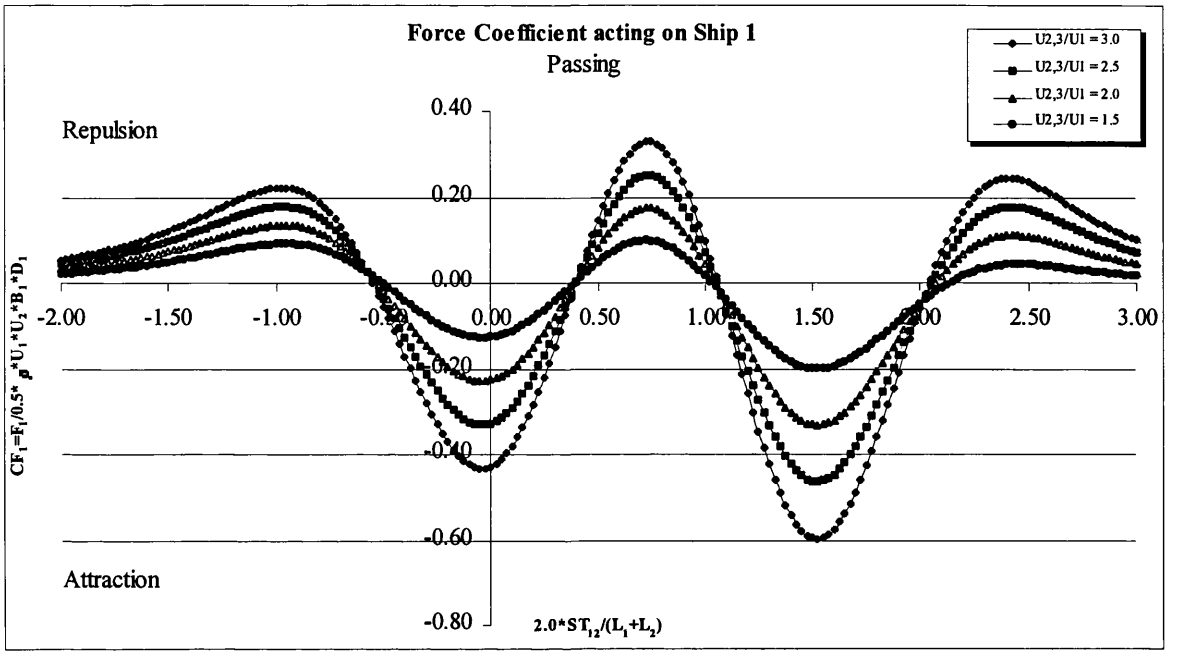

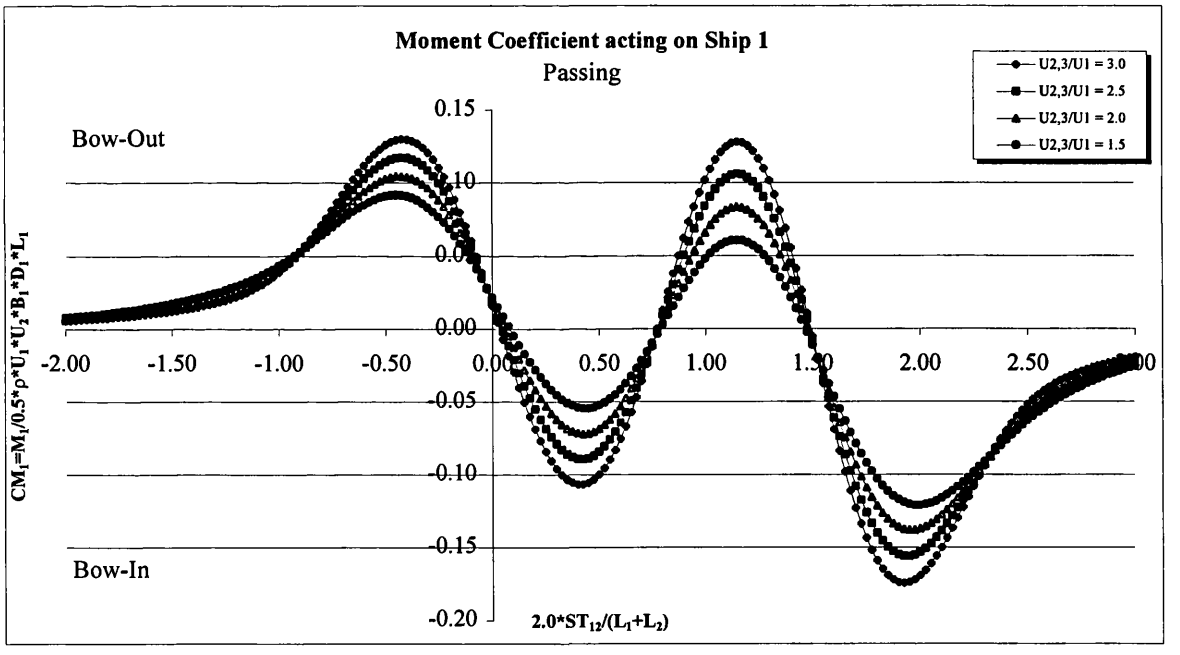

Figs 6.10a,b The lateral force and yaw moment coefficients acting on Ship 1 for various ship speeds, (three ships passing)

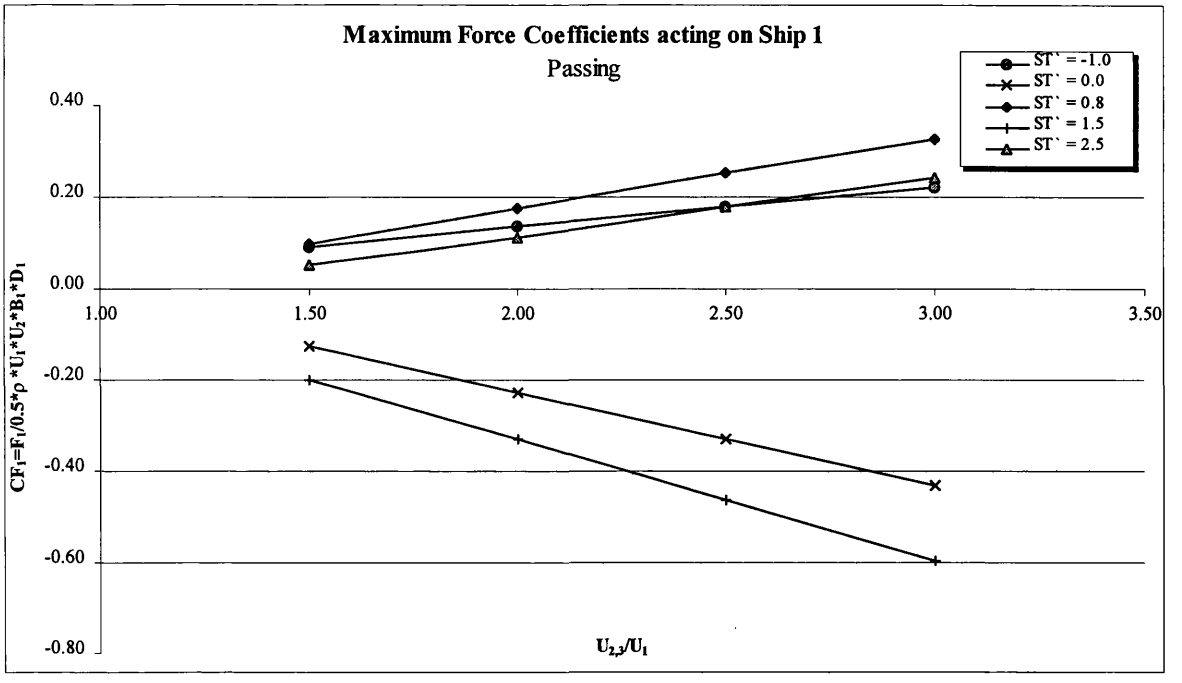

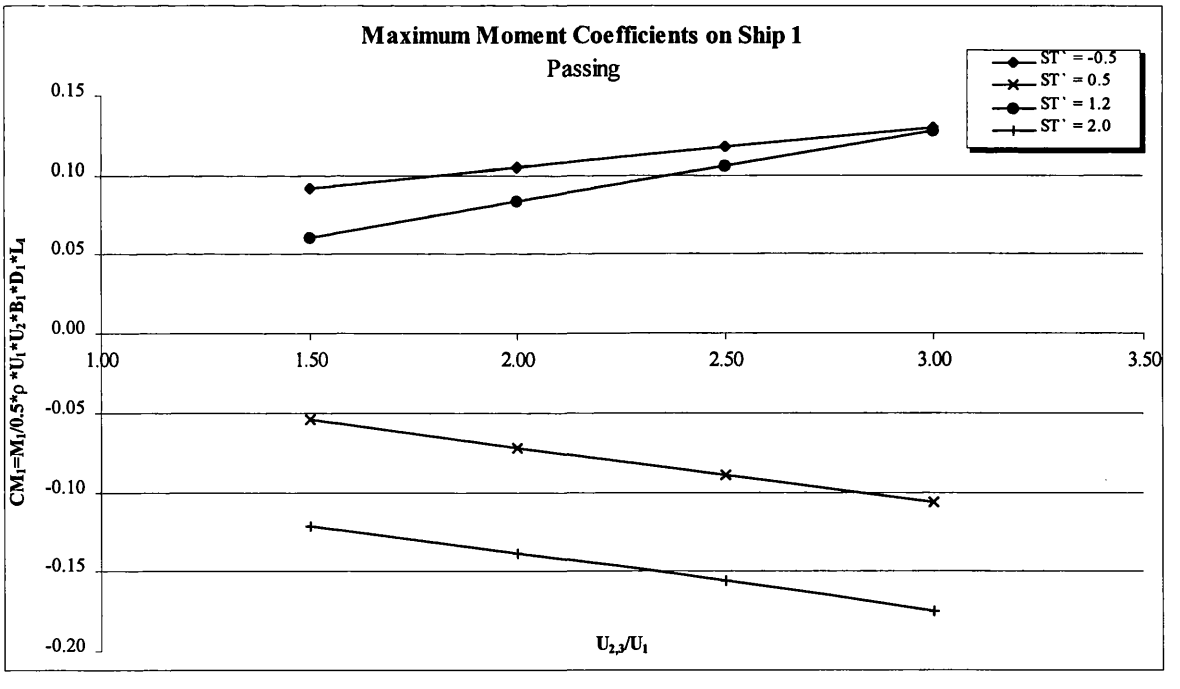

Figs 6.11a,b Maximum lateral force and yaw moment coefficients acting on Ship 1 for various ship speeds, (three ships passing)

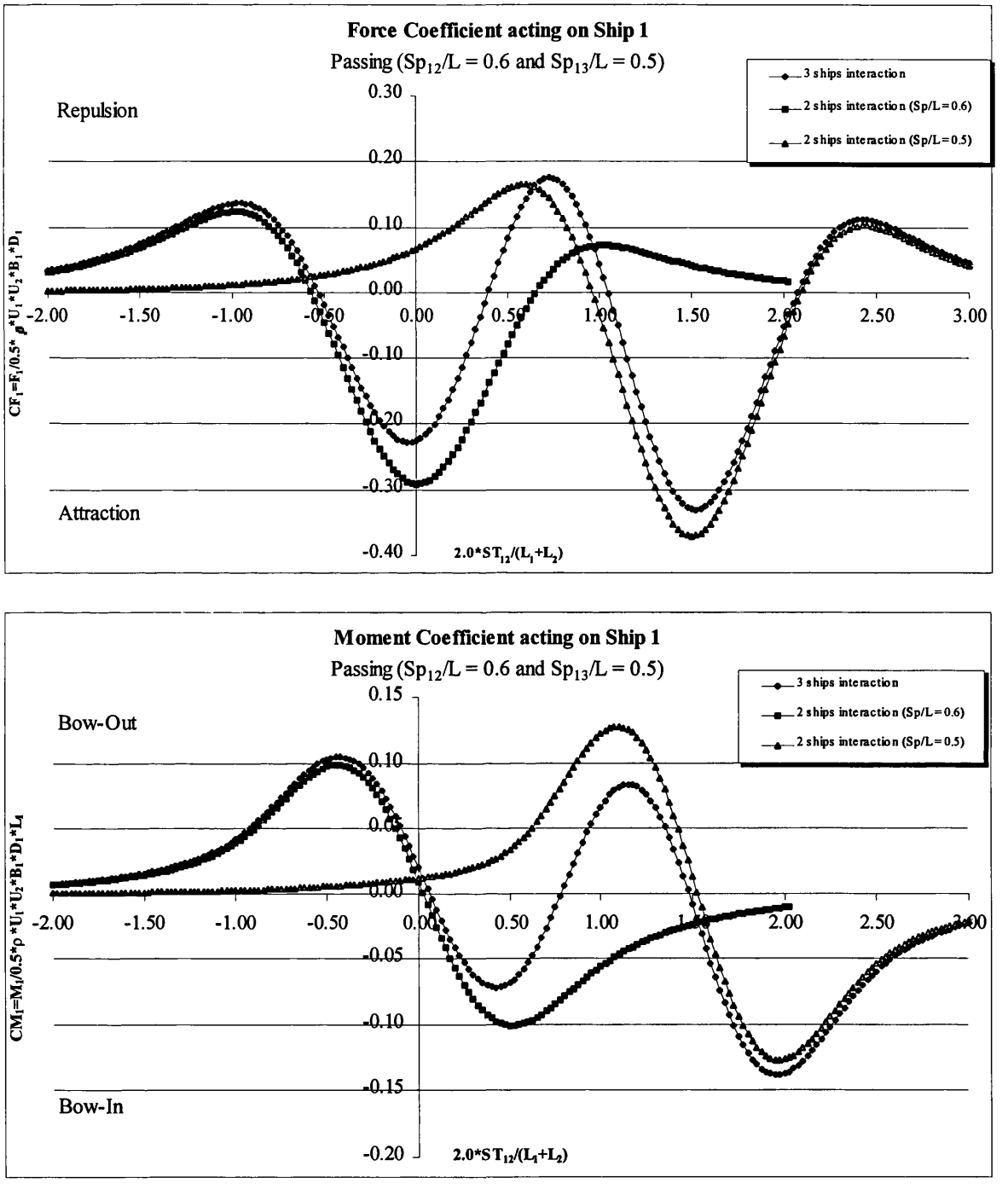

Figs 6.12a,b Comparisons of the lateral force and yaw moment coefficients acting on Ship 1 between two and three ships passing manoeuvre.

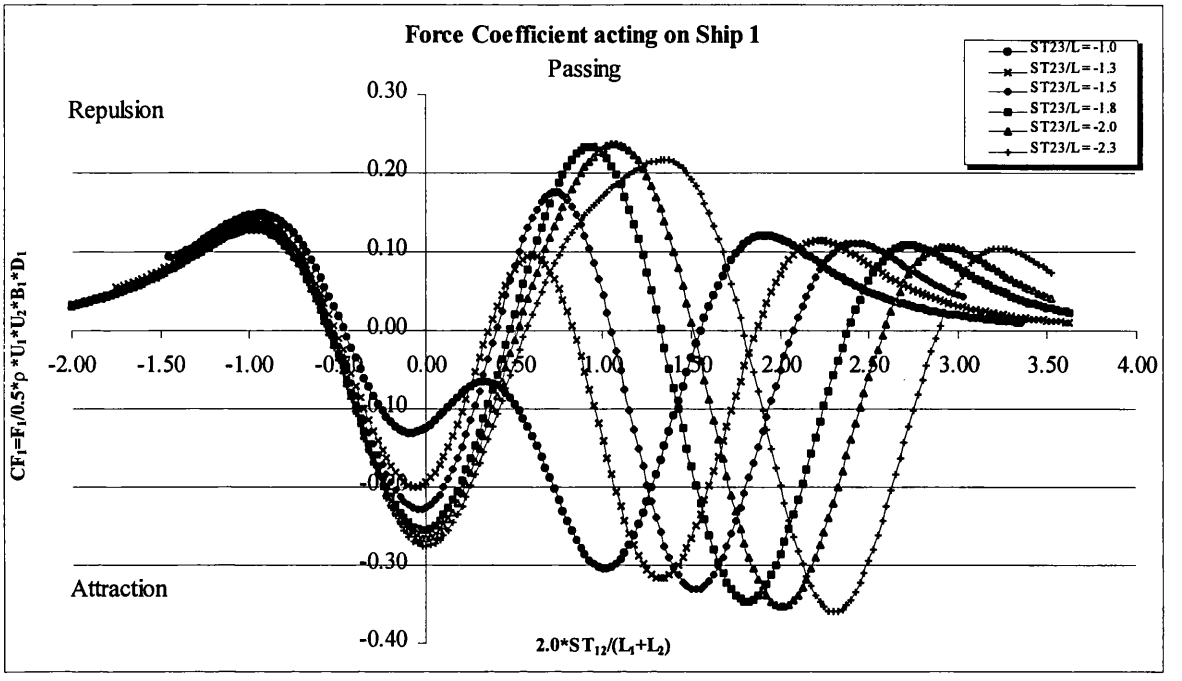

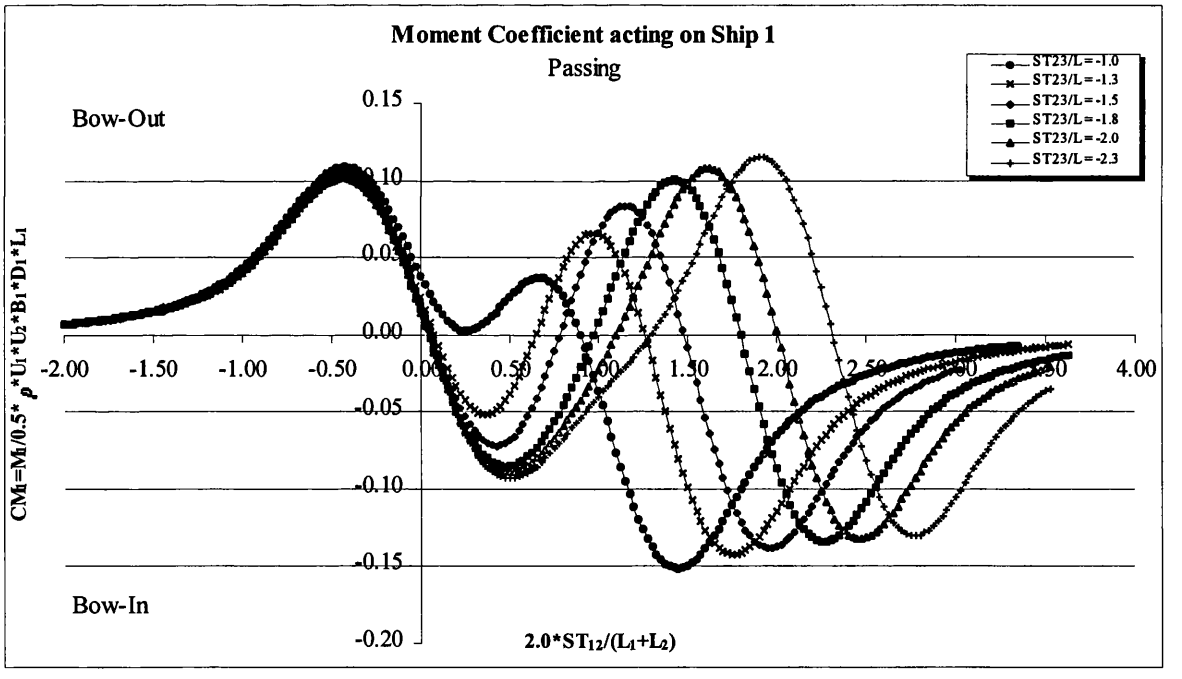

Figs 6.13a,b The lateral force and yaw moment coefficients acting on Ship 1 for various longitudinal distances between Ship 2 and Ship 3, (three ships passing)

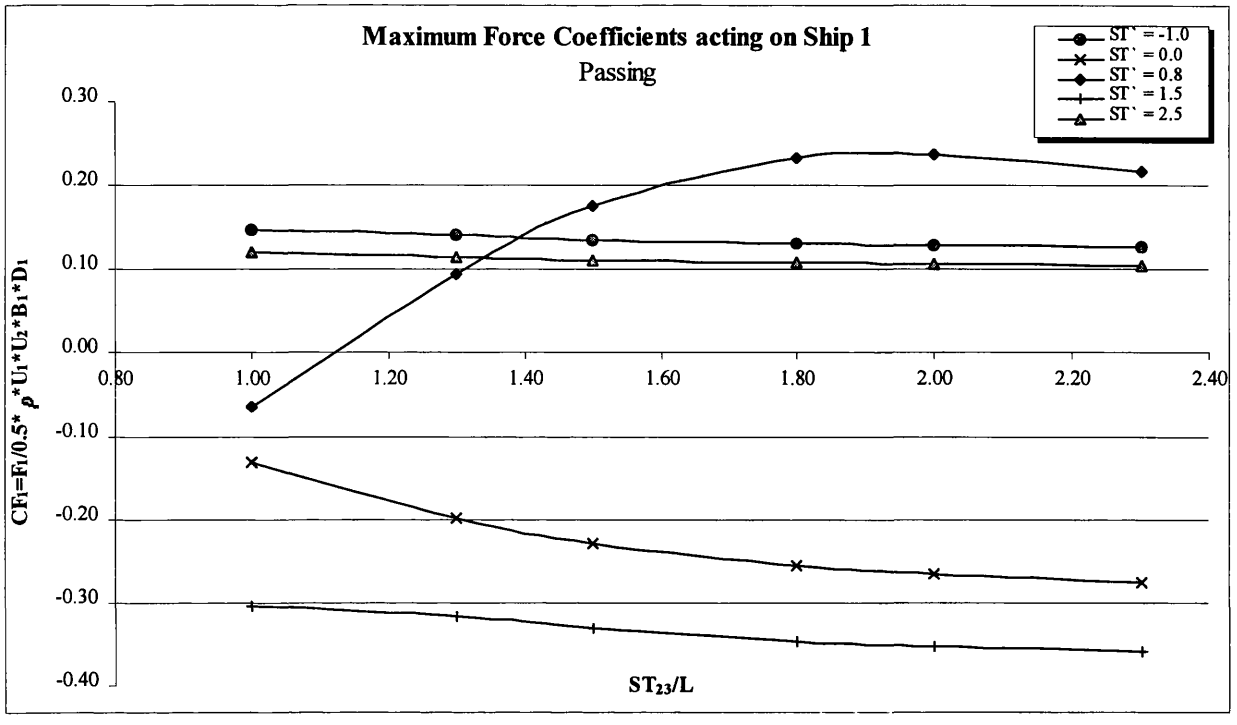

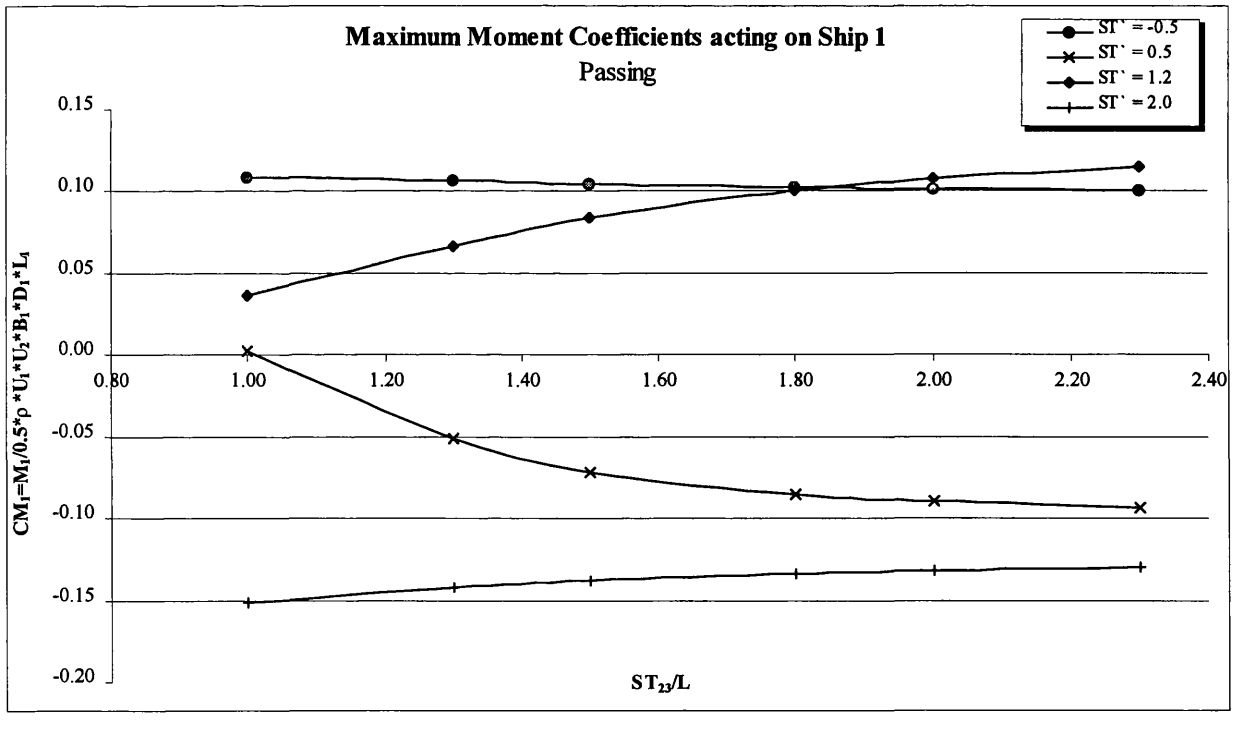

Figs 6.14a,b Maximum lateral force and yaw moment coefficients acting on Ship 1 for various longitudinal distances between Ship 2 and Ship 3, (three ships passing)

CHAPTER 7

CONCLUSIONS AND RECOMMENDATIONS

7.1 CONCLUSIONS

The aims of this research were to calculate interaction forces and moments on two and three ships in meeting and passing conditions. A number of parameters have been investigated to obtain a larger database of the interactive lateral force and yaw moment coefficients.

Numerical calculations are carried out using a FORTRAN 77 program based on discrete vortex distribution method. This program can calculate the lateral forces and yaw moments for both the two and the more complicated three ships interaction manoeuvre. The program is a development of a more general method and tackles problems resulting from varying several parameters (such as water depth, separation distance, ship size and ship speed.) However, the ships are limited to travel in parallel straight lines.

(i) Verification

For verification of the present method, several comparisons are made with previous experimental data both from Yasukawa (1983) and Dand (1981b), and theoretical predictions from Yasukawa (1983). The magnitudes of the lateral force and yaw moment coefficients obtained from the present method in the two ships meeting conditions are found to compare well with Yasukawa's experimental results. Yasukawa's measured values show phase discrepancies for the hydrodynamic forces and moments that do not appear in the computed data. Dand described problems involving a systematic feature of phase lag in his experimental results, but managed to solve this problem. This may explain why Yasukawa's experimental data have the same force and moment transit for the encountering manoeuvre as the present method but with a constant phase shift of the peak values. Besides, Yasukawa did not have a phase lag in his computed data, and comparisons with the present method show a very good agreement, both qualitatively and quantitatively, with these results.

Comparisons with Dand's experimental data show good qualitatively agreement both for the non-dimensionalized interaction forces and moments for two ships meeting.
Yasukawa and Dand did also conduct experiments for the situations of two ships passing. Yasukawa's measurements were carried out on a stationary model when

being passed by another model. Since the present method can not take zero speed as input, this situation is simulated by giving the speed of the overtaken speed as 0.001m/s. No phase lag were recorded by Yasukawa, and the qualitatively agreement is good. Furthermore, the lateral force and yaw moment coefficients obtained from the present method show only small differences, both in tendencies and magnitudes, with those from Yasukawa's predicted results.

Again, comparisons with Dand's experimental results shows good qualitatively agreement.

The present method is found to predict the ship interaction forces and moments reliably and with acceptable accuracy both for the two ships meeting and passing manoeuvre, based on the comparisons above. This engenders confidences in the program and allows the research to be progressed with assurance.

(ii) Two ship interaction

When two ships encounter each other in a channel they both experience a similar force and moment pattern: firstly, a repulsion force, then an attraction force and finally another repulsion force. The moment is initially bow-out in nature followed effectively by two successive bow-in peaks. The recovery between these peaks is usually a bow-in minimum rather than a bow-out peak, but for small separation distances a substantial bow-out peak exists between the two bow-in maxima.

In an overtaking manoeuvre, the slower ship experience a repulsion-attraction-repulsion force pattern while the moment exhibits a bow-out – bow-in behavior. In contrast, the faster passing ship experiences an attraction-repulsion force variation with a bow-in – bow-out moment variation.

A substantial investigation into the effects of the water depth, separation distance, ship size and ship speed has been carried out. The lateral forces and yaw moments are found to increase rapidly as the water gets shallower and the separation distance decreases both for the two ships meeting and passing situations. Furthermore, if a ship encounters a bigger and faster ship, it experiences larger hydrodynamic forces and moments.

It is apparent that the slower ship in the two ships passing manoeuvre experiences several times larger lateral forces and moments than the faster[1] ship. The interaction forces and moments acting on the slower ship increase rapidly too if the speed and size of the overtaking ship increase.

(iii) New empirical formulae

New empirical formulae[2] are derived for the maximum lateral force and yaw moment coefficients, both for the two ships meeting and passing manoeuvre, which takes into account the effects of water depth, separation distance, ship size and ship speed. These maximums are most important from viewpoint of safety of navigation.

The various maximum lateral force coefficients acting on Ship 1 when encountering Ship 2 is calculated using the new empirical formulae:

$$CF_i = Y_i^{ms}\left(1+{Sp}/{L_1}\right)^{\alpha_i}\left[1+Y_i^{md}\left({D_1}/{H}\right)\right]^{\beta_i}\left({H}/{D_1}\right)^{\beta_i}\left({L_1}/{L_2}\right)^{\delta}\left[1+Y_i^{mu}\left({\Delta U}/{U_1}\right)\right] \qquad i = 1,2,3$$

where m denotes the meeting manoeuvre and
i = 1 denotes the bow-bow situation
i = 2 denotes the midship-midship situation
i = 3 denotes the stern-stern situation

and $\Delta U = U_2 - U_1$

Similar the various maximum yaw moment coefficients acting on Ship 1 is calculated by using the following new empirical formulae:

$$CM_i = N_i^{ms}\left(1+{Sp}/{L_1}\right)^{\varepsilon_i}\left[1+N_i^{md}\left({D_1}/{H}\right)\right]^{\varphi_i}\left({H}/{D_1}\right)^{\varphi_i}\left({L_1}/{L_2}\right)^{\delta}\left[1+N_i^{mu}\left({\Delta U}/{U_1}\right)\right] \qquad i = 1,2,3,4$$

where m denotes the meeting situation and
i = 1 denotes the bow-bow situation
i = 2 denotes the immediately before midship-midship situation (Fore-Fore)
i = 3 denotes the immediately after midship-midship situation (Aft-Aft)
i = 4 denotes the stern-stern situation

and $\Delta U = U_2 - U_1$

[1] Verified for U_1/U_2 ratios above 1.3.
[2] The restrictions on use of the new empirical formulae in Chapters 3 and 4 still apply.

The different constants for maximum lateral force and yaw moment coefficients are seen in the Tables 3.9 and 3.10 respectively given in Chapter 3.5.4.

New empirical formulae are also derived both for the faster (Ship 1) and slower ship (Ship 2) in an overtaking manoeuvre. The various maximum lateral force coefficients acting on the faster Ship 1 is computed using the following formulae:

$$CF1_i = Y1_i^{ps}\left(Sp/L_1\right)^{\kappa_i}\left[1+Y1_i^{pd}\left(D_1/H\right)\right]^{\lambda_i}\left(H/D_1\right)^{\lambda_i}\left(L_1/L_2\right)^{\delta}\left[1+Y1_i^{pu}/2+Y1_i^{pu}\left(\Delta U/U_1\right)\right] \qquad i = 1,2$$

where p denotes the passing manoeuvre and
i = 1 denotes the bow-stern situation
i = 2 denotes the midship-midship situation

and $\Delta U = U_2 - U_1$

Similarly, the new empirical formula for the maximum yaw moment coefficients is found to be:

$$CM1_i = N1_i^{ps}\left(Sp/L_1\right)^{\mu_i}\left[1+N1_i^{pd}\left(D_1/H\right)\right]^{\nu_i}\left(H/D_1\right)^{\nu_i}\left(L_1/L_2\right)^{\delta}\left[1+N1_i^{pu}/2+N1_i^{pu}\left(\Delta U/U_1\right)\right] \qquad i = 1,2$$

where p denotes the passing manoeuvre and
i = 1 denotes the bow-midship situation
i = 2 denotes the stern-midship situation

and $\Delta U = U_2 - U_1$

For the slower ship (Ship 2), the following new empirical formulae is used to calculate the maximum lateral force coefficients:

$$CF2_i = Y2_i^{ps}\left(1+Sp/L_2\right)^{\tau_i}\left[1+Y2_i^{pd}\left(D_1/H\right)\right]^{\upsilon_i}\left(H/D_1\right)^{\upsilon_i}\left(L_2/L_1\right)^{\delta}\left[1+Y2_i^{pu}+Y2_i^{pu}\left(\Delta U/U_2\right)\right] \qquad i = 1,2,3$$

where p denotes the passing manoeuvre and
i = 1 denotes the bow-stern situation
i = 2 denotes the midship-midship situation
i = 3 denotes the stern-bow situation

and $\Delta U = U_2 - U_1$

The new empirical formula for the maximum yaw moment coefficients is on the following form:

$$CM2_i = N2_i^{ps}\left(1+{Sp}/{L_2}\right)^{\omega_i}\left[1+N2_i^{pd}\left({D_2}/{H}\right)\right]^{\psi_1}\left({H}/{D_2}\right)^{\psi_1}\left({L_2}/{L_1}\right)^{\delta}\left[1+N2_i^{pu}+N2_i^{pu}\left({\Delta U}/{U_2}\right)\right] \qquad i = 1,2$$

where and p denotes the passing manoeuvre and
i = 1 denotes the bow-midship situation
i = 2 denotes the stern-midship situation

and $\Delta U = U_2 - U_1$

All the different constants for the various maximum lateral force and yaw moment coefficients are given in the Tables 4.5 to 4.8 in Chapter 4.5.4

(iv) Practical application

These new empirical formulae are used to identify the conditions where safe operations are not possible both for the two ships meeting and two ships passing manoeuvre. From the viewpoint of safety of navigation the side interaction force is not intrinsically dangerous. However, the lack of sufficient rudder moment puts ships at risk. In close encounters in restricted waters the rudder moment is, in many situations, less than the interaction yaw moment. (For example, if a ship is overtaken by a 25% larger ship travelling at twice its speed in waters 30% of its draught minimum separation for safe operation to be possible is then 0.52 times its length.) However, it should be born in mind that even though a ship is travelling under conditions that are below the point of rudder adequacy, it is not necessarily a sufficient condition for a collision to take place (either with the other ship or the channel wall). This is because of the transient nature of the interaction.

(v) Three ship interaction

Research is also carried out on the more complicated problem involving three ships in both meeting and passing manoeuvre. Previous investigation into this problem is very limited, but a comparison with Yasukawa's predicted lateral force and moment coefficients show very good qualitatively and qualitatively agreement.

For the three ships meeting manoeuvre, Ship 1 is encountering first Ship 3 followed by Ship 2 at some distance. It is apparent that the potentially most hazardous part of the transit is when Ship 1 is interacting with both Ship 2 and Ship 3. As a result, a '3 ship interaction' manoeuvre is considered to be more dangerous than a '2 ship manoeuvre'. The parametric study into the effect of the water depth and separation distance shows that the danger of unsafe operations increases as the water gets shallower and the separation distance decreases. The ship size and ship speed influences the lateral forces and moments too.

The parametric study also reveals that Ship 1 experiences largest repulsion forces when the longitudinal distance, or stagger, between the midships of Ship 2 and Ship 3 is 1.8 times the ship length when all three ships are of the same size. These peaks decrease for larger and smaller staggers.

In the three ships passing manoeuvre, Ship 1 is the slower ship while overtaken first by Ship 2 followed by Ship 3 at some distance. Again, the lateral forces and yaw moments increase as the water depth and separation distance decrease. Ship 1 also experiences larger interaction forces and moments when the speed and size of the overtaking ships are increased. This tendency is common to the three ships meeting manoeuvre.

It should be noted that the duration of the passing conditions is longer than in the meeting condition. The possibility of collision or ramming of ships is greater in the passing transit, and especially careful navigation must be applied when Ship 1 is situated between Ship 2 and Ship 3.

The results allow conditions for unsafe operations to be identified. Furthermore, the research has the potential to improve the management of operations in crowded waterways, harbours, channels, ports, etc.

7.2 RECOMMENDATIONS

Owing to the extensive time required tackling a large number of experimental conditions for predicting ship interaction forces and moments some recommendations are made for future work.

Even though some authors (Yasukawa (1983) and Dand (1981b)) have made measurements on ships in two ships encountering and overtaking manoeuvres, more experimental data are needed. Furthermore, no one has attempted experiments for the situations where three ships are interacting. Since waterways in the future will be more crowded, measurements of the lateral forces and yaw moments acting on ships interacting with several ships would illustrate how they influence each other.

Based on the present method, simulation studies can be carried out for various water depths, separation distance between ships, ship size and ship speed, both for the two and three ship interaction problems. The control limit for keeping the ships course for safety of navigation can then be found. Furthermore, analysis with active rudder and the ships free to deviate would make it possible to produce the ships trajectories for various interaction manoeuvres. Such a study can then be used to simulate accident scenarios.

The next logical step is to investigate and calculate the interaction forces and moments acting on ships when they are travelling at oblique paths. The potential hazardous situations when operating in harbours, inland waterways etc. can then be identified.

REFERENCES

Beck, R.F. (1977), "Forces and moments on a ship moving in a shallow channel.", Journal of Ship Research , Vol. 21, pp 107-119.

Beck, R.F., Tuck, E.O. and Newman, J.N. (1975), "Hydrodynamic forces on ships in dredged channels.", Journal of Ship Research , Vol. 19, pp 166 -171.

Clarke, D. (1983), "The application of manoeuvring criteria in hull design", Transactions RINA, Vol. 125, pp 45 – 68.

Dand, I.W. (1976a), "Hydrodynamic aspects of shallow water collision" ,Transactions RINA, Vol. 118, pp 323 - 346.

Dand, I.W. (1976b), "Ship-ship interaction in shallow water.", 11th symposium on Naval Hydrodynamics, London.

Dand, I.W. (1981a), "Simulation of the behaviour of a moored ship when passed by other ships.", National Maritime Institute, R 111.

Dand, I.W. (1981b), "Some measurements of interaction between ship models passing on parallel courses.", National Maritime Institute, R 108.

Dand, I.W. (1981c), "Some measurements of interaction induced by surface piercing and flooded banks.", National Maritime Institute, R 110.

Dand, I.W. (1994), "Interaction.", Nautical Institute conference, pp 1-20.

Hunley, W.H. (1969), "Anchor, mooring and towing arrangements" , Ship Design and Construction, pp 377-404.

James, R.M. (1972), "On the remarkable accuracy of the vortex lattice method", Computer Methods in Applied Mechanics and Engineering 1, pp 59-79.

Kijima, K. and Yasukawa, H. (1985) "Manoeuvrability of ships in narrow waterway" Journal of the Society of Naval Architects of Japan, Vol. 23, pp 25-37.

Kijima, K. and Furukawa, Y. (1994) "Ship manoeuvring motion in the proximity of piers" , Proceedings of the International Committee on Manoeuvring and Control of Marine Craft, Southampton, pp 211-222.

Newman, J.N. (1969), "Lateral motion of a slender body between two parallel walls.", Journal of Fluid Mechanics, Vol. 39, pp 97-115.

Sedov, L.I. (1969), "Two dimensional problems in hydrodynamics and aerodynamics", John Wiley, New York.

Tan, W.T. (1979), "Unsteady hydrodynamic interaction of ships in the proximity of fixed objects." , Master's thesis, Department of Ocean Engineering, M.I.T

Taylor, P.J. (1973), "The blockage coefficient for flow about an arbitrary body immersed in a channel.", Journal of Ship Research , Vol. 17, pp 97-105.

Tuck, E.O. (1966), "Shallow water flow past slender bodies.", Journal of Ship Research , Vol. 26, pp 81-95.

Tuck, E.O. (1967), " Sinkage and trim in shallow water of finite width.", Schiffstechnik, Vol. 14, pp 92-94.

Tuck, E.O. and Newman, J.N. (1974), " Hydrodynamic interaction between ships.", 10th Symposium on Naval Hydrodynamics, pp 35-70.

Varyani, K.S, Hamoudi, B and McGregor, R.C. (1997) "Interactive forces between three ships in a restricted waterway. ", Proceeding of the International Federation of Automatic Control Conference on Manoeuvring and Control of Marine Craft (MCMC 97), Brijuni, Croatia, 10-12 Sept 1997, pp 127-133.

Varyani, K.S, McGregor, R.C. and Wold, P. (1998) "Interactive forces between several ships meeting in confined waters. ", Control Engineering Practice 6, pp 637 - 642.

Wold, P. (1997) "Squat on monohull ships in shallow water." , University of Glasgow, Department of Naval Architecture and Ocean Engineering, Technical Report NAOE 98-27.

Yasukawa, H. (1983), "Research of ship manoeuvrability in restricted channel." , Kyushu University, Master's thesis.

Yeung, R.W. (1978), "On the interaction of slender ships in shallow water." Journal of Fluid Mechanics, Vol. 85, pp 143-159.

Yeung, R.W. and Tan W.T. (1980), "Hydrodynamic interaction of ships with fixed obstacles", Journal of Ship Research, Vol. 24, pp 50-59.

APPENDIX

APPENDIX 1

GREEN FUNCTIONS

The Green Functions defined by eqns (2.21), (2.22) and (2.23) can be obtained by conformal transformation using the following mapping function:

$$\zeta = e^{(\pi/w)kz} \tag{A1.1}$$

where z and ζ are complex variables representing point on the physical and mapped plane. z is defined as z = x + iy. The complex potentials for a source and a vortex located in the ζ plane satisfying the rigid boundary condition are of the following form:

$$\left.\begin{aligned} f^{(\sigma)} &= \ell n(\zeta-\zeta_0)+\ell n(\zeta-\bar{\zeta}_0) \\ f^{(\gamma)} &= -i\ell n(\zeta-\zeta_0)+i\ell n(\zeta-\bar{\zeta}_0) \end{aligned}\right\} \tag{A1.2}$$

where ζ_0 denotes the location of the source or vortex and $\bar{\zeta}_0$ is the complex conjugate of ζ_0.

The Green Functions can be obtained by taking the real part of eqn (A1.2). By taking the complex derivative of eqn (A1.2), the following expressions for the complex velocities are obtained:

$$\left.\begin{aligned} \omega^{(\sigma)} &= \frac{df^{(\sigma)}}{dz} = \left[\frac{1}{\zeta-\zeta_0}+\frac{1}{\zeta-\bar{\zeta}_0}\right]\frac{\partial\zeta}{\partial z} \\ \omega^{(\gamma)} &= \frac{df^{(\gamma)}}{dz} = \left[-\frac{i}{\zeta-\zeta_0}+\frac{i}{\zeta-\bar{\zeta}_0}\right]\frac{\partial\zeta}{\partial z} \end{aligned}\right\} \tag{A1.3}$$

where the complex velocities are defined as $\omega^{(\sigma,\gamma)} = u - iv$.

The normal velocities are then given by the following:

$$\left.\begin{aligned}\frac{\partial G^{(\sigma)}}{\partial y_i} &= -\mathrm{Im}\left[\omega^{(\sigma)} e^{\zeta\theta_i}\right] \\ \frac{\partial G^{(\gamma)}}{\partial y_i} &= -\mathrm{Im}\left[\omega^{(\gamma)} e^{\zeta\theta_i}\right]\end{aligned}\right\} \qquad \text{(A1.4)}$$

where Im denotes the imaginary part and θ_i is the angular displacement of the $0_i x_i y_i$ coordinate system relative to the 0xy system. When ship travels in the positive direction of x-axis, θ_i equals zero and in the negative direction, θ_i equals π.

APPENDIX 2

CALCULATION OF RUDDER DERIVATIVES (From Clarke (1983))

The side force Y created by the rudder is calculated on the basis that the rudder acts like a low aspect ratio wing, so that:

$$Y = \tfrac{1}{2}\rho c^2 A C_L \qquad \text{(A2.1)}$$

where c is water speed past the rudder, A is the rudder area and C_L is the lift coefficient. If this side force is non-dimensionalized in the usual way, by the factor $^1/_2\rho U^2 L^2$ then we have:

$$Y' = \left(\frac{A}{LD}\right)\left(\frac{D}{L}\right)C_L\left(\frac{c}{U}\right)^2$$

from which

$$Y'_\delta = \left(\frac{A}{LD}\right)\frac{D}{L}\left(\frac{\partial C_L}{\partial \delta}\right)\left(\frac{c}{U}\right)^2 \qquad \text{(A2.2)}$$

and since the rudder is approximately half the ship length aft of amidships:

$$N'_\delta = -\tfrac{1}{2}Y'_\delta \qquad \text{(A2.3)}$$

Although the lift curve slope of the rudder $\partial C_L/\partial\delta$ and the velocity ratio $(c/U)^2$ are variables which are different for every ship, their product has been assumed constant throughout the analysis, so that:

$$\left(\frac{\partial C_L}{\partial \delta}\right)\left(\frac{c}{U}\right)^2 = 3.0 \qquad \text{(A2.4)}$$

which is a typical value for single screw ships.

APPENDIX 3

FIGURES FOR TWO SHIPS MEETING

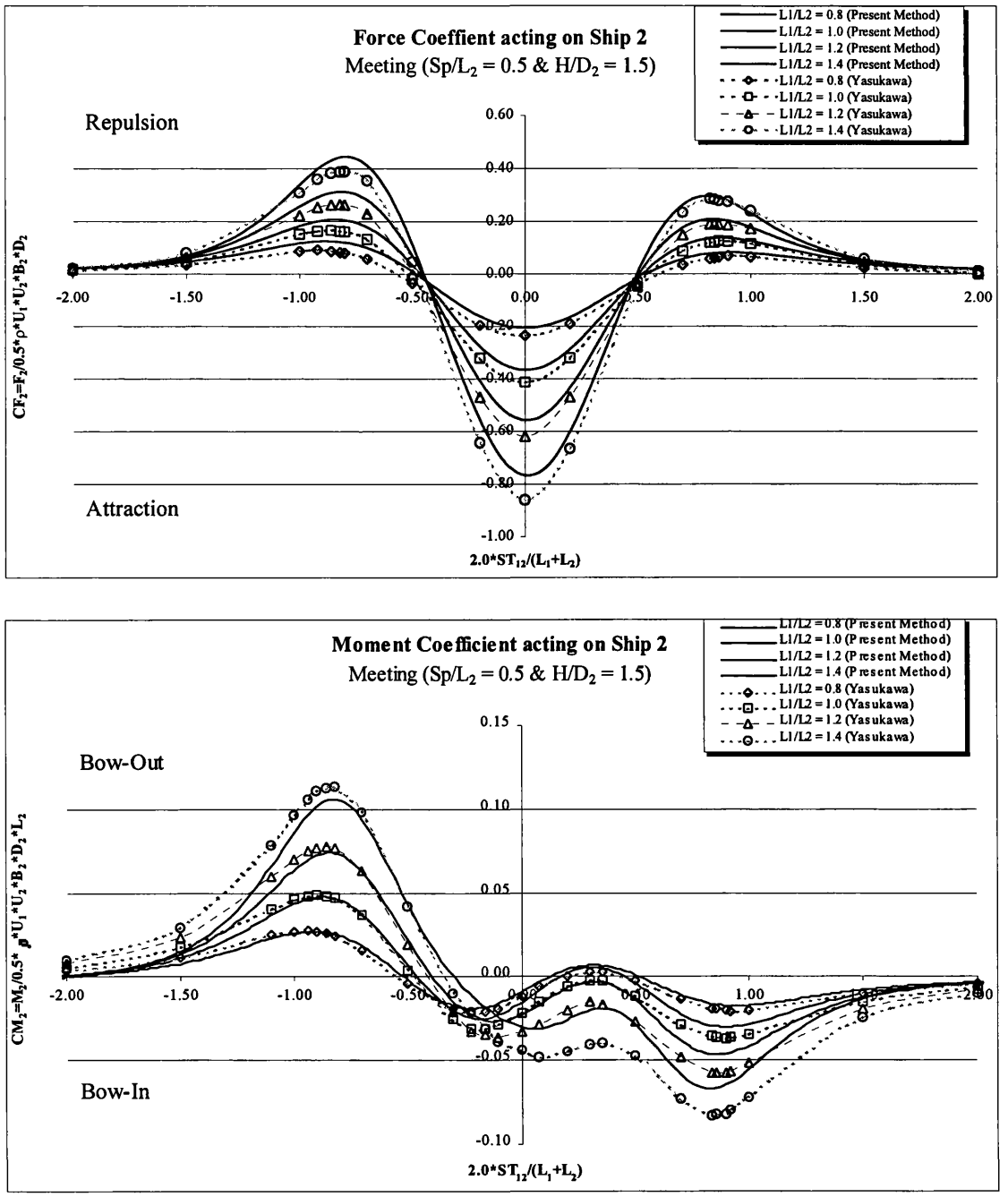

Fig A3.1 Comparison of the lateral force and yaw moment coefficients with Yasukawa's theoretical data for various ship sizes, (two ships meeting, $U_1/U_2 = 1.0$)

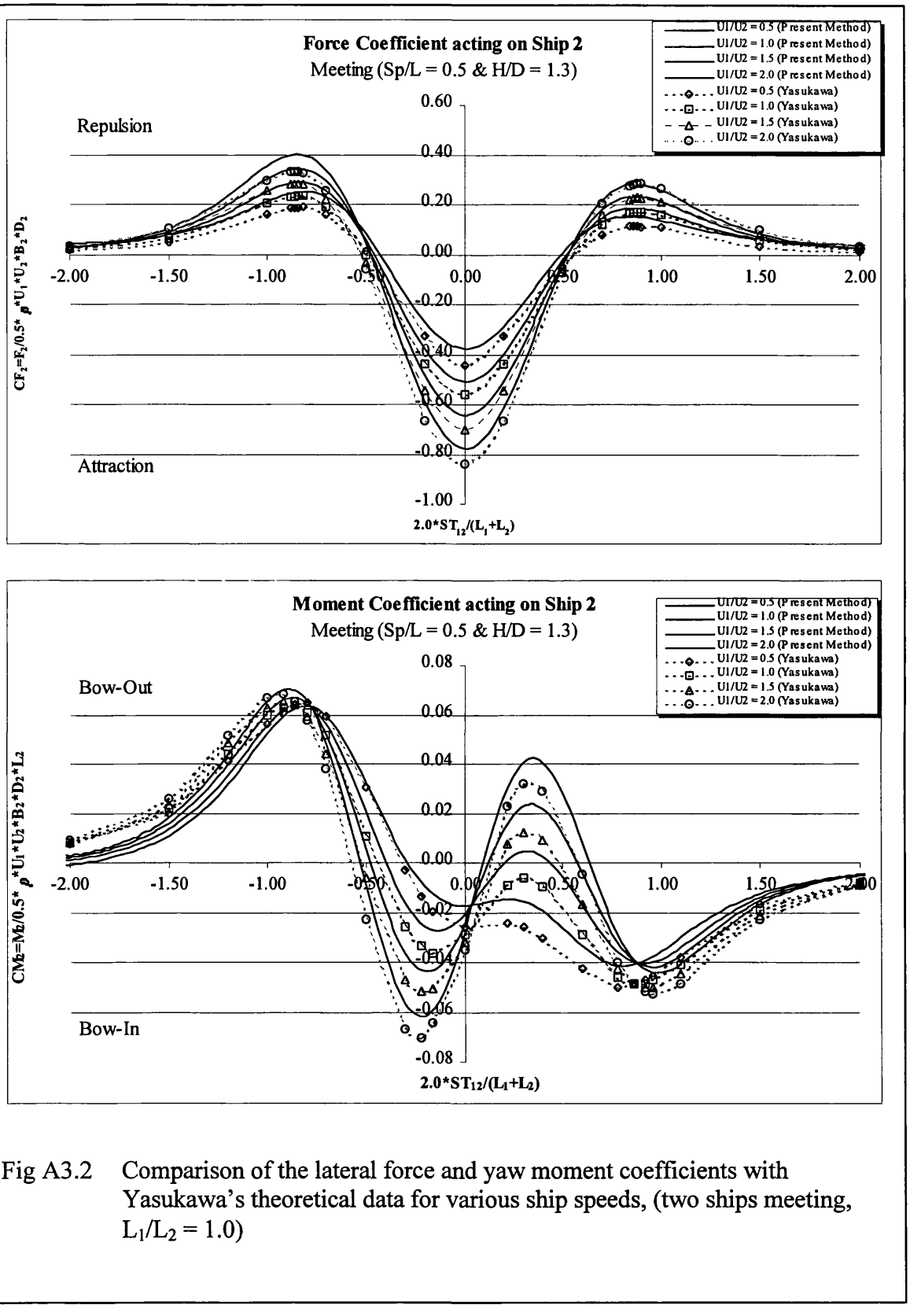

Fig A3.2 Comparison of the lateral force and yaw moment coefficients with Yasukawa's theoretical data for various ship speeds, (two ships meeting, $L_1/L_2 = 1.0$)

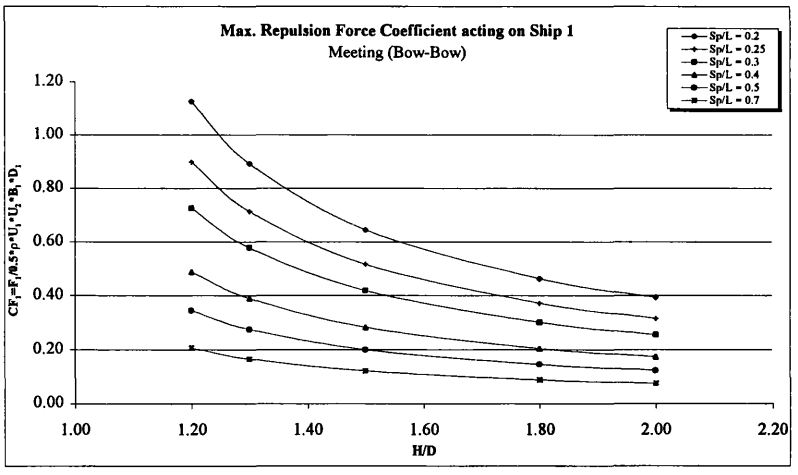

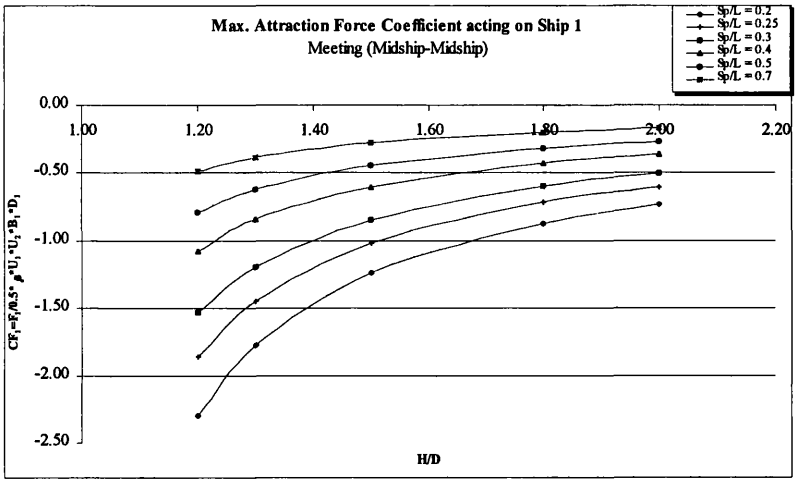

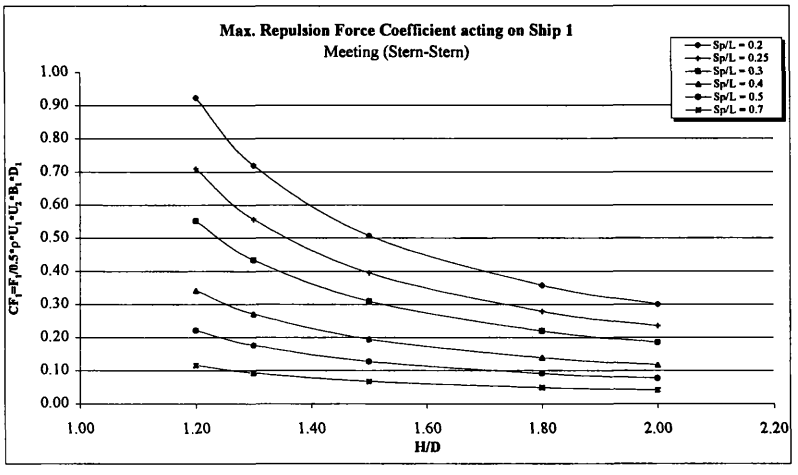

Fig A3.3 Maximum lateral force coefficients acting on Ship 1 for various water depths and separation distances, (two ships meeting, $L_1/L_2 = 1.0$ and $U_1/U_2 = 1.0$)

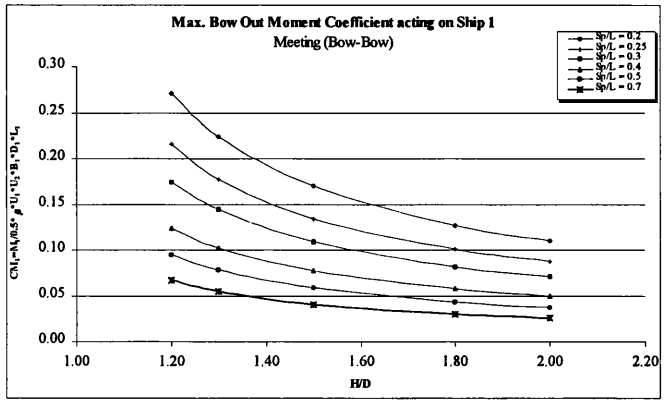

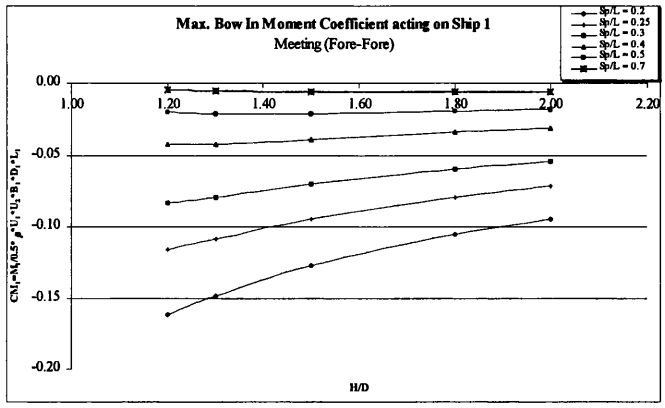

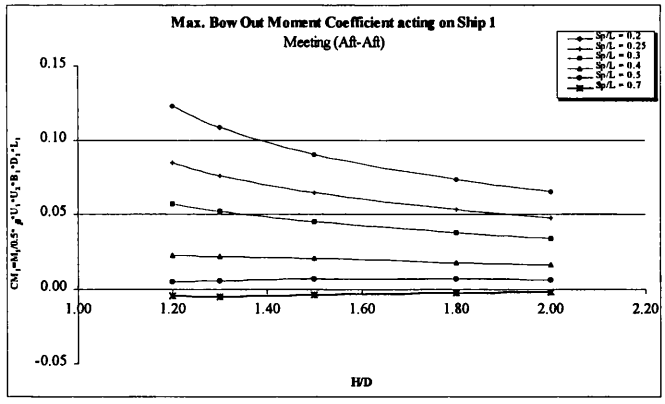

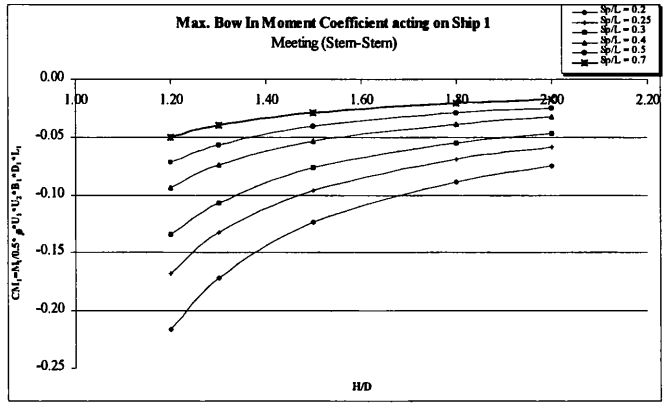

Fig A3.4 Maximum yaw moment coefficients acting on Ship 1 for various water depths and separation distances, (two ships meeting, $L_1/L_2 = 1.0$ and $U_1/U_2 = 1.0$)

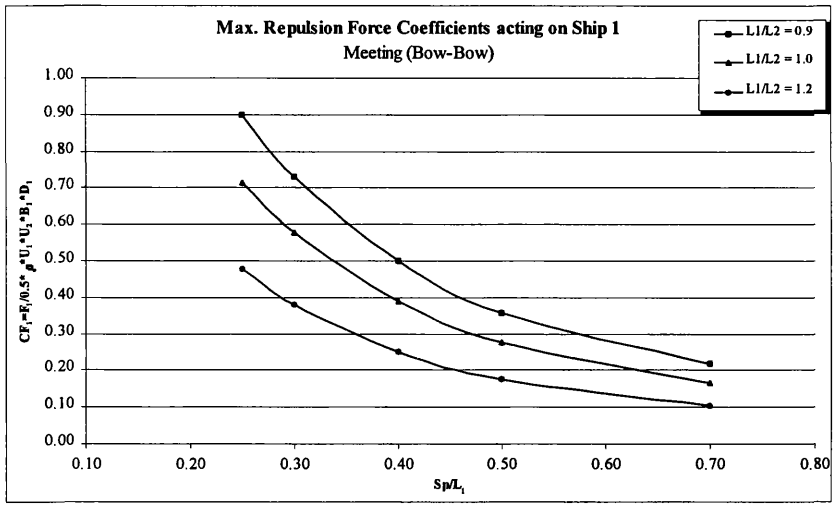

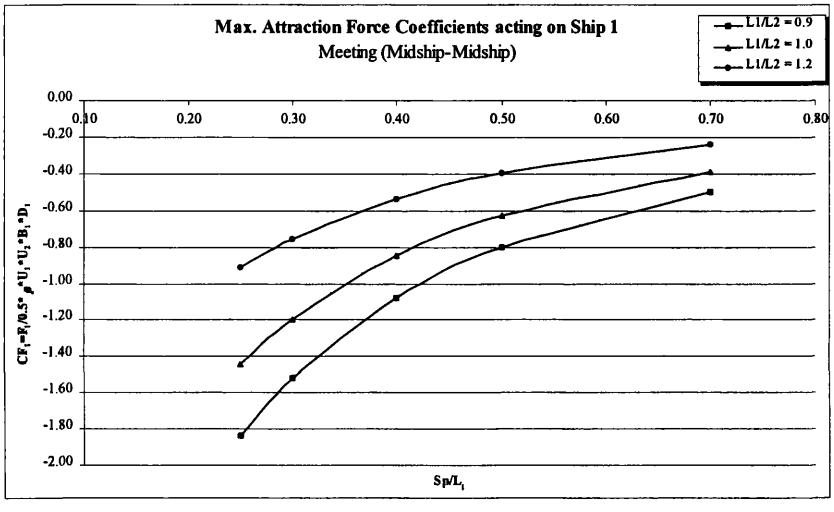

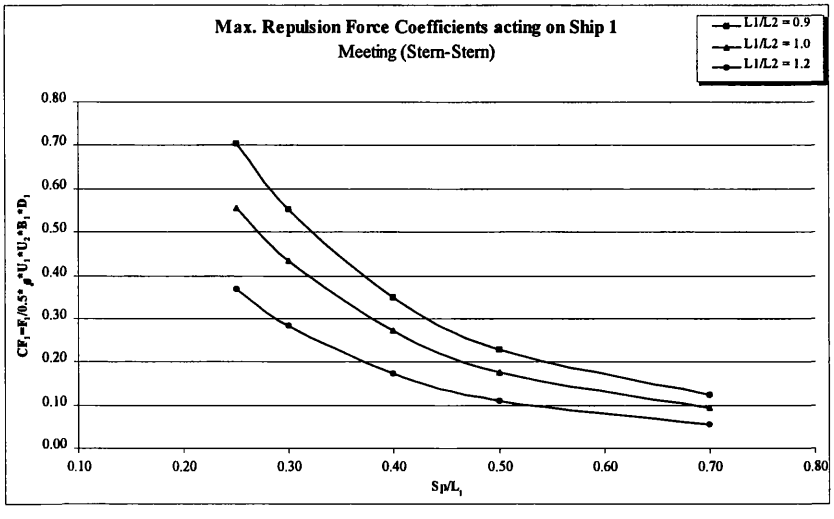

Fig A3.5 Maximum lateral force coefficients acting on Ship 1 for various ship sizes and separation distances, (two ships meeting, $H/D_1 = 1.3$ and $U_1/U_2 = 1.0$)

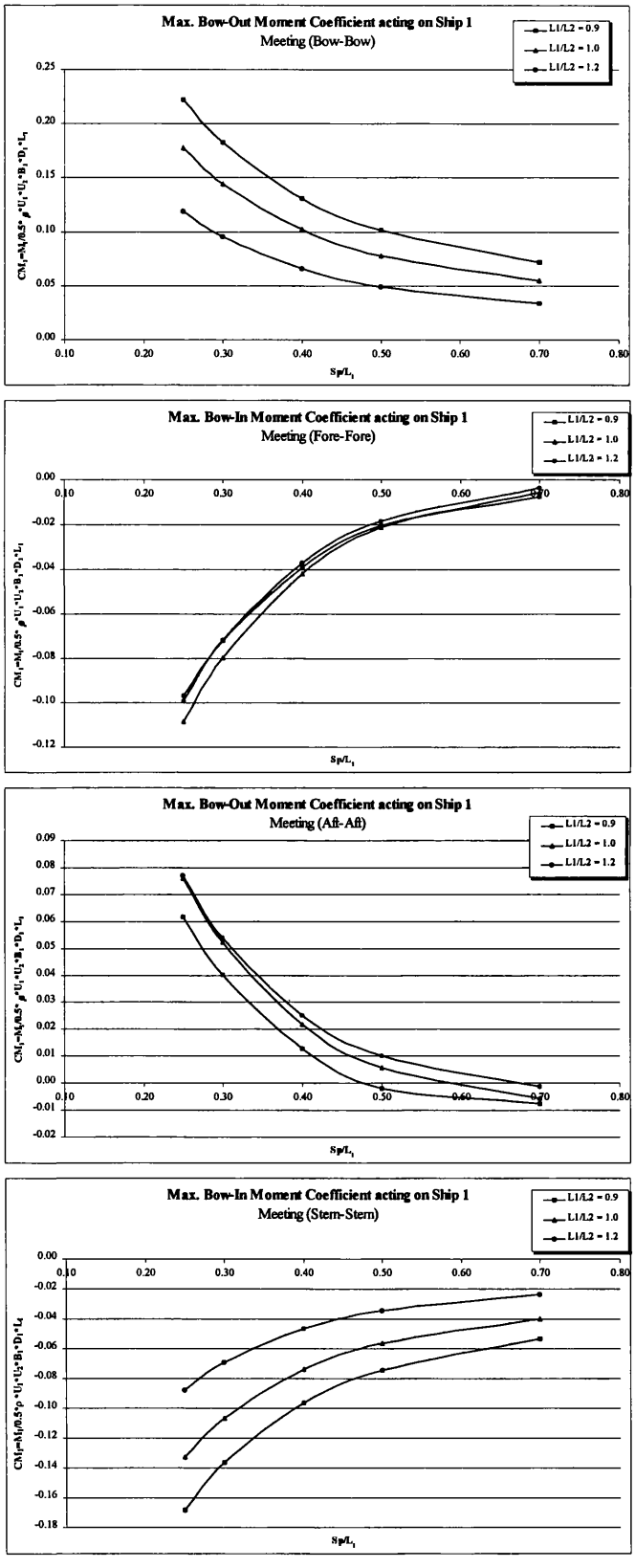

Fig A3.6 Maximum yaw moment coefficients acting on Ship 1 for various ship sizes and separation distances, (two ships meeting, $H/D_1 = 1.3$ and $U_1/U_2 = 1.0$)

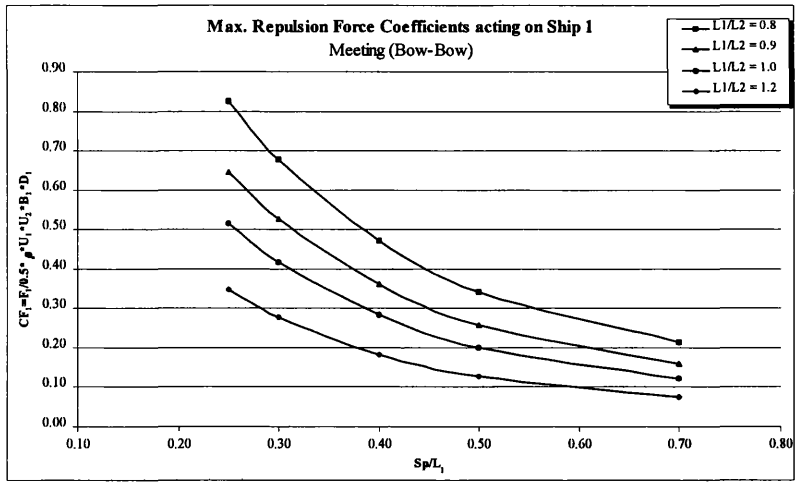

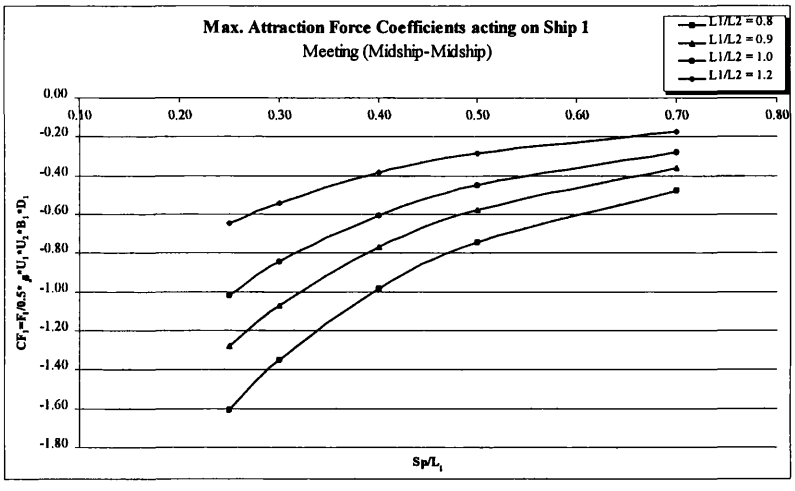

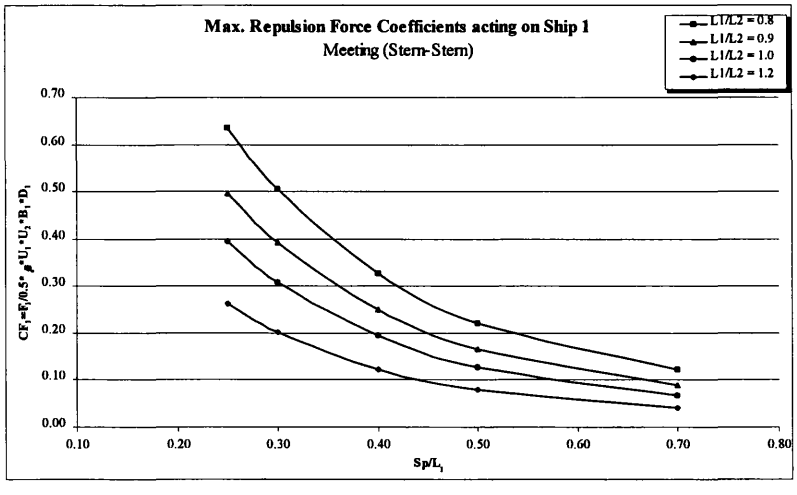

Fig A3.7 Maximum lateral force coefficients acting on Ship 1 for various ship sizes and separation distances, (two ships meeting, $H/D_1 = 1.5$ and $U_1/U_2 = 1.0$)

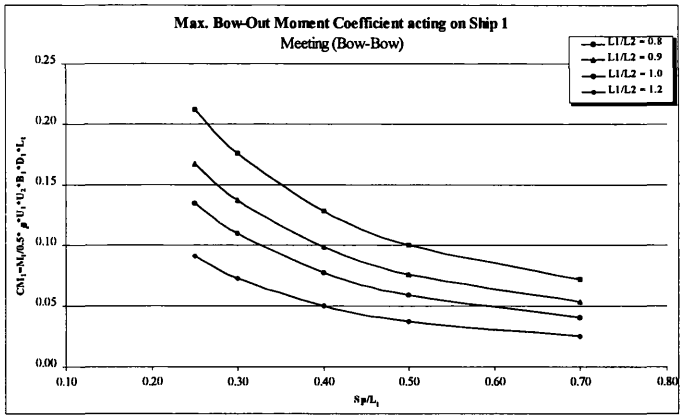

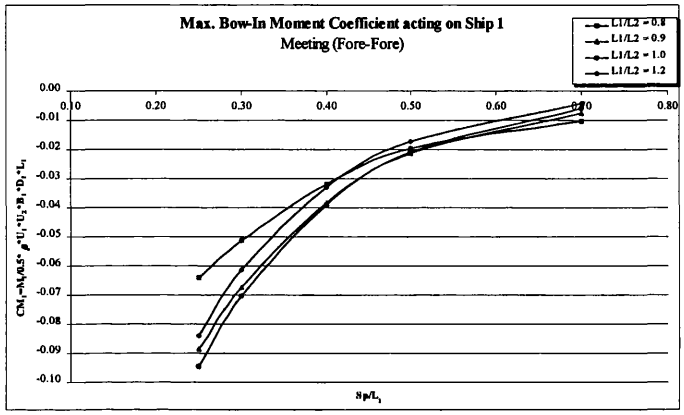

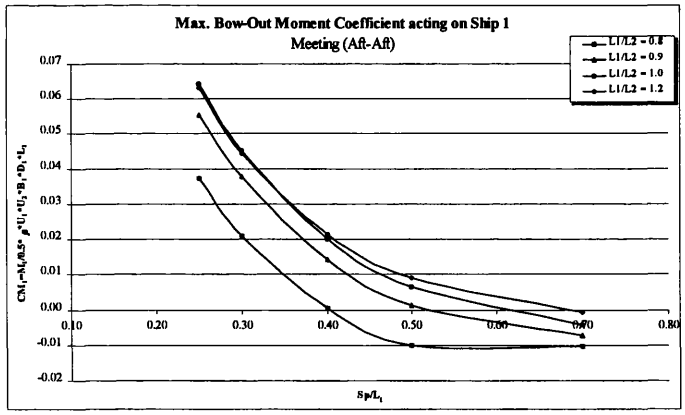

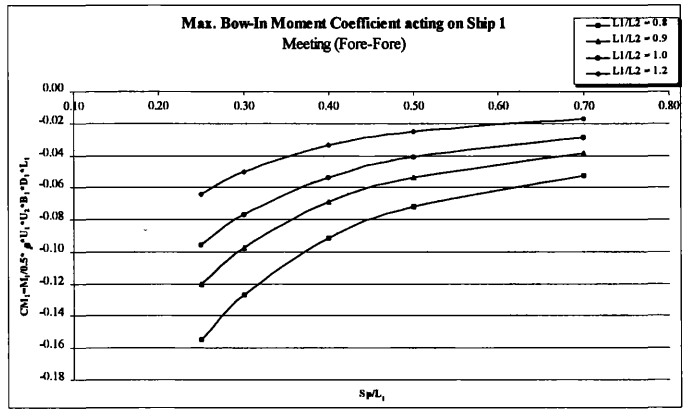

Fig A3.8 Maximum yaw moment coefficients acting on Ship 1 for various ship sizes and separation distances, (two ships meeting, $H/D_1 = 1.5$ and $U_1/U_2 = 1.0$)

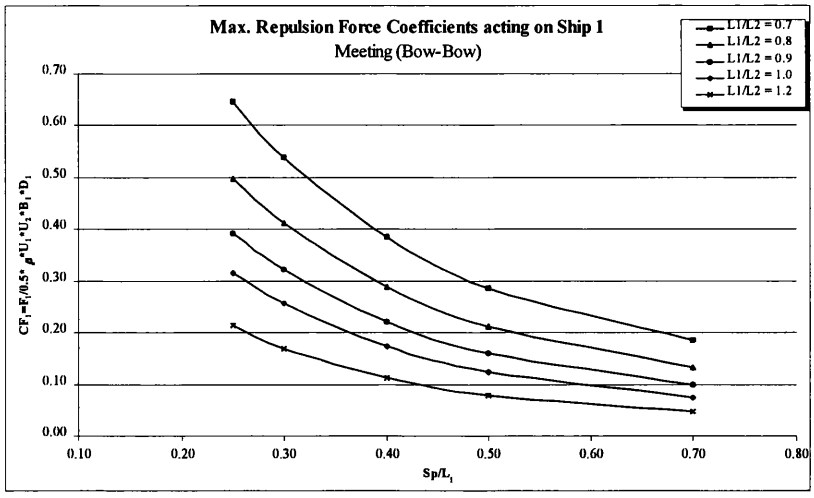

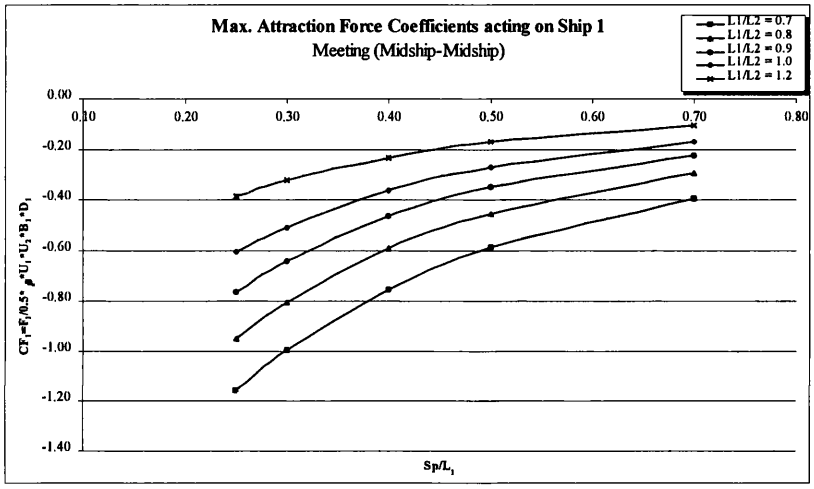

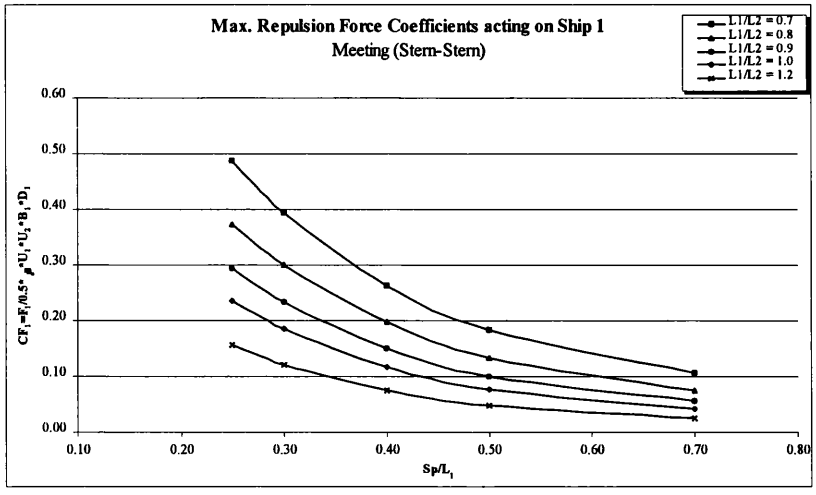

Fig A3.9 Maximum lateral force coefficients acting on Ship 1 for various ship sizes and separation distances, (two ships meeting, $H/D_1 = 2.0$ and $U_1/U_2 = 1.0$)

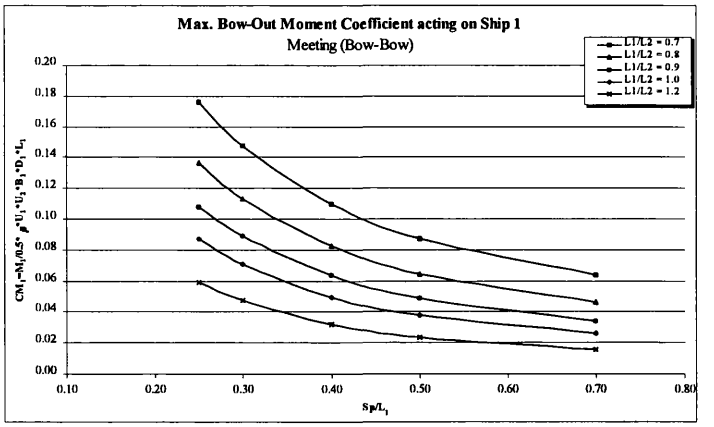

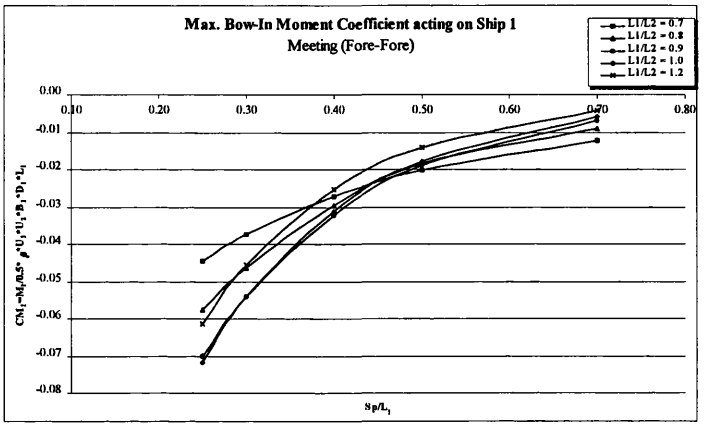

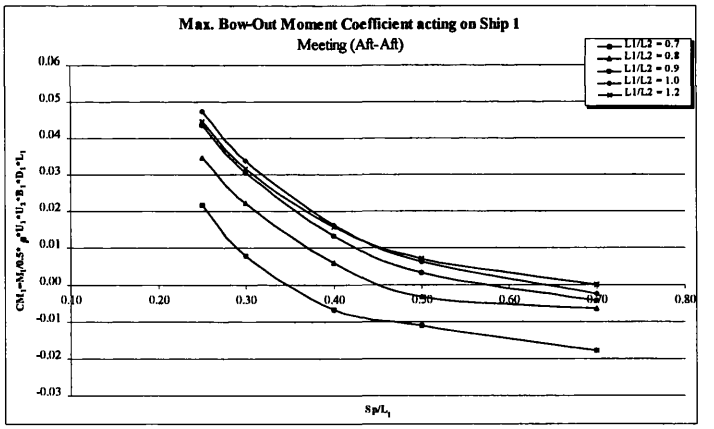

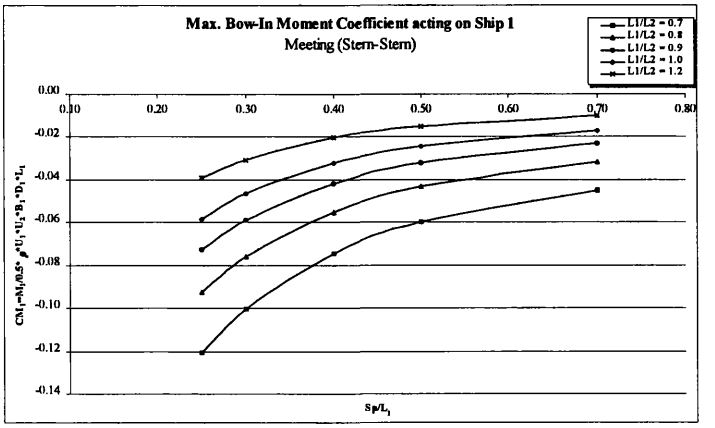

Fig A3.10 Maximum yaw moment coefficients acting on Ship 1 for various ship sizes and separation distances, (two ships meeting, $H/D_1 = 2.0$ and $U_1/U_2 = 1.0$)

APPENDIX 4

FIGURES TWO SHIPS PASSING

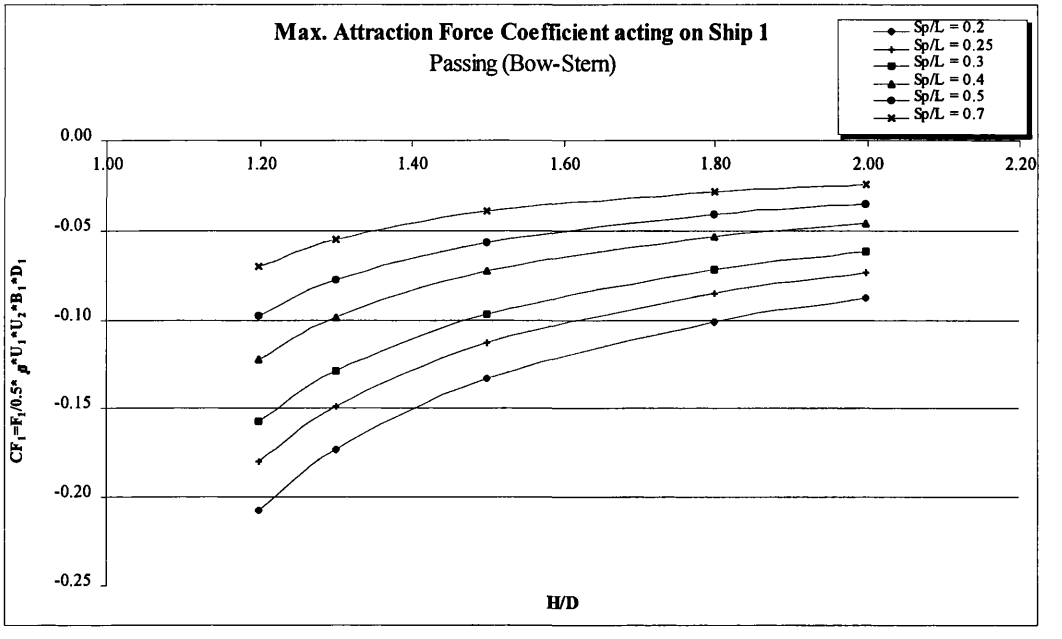

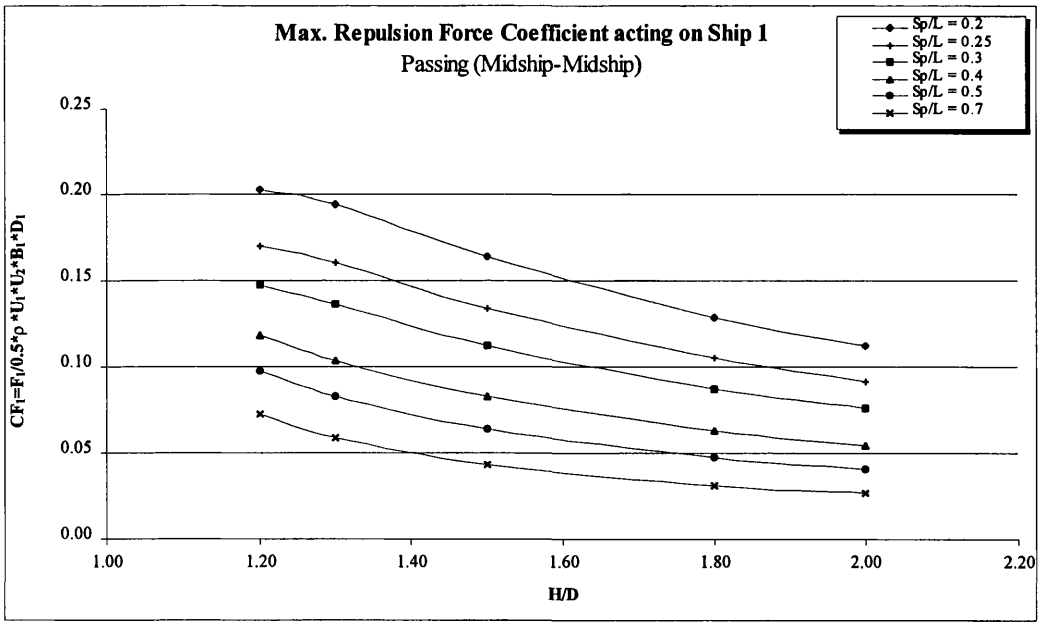

Fig A4.1 Maximum lateral force coefficients acting on the faster Ship 1 for various water depths and separation distances, (two ships passing, $L_1/L_2 = 1.0$ and $U_1/U_2 = 2.0$)

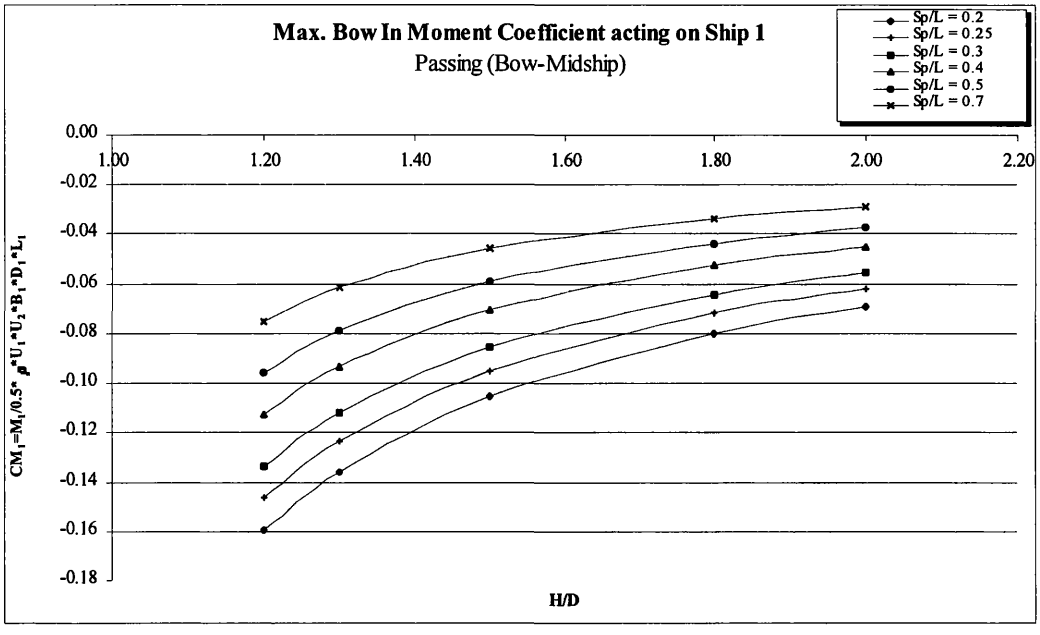

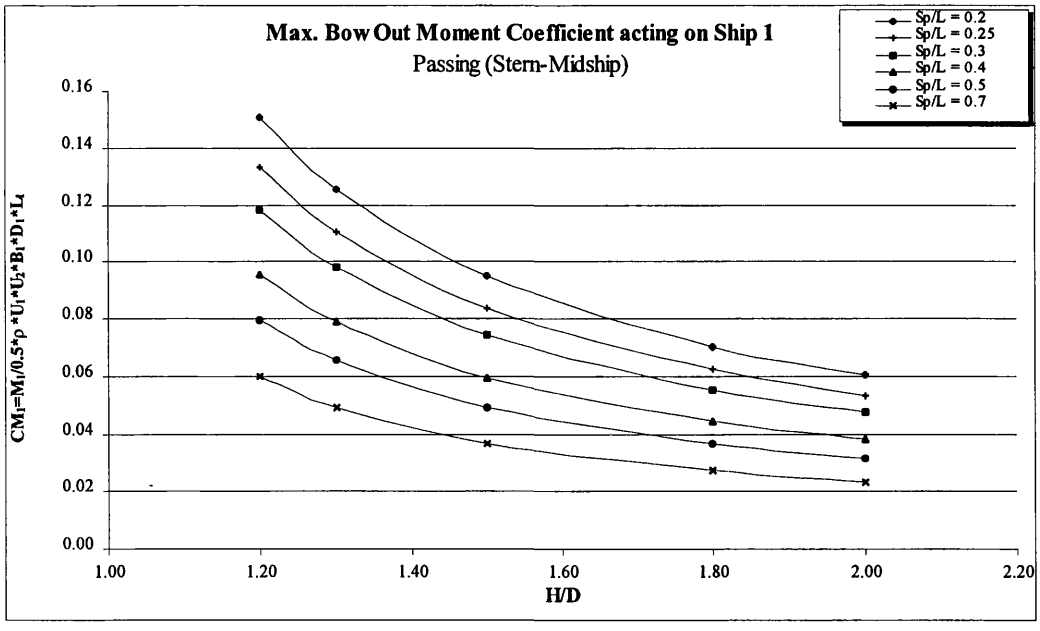

Fig A4.2 Maximum yaw moment coefficients acting on the faster Ship 1 for various water depths and separation distances, (two ships passing, $L_1/L_2 = 1.0$ and $U_1/U_2 = 2.0$)

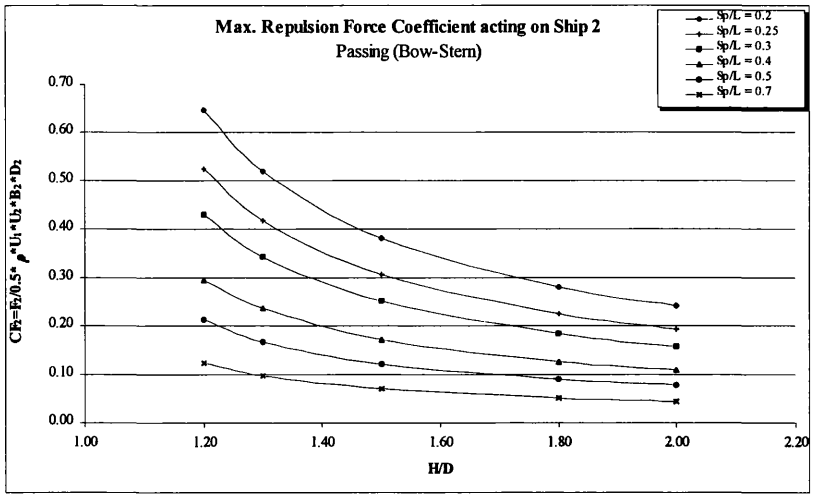

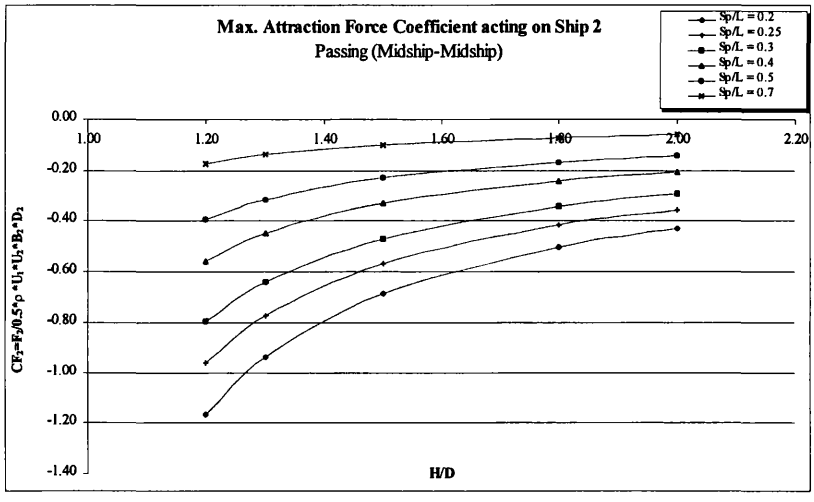

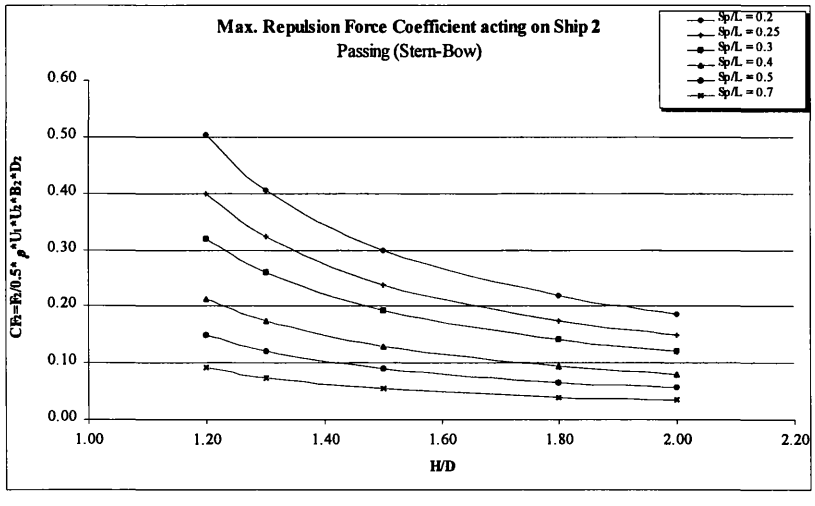

Fig A4.3 Maximum lateral force coefficients acting on the slower Ship 2 for various water depths and separation distances, (two ships passing, $L_1/L_2 = 1.0$ and $U_1/U_2 = 2.0$)

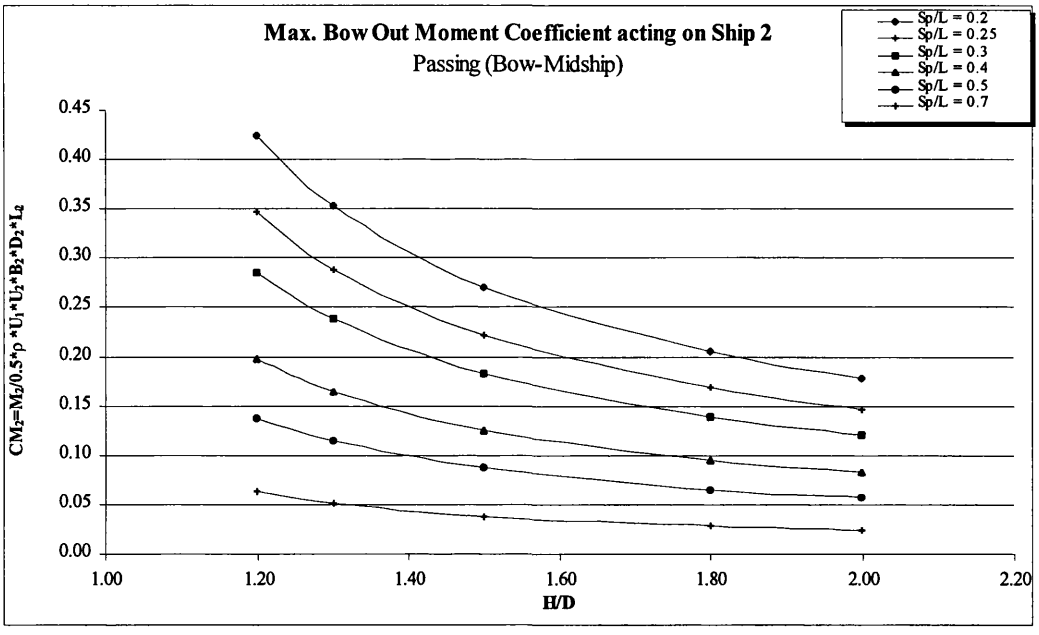

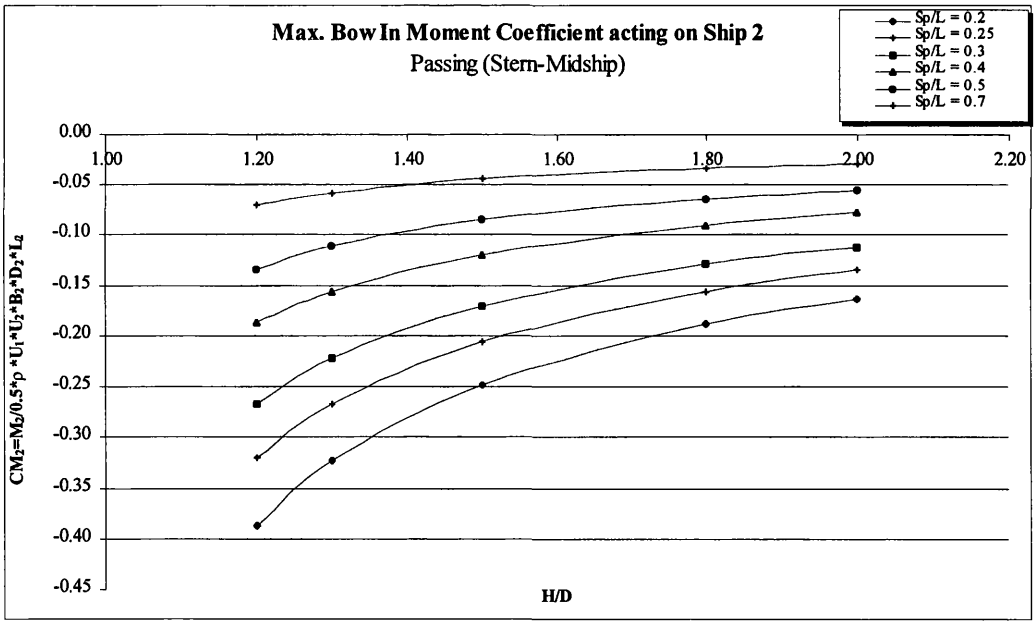

Fig A4.4 Maximum yaw moment coefficients acting on the slower Ship 2 for various water depths and separation distances, (two ships passing, $L_1/L_2 = 1.0$ and $U_1/U_2 = 2.0$)

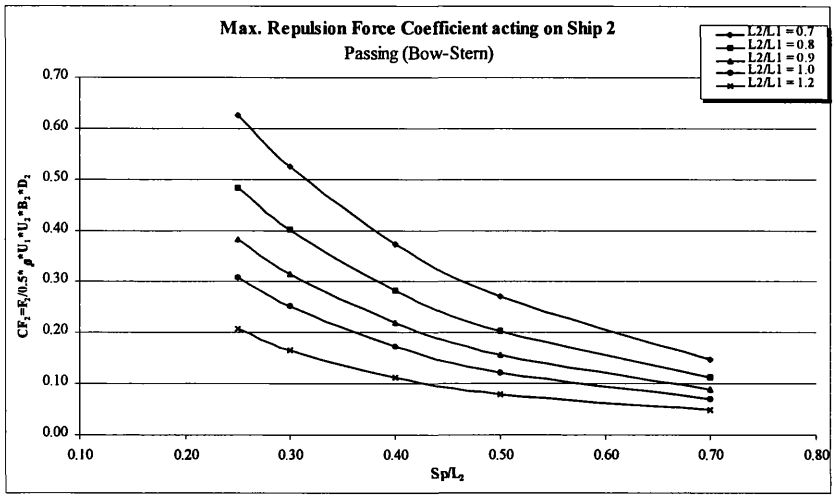

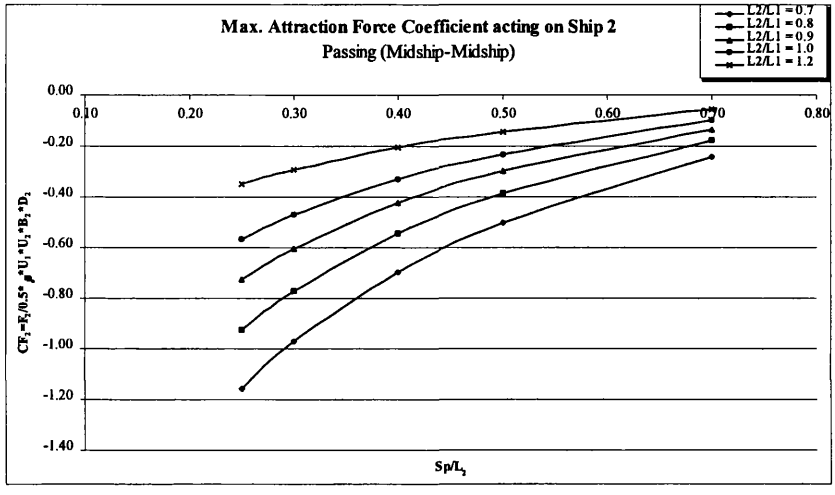

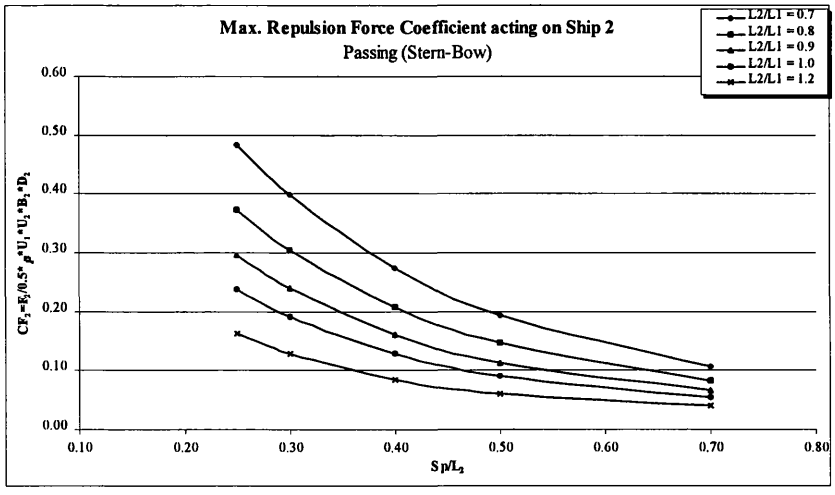

Fig A4.5 Maximum lateral force coefficients acting on the slower Ship 2 for various ship sizes and separation distances, (two ships passing, $H/D_2 = 1.5$ and $U_1/U_2 = 2.0$)

APPENDIX 5

FIGURES FOR THREE SHIPS MEETING

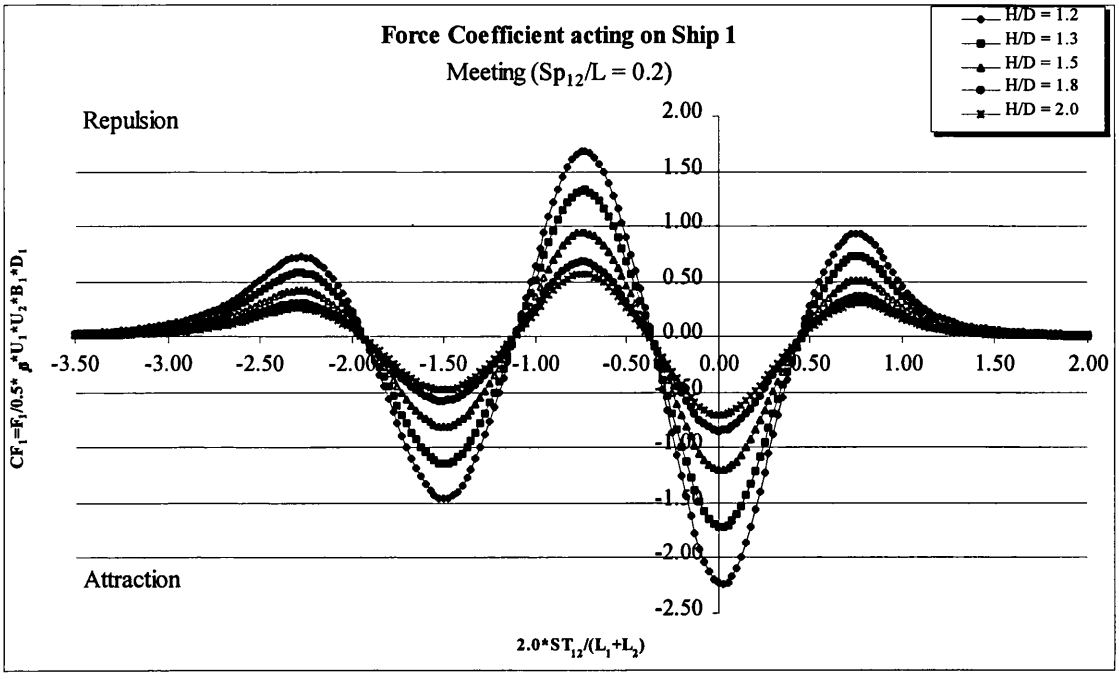

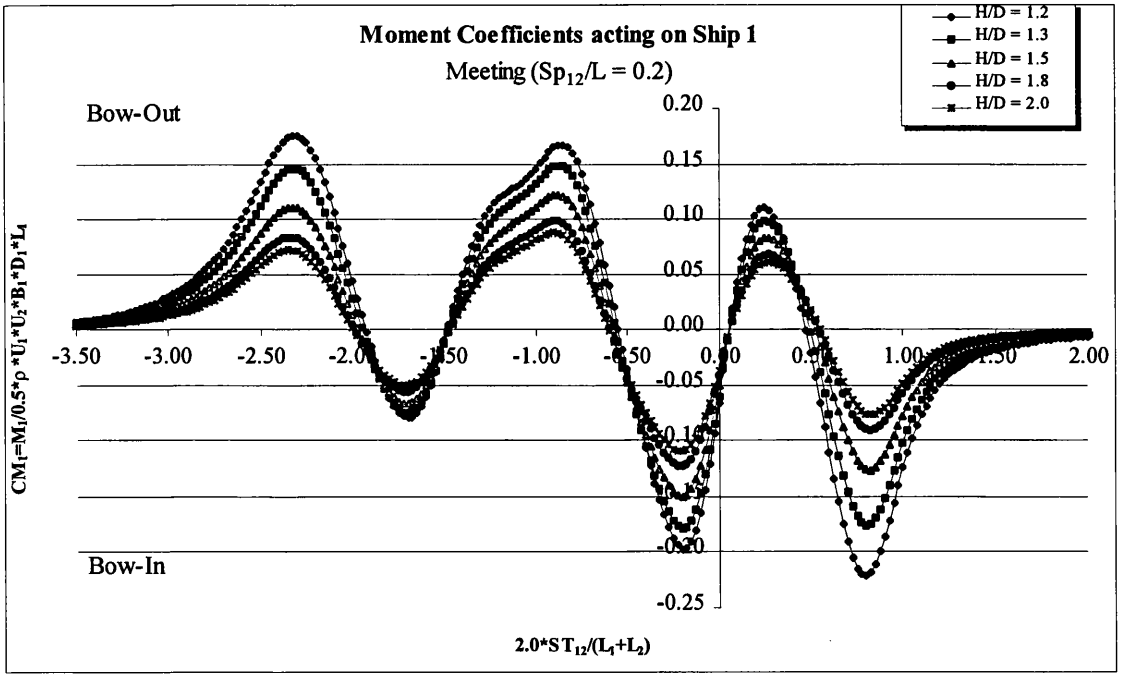

Fig A5.1 The lateral force and yaw moment coefficients acting on Ship 1 for various water depths, (three ships meeting, $Sp_{12}/L = 0.2$, $Sp_{13}/L = 0.3$ and $U_{2,3}/U_1 = 1.0$)

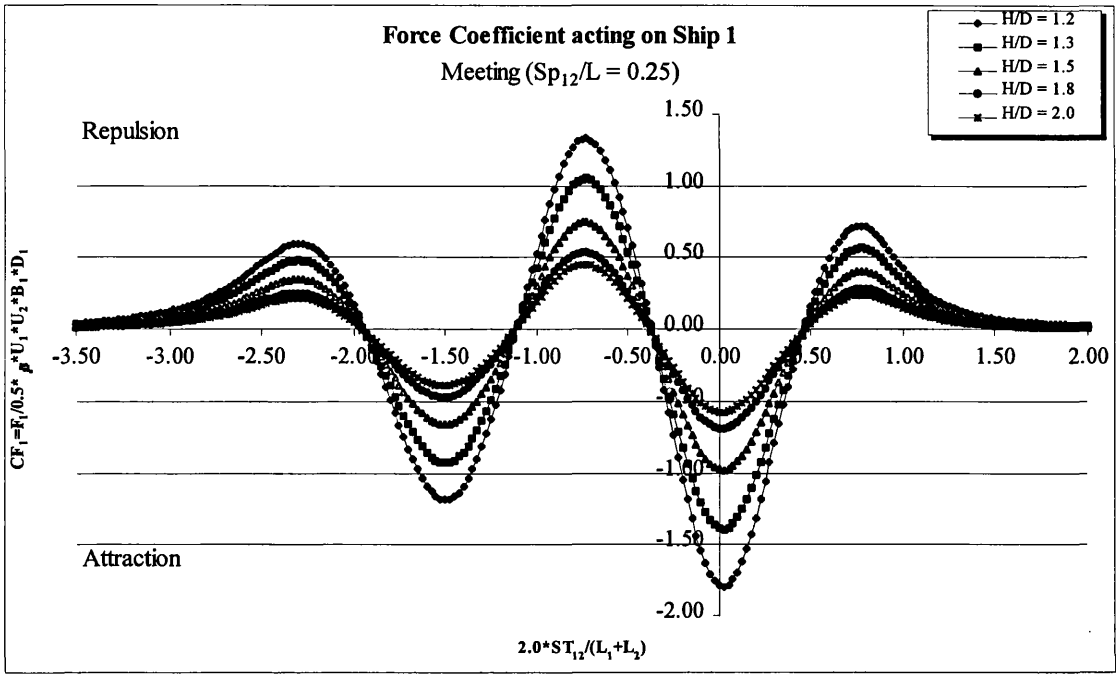

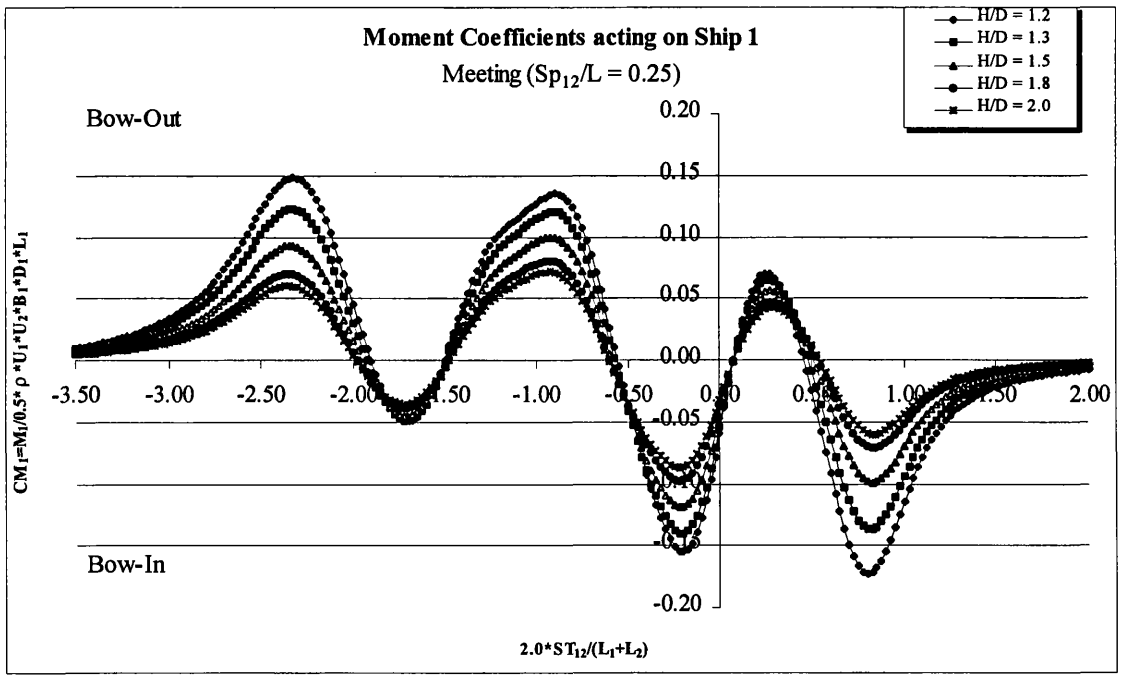

Fig A5.2 The lateral force and yaw moment coefficients acting on Ship 1 for various water depths, (three ships meeting, $Sp_{12}/L = 0.25$, $Sp_{13}/L = 0.35$ and $U_{2,3}/U_1 = 1.0$)

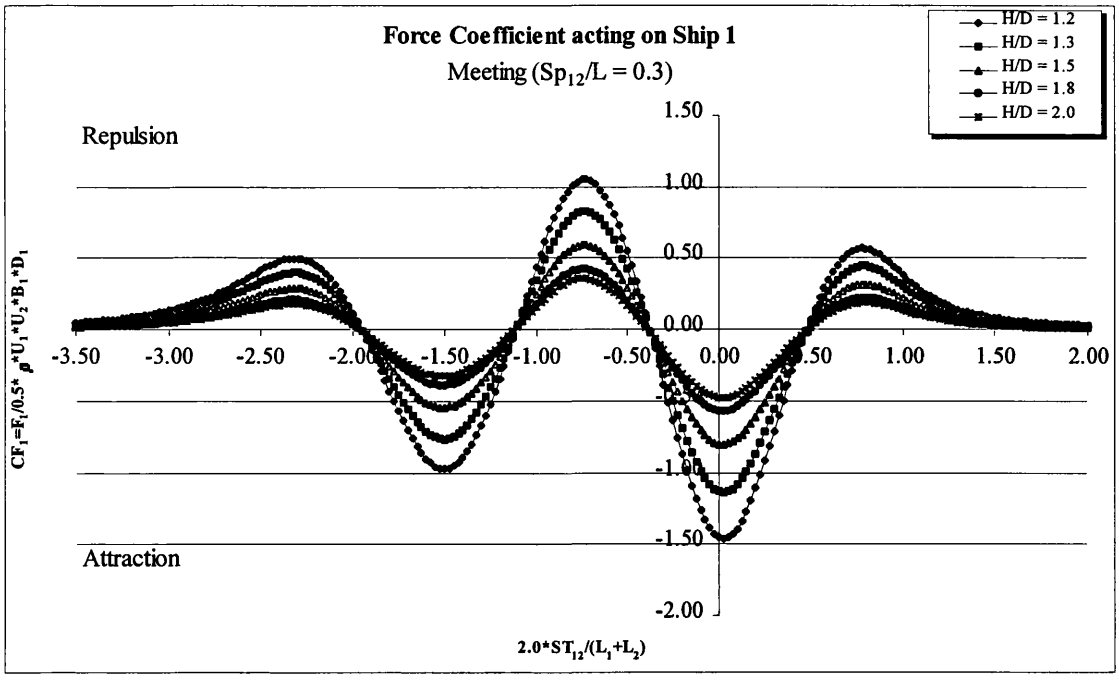

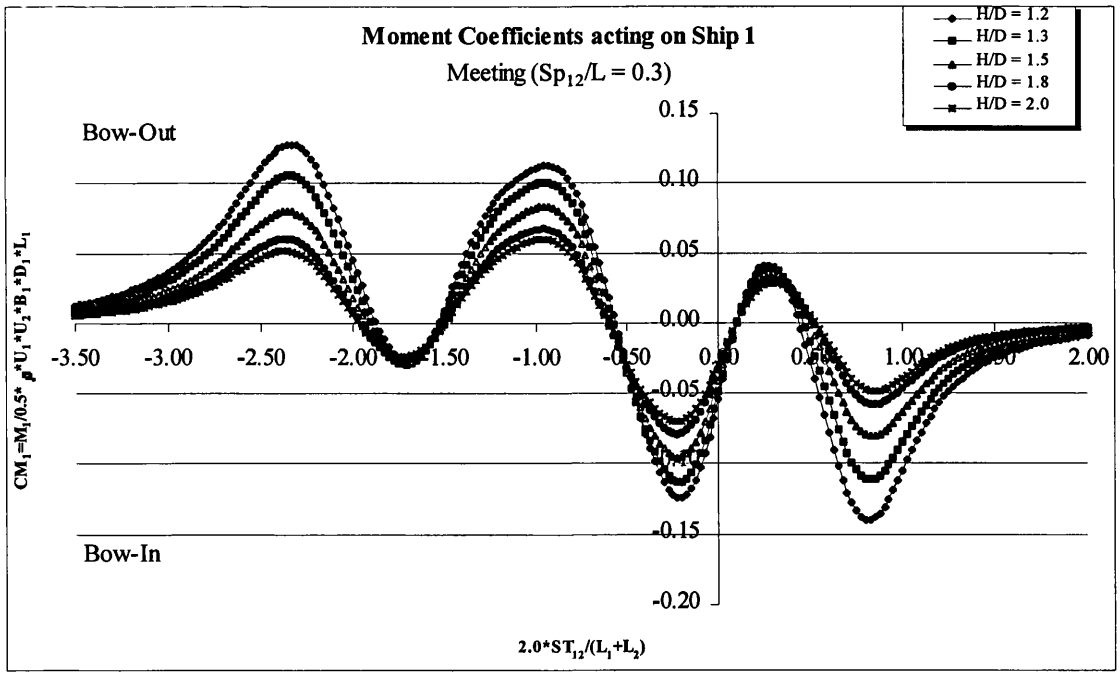

Fig A5.3 The lateral force and yaw moment coefficients acting on Ship 1 for various water depths, (three ships meeting, $Sp_{12}/L = 0.3$, $Sp_{13}/L = 0.4$ and $U_{2,3}/U_1 = 1.0$)

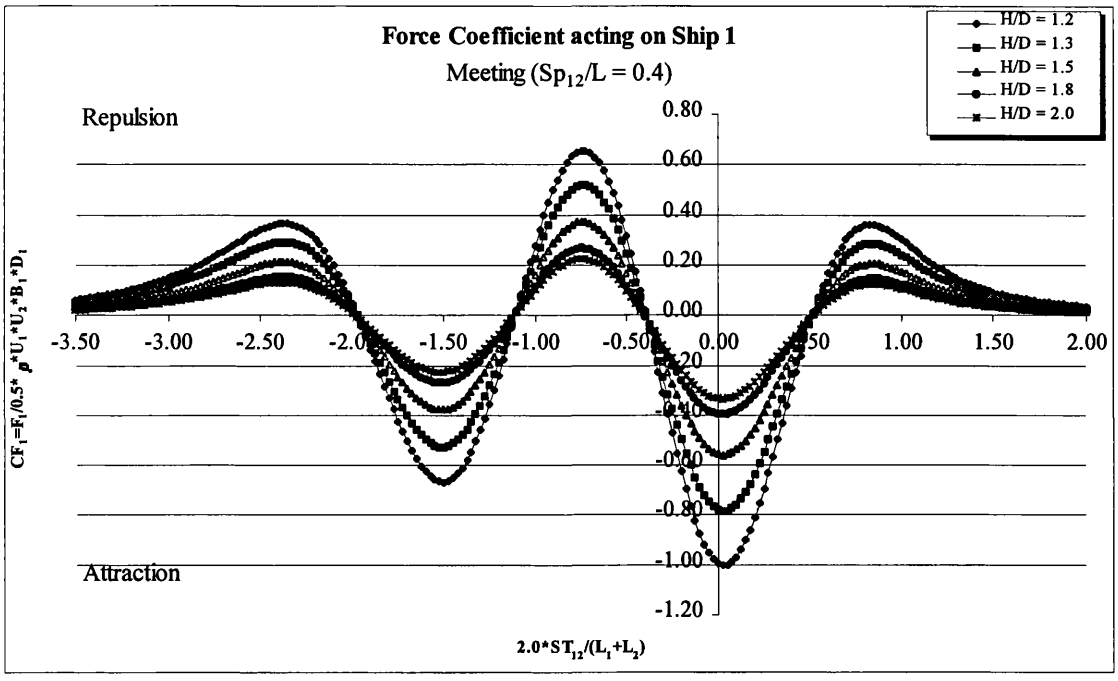

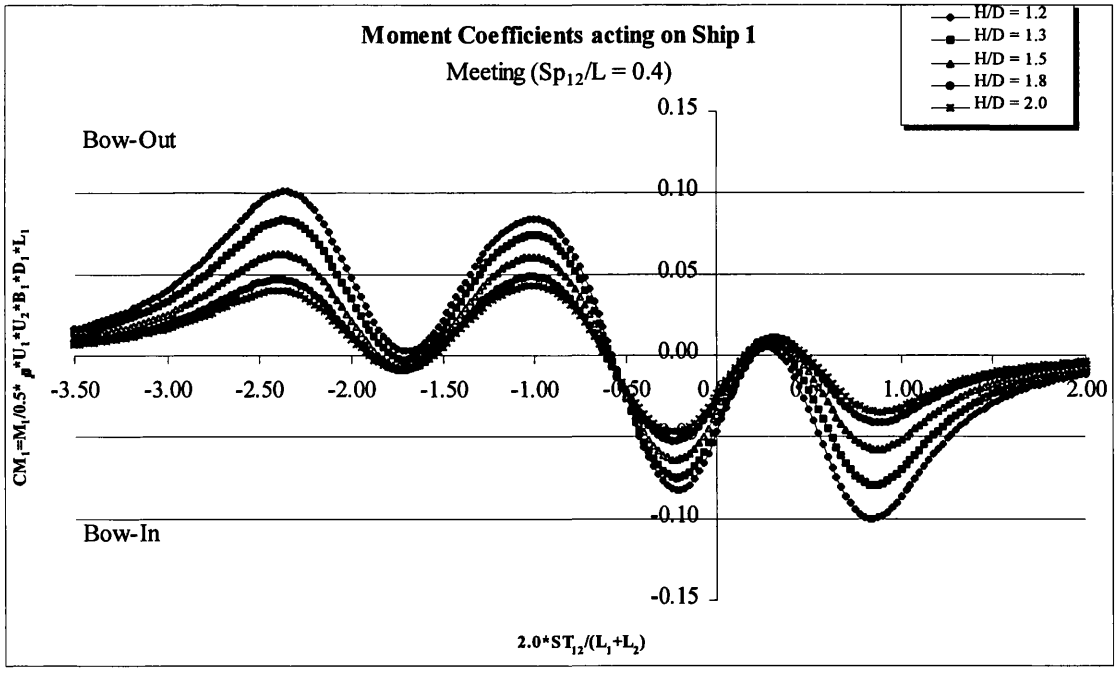

Fig A5.4 The lateral force and yaw moment coefficients acting on Ship 1 for various water depths, (three ships meeting, $Sp_{12}/L = 0.4$, $Sp_{13}/L = 0.5$ and $U_{2,3}/U_1 = 1.0$)

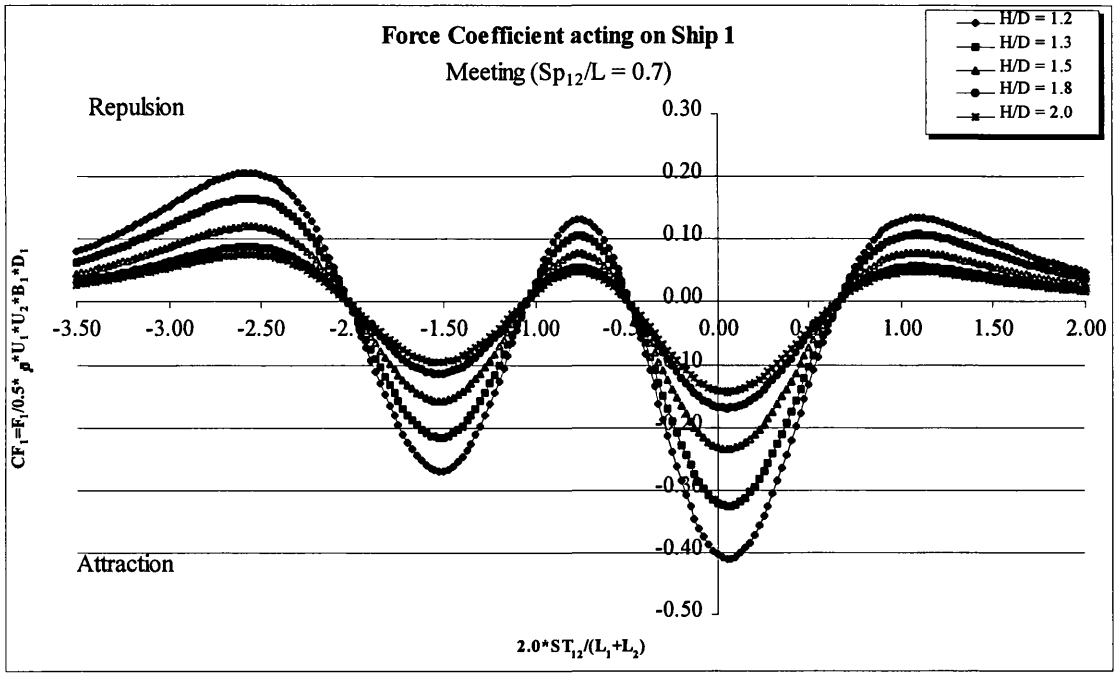

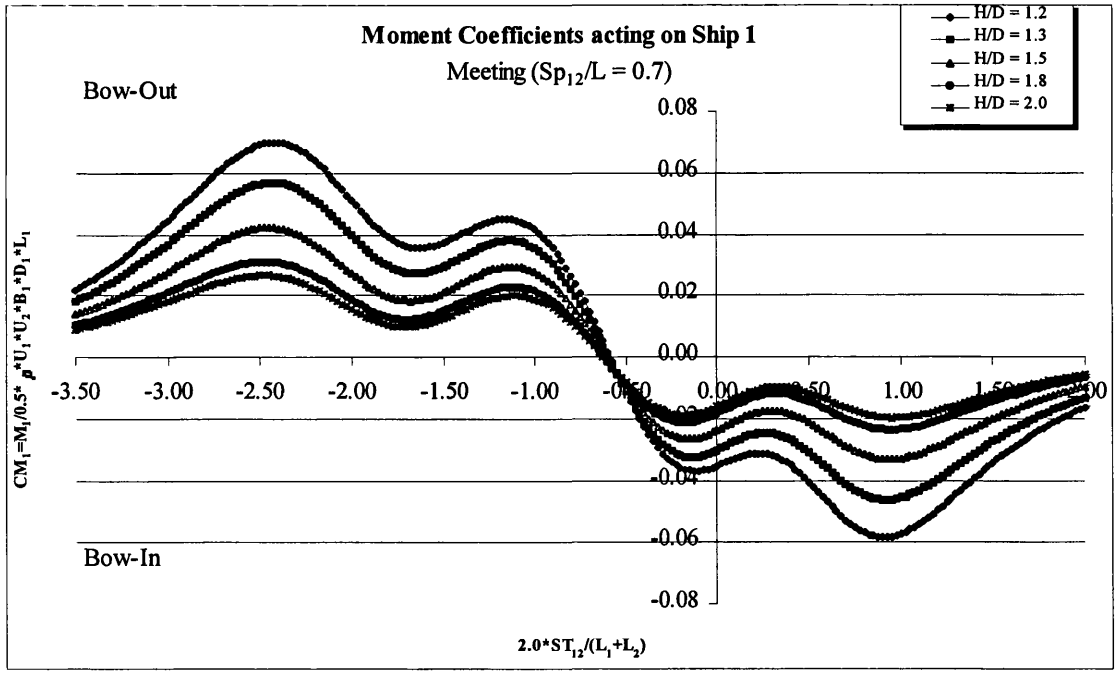

Fig A5.5 The lateral force and yaw moment coefficients acting on Ship 1 for various water depths, (three ships meeting, $Sp_{12}/L = 0.7$, $Sp_{13}/L = 0.8$ and $U_{2,3}/U_1 = 1.0$)

APPENDIX 6

THREE SHIPS PASSING

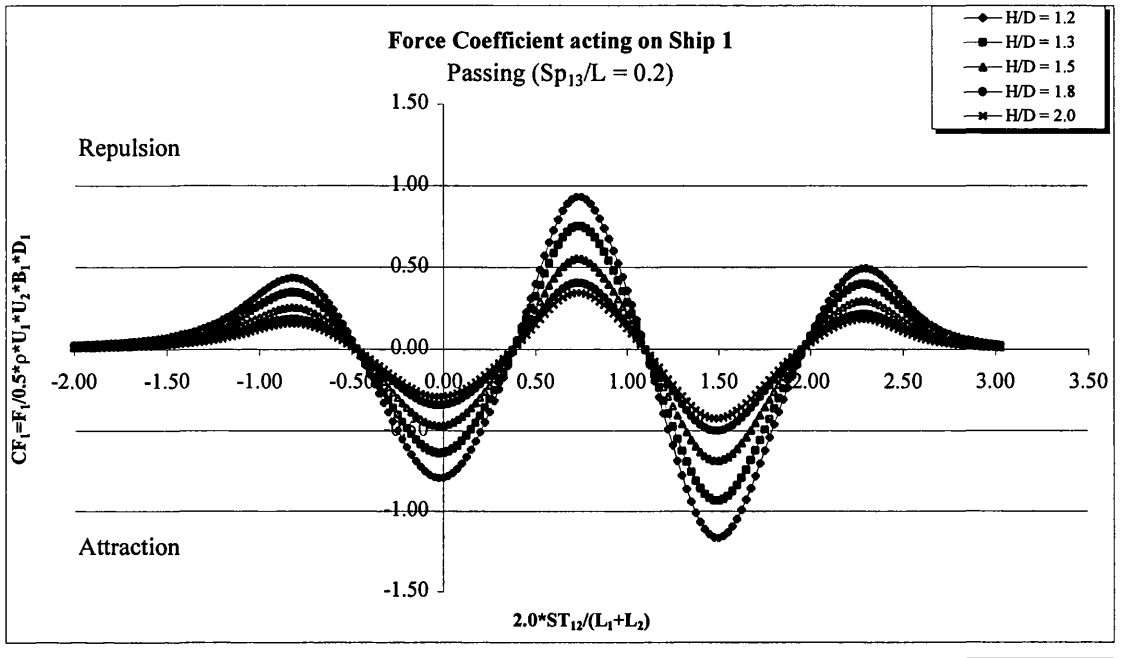

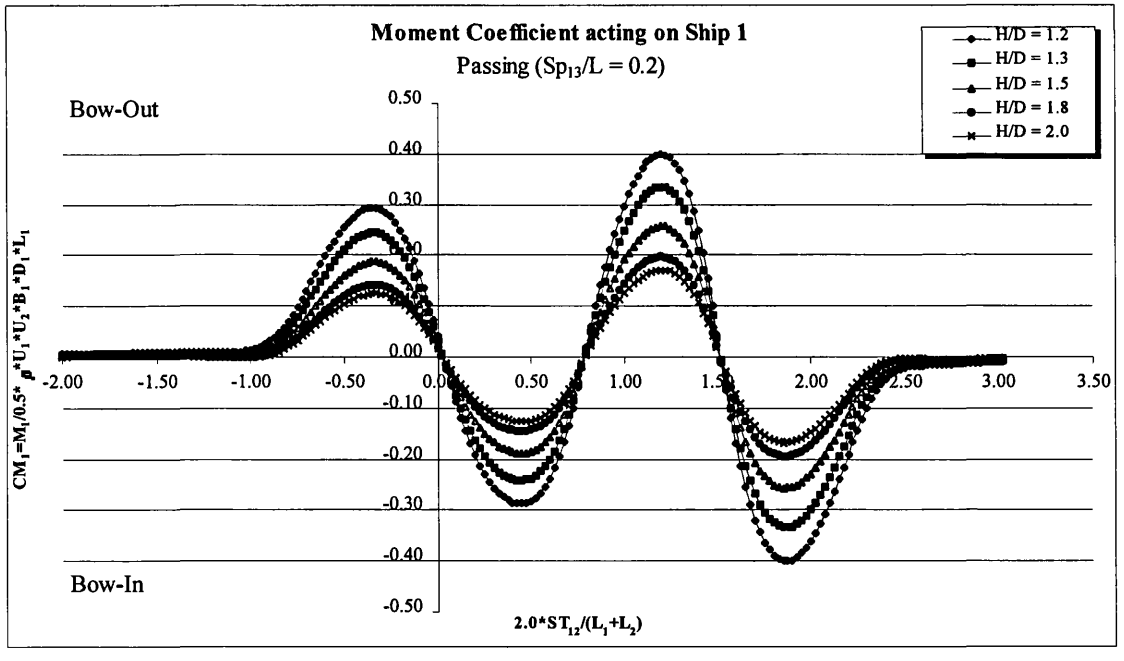

Fig A6.1 The lateral force and yaw moment coefficients acting on Ship 1 for various water depths, (three ships passing, $Sp_{12}/L = 0.3$, $Sp_{13}/L = 0.2$ and $U_{2,3}/U_1 = 2.0$)

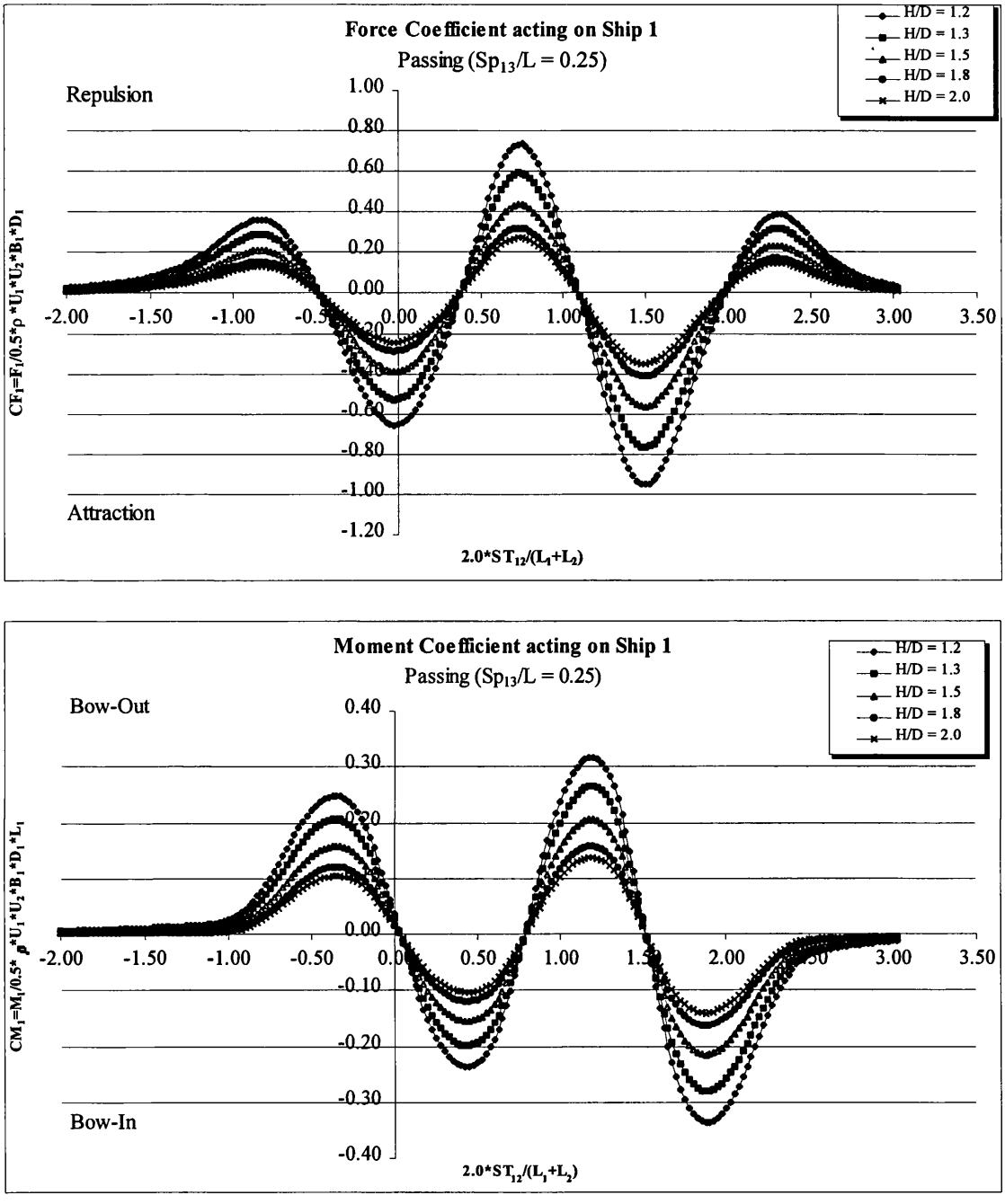

Fig A6.2 The lateral force and yaw moment coefficients acting on Ship 1 for various water depths, (three ships passing, $Sp_{12}/L = 0.35$, $Sp_{13}/L = 0.25$ and $U_{2,3}/U_1 = 2.0$)

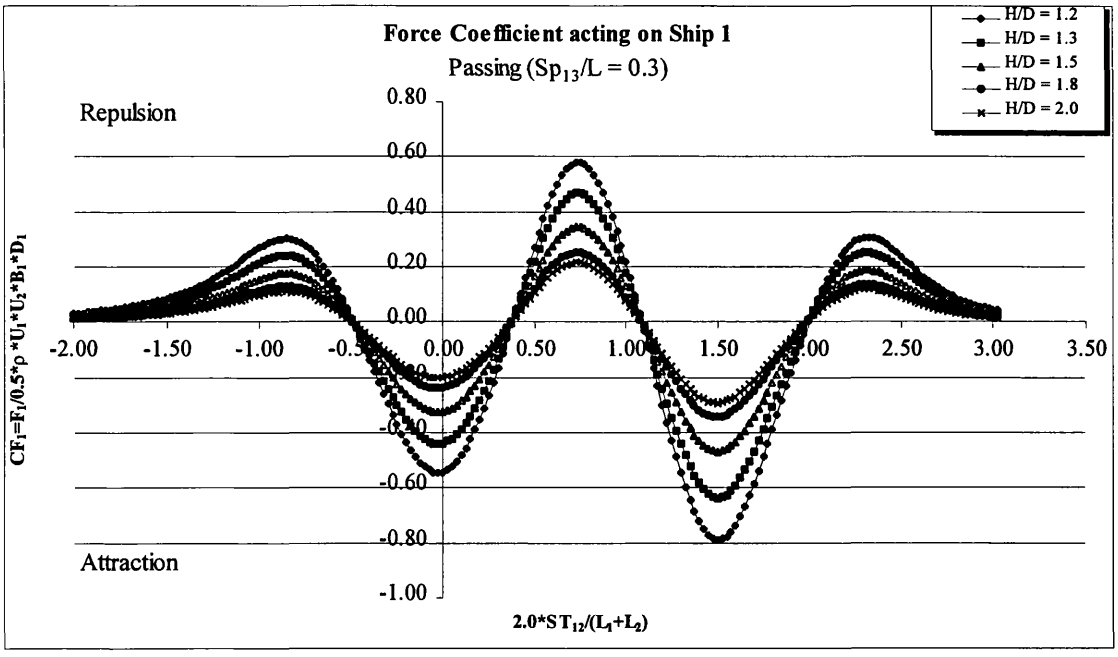

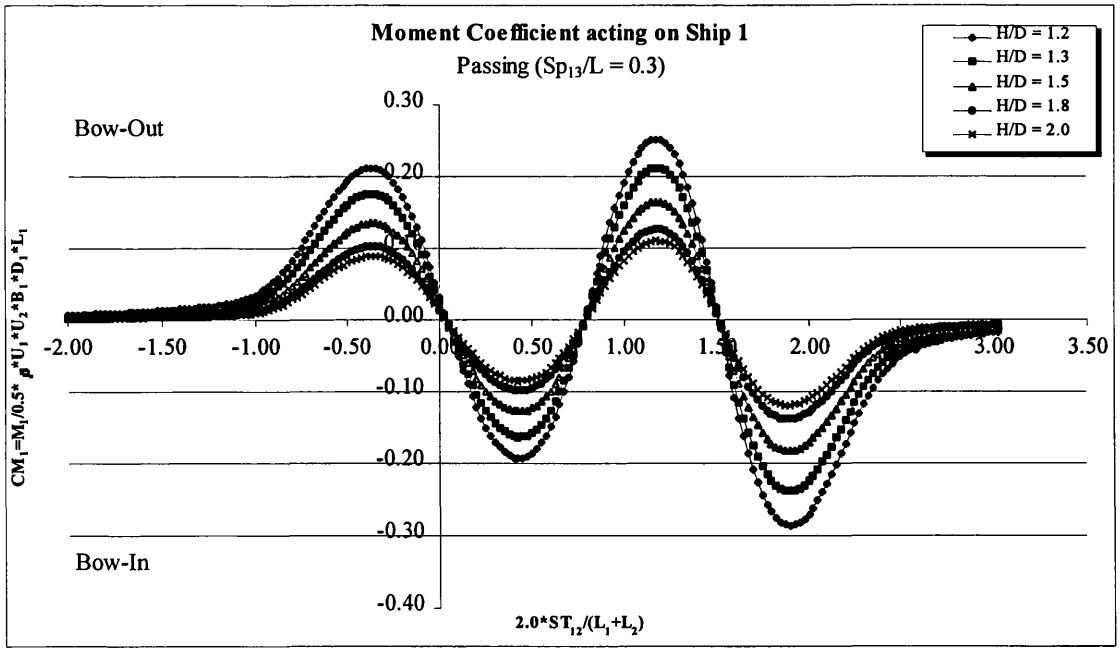

Fig A6.3 The lateral force and yaw moment coefficients acting on Ship 1 for various water depths, (three ships passing, $Sp_{12}/L = 0.4$, $Sp_{13}/L = 0.3$ and $U_{2,3}/U_1 = 2.0$)

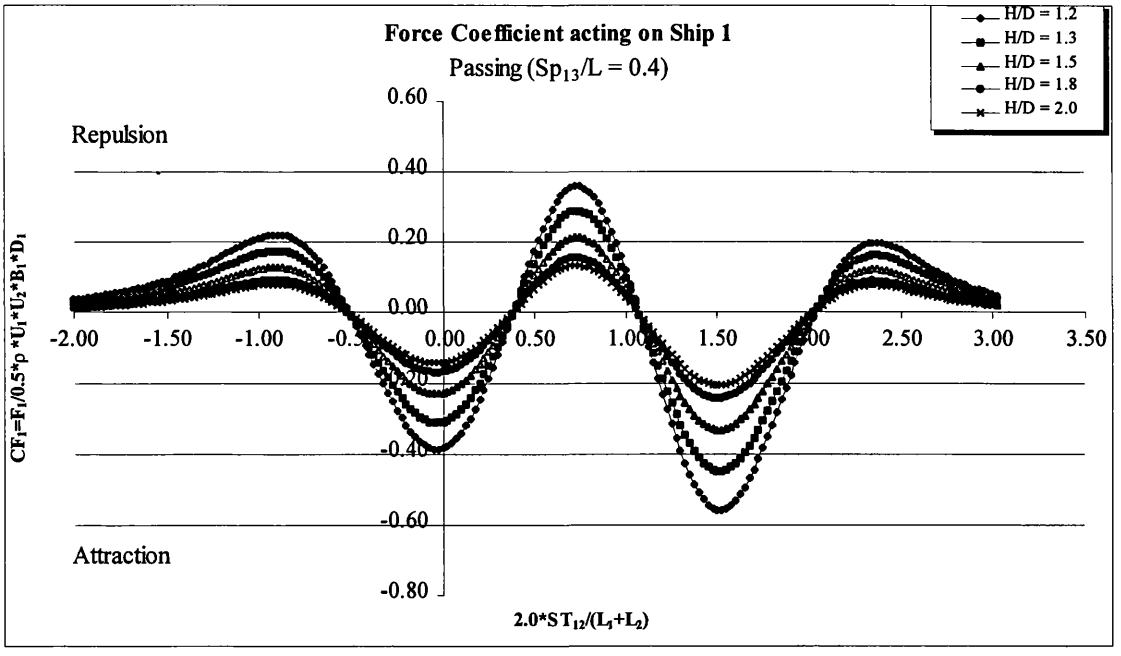

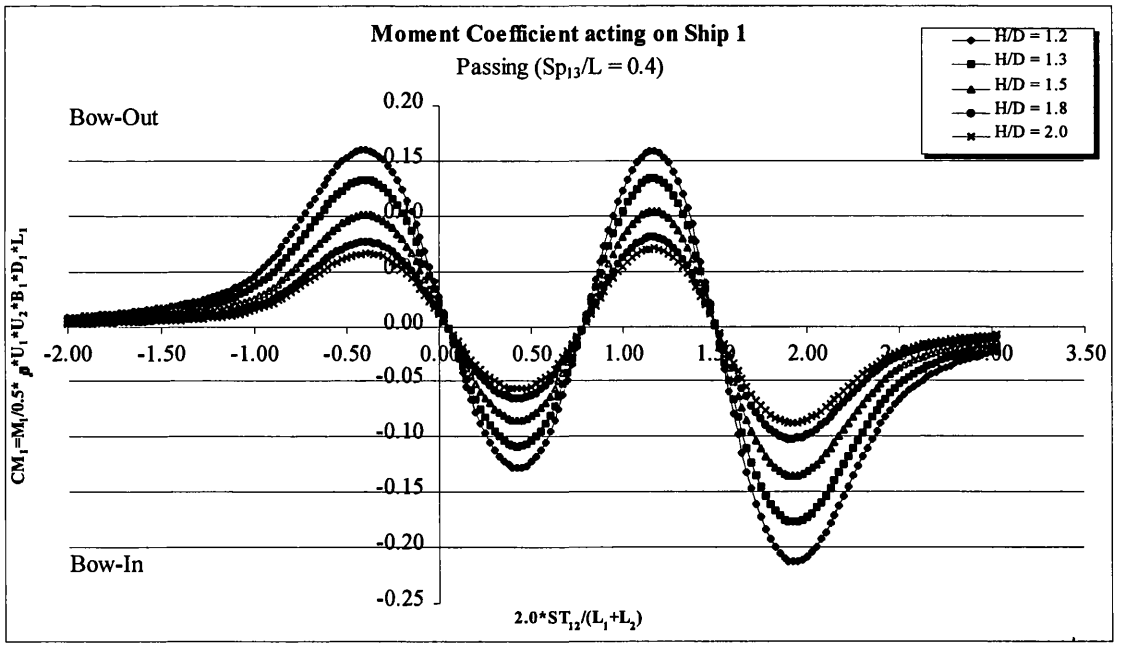

Fig A6.4 The lateral force and yaw moment coefficients acting on Ship 1 for various water depths, (three ships passing, $Sp_{12}/L = 0.5$, $Sp_{13}/L = 0.4$ and $U_{2,3}/U_1 = 2.0$)

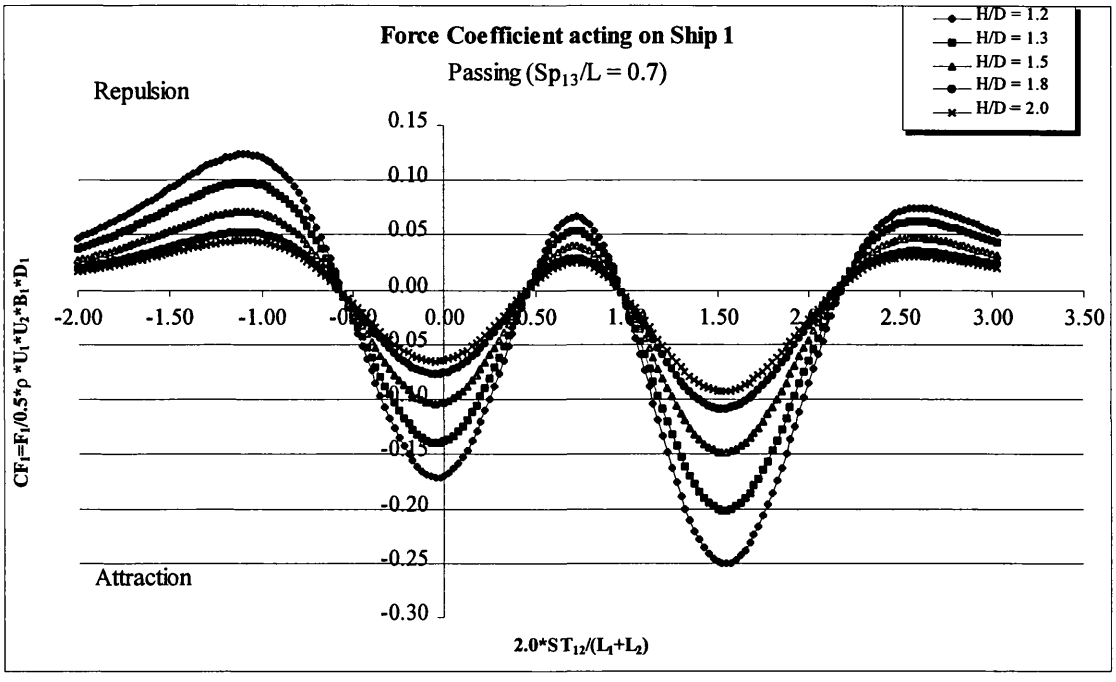

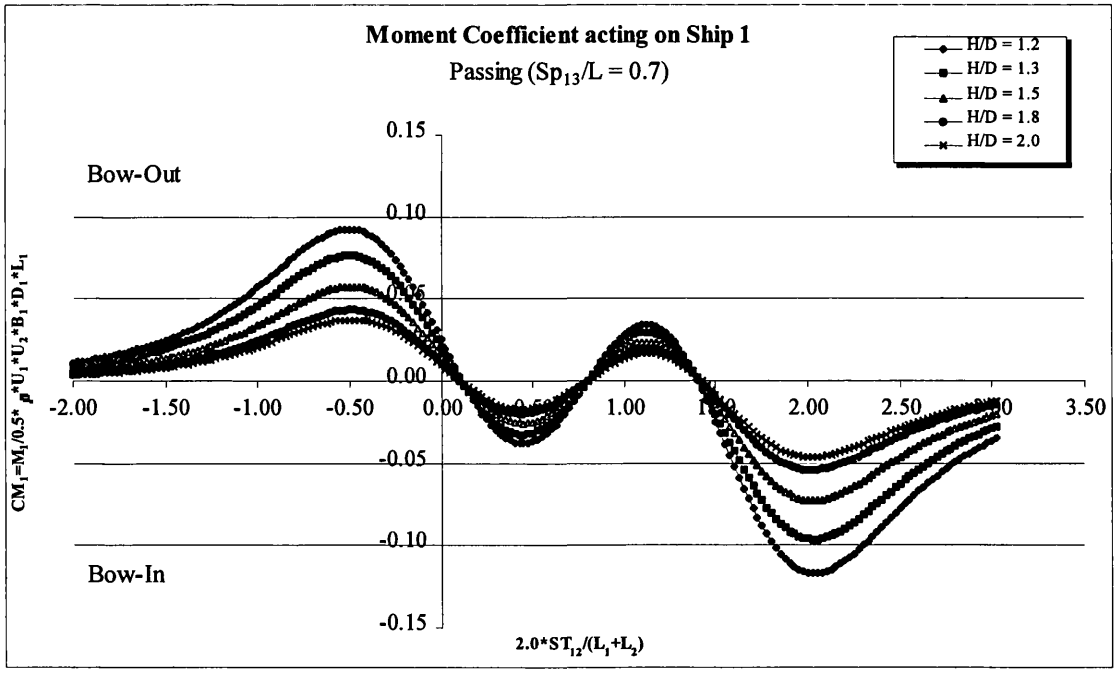

Fig A6.5 The lateral force and yaw moment coefficients acting on Ship 1 for various water depths, (three ships passing, $Sp_{12}/L = 0.8$, $Sp_{13}/L = 0.7$ and $U_{2,3}/U_1 = 2.0$)